REPUBLIQUE DU CAMEROUN
Paix – Travail – Patrie

UNIVERSITE DE YAOUNDE I

FACULTE DES SCIENCES

CENTRE DE RECHERCHE ET DE FORMATION DOCTORALE EN SCIENCES, TECHNOLOGIES ET GÉOSCIENCES

UNITE DE RECHERCHE ET DE FORMATION DE CHIMIE ET APPLICATION

REPUBLIC OF CAMEROON
Peace – Work – Fatherland

THE UNIVERSITY OF YAOUNDE I

FACULTY OF SCIENCES

POSTGRADUATE SCHOOL OF SCIENCE, TECHNOLOGY AND GEOSCIENCES

RESEARCH AND POSTGRADUATE TRAINING UNIT FOR CHEMISTRY AND APPLICATION

DEPARTMENT OF ORGANIC CHEMISTRY
DÉPARTEMENT DE CHIMIE ORGANIQUE

LABORATORY OF BIOORGANIC AND MEDECINAL CHEMISTRY
LABORATOIRE DE CHIMIE MEDICINALE ET BIOORGANIQUE

PHYTOCHEMICAL STUDIES OF *Psorospermum guineense* hochr (HYPERICACEAE) AND *Alstonia scholaris* (l) r. br. (APOCYNACEAE), SYNTHESIS, ANTI-BREAST CANCER ACTIVITY AND MOLECULAR DOCKING STUDIES

Thesis presented and publicly defended in partial fulfillment of the conditions for the award of Doctorate/Ph.D Degree in Organic Chemistry
Option: Natural Products and Organic Synthesis

By:

GHANSENYUY SALOME YUWONG
Registration number: 08T1006
Master's Degree in Organic Chemistry

Co-supervised by :

FOLEFOC NGOSONG Gabriel
Associate Professor
University of Yaounde I

EYONG KENNETH Oben
Associate Professor
University of Yaounde I

2023/2024 Academic year

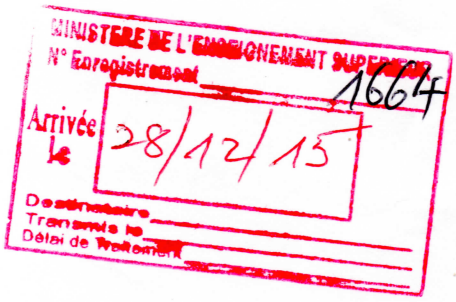

Ghansenyuy Salome Yuwong

672566455/salosuccess@yahoo.com

Ph.D. student -Organic Chemistry

University of Yaoundé 1

28/12/2015

The Minister of Higher Education,

Yaoundé-Cameroon.

Sir,

A LETTER OF APPRECIATION FOR FINANCIAL ASSISTANCE RECIEVED

I write to express my very sincere gratitude for the financial assistance which I received from your ministry to buy some basic needs for my research work. I say 'THANK YOU' for such an initiative which gave me hope and encouraged me to keep up the hard work in my studies.

I requested for financial assistance to enable me get some pressing needs particularly; chemicals for laboratory research work, pay my school fees and get a good laptop.

I received a cash award of 200 000 frs on Friday the 18th September 2015 which I spent as follows:

Item	Amount spent
Purchase of chemicals in the laboratory	120 000frs
Payment of school fees for 2014/2015 academic year	50 000frs
Labtop repairs	30 000frs
Purchase of a new laptop charger	10 000frs
Total	**200 000frs**

I remain grateful for the award I received. May God pour out very rich blessings on the Cameroon ministry of Higher Education and may her efforts be fruitful.

Yours faithfully,

Ghansenyuy Salome Yuwong

CERTIFICATE OF ATTENDANCE

The Higher Institute for Growth in HEalth Research for Women (HIGHER Women) hereby certifies that

Ms. GHANSENYUY Salome YUWONG

attended the training workshop titled

ADVANCING THE CAREER OF EMERGING WOMEN IN HIGHER EDUCATION AND RESEARCH FOR HEALTH

31 August – 4 September 2015

Monastère Notre Dame des Bénédictins du Mont-Fébé, Yaoundé,

Cameroon

Prof. Rose Gana Fomban Leke
HIGHER Women Consortium

CERTIFICATE OF ATTENDANCE

The Higher Institute for Growth in HEalth Research for Women (HIGHER Women) hereby certifies that

Ms. GHANSENYUY Salome YUWONG

attended the

« PROPOSAL WRITING WORKSHOP »

6 – 8 July 2016

Monastère Notre Dame des Bénédictins du Mont-Fébé, Yaoundé,

Cameroon

Prof. Rose Gana Fomban Leke
HIGHER Women Consortium

2

HIGHER Women
Still We Rise

CERTIFICATE OF ATTENDANCE

The Higher Institute for Growth in HEalth Research (HIGHER Women) Consortium hereby certifies that

Mrs. Salome YUWONG

attended the « **Strengthening Skills to Propel Women's Research Careers**» Seminar

27 – 28 July 2017
OCEAC, Yaoundé,
Cameroon

Prof. Rose Gana Fomban Leke
HIGHER Women Consortium

MINISTÈRE DE LA FONCTION PUBLIQUE ET DE LA RÉFORME ADMINISTRATIVE

SECRÉTARIAT GÉNÉRAL

DIRECTION DU DÉVELOPPEMENT DES RESSOURCES HUMAINES DE L' ETAT

SOUS DIRECTION DU RENFORCEMENT DES CAPACITÉS

SERVICE DE GESTION DES STAGIAIRES

BUREAU DU FICHIER ET DES STATISTIQUES

REPUBLIQUE DU CAMEROUN
Paix - Travail - Patrie

MINISTERE DES FINANCES
Direction Générale du Budget
31 .08. 2017
Contrôle Financier Central auprès du MINFOPRA
VISA BUDGETAIRE
11003798

ARRETE N° _____ /MFPRA/SG/DDRHE/SDRC/SGS/BFS

Autorisant Mademoiselle GHANSENYUY SALOME YUWONG (Mle 790972-E) à effectuer un Stage de formation.

LE MINISTRE DE LA FONCTION PUBLIQUE ET DE LA REFORME ADMINISTRATIVE

Vu la constitution ;
Vu le décret n°94/199 du 07 octobre 1994 portant Statut Général de la Fonction Publique de l'Etat, modifié et complété par le décret N° 2000/287 du 12 octobre 2000 ;
Vu le décret n°2000/697/PM du 13 septembre 2000 fixant le régime de la formation permanente des fonctionnaires ;
Vu le décret n°2000/359 du 05 décembre 2000 portant statut particulier des fonctionnaires des corps de l'Education Nationale ;
Vu le décret n° 2011/408 du 09 décembre 2011 portant organisation du Gouvernement;
Vu le décret n° 2011/410 du 09 décembre 2011 portant formation du Gouvernement;
Vu le décret n° 2012/537 du 19 novembre 2012 portant organisation du Ministère de la Fonction Publique et de la Réforme Administrative;
Vu le décret n°2015/434 du 02 octobre 2015 portant réaménagement du Gouvernement.

ARRETE :

Article 1er : Mademoiselle GHANSENYUY SALOME YUWONG, Professeur des Lycées d'Enseignement Secondaire Général, est autorisée à effectuer un stage de formation à l'Université de Karachi au Pakistan pour une période de trois cent soixante-quatre (364)jour(s) allant du 1er septembre 2017 au 31 août 2018 en vue de finaliser ses Travaux de Recherches Doctorales en Chimie.

Article 2 : Pendant la durée du stage, l'intéressée cumilera avec la Bourse de "The World Academy of Science (TWAS)" dont elle est bénéficiaire, son salaire indiciaire assorti du complément forfaitaire de solde et éventuellement des prestations familiales à l'exclusion de toute autre prime ou indemnité.

Article 3 : L'intéressée devra se présenter au Ministère de la Fonction Publique et de la Réforme Administrative, Direction du Développement des Ressources Humaines de l'Etat, le 30 septembre 2018, munie de son rapport des travaux de thèse, d'une attestation de suivi régulier de la formation délivrée par les services diplomatiques compétents et d'un certificat de reprise de service, faute de quoi, il sera procédé à la constatation de son absence.

Article 4 : Le présent arrêté sera enregistré et communiqué partout où besoin sera.

Yaoundé, le 08 SEPT 2017

AMPLIATIONS
-MINFI/SOLDE/TRESOR
-DGSN
-MINREX/AMBACAM/PAKISTAN
-MINESEC/INTERESSEE
-DOSSIER/CHRONO
-ARCHIVES

REPUBLIQUE DU CAMEROUN
Republic of Cameroun
The Minister
MINISTRY OF PUBLIC SERVICE AND ADMINISTRATIVE REFORMS
MINISTÈRE DE LA FONCTION PUBLIQUE ET DE LA RÉFORME ADMINISTRATIVE
Le Ministre

ANGOUING Michel Ange

SIGIPES Edition du 30/08/2017

Sandia National Laboratories

CRDF GLOBAL
INSPIRED BY PEOPLE | DRIVEN BY SCIENCE

This is to Certify that

Dr. / Mr. / Ms. **Ghansenyuy Salome Yuwong**

has participated in the series of Webinar entitled, **"Women in Science: Chemical Safety and Security"** on March 7 and 8, 2018. It was jointly organized by the International Center for Chemical and Biological Sciences (ICCBS), Sandia National Laboratories (SNL) and CRDF Global (USA).

Andrew W. Nelson, PhD MPH
Sandia National Laboratories
USA

Prof. Dr. M. Iqbal Choudhary *H.I. S.I. T.I.*
Director, ICCBS
Pakistan

PCMD

United Nations
Educational, Scientific and
Cultural Organization

INTERNATIONAL CENTER FOR CHEMICAL AND BIOLOGICAL SCIENCES

(H.E.J. Research Institute of Chemistry, and Dr. Panjwani Center for Molecular Medicine and Drug Research)
University of Karachi, Karachi-75270, Pakistan

Prof. Dr. Muhammad Iqbal Choudhary
Director *Hilal-e-Imtiaz, Sitara-e-Imtiaz, Tamgha-e-Imtiaz*

Distinguished National Professor
D. Sc., Ph.D., C.Chem., Meritorious Professor
Member National Commission for Science and Technology
Fellow of the Academy of Sciences for the Developing World (TWAS)
Fellow of the Islamic World Academy of Sciences
Fellow of the Pakistan Academy of Sciences
Fellow of the Royal Society of Chemistry
Fellow of the Chemical Society of Pakistan
Fellow of International Union of Pure and Applied Chemistry
Fellow of LEAD International
Fellow of the World Innovation Foundation

Tel. Off : (92-21) 34824924-5, 34819010
UAN : 111-222-292 (Ext.106)
Telefax : (92-21) 99261713, 34819018
E-mail : iqbal.choudhary@iccs.edu
pcmd@cyber.net.pk
Web : www.iccs.edu

31.05.2018

ATTESTATION OF EFFECTIVE TRAINING AT THE INTERNATIONAL CENTER FOR CHEMICAL AND BIOLOGICAL SCIENCES (ICCBS), UNIVERSTITY OF KARACHI-PAKISTAN: UNDERGONE BY Ms. GHANSENYUY SALOME YUWONG

This is to certify that **Ms. GHANSENYUY SALOME YUWONG**, a TWAS-ICCBS Research Scholar (2016 award scheme), successfully completed her postgraduate(Ph.D.) research fellowship in Organic Chemistry at the H.E.J. Research Institute of Chemistry, International Center for Chemical and Biological Sciences (ICCBS), University of Karachi-75270, Pakistan. During her stay (Dec 5th, 2017 to June 4th, 2018), she worked on two medicinal plant extracts. With the help of modern equipment and modern techniques, she acquired a good expertise in separation analyses, and spectroscopic techniques.

Ms. Yuwong was not only able to enhance her knowledge on scientific research, but also on diversified topics that include, scientific writing, laboratory safety practices, chemical risk management, and assessment of chemical risk, through attending several workshops, seminars and webinars at the ICCBS conducted by leading local and foreign experts and scientists.

She is a skillful and diligent researcher who carried out her research with frugality by following the appropriate protocols. She is mentally alert, creative and was fully committed to her research work during her tenure at the ICCBS. Furthermore, she enjoyed learning local culture, and also learned about cultural practices during her stay. She however, encountered a difficulty as her visa extension did not go through hence she couldn't stay for up to 12 months as was previewed earlier, she was advised to reapply and come back for another 6 months' stay.

I am confident that Ms. Salome Yuwong will positively impact her University as well as her country and society at large, with the knowledge she acquired during her tenure. I wish her best of luck in her future, and research endeavors.

PROF. DR. M. IQBAL CHOUDHARY, *H.I., S.I., T.I.*
Director, ICCBS

THE AFRICA-EU PARTNERSHIP
LE PARTENARIAT AFRIQUE-UE

CONSEIL AFRICAIN ET MALGACHE POUR L'ENSEIGNMENT SUPERIEUR

GUNI GLOBAL UNIVERSITY NETWORK FOR INNOVATION

AfriQAN

CERTIFICATE OF PARTICIPATION

This is to certify that

GHANSENYUY SALOME YUWONG

participated actively at the

10th International Conference and Workshops on Quality Assurance in Higher Education in Africa and the 2018 AfriQAN General Assembly on

Higher Education Quality Assurance and the Promotion of Synergies Among Science, Technology and Humanities: Towards the Attainment of the SDGs in Africa

Yaoundé, Cameroon | September 17-20, 2018

Professor Juma Shabani
Chairman, ICQAHEA

Professor Peter Okebukola
President, GUNi-Africa

Professor Jonathan Mba
Coordinator, AfriQAN

CERTIFICATE OF RECOGNITION

The Higher Institute for Growth in HEalth Research for Women (HIGHER Women) Consortium hereby congratulates

Ms Ghansenyuy Salome Yuwong

for having facilitated workshop on

WOMEN IN RESEARCH FOR HEALTH: CAREER, FAMILY AND SOCIETY

5 - 7 September 2019, Monastère des Bénédictins, Mont-Febe, Yaoundé, Cameroon

Prof. Rose Gana Fomban Leke
HIGHER WOMEN Consortium
Founder/President

2023 Annual Meeting
October 18-22

HYATT REGENCY CHICAGO | CHICAGO, ILLINOIS USA

ajtmh.org astmh.org #TropMed23

CERTIFICATE OF ATTENDANCE

This certificate is presented to

Ghansenyuy Salome Yuwong

for attending the **American Society of Tropical Medicine and Hygiene 2023 Annual Meeting**
at the Hyatt Regency Chicago, Chicago IL, USA
October 18 - 22, 2023

Daniel Bausch, President

Christy A. Petersen, Scientific Program Chair

Karen Goraleski, CEO

ATTESTATION OF PARTICIPATION

The Higher Institute for Growth in HEalth Research for Women *(**HIGHER Women**)* Consortium certifies that

GHANSENYUY Salome YUWONG

participated at the 7th Annual Workshop on the theme ***Women in Health Research: Breaking Boundaries*** from 20th to 21st September 2024, Conference Hall IMPM, Ministry of Scientific Research and Innovation, Yaoundé, Cameroon.

Professor Rose G.F. LEKE

PRESIDENT

Certificate of Attendance

This certificate recognizes:

Ghansenyuy Salome Yuwong

Attended the

American Society of Tropical Medicine and Hygiene 2024 Annual Meeting

November 13 – November 17, 2024

New Orleans Ernest N. Morial Convention Center

New Orleans, Louisiana

Linnie Golightly, President

David Hamer, Scientific Program Chair

Jamie Nishi, CEO

CERTIFICATE OF ATTENDANCE

This certifies that

GHANSENYUY SALOME YUWONG

attended the ACS Spring 2025 Conference
March 23-27, 2025
San Diego, CA, USA

Liz Huh
DIRECTOR, MEETINGS & EVENTS

AMERICAN SOCIETY FOR MICROBIOLOGY

Certificate of Completion

This certifies that

Ghansenyuy Salome Yuwong

has successfully completed the following professional development webinar training:

MANAGING BURNOUT AND RESILIENCY

Webinar Duration: 1.5 hours
Provided by: ASM Education Department

Shelley Payne, Chair, ASM Education Committee

April 17, 2025

Date of Completion

ASTMH

AMERICAN SOCIETY OF TROPICAL MEDICINE & HYGIENE

ADVANCING GLOBAL HEALTH SINCE 1903

This certifies that

Ghansenyuy Salome Yuwong

ID 79931

Predoctoral Student Member
In good standing of the

American Society of Tropical Medicine and Hygiene
2024-2025

Kent Kester, MD, FASTMH
Chair, ASTMH Membership Committee

Jamie Bay Nishi, MS
CEO

AMERICAN SOCIETY FOR MICROBIOLOGY

2025 Certificate of Membership

Ghansenyuy Salome Yuwong

is a Global Outreach - Student Member
of the American Society for Microbiology, entitled to
all the rights and privileges associated therewith
as specified by the Bylaws of the Society

Theresa M Koehler
President

Robin Patel
Secretary

Peggy Cotter
Membership Committee Chair

American Society of Pharmacognosy

CERTIFICATE OF MEMBERSHIP

PRESENTED TO

Ghansenyuy Salome Yuwong

to certify professional associate membership in the **American Society of Pharmacognosy (ASP)**. Membership expires on December 31, 2027.

Laura Stoll

Laura Stoll
ASP Business Manager

February 28, 2025

Date

American Society of Pharmacognosy

ACS Chemistry for Life®

American Chemical Society

THIS IS TO CERTIFY THAT

GHANSENYUY SALOME YUWONG

is a Member of the American Chemical Society, entitled to all rights and privileges associated therewith as specified in the ACS Governing Documents of the Society.

Dorothy J. Phillips

Dorothy J. Phillips, Ph.D.
2025 American Chemical Society President

Albert G. Horvath
Chief Executive Officer (CEO)

REPUBLIQUE DU CAMEROUN
****
Paix - Travail - Patrie
****
UNIVERSITE DE YAOUNDE I
****
CENTRE DE RECHERCHE ET DE FORMATION DOCTORALE EN SCIENCES, TECHNOLOGIE ET GEOSCIENCES
****
UNITE DE RECHERCHE DE FORMATION DOCTORALE EN CHIMIE ET APPLICATIONS
****

REPUBLIC OF CAMEROON
****
Peace - Work - Fatherland
****
THE UNIVERSITY OF YAOUNDE I
****
POSTGRADUATE SCHOOL OF SCIENCE, TECHNOLOGY AND GEOSCIENCES
****
DOCTORAL RESEACH UNIT IN CHEMESTRY AND APPLICATIONS
****

DEPARTEMENT DE CHIMIE ORGANIQUE
DEPARTMENT OF ORGANIC CHEMISTRY

Attestation Of Thesis Correction of Miss Ghansenyuy Salome Yuwong

We hereby attest that the thesis entitled, «**Phytochemical studies of *Psorospermum guineense* hochr (Hypericaceae) and *Alstonia scholaris* (l) r. br. (Apocynaceae), synthesis, anti-breast cancer activity and molecular docking studies**», presented by Miss Ghansenyuy Salome Yuwong, Matricule 08T1006, has been revised according to the recommandations of the jury members before whom this thesis was defended on June 7th, 2025 at the University of Yaounde 1.

In witness whereof, the present certification is issued to serve wherever applicable.

Issued in Yaoundé, on 4../..7./2025

Members of Jury

President

ATCHADE Alex De Théodore, Professor

Supervisors

EYONG Kenneth Oben, Associate Professor

FOLEFOC Gabriel Ngosong, Associate Professor

Examiners

MBAH James Ajeck, Professor

ABOUEM À ZINTCHEM Auguste

Associate Professor

DJUIDJE NGOUNOUE Marceline,

Associate Professor

<UNIVERSITÉ DE YAOUNDÉ I **Faculté des Sciences** Division de la Programmation et du Suivi des Activités Académiques		**THE UNIVERSITY OF YAOUNDE I** **Faculty of Science** Division of Programming and Follow-up of Academic Affaires
LISTE DES ENSEIGNANTS PERMANENTS		**LIST OF PERMANENT TEACHING STAFF**

ANNÉE ACADEMIQUE 2024/2025

(Par Département et par Grade)

DATE D'ACTUALISATION AVRIL 2025

ADMINISTRATION

DOYEN : OWONO OWONO Luc Calvin, *Maître de Conférences*
VICE-DOYEN / DPSAA: NDJIGUI Paul-Désiré, *Professeur*
VICE-DOYEN / DSSE : NYEGUE Maximilienne Ascension, *Professeur*
VICE-DOYEN / DRC : NOUNDJEU Pierre, *Maître de Conférences*
Chef Division Administrative et Financière : NDOYE FOE Florentine Marie Chantal, *Maître de Conférences*
Chef Division des Affaires Académiques, de la Recherche et de la Scolarité DAARS : AJEAGAH Gideon AGHAINDUM, *Professeur*

1- DÉPARTEMENT DE BIOCHIMIE (BC) (39)

N°	NOMS ET PRÉNOMS	GRADE	OBSERVATIONS
1.	BIGOGA DAIGA Jude	Professeur	En poste
2.	FEKAM BOYOM Fabrice	Professeur	En poste
3.	KANSCI Germain	Professeur	En poste
4.	MBACHAM FON Wilfred	Professeur	En poste
5.	MOUNDIPA FEWOU Paul	Professeur	*Chef de Dpt*
6.	NGUEFACK Julienne	Professeur	En poste
7.	NJAYOU Frédéric Nico	Professeur	En poste
8.	OBEN Julius ENYONG	Professeur	En poste
9.	ACHU Merci BIH	Maître de Conférences	En poste
10.	AKINDEH MBUH NJI	Maître de Conférences	En poste
11.	ATOGHO Barbara MMA	Maître de Conférences	En poste
12.	AZANTSA KINGUE GABIN BORIS	Maître de Conférences	En poste
13.	BELINGA née NDOYE FOE F. M. C.	Maître de Conférences	Chef DAF / FS
14.	DAKOLE DABOY Charles	Maître de Conférences	En poste
15.	DONGMO LEKAGNE Joseph Blaise	Maître de Conférences	En poste
16.	DJUIDJE NGOUNOUE Marceline	Maître de Conférences	En poste
17.	DJUIKWO NKONGA Ruth Viviane	Maître de Conférences	En poste
18.	EFFA ONOMO Pierre	Maître de Conférences	En poste
19.	EWANE Cécile Annie	Maître de Conférences	En poste
20.	KENGNE NOUEMSI Anne Pascale	Maître de Conférences	En poste

21.	KOTUE TAPTUE Charles	Maître de Conférences	En poste
22.	LUNGA Paul KEILAH	Maître de Conférences	En poste
23.	MANANGA Marlyse Joséphine	Maître de Conférences	En poste
24.	MBONG ANGIE M. Mary Anne	Maître de Conférences	En poste
25.	MOFOR née TEUGWA Clotilde	Maître de Conférences	Doyen FS / Uds
26.	NANA Louise épouse WAKAM	Maître de Conférences	En poste
27.	NGONDI Judith Laure	Maître de Conférences	En poste
28.	Palmer MASUMBE NETONGO	Maître de Conférences	En poste
29.	PECHANGOU NSANGOU Sylvain	Maître de Conférences	En poste
30.	TCHANA KOUATCHOUA Angèle	Maître de Conférences	En poste
31.	AKINDEH MBUH NJI	Chargé de Cours	En poste
32.	BEBEE Fadimatou	Chargée de Cours	En poste
33.	BEBOY EDJENGUELE Sara N.	Chargé de Cours	En poste
34.	FONKOUA Martin	Chargé de Cours	En poste
35.	KOUOH ELOMBO Ferdinand	Chargé de Cours	En poste
36.	MBOUCHE FANMOE Marceline Joëlle	Chargé de Cours	En poste
37.	OWONA AYISSI Vincent Brice	Chargé de Cours	En poste
38.	WILFRED ANGIE Abia	Chargé de Cours	En poste
39.	FOUPOUAPOUOGNIGNI Yacouba	Chargé de Cours	En poste
40.	BAKWO BASSOGOG Christian Bernard	Chargé de Cours	En poste
41.	EYENGA Eliane Flore	Chargé de Cours	En poste
42.	MADIESSE KEMGNE Eugenie Aimée	Chargé de Cours	En poste
43.	MANJIA NJIKAM Jacqueline	Chargé de Cours	En poste
44.	WOGUIA Alice Louise	Chargé de Cours	En poste

2- DÉPARTEMENT DE BIOLOGIE ET PHYSIOLOGIE ANIMALES (BPA) (51)

1.	AJEAGAH Gideon AGHAINDUM	Professeur	*DAARS/FS*
2.	BILONG BILONG Charles-Félix	Professeur	Chef de Département
3.	DIMO Théophile	Professeur	En Poste
4.	DJIETO LORDON Champlain	Professeur	En Poste
5.	DZEUFIET DJOMENI Paul Désiré	Professeur	En Poste
6.	ESSOMBA née NTSAMA MBALA	Professeur	*Vice Doyen/FMSB/UYI*
7.	FOMENA Abraham	Professeur	En Poste
8.	KEKEUNOU Sévilor	Professeur	En poste
9.	NJAMEN Dieudonné	Professeur	En poste
10.	NJIOKOU Flobert	Professeur	En Poste
11.	NOLA Moïse	Professeur	En poste
12.	TAN Paul VERNYUY	Professeur	En poste
13.	TCHUEM TCHUENTE Louis Albert	Professeur	*Inspecteur de service Coord.Progr./MINSANTE*
14.	ZEBAZE TOGOUET Serge Hubert	Professeur	En poste

15.	ALENE Désirée Chantal	Maître de Conférences	*Chef Service/ MINESUP*
16.	BILANDA Danielle Claude	Maître de Conférences	En poste
17.	DJIOGUE Séfirin	Maître de Conférences	En poste
18.	JATSA BOUKENG Hermine épse MEGAPTCHE	Maître de Conférences	En Poste
19.	LEKEUFACK FOLEFACK Guy B.	Maître de Conférences	En poste
20.	MBENOUN MASSE Paul Serge	Maître de Conférences	En poste
21.	MEGNEKOU Rosette	Maître de Conférences	En poste
22.	MONY Ruth épse NTONE	Maître de Conférences	En Poste
23.	NGUEGUIM TSOFACK Florence	Maître de Conférences	En poste
24.	NGUEMBOCK	Maître de Conférences	En poste
25.	TOMBI Jeannette	Maître de Conférences	En poste

26.	ATSAMO Albert Donatien	Chargé de Cours	En poste
27.	BASSOCK BAYIHA Etienne Didier	Chargé de Cours	En poste
28.	DONFACK Mireille	Chargée de Cours	En poste
29.	ESSAMA MBIDA Désirée Sandrine	Chargée de Cours	En poste
30.	ETEME ENAMA Serge	Chargé de Cours	En poste
31.	FEUGANG YOUMSSI François	Chargé de Cours	En poste
32.	GONWOUO NONO Legrand	Chargé de Cours	En poste
33.	GOUNOUE KAMKUMO Raceline	Chargée de Cours	En poste
34.	KANDEDA KAVAYE Antoine	Chargé de Cours	En poste
35.	KOGA MANG DOBARA	Chargé de Cours	En poste
36.	LEME BANOCK Lucie	Chargé de Cours	En poste
37.	MAHOB Raymond Joseph	Chargé de Cours	En poste
38.	METCHI DONFACK MIREILLE FLAURE EPSE GHOUMO	Chargé de Cours	En poste
39.	MOUNGANG Luciane Marlyse	Chargée de Cours	En poste
40.	MVEYO NDANKEU Yves Patrick	Chargé de Cours	En poste
41.	NGOUATEU KENFACK Omer Bébé	Chargé de Cours	En poste
42.	NJUA Clarisse Yafi	Chargée de Cours	*Chef Div. Uté Bamenda*
43.	NOAH EWOTI Olive Vivien	Chargée de Cours	En poste
44.	TADU Zephyrin	Chargé de Cours	En poste
45.	TAMSA ARFAO Antoine	Chargé de Cours	En poste
46.	YEDE	Chargé de Cours	En poste
47.	YOUNOUSSA LAME	Chargé de Cours	En poste

48.	AMBADA NDZENGUE GEORGIA ELNA	Assistante	En poste
49.	FOKAM Alvine Christelle Epse KEGNE	Assistante	En poste
50.	MAPON NSANGOU Indou	Assistant	En poste
51.	NWANE Philippe Bienvenu	Assistant	En poste

3- DÉPARTEMENT DE BIOLOGIE ET PHYSIOLOGIE VÉGÉTALES (BPV) (33)

1.	AMBANG Zachée	Professeur	*Chef DAARS /UYII*
2.	DJOCGOUE Pierre François	Professeur	En poste
3.	MBOLO Marie	Professeur	En poste
4.	MOSSEBO Dominique Claude	Professeur	En poste
5.	YOUMBI Emmanuel	Professeur	*Chef de Dpt*
6.	ZAPFACK Louis	Professeur	En poste

7.	ANGONI Hyacinthe	Maître de Conférences	En poste
8.	BIYE Elvire Hortense	Maître de Conférences	En poste
9.	MALA Armand William	Maître de Conférences	En poste
10.	MBARGA BINDZI Marie Alain	Maître de Conférences	*DAAC /UDla*
11.	NDONGO BEKOLO	Maître de Conférences	*CE / MINRESI*
12.	NGODO MELINGUI Jean Baptiste	Maître de Conférences	En poste
13.	NGONKEU MAGAPTCHE E. L.	Maître de Conférences	*CT / MINRESI*
14.	TONFACK Libert Brice	Maître de Conférences	En poste
15.	TSOATA Esaïe	Maître de Conférences	En poste
16.	ONANA JEAN MICHEL	Maître de Conférences	En poste

17	DJEUANI Astride Carole	Chargé de Cours	En poste
18	GOMANDJE Christelle	Chargée de Cours	En poste
19	GONMADGE CHRISTELLE	Chargée de Cours	En poste
20	MAFFO MAFFO Nicole Liliane	Chargé de Cours	En poste
21	MAHBOU SOMO TOUKAM. Gabriel	Chargé de Cours	En poste
22	NGALLE Hermine BILLE	Chargée de Cours	En poste
23	NNANGA MEBENGA Ruth Laure	Chargé de Cours	En poste
24	NOUKEU KOUAKAM Armelle	Chargé de Cours	En poste
25	NSOM ZAMBO EPSE PIAL ANNIE CLAUDE	Chargé de Cours	*En détachement/UNESCO MALI*
26	GODSWILL NTSOMBOH NTSEFONG	Chargé de Cours	En poste
27	KABELONG BANAHO Louis-Paul-Roger	Chargé de Cours	En poste
28	KONO Léon Dieudonné	Chargé de Cours	En poste
29	LIBALAH Moses BAKONCK	Chargé de Cours	En poste
30	LIKENG-LI-NGUE Benoit C	Chargé de Cours	En poste
31	TAEDOUNG Evariste Hermann	Chargé de Cours	En poste
32	TEMEGNE NONO Carine	Chargé de Cours	En poste
33	MANGA NDJAGA JUDE	Assistant	En poste

4- DÉPARTEMENT DE CHIMIE INORGANIQUE (CI) (31)

1.	GHOGOMU Paul MINGO	Professeur	*Ministre Chargé deMiss.PR*
2.	NANSEU Njiki Charles Péguy	Professeur	En poste
3.	NDIFON Peter TEKE	Professeur	*CT MINRESI*

4.	NENWA Justin	Professeur	En poste
5.	NGOMO Horace MANGA	Professeur	*Vice Chancelor/UB*
6.	NJIOMOU C. épse DJANGANG	Professeur	En poste
7.	NJOYA Dayirou	Professeur	En poste

8.	ACAYANKA Elie	Maître de Conférences	En poste
9.	EMADACK Alphonse	Maître de Conférences	En poste
10.	KAMGANG YOUBI Georges	Maître de Conférences	En poste
11.	KEMMEGNE MBOUGUEM Jean C.	Maître de Conférences	En poste
12.	KENNE DEDZO GUSTAVE	Maître de Conférences	En poste
13.	MBEY Jean Aime	Maître de Conférences	En poste
14.	NDI NSAMI Julius	Maître de Conférences	*Chef de Département*
15.	NEBAH Née NDOSIRI Bridget NDOYE	Maître de Conférences	*Sénatrice/SENAT*
16.	NYAMEN Linda Dyorisse	Maître de Conférences	En poste
17.	PABOUDAM GBAMBIE AWAWOU	Maître de Conférences	En poste
18.	TCHAKOUTE KOUAMO Hervé	Maître de Conférences	En poste
19.	BELIBI BELIBI Placide Désiré	Maître de Conférences	*Chef Service/ ENS Bertoua*
20.	CHEUMANI YONA Arnaud M.	Maître de Conférences	En poste
21.	KOUOTOU DAOUDA	Maître de Conférences	En poste

22.	MAKON Thomas Beauregard	Chargé de Cours	
23.	NCHIMI NONO KATIA	Chargé de Cours	En poste
24.	NJANKWA NJABONG N. Eric	Chargé de Cours	En poste
25.	PATOUOSSA ISSOFA	Chargé de Cours	En poste
26.	SIEWE Jean Mermoz	Chargé de Cours	En poste

27.	BOYOM TATCHEMO Franck W.	Assistant	En Poste

5- DÉPARTEMENT DE CHIMIE ORGANIQUE (CO) (38)			
1.	Alex de Théodore ATCHADE	Professeur	*DEPE /Univ. Bertoua*
2.	DONGO Etienne	Professeur	*Vice-Doyen/FSE/UYI*
3.	MKOUNGA Pierre	Professeur	En poste
4.	NGOUELA Silvère Augustin	Professeur	*Chef de Département UDS*
5.	PEGNYEMB Dieudonné Emmanuel	Professeur	*Recteur UBertoua/ Chef de Département*
6.	MBAZOA née DJAMA Céline	Professeur	En poste

7.	AMBASSA Pantaléon	Maître de Conférences	En poste
8.	EYONG Kenneth OBEN	Maître de Conférences	*Directeur/ ENSET Bambili*
9.	FOTSO WABO Ghislain	Maître de Conférences	En poste
10.	KAMTO Eutrophe Le Doux	Maître de Conférences	En poste
11.	KENMOGNE Marguerite	Maître de Conférences	En poste
12.	MVOT AKAK CARINE	Maître de Conférences	En poste

13.	NGO MBING Joséphine	Maître de Conférences	*Chef de Cellule MINRESI*
14.	NGONO BIKOBO Dominique Serge	Maître de Conférences	*C.E.A/ MINESUP*
15.	NOTE LOUGBOT Olivier Placide	Maître de Conférences	*DAAC/Uté Bertoua*
16.	NOUNGOUE TCHAMO Diderot	Maître de Conférences	En poste
17.	OUAHOUO WACHE B. M.	Maître de Conférences	En poste
18.	TABOPDA KUATE Turibio	Maître de Conférences	En poste
19.	TAGATSING FOTSING Maurice	Maître de Conférences	En poste
20.	ZONDEGOUMBA Ernestine	Maître de Conférences	En poste

21.	NGNINTEDO Dominique	Chargé de Cours	En poste
22.	NGOMO Orléans	Chargée de Cours	En poste
23.	SIELINOU TEDJON Valérie	Chargé de Cours	En poste
24.	MESSI Angélique Nicolas	Chargé de Cours	En poste
25.	TCHAMGOUE Joseph	Chargé de Cours	En poste
26.	TSAMO TONTSA Armelle	Chargé de Cours	En poste
27.	TSEMEUGNE Joseph	Chargé de Cours	En poste
28.	MUNVERA MFIFEN Aristide	Chargé de Cours	En poste
29.	NONO NONO Éric Carly	Chargé de Cours	En poste
30.	OUETE NANTCHOUANG J. L.	Chargé de Cours	En poste
31.	TSAFFACK Maurice	Chargé de Cours	En poste

32.	NDOGO ETEME Olivier	Assistant	En poste
33.	Chimeze Valery	Assistant	En poste

6- DÉPARTEMENT D'INFORMATIQUE (IN) (22)

1.	ATSA ETOUNDI Roger	Professeur	*Chef Div.MINESUP*
2.	FOUDA NDJODO Marcel L.	Professeur	*Chef Dpt ENS/Chef IGA.MINESUP*

3.	NDOUNDAM Réné	Maître de Conférences	En poste
4.	TSOPZE Norbert	Maître de Conférences	En poste

5.	ABESSOLO ALO'O Gislain	Chargé de Cours	*Sous-Directeur/MINFOPRA*
6.	AMINOU Halidou	Chargé de Cours	*Chef de Département*
7.	DJAM Xaviera YOUH – KIMBI	Chargé de Cours	En Poste
8.	DOMGA KOMGUEM Rodrigue	Chargé de Cours	En poste
9.	EBELE Serge Alain	Chargé de Cours	En poste
10.	HAMZA Adamou	Chargé de Cours	En poste
11.	JIOMEKONG AZANZI Fidel	Chargé de Cours	En poste
12.	KOUOKAM KOUOKAM E. A.	Chargé de Cours	En poste
13.	MELATAGIA YONTA Paulin	Chargé de Cours	En poste
14.	MONTHE DJIADEU Valery M.	Chargé de Cours	En poste

15.	OLE OLE Daniel Claude Delort	Chargé de Cours	*Dir. adjoint ENSET. Ebolowa*
16.	TAPAMO Hyppolite	Chargé de Cours	En poste

17.	BAYEM Jacques Narcisse	Assistant	En poste
18.	EKODECK Stéphane Gaël Raymond	Assistant	En poste
19.	MAKEMBE. S . Oswald	Assistant	En poste
20.	MESSI NGUELE Thomas	Assistant	En poste
21.	NKONDOCK. MI. BAHANACK.N.	Assistant	En poste
22.	NZEKON NZEKO'O ARMEL JACQUES	Assistant	En poste

7- DÉPARTEMENT DE MATHÉMATIQUES (MA) (31)

1.	AYISSI Raoult Domingo	Professeur	**Chef de Département**
2.	EMVUDU WONO Yves S.	Professeur	*Inspecteur MINESUP*
3.	KIANPI Maurice	Maître de Conférences	En poste
4.	MBANG Joseph	Maître de Conférences	En poste
5.	MBEHOU Mohamed	Maître de Conférences	En poste
6.	MBELE BIDIMA Martin Ledoux	Maître de Conférences	En poste
7.	NOUNDJEU Pierre	Maître de Conférences	*Chef Service des Programmes & Diplômes/FS/UYI*
8.	TAKAM SOH Patrice	Maître de Conférences	En poste
9.	TCHAPNDA NJABO Sophonie B.	Maître de Conférences	*Directeur/AIMS Rwanda*
10.	TCHOUNDJA Edgar Landry	Maître de Conférences	En poste

11.	AGHOUKENG JIOFACK Jean Gérard	Chargé de Cours	*Chef Cellule MINEPAT*
12.	BOGSO ANTOINE MARIE	Chargé de Cours	En poste
13.	CHENDJOU Gilbert	Chargé de Cours	En poste
14.	DJIADEU NGAHA Michel	Chargé de Cours	En poste
15.	DOUANLA YONTA Herman	Chargé de Cours	En poste
16.	KIKI Maxime Armand	Chargé de Cours	En poste
17.	MBAKOP Guy Merlin	Chargé de Cours	En poste
18.	MENGUE MENGUE David Joe	Chargé de Cours	*Chef Dpt /ENS Uté Maroua*
19.	NGUEFACK Bernard	Chargé de Cours	En poste
20.	NIMPA PEFOUKEU Romain	Chargée de Cours	En poste
21.	OGADOA AMASSAYOGA	Chargée de Cours	En poste
22.	POLA DOUNDOU Emmanuel	Chargé de Cours	*En stage*
23.	TCHEUTIA Daniel Duviol	Chargé de Cours	En poste
24.	TETSADJIO TCHILEPECK M. E.	Chargé de Cours	En poste

25.	BITYE MVONDO Esther Claudine	Assistante	En poste
26.	FOKAM Jean Marcel	Assistant	En poste
27.	LOUMNGAM KAMGA Victor	Assistant	En poste
28.	MBATAKOU Salomon Joseph	Assistant	En poste
29.	MBIAKOP Hilaire George	Assistant	En poste
30.	MEFENZA NOUNTU Thiery	Assistant	En poste
31.	TENKEU JEUFACK Yannick Léa	Assistant	En poste

8- DÉPARTEMENT DE MICROBIOLOGIE (MIB) (22)

1.	ESSIA NGANG Jean Justin	Professeur	*Chef de Département*
2.	NYEGUE Maximilienne Ascension	Professeur	*VICE-DOYEN / DSSE/FS/UYI*
3.	NWAGA Dieudonné M.	Professeur	En poste

4.	ASSAM ASSAM Jean Paul	Maître de Conférences	En poste
5.	BOUGNOM Blaise Pascal	Maître de Conférences	En poste
6.	BOYOMO ONANA	Maître de Conférences	En poste
7.	KOUITCHEU MABEKU Epse KOUAM Laure Brigitte	Maître de Conférences	En poste
8.	RIWOM Sara Honorine	Maître de Conférences	En poste
9.	SADO KAMDEM Sylvain Leroy	Maître de Conférences	En poste

10.	BODA Maurice	Chargé de Cours	En position d'absence irrégulière
11.	ESSONO OBOUGOU G. G.	Chargé de Cours	En poste
12.	NJIKI BIKOÏ Jacky	Chargée de Cours	En poste
13.	TCHIKOUA Roger	Chargé de Cours	En poste
14.	ESSONO Damien Marie	Chargé de Cours	En poste
15.	LAMYE Glory MOH	Chargé de Cours	En poste
16.	MEYIN A EBONG Solange	Chargée de Cours	En poste
17.	NKOUDOU ZE Nardis	Chargé de Cours	En poste
18.	TAMATCHO KWEYANG Blandine Pulchérie	Chargée de Cours	En poste
19.	TOBOLBAÏ Richard	Chargé de Cours	En poste

20.	MONI NDEDI Esther Del F.	Assistante	En poste
21.	NKOUE TONG ABRAHAM	Assistant	En poste
22.	SAKE NGANE Carole Stéphanie	Assistante	En poste

9. DEPARTEMENT DE PYSIQUE(PHY) (43)

1.	BEN- BOLIE Germain Hubert	Professeur	En poste
2.	DJUIDJE KENMOE épouse ALOYEM	Professeur	En poste
3.	EKOBENA FOUDA Henri Paul	Professeur	*Vice-Recteur. Uté Ngaoundéré*
4.	ESSIMBI ZOBO Bernard	Professeur	En poste
5.	NANA ENGO Serge Guy	Professeur	En poste
6.	NANA NBENDJO Blaise	Professeur	En poste
7.	NDJAKA Jean Marie Bienvenu	Professeur	*Chef de Département*
8.	NJANDJOCK NOUCK Philippe	Professeur	En poste
9.	NOUAYOU Robert	Professeur	En poste
10.	PEMHA Elkana	Professeur	En poste
11.	SAIDOU	Professeur	*Chef de centre/IRGM/MINRESI*
12.	TABOD Charles TABOD	Professeur	*Doyen FSUniv/Bda*
13.	TCHAWOUA Clément	Professeur	En poste
14.	WOAFO Paul	Professeur	En poste
15.	ZEKENG Serge Sylvain	Professeur	En poste

16.	BIYA MOTTO Frédéric	Maître de Conférences	*DG/HYDRO Mekin*
17.	BODO Bertrand	Maître de Conférences	En poste
18.	ENYEGUE A NYAM épse	Maître de Conférences	En poste
19.	EYEBE FOUDA Jean sire	Maître de Conférences	En poste
20.	FEWO Serge Ibraïd	Maître de Conférences	En poste
21.	HONA Jacques	Maître de Conférences	En poste
22.	MBINACK Clément	Maître de Conférences	En poste
23.	MBONO SAMBA Yves C. U.	Maître de Conférences	En poste
24.	NDOP Joseph	Maître de Conférences	En poste
25.	SIEWE SIEWE Martin	Maître de Conférences	En poste
26.	SIMO Elie	Maître de Conférences	En poste
27.	VONDOU DerbetiniAppolinaire	Maître de Conférences	En poste
28.	WAKATA née BEYA Annie	Maître de Conférences	*Directeur/ENS/UYI*

29.	ABDOURAHIMI	Chargé de Cours	En poste
30.	CHAMANI Roméo	Chargé de Cours	En poste
31.	EDONGUE HERVAIS	Chargé de Cours	En poste
32.	FOUEDJIO David	Chargé de Cours	*Chef Cell. MINADER*
33.	MELI'I Joelle Larissa	Chargée de Cours	En poste
34.	MVOGO ALAIN	Chargé de Cours	En poste
35.	WOULACHE Rosalie Laure	Chargée de Cours	*Absente depuis Janvier 2022*
36.	AYISSI EYEBE Guy François Valérie	Chargé de Cours	En poste
37.	DJIOTANG TCHOTCHOU Lucie Angennes	Chargée de Cours	En poste
38.	OTTOU ABE Martin Thierry	Chargé de Cours	En poste

39.	TEYOU NGOUPOU Ariel	Chargé de Cours	En poste

40.	KAMENI NEMATCHOUA Modeste	Assistant	En poste
41.	LAMARA Maurice	Assistant	En poste
42.	NGA ONGODO Dieudonné	Assistant	En poste
43.	WANDJI NYAMSI William	Assistant	En poste

10- DÉPARTEMENT DE SCIENCES DE LA TERRE (ST) (42)

1.	BITOM Dieudonné-Lucien	Professeur	*Doyen / FASA / UDs*
2.	FOUATEU Rose épse YONGUE	Professeur	En poste
3.	NDAM NGOUPAYOU Jules-Remy	Professeur	En poste
4.	NDJIGUI Paul Désiré	Professeur	*Chef de Département*
5.	NGOS III Simon	Professeur	En poste
6.	NKOUMBOU Charles	Professeur	En poste
7.	NZENTI Jean-Paul	Professeur	En poste

8.	ABOSSOLO née ANGUE Monique	Maître de Conférences	*Vice-Doyen / DRC*
9.	BISSO Dieudonné	Maître de Conférences	*Directeur/Projet Barrage Memve'ele*
10.	EKOMANE Emile	Maître de Conférences	En poste
11.	FUH Calistus Gentry	Maître de Conférences	*Sec. D'Etat/MINMIDT*
12.	GANNO Sylvestre	Maître de Conférences	En poste
13.	GHOGOMU Richard TANWI	Maître de Conférences	*Chef de Département /Uté Maroua*
14.	MOUNDI Amidou	Maître de Conférences	CT/ MINIMDT
15.	NGO BIDJECK Louise Marie	Maître de Conférences	En poste
16.	NGUEUTCHOUA Gabriel	Maître de Conférences	CEA/MINRESI
17.	NJILAH Isaac KONFOR	Maître de Conférences	En poste
18.	NYECK Bruno	Maître de Conférences	En poste
19.	ONANA Vincent Laurent	Maître de Conférences	*Chef service Maintenance & du Matériel/UYII*
20.	TCHAKOUNTE J. épse NUMBEM	Maître de Conférences	*Chef.cell / MINRESI*
21.	TCHOUANKOUE Jean-Pierre	Maître de Conférences	En poste
22.	TEMGA Jean Pierre	Maître de Conférences	En poste
23.	YENE ATANGANA Joseph Q.	Maître de Conférences	*Chef Div. /MINTP*
24.	ZO'O ZAME Philémon	Maître de Conférences	*DG/ART*

25.	ANABA ONANA Achille Basile	Chargé de Cours	En poste
26.	BEKOA Etienne	Chargé de Cours	En poste

27.	ELISE SABABA	Chargé de Cours	En poste
28.	ESSONO Jean	Chargé de Cours	En poste
29.	EYONG JOHN TAKEM	Chargé de Cours	En poste
30.	MAMDEM TAMTO L. E.	Chargé de Cours	En poste
31.	MBESSE CECILE OLIVE	Chargée de Cours	En poste
32.	MBIDA YEM	Chargé de Cours	En poste
33.	METANG Victor	Chargé de Cours	En poste
34.	MINYEM Dieudonné	Chargé de Cours	*CD/ Uté Maroua*
35.	NGO BELNOUN Rose Noël	Chargée de Cours	En poste
36.	NOMO NEGUE Emmanuel	Chargé de Cours	En poste
37.	NTSAMA ATANGANA Jacqueline	Chargé de Cours	En poste
38.	TCHAPTCHET TCHATO De P.	Chargé de Cours	En poste
39.	TEHNA Nathanaël	Chargé de Cours	En poste
40.	FEUMBA Roger	Chargé de Cours	En poste
41.	MBANGA NYOBE Jules	Chargé de Cours	En poste

42.	NGO'O ZE ARNAUD	Assistant	En poste

Répartition chiffrée des Enseignants de la Faculté des Sciences de l'Université de Yaoundé I

NOMBRE D'ENSEIGNANTS					
DÉPARTEMENT	**Professeurs**	**Maîtres de Conférences**	**Chargés de Cours**	**Assistants**	**Total**
BCH	8 (00)	14 (10)	15 (05)	02 (01)	**39 (16)**
BPA	14 (01)	11 (07)	22 (07)	04 (02)	**51 (17)**
BPV	06 (01)	10(01)	16 (09)	01 (00)	**33 (11)**
CI	09(01)	14(04)	08 (01)	00 (00)	**31 (06)**
CO	07 (01)	19 (05)	12 (03)	02 (00)	**38(09)**
IN	02 (00)	02 (00)	12 (01)	06 (00)	**22 (01)**
MAT	02 (00)	08 (00)	14 (01)	07 (01)	**31 (02)**
MIB	03 (01)	06 (02)	10 (03)	03 (02)	**22 (08)**
PHY	15 (01)	13 (02)	11 (03)	04 (00)	**43 (06)**
ST	07 (01)	16 (03)	18 (04)	01 (00)	**42(08)**
Total	**73 (07)**	**113 (34)**	**135 (36)**	**32 (07)**	**352 (84)**

Soit un total de **353 (84)** dont :

- Professeurs **73 (07)**
- Maîtres de Conférences **113 (34)**
- Chargés de Cours **137 (37)**
- Assistants **29 (01)**

( ) = Nombre de Femmes **84**

DEDICATION

To my:

Biological parents; BONGNAVTI Theresia of blessed memory

And

YUWONG Gaius.

And to the Garden for Education and Healing, Bamenda.

ACKNOWLEDGEMENTS

This work was done through inputs from several directions which positively influenced this achievement. I am grateful even to those whose names are not particularly mentioned.

- I wish to thank **Professor FOLEFOC NGOSONG Gabriel**, for receiving me into his research team, allowing me to accomplish this work and above all, for his fatherly care during the most challenging moments of the work.
- I wish to appreciate **Professor EYONG OBEN Kenneth**, to whom I owe deep gratitude for initiating me into research, the confidence he placed in me, for his advice, constant encouragement, availability, rigor throughout the laboratory work period and for providing me all the necessary facilities.
- I extend my heartfelt gratitude to my host supervisor, **Professor MUHAMMAD Shaiq Ali,** for his excellent supervision, day to day encouragement and guidance which I received throughout my research stay at the International Center for Chemical and Biological Sciences (ICCBS), Pakistan.
- I am thankful to **Professor PEGNYEMB Dieudonné Emmanuel,** Head of the Department of Organic Chemistry, University of Yaounde I for his several advices and encouragement as well as his devotion in managing the Department.
- I am thankful to my dear friend and Bachelor level classmate back then at the University of Buea, **Dr**. **NZUWAH Nziko Vincent de Paul,** Assistant Professor at the Department of Chemistry, Hampton University-USA, for running some of the NMR analyses.
- I do appreciate my laboratory team mates; **Dr. SIDJUI Lazare, Dr. BAIRY Guérison, Dr. KETSEMEN Hervé, YEMBACK Pierre, OMDIM Irène, NYEMECK Suzanne, YURI Paul, MESSOMO Joseph Ghislain and TSAMO NOUMEDEM Cynthia** for their moral support, constructive criticism and availability to assist in one way or the other and most especially the scientific thoughts we shared in a warm environment.
- I am grateful to TWAS-ICCBS for the Post-Graduate fellowship offered to me during my PhD research period.
- I thank our collaborators at; Bahria University-Pakistan, Baylor University-USA and University of Johannesburg-South Africa for carrying out some of our analyses.

- I am grateful to **Professor Jeremiah GASSENMITH** for the opportunity offered to me at the end of my Ph.D to have a contact with his team at the University of Texas at Dallas which greatly opened my thoughts to the realities of advanced science and the use of mordern laboratory techniques. I thank his student **Miss Nancy TRAN** whom I met at the American Chemical Society Spring meeting 2025 presenting a work similar to mine, for doing all to link me up to their team and for the time we spent at the University of Dallas.
- I thank the Ministry of Secondary Education in Cameroon for the study leave granted to me to permit me carry on part of my studies in Pakistan under the TWAS-ICCBS Fellowship program.
- I thank the Ministry of Higher Education in Cameroon, the Presbyterian Church in Camerooon - Nsimeyong Congregation and the Bui Family Union USA for financial support at some moment of my research work.
- I am grateful to all the platforms through which I received professional and holistic mentorship, and adequate training during the period of my research project especially during the very challenging moments. These are; the Higher Women's consortium, PCC Nsimeyong Educational Mentoring platform, the American Society of Tropical Medicine and Hygiene, the American Society for Microbiology, the American Chemical Society, the American society of Pharmacognosy and the American Association for Cancer Research.
- I particularly thank some HIGHER Women mentors, **Professor LEKE Rose FOMBAN GANA, Professor Judith NDONGO TORIMIRO, Professor DJUIJE Marceline NGOUONOUE, Dr. KWEDI Sylvie NOLNA** and **Dr. AMANI Adidja,** for helping me in unique ways to meet my goals especially towards the end of my PhD research cycle.
- My profound gratitude goes to my Bachelor level mates from the University of Buea; **Dr. NDONTSA Elizabeth, Dr. NJUMA Olive Ewule, Dr. DICKMU Gerald, Dr. NUBED Lina and Dr. NEH Louiza Bako** who set the pace in completing their PhD studies years ago, challenging me positively to stay on through their encouraging words.
- I thank my Masters level friends; **Dr. TARKWA Jean Baptiste, Dr. NZIAKOU Yannick, Dr. ACHE Roland Ndifor, Dr. CHI Godloves FRU, Dr. AKONGMWI Mirabel, Dr. MAZA Hermine, Dr. AMAAH Colette, Dr. HAPPI MOUTHE**

Gervais, Dr. EMADE Karine KWENE, Dr. ABE Noah Pierre and Miss TIWA MADO Sandrine and **Mr. BALEBA Roger** for the moments we shared together and their great determination which inspired me to stay on.

- Special thanks to my batchmates from *ENS* Yaoundé; **Dr. TCHAMGOUE Joseph, Dr. MBOUOPDA POUPI Albert Brandt, Dr. FOTSING NKUIGUE Patrick, Dr. KAGHO KENOU Donald Ulrich, Dr. YANKE MBOKANA Jenna Geralde** and **Dr. ESSOMA Jean Serge,** for braving through the challenges in our context to excel and for their sincere encouragement.
- I owe deep thanks to my seniors; **Dr. TENDE Renz, Dr, SONE Charles, Dr. NKAM Giftus NTAMBO, Dr. CHEWACHONG Godwill MIH, Dr. NEBA Ritley** and **Dr. NKAFU Germaine**, for setting the pace for me to follow on and especially for their individual concern for my educational progress.
- I am grateful to the Cameroonians with whom I lived in Pakistan as a family during my research stay at ICCBS; **Professor FONGANG FOTSING Yannick Stephane, Professor SOH Désiré, Dr. Alfred NGENGE TAMFU, Dr. FEUMO FEUSSO Hermann Marius, Dr. BISSIM Samuel Magloire, Dr. MUNVERA MFIFEN Aristide, Dr. TSOPMEJIO Jean Paul, Dr. TABEKOUENG Georges Bellier, Dr. Zeukang Rostanie and Dr. AKOSONG Emmanuel,** for setting the pace and for all their encouragement when I almost gave up.
- I thank **Dr. USO Excellence OFFIONG** for his timely intervention at the last phase of my PhD cycle. I am indented to his qualitative and quantitative investment in my life in diverse dimensions.
- I thank my colleagues in the Government Bilingual High Schools I have served as chemistry teacher; Foumban and Limbe for their kind collaboration.
- My sincere thanks go to members of the World changers Association with whom I shared my dreams especially; **Engineer KUM KUMBONG Yandy, Engineer LUKONG Terence KIBULA, Dr. Leonard NGARKA, Dr. NGANYU TANYU Derick, Miss WONG Mariette, Dr. SIEWE Joseph, Dr. NFOR Leonard, Dr. BIHNWI Comfort, Dr. MUNANG Yvonne, Dr. TOH Bemsibom, Dr. Emma WOKS, Dr. AYUKETAH Pearl, Dr. NGO BAMA Solange, Dr. EKWOGE Hilda TONGEH, Mrs. ATEH Onorine, Mrs NFOR Odette, Dr. EBUDE Yolande, Dr. TEGOMOH Brian, Engineer TANYI Randall, Dr. TANSAH Vanessa, Dr.**

MUTIA KEHWALLAH and **Dr. ATAH Jude,** for their encouragement and especially for believing in my research aspirations.

- I thank all the Pastors who served in the Presbyterian Church in Camerooon-Nsimeyong Congregation during the period of my studies for their counsel and support throughout my study period. I particularly appreciate; **Rev. MASOK BASSAM Emmanuel**, **Rev. MBINDA Bulex**, **Rev. KANG Denis**, **Rev. MOTOPOH Alfred ESIMAI**, **Rev. BERNDZEH Theresia**, **Rev. ENOW Michael AGBOR** and **Rev. MBAKWA Juliette** amongst others, for the committed moral support through the challenging times.
- I greatly appreciate the coordinators of the Diakonia committee of PCC Nsimeyong; **Dr. NKELE NDEKI NGOH** and **Dr. NGU Pius MOKOM** and all the committee members for their enormous support towards my welfare throughout the study period.
- I thank the members of the session of PCC Nsimeyong with whom I served within the period 2019 to 2024 led by the chairman, **Emeritus Elder CHE Philip AMABO** and his Vice, **Elder ACHU Eunice**, for their support in every dimension.
- I owe special thanks to my congregational fathers and mothers of PCC Nsimeyong; **Professor MBU Robinson, Professor AGWARA Moise ONDOH**, **Mr. ENOW OROCK Stephen, Chief Dr. ORUH Julius, Senator Elizabeth Regina MUNDI, Commissioner TANG Lawrence, Elder/Mrs. TAKANG Collette, Mrs. YUFENYUY Anastasia** and **Mrs. CHANG Deborah,** for their unquantifiable support.
- My gratitude goes to my uncles, aunts and their spouses; **Rev. Sr. DINYUY Ann, Mr. NGWANG Didacus, Dr. VERLA Vincent, Mr. YEFON Henry KPUDIY, Mr. KIMAH Constantine, Rev. Dr. NYUYKI Peter SIYSI, Miss BONGNYANG Eveline, Mrs. GHAM SUIRU Alice** and **Mrs**. **FITIKEM Evera** for their countless support throughout these numerous years of research and for the responsibilities they shouldered, especially for the attentive care given to my beloved father while I was out on studies.
- I thank my brothers and cousins; **Rev/Fr. Francline BANADZEM JAVLON, DINDZEE, Mr. MYENNE Hanson**, **Dr. /Mrs. SINYUY Geraldine, Mr. NYUYBATI Augustus, Mr. NDZEBEME Pilate, Rev. NDOFOR Theresia, Mr. YIVEN Divine, Mr. WIRKOM Mark, Mrs. LAMOH Nicoline, Mrs. JAILA**

Shalom, Miss VERLA Joyce, and **Miss BONGKIYNYUY Nancy** for their encouragement during the difficult moments.

- I owe profound thanks to my friends and well-wishers of PCC Nsimeyong congregation; **Mgr. TEKE Seraphine, Miss CHANA Blanch, Mr. GARA Andreas TAWUM, Dr. & Mrs. AWAH Laive, Dr.&Dr./Mrs. WALINJOM Joshua, Dr. & Mrs. AGBOR OBEN Emmanuel, Mr./Mrs. ADIG Emmanuel, Mr./Mrs. KAH Dickson, Mr./Mrs. FORSAH Clement, Miss MAFOR Daisy, Miss NGEGA Vanessa, Mr./Mrs. FORSAH Clement** and **Mr. MBAH Emmanuel FONDJINAM,** for their support during the challenging moments.
- I very deeply thank amongst many others, the following persons with whom I shared a close fellowship towards the last year of my PhD; **Miss DEDEH Marie, Mr. TEH Hope, Miss KENG Grasida, Miss LAISIN Clotild, Miss NGWEY Penanje, Miss UNGITOH Carine, Miss TANI Glory, Miss LENDZE Verina, Mr. ZAOLEFACK Emmanuel, Miss BINGMEH Harriet, Miss WACHEE Stephanie and Miss BEI Edith,** for their support and encouragement.

TABLE OF CONTENTS

LIST OF ABREVIATIONS AND SYMBOLS

CI	**:**	Confidence Interval
COSY	**:**	Correlation Spectroscopy
d	**:**	Doublet
dd	**:**	Doublet of doublet
DEPT	**:**	Distortionless Enhancement by Polarisation Transfer
DMSO	**:**	Dimethylsulfoxide
HER 2	**:**	Human Epidermal Growth Factor Receptor 2
HETCOR	**:**	Heteronuclear correlation
HMBC	**:**	Hetenonuclear Multiple Bond Correlation
HSQC	**:**	Heteronuclear Single Quantum Correlation
IC	**:**	Intervale de confiance
IC_{50}	**:**	Inhibition concentration at 50 %
IR	**:**	Infrared Spectroscopy
LC-MS		Liquid Chromatography Mass Spectrometry
m	**:**	Multiplet
MS	**:**	Mass Spectrometry
q	**:**	Quadruplet
R.M.S.D.	**:**	Root Mean Square Deviation
TNBC	**:**	Triple Negative Breast Cancer
s	**:**	Singlet
t	**:**	Triplet
δ	**:**	Chemical shift
λ	**:**	Wavelength
MD	**:**	Molecular docking
∆G	**:**	Gibbs free energy

LIST OF FIGURES

LIST OF TABLES

LIST OF SCHEMES

ABSTRACT

The present work focuses on the chemical study of *Psorospermum guineense* and *Alstonia scholaris,* two medicinal plants used in the treatment of cancer from a rational approach, and associated carcinogenic processes such as tumor cell proliferation, differentiation, and apoptosis.

By means of various liquid phase chromatographic techniques such as Flash Chromatography, Column Chromatography (CC) and Thin Layer Chromatography (TLC), seventeen (17) compounds were isolated from the CH_2Cl_2/MeOH (1:1) extract of the twigs of *Psorospermum guineense* and the EtOH extract of the leaves of *Alstonia scholaris.* The structures of these compounds were determined by interpretation of their UV, IR, MS (EI-MS, ESI-MS and LC-MS), 1D (^{1}H, ^{13}C, DEPT) and 2D (HSQC, HMBC, ^{1}H -^{1}H COSY) NMR data and in some cases by comparison of their data with those reported in the literature or by comparative TLC with available authentic samples.

The phytochemical study of the leaves of *Alstonia scholaris* has resulted in the isolation and characterization of nine known compounds (three (03) triterpenes, two (02) alkaloids, one (01) phenyl propanoid and three (03) steroids), namely: betulin, α-amyrin acetate, mixture of β-sitosterol and stigmasterol, tetratriacontyl-trans-*p*-coumarate, ursolic acid, β-sitosterol glucoside, picralstonine and scholaricine. While, structures of purified compounds from the twigs of *Psorospermum guineense* (five (5) anthraquinones and three (03) triterpenes) were determined as 3-geranyloxyemodin, 3-β-fridelanol, 3-geranyloxyemodin anthrone, 2- geranylemodin, acetylvismione D, betulinic acid, ursolic acid and emodin.

Single crystal x-ray diffraction analysis was used to confirm the relative configuration and conformation of 3-geranyloxyemodin.

To introduce privilege medicinal scaffold, five (05) of these compounds (3-geranyloxyemodin, 2-geranylemodin, betulin, α-amyrin acetate and ursolic acid) were subjected to SeO_2 oxidation. Betulin and α-amyrin acetate under SeO_2 oxidation condition afforded new acrylaldehye derivatives. Betulin afforded betulin acrylaldehyde while α-amyrin acetate afforded lupeolacetate acrylaldehyde in an intriguing mechanism with the conversion of ursane to lupane scaffold. There was no reaction with ursolic acid meanwhile, the

ABSTRACT

compounds 3-geranyloxyemodin and 2-geranylemodin afforded two (02) major products each.

3-geranyloxyemodin afforded (2*E*,6*E*)-8-((4,5-dihydroxy-7-methyl-9,10-dioxo-9,10-dihydroanthracen-2-yl)oxy)-2,6-dimethylocta-2,6-dienal and 1,8-dihydroxy-3-(((2*E*,6*Z*)-8-hydroxy-3,7-dimethylocta-2,6-dien-1-yl)oxy)-6-methylanthracene-9,10-dione.

2-geranylemodin afforded (2*E*,6*E*)-2,6-dimethyl-8-(1,3,8-trihydroxy-6-methyl-9,10-dioxo-9,10-dihydroanthracen-2-yl)octa-2,6-dienal and 1,3,8-trihydroxy-2-((2*E*,6*Z*)-8-hydroxy-3,7-dimethylocta-2,6-dien-1-yl)-6-methylanthracene-9,10-dione.

All the six (o6) synthesized compounds were new drivatives.

Preliminary cytotoxicity assays against the triple negative (MDA-MB-231) breast cancer cell indicated that Ursolic acid was the most active amongst the isolated compounds, with an IC_{50} value of 9.88 µM and 95% CI of 9.03-10.5 µM. On the other hand, the transformed compound, lupeol acetate acryl aldehyde with the privilege α,β-unsaturated carbonyl scaffold showed an increase in activity against MDA MB 231 breast cancer cell line with an IC_{50} of 4.63 ± 0.09 µg/ml. To determine possible mode of action for these compounds, they were screened on some cancer targets; acetylvismione D exhibited best antioxidant activity (20.8 ± 0.15 µM), scholaricine exhibited best lipoxygenase inhibitory activity (15.2 ± 0.41 µM) which were all better compared to the reference drugs beta hydroxyl acid (BHA) (44.2 ± 0.07 µM) and baicalein (22.6 ± 0.08 µM) respectively. Betulin gave the best urease inhibition activity (29.5 ± 0.91 µM) whose IC_{50} value was slightly higher than that of the reference compound used thiourea (24.2± 0.09 µM). The plausible binding interactions between the tested compounds and the enzyme target lipoxygenase were predicted through molecular docking studies. These results reveal that H-bonding, dipole-dipole, Pi-Pi stacked were the most important interactions.

Keywords: *Psorospermum guineense* - *Alstonia scholaris* - cytotoxicity - lipoxygenase - molecular docking - betulin acrylaldehyde - lupeol acetate acryl aldehyde

RESUME

Le présent travail porte sur l'étude chimique de *Psorospermum guineense* et *Alstonia Scholaris*, deux plantes médicinales utilisées en pharmacopée traditionnelle pour traiter le cancer de manière rationnelle et les processus cancérigènes associés tels que la prolifération, la différenciation et l'apoptose des cellules tumorales.

Au total dix-sept (17) composés ont été isolés de l'extrait au CH_2Cl_2/MeOH (1:1) des tiges de *Psorospermum guineense* et de l'extrait éthanolique des feuilles d'*Alstonia scholaris* au moyen de techniques de chromatographie usuelles telles que la Chromatographie sur Colonne (CC) et la Chromatographie sur Couche Mince (CCM). Les structures de ces composés ont été déterminées par interprétation de leurs données UV, IR, MS (EI-MS, ESI-MS and LC-MS), RMN 1D (^{1}H, ^{13}C, DEPT) et 2D (HSQC, HMBC, COSY), par comparaison de leurs données avec celles rapportées dans la littérature ou par CCM comparative avec des échantillons authentiques disponibles.

L'étude phytochimique des feuilles d'*Alstonia scholaris* a conduit à l'isolement et caracterisation de neuf composés connus (trois (03) triterpènes, two (02) alkaloids, une (01) phenyl propanoide et trois (03) steroides) à savoir: bétuline, α-acétate d'amyrine, mélange de β-sitostérol et stigmastérol, tétratriacontyl-trans-*p*–coumarate, acide ursolique, β - sitostérol glucoside, picralstonine et schlolaricine. Alorsque, les structures des composé purifiés issus des brindilles de *Psorospermum guineense* (cinq (5) anthraquinones et six (06) triterpènes) *ont* été determiné comme étant 3-géranyloxyémodine, 3-β–fridelanol, 3-géranyloxyémodine anthrone, 2-géranylémodine, acétylvismione D, acide bétulinique, acide ursolique et émodine.

Une analyse par diffraction des rayons X sur monocristal a été utilisée pour confirmer la configuration et la conformation relatives du 3-geranyloxyemodin.

Pour introduire un squelette médicinal privilégié, cinq (05) de ces composés (3-géranyloxyémodine, 2- géranylémodine, bétuline, l'acétate d'α - amyrine et l'acide ursolique) ont été soumis à une oxydation par le dioxyde de sélénium (SeO_2). La bétuline et l'acétate d'α-amyrine dans ces conditions ont donné de nouveaux dérivés d'acrylaldéhyde. La bétuline a conduit à la bétuline acrylaldéhyde tandis que l'α - acétate d'amyrine a donné l'aldéhyde acrylique de lupéolacétate dans un mécanisme intrigant avec la conversion du squelette ursane au squelette lupane. La réaction avec l'acide ursolique n'a pas eu lieu tandisque les composés, 3- géranyloxyémodine et 2- géranylémodine ont fourni deux(2) derivés nouveaux chaqu'un.

RESUME

3-géranyloxyémodine a fourni (2*E*,6*E*)-8-((4,5-dihydroxy-7-méthyl-9,10-dioxo-9,10-dihydroanthracèn-2-yl)oxy)-2,6-diméthylocta-2,6-diénal et 1,8-dihydroxy-3-(((2*E*,6*Z*)-8-hydroxy-3,7-diméthylocta-2,6-dién-1-yl)oxy)-6-méthylanthracène-9,10-dione ;

2-géranylémodine a fourni (2*E*,6*E*)-2,6-diméthyl-8-(1,3,8-trihydroxy-6-méthyl-9,10-dioxo-9,10-dihydroanthracèn-2-yl)octa-2,6-diénal et 1,3,8-trihydroxy-2-((2*E*,6*Z*)-8-hydroxy-3,7-diméthylocta-2,6-dièn-1-yl)-6-méthylanthracène-9,10-dione.

Tous les six (06) composés synthésisés été les dérivés nouveaux.

Des tests de cytotoxicité préliminaires contre les cellules cancéreuses du sein MDA-MB-231 ont indiqué que l'acide ursolique était le plus actif parmi les composés isolés, avec une valeur IC_{50} de 9,88 μM et un IC à 95 % de 9,03-10,5 μM. D'autre part, le composé transformé, aldéhyde acrylique de lupéol acétate avec le groupe carbonyle α,β-insaturé a montré une augmentation de l'activité contre la lignée cellulaire de cancer du sein MDA MB 231 avec une IC_{50} de 4, 63 ± 0, 09 μg / ml. Afin de déterminer le mode d'action possible de ces composés, ils ont été criblés sur certaines cibles cancéreuses. L'acétylvismione D a présenté une meilleure activité inhibitrice de la lipoxygénase (19,8 ± 0,16) et une meilleure activité antioxydante (20,8 ± 0,15) par rapport aux médicaments de référence, la baicaléine (22,6 ± 0,08 μM) et l'acide bêta-hydroxylé (BHA) (44,2 ± 0,07) respectivement. Pour apporter une plus-value à l'activité inhibitrice du composé le plus actif (acétylvismione D) sur la lipoxygénase, nous avons effectué l'amarrage moléculaire ce qui nous a permis de déterminer les types d'interactions qui existe entre cette enzyme et ce composé. Les interactions de liaison plausibles entre les composés testés et la cible enzymatique, la lipoxygénase ont été prédit par des études d'amarrage moléculaires. Ces résultats ont montré que les liaisons hydrogènes, dipole-dipole, Pi-Pi a étaient les interactions les plus importants.

Mots-clés: *Psorospermum guineense* - *Alstonia scholaris* - diffraction des rayons X – cytotoxicité - lipoxygénase - amarrage moléculaire - bétuline acrylaldehyde - lupeolacétate acrylaldehyde

GENERAL INTRODUCTION

Cancer is one of the leading causes of mortality worldwide **(Kashetti, 2020)** with 18.1 million new cancer cases and 9.6 million deaths reported in 2021 **(WHO, 2021)**. It is characterized by irregular proliferation of malignant cells in a series of stages with different biochemical, molecular and cellular events **(Omara *et al*., 2020)**. Cancer is caused by both internal factors (such as mutations, hormones and immune conditions) and external factors like chemicals, radiation and infectious microorganisms **(Lieu *et al*., 2023)**. This could be attributed to changes in lifestyle such as smoking, unhealthy eating, lack of physical exercise and excessive consumption of alcohol **(Sanderson *et al*., 2009)**.

Breast cancer is the second most common cancer in women after lung cancer and a leading cause of death **(Kathryn *et al*., 2011)**. 6000 Cameroonian women died of cancer and the breast is the most affected with 2625 new cases recorded between 2010 and 2015 **(Zingue *et al*., 2021)**. Treatment of breat cancer involves chemotherapy using tamoxifen (**1**), radiotherapy or surgery. The treatment is costly, and resistance of tumor cells to the available antineoplastic drugs has exacerbated the cost **(WHO, 2021)**. New families of active compounds are needed especially from natural sources in order to decrease the risk of resistance.

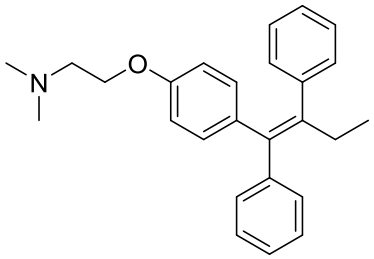

Tamoxifen **(1)**

The families Hypericaceae and Apocynaceae and most especially the species *Psorospermum guineense* and *Alstonia scholaris* are used in traditional medicine to treat different illnesses such as malaria and cancer **(Manjeshwar, 2011; Abhijit, 2011)**. These species are rich in secondary metabolities such as quinones, triterpenes and alkaloids but little information is known of the mode of action of these compounds in the treatment of cancer. *Psorospermum guineense* is typically found in the North west and center regions of Cameroon (**Nguemeving, *et al*., 2006)** meanwhile *Alstonia scholaris* is found in the middle East especially in Pakistan **(Atta-Ur-Rahmann *et al*., 1985)**.

In the search for anti-cancer agents, various classes of compounds including quinones, triterpenes and alkaloids have been isolated, chemically transformed by hemisythesis,

evaluated against a breast cancer cell line and molecular docking for mode of action studies carried out.

Our research question is; can compounds from the leaves of *Alstonia scholaris* and the twigs of *Psorospermum guineense* be potential anti cancer agents? We set as research hypothesis; Compounds from *Alstonia scholaris* and *Psorospermum guineense* can inhibit lipoxygenase and urease which are key enzymes that intervene in the process of cancer development.

The general objective of this work is to carry out phytochemical studies of *Psorospermum guineense* and *Alstonia scholaris*, structural modification of some isolated compounds, anti-breast cancer activity and molecular docking studies. The operational objectives are:

- To extract and isolate secondary metabolites from the crude extracts of the twigs of *Psorospermum guineense* and leaves of *Alstonia scholaris* using hexane and ethyl acetate;
- To characterize secondary metabolites isolated from the crude extracts of the twigs of *Psorospermum guineense* and leaves of *Alstonia scholaris* using NMR, IR, etc;
- To carry out structure modification of isolated compounds for structure activity relationship and to introduce privilege medicinal scaffold;
- To carry out biological activities (anti-breast cancer activity on triple negative (MDA MB-231) breast cancer cell lines, anti-oxidant and enzyme (lipoxygenase and urase) inhibition activities) and molecular docking studies of the of obtained compounds on the enzyme lipoxygenase for identification of binding interactions between ligand and target (enzyme).

This dissertation is presented in three parts which are; a literature review, the results obtained in the course of our work and finally the experimental section.

CHAPTER I: LITERATURE REVIEW

I.1 LITERATURE REVIEW ON *Alstonia scholaris* (Apocynaceae) and *Psorospermum guineense* (Hypericaceae)

I.1.1 Literature review on *Alstonia scholaris*

I.1.1.1 Apocynaceae family

The Apocynaceae family comprises of about 200 genera and 2000 species of tropical trees, shrubs and vines **(www.botany.hawaii.edu)**. The plants of this family often have milky or clear latex, the leaves are simple, usually opposite or whorled, the flowers often have a narrow tubular base and spreading lobes while the fruit is usually a berry, drupe or a follicle or pair of follicles, splitting to release the small seeds which usually have a coma of fine hairs to aid wind dispersal (**www.keys.lucidcentral.org**). Amongst the genera of this family is the *Alstonia* genus.

I.1.1.2 *Alstonia* genus

Plants of the genus *Alstonia* (Apocynaceae), which are usually shrubs or trees, are distributed over the tropical parts of Central America, Africa, and Asia, with the center of diversity in the Malesian region **(Tan *et al.*, 2010)**. It was named by Robert Brown in 1811, after Charles Alston (1685-1760), Professor of botany at Edinburgh from 1716-1760 **(Anupam *et al.*, 2015)**. *Alstonia* consists of about 40-60 species, native to tropical and subtropical Africa, central America, south east Asia, Polynesia and Australia **(Anupam *et al.*, 2015)**. Many *Alstonia* species are commercial Timber called *pule* or *pulai* in Indonesia and Malasia, which produced light timber **(Anupam *et al.*, 2015)**. Approximately 155 species belonging to the genus *Alstonia* **(Komal *et al.*, 2020)**. Amongst the species of this genus is the species *Alstonia scholaris*.

I.1.1.3 *Alstonia scholaris* species

Initially, this plant was named *Echites scholaris* in 1767 by Linnaeus. In 1811, Robert Brown named it as *Alstonia scholaris* in honor of Charles Alston, a renowned professor of botany and Materia Medica, at the University of Edinburgh (1740–1760). In 1841, Rhumphius gave the probable origin of name *scholaris* as the wood of this plant was used to make the writing slates for school children **(Komal *et al.*, 2020)**.

I.1.1.3.1 Botanical aspect of *Alstonia scholaris*

Alstonia scholaris is a tree that can reach heights of about 40–45 m when mature.

Bark and trunk: The bark is slightly cracked or corky with shades of brown or greyish brown outer bark and yellow to brown inner bark. It has the characteristic milky white latex, which freely flows out after a slight cut of bark. It has a fluted bole that can grow up to 10 m in the case of the larger trees **(Komal *et al.*, 2020)**.

Leaves: Leaves are organized in simple whorls (4–8 whorls) in the upper axils with secondary veins perpendicular to midrib. The shape of leaf is bluntly acuminate with elliptical or elliptically lanceolate, glabrous or sparsely hairy lamina which tapers towards the base having a size about 11–23 9 4–8 cm. It has a dark green upper surface and slightly paler lower surface. It has an entire margin and coriaceous blade along with 1–1.5 cm long leaf stalk and rounded or slightly pointed tip **(Komal *et al.*, 2020)**.

Flowers or inflorescences: It has strongly perfumed 120 cm long branched terminal panicle inflorescence. Flowers are white, cream or green color and 7–10 cm long and are densely clustered. It has 1.5–4 mm long hairy lobes, sparsely/densely pubescent tube with short pedicel **(Komal *et al.*, 2020)**.

Fruits: The fruits are brown-green woody dry pendulous, twolobed and dehiscent follicle. The follicles are cylindrical, slender of size 21–56 x 0.2–0.3 cm. Fruits are spindle shaped grouped and arranged in the pairs containing numerous seeds **(Komal *et al.*, 2020)**.

Seeds: Seeds are brown colored, flat oblong about 4–5 x 0.9 – 1.2 mm. The seeds have 7–13 mm long tuft of hair at both the ends **(Komal *et al.*, 2020)**.

Figure 1: (a) Leaves, (b) bark, (c) flowers (Vanita and Deepali, 2018)

I.1.1.3.2 Taxonomical classification, Synonymns and Common names

i. Taxonomical classification of *Alstonia scholaris* (Anupam *et al*., 2016)

Kingdom	:	Plantae
Superdivision	:	Embryophyata
Division	:	Tracheophyata
Subdivision	:	Spermatophytina
Class	:	Magnoliopsida
Order	:	Gentianales
Family	:	Apocynaceae
Tribe	:	Plumeriae
Subtribe	:	Alstoniinae
Genus	:	*Alstonia*
Species	:	*Alstonia scholaris*

ii. Synonynms and Common names of *Alstonia scholaris*

Some synonyms of *Alstonia scholaris* are**:** *Echites scholaris*, *Alstonia kurzii*, *Tabernaemontana alternifolia*, *Acokanthera scholaris*, and *Echite spala* **(Vanita and Deepali, 2018)**. Table 1 below gives a list of some common names of *Alstonia scholaris* in various languages **(Mangalore *et al*., 2012; Manjeshwar, 2011)**.

Table 1: Common names used for *Alstonia scholaris* in various languages

Language	Name(s)	Reference
Sanskrit	Saptaparna, Saptaparni, phalagaruda, Vishalalvaka, Vishamachhda, Ayugmaparna, Payasya, Jivani, Kshalrya, Madagandha, Grahashi, Grahanashana	**Mangalore *et al*., 2012; Manjeshwar, 2011**
English	Devil's tree, birrba, black board tree, dita bark, milk wood, pine, milky pine, white cheese wood	
Bengali	Chattin	
Burmese	Lettok	**Manjeshwar, 2011**
Javanese	Pule	
Kannada	Hale	
Konkani	Santhani	
Malay	Pulai, pulai linlin, Ezhilampala, Mukkampala, Pala, yakshi pala	
Oriya	Chhatiana, Chhanchania; Silgandha	
Sindhi	Rukattana, Sapthaparna	
Sino Tibetan	Tinpet	
Tamil	Pala, Elilaipillai, Mukumpalei, Wedrase	
Thai	Sattaban, teenpet, teenpethasaban	
Vietnamese	Caay mof cua, caay suwxa	

I.1.1.3.3 Habitat and distribution of *Alstonia scholaris*

i. Habitat of *Alstonia scholaris*

Alstonia scholaris is grown in the lowland and mountain rainforests **(Abhijit, 2011)**. It is evergreen tropical tree of Indian subcontinent and Southeast Asia. The plant is native of India, Srilanka, Pakistan, Nepal, Thailand, Burma, Malaysia, South East Asia, Africa, Northern Australia, Solomon Islands and South China. It was introduced in the southern USA where it is grown as an ornamental plant **(Anupam *et al*., 2015)**.

ii. Distribution of *Alstonia scholaris*

Alstonia scholaris is the most widespread species of the genus Alstonia. It is widely found in deciduous and mixed forests ecosystem native to India, China, Australia, Indonesia, Malaysia, Myanmar, Nepal, Papua New Guinea, Philippines, Sri Lanka, Thailand, and Viet Nam **(Komal *et al.*, 2020)**. The figure below shows the geographical distribution of *Alstonia scholaris.*

Figure 2: Geographical distribution of *Alstonia scholaris*

(www.researchgate.net/figure/Geographical-distribution-of-A-scholaris-Color-figure-online_fig1_339273223)

I.1.1.3.4 Uses of *Alstonia scholaris*

i. Ethnomedicinal or Traditional Uses

Alstonia scholaris has been used since time immemorial for its medicinal value and is recognised in the Indian, British and French Pharmacopoeias. All parts of the plant are utilized, among which the bark is the most extensively used. In Ayurveda, the traditional system of Indian medicine, the bark is used in various compound formulations. The mostn important are the saptaparnaghana vati, saptachchhadadi kvatha, saptachchhadadi taila, saptaparnasatvadi vati, and mahatikta ghrita.

Alstonia scholaris is also an important component of the proprietary polyherbal preparation Ayush-64, National Research Development Corporation (NRDC) and is marketed in India to treat malaria **(Manjeshwar, 2011).** In various traditions, the decoction prepared from the plant is bitter and used as a tonic, alternative, febrifuge, acrid, thermogenic, digestive, laxative, anthelmintic, astringen, febrifuge, anti-pyretic, depurative, galactogogue, stomachic, cardiotonic and tonic. It is useful in fever, malarial fever, abdominal disorders, diarrhoea, dysentery, dyspepsia, leprosy, skin diseases, pruritus,

tumors, chronic and foul ulcers, asthma, bronchitis, cardiopathy, helminthiasis, agalactia and debility. It is given as postnatal conditions to mothers for increasing lactation, and to improve digestion and relieve post-delivery weakness. It is also useful against snake-bite. The systemic consumption of the decoction prepared from the barks is believed to prevent *Alstonia scholaris* has been used since time immemorial for its medicinal value and is recognised in the Indian, British and French Pharmacopoeias. All parts of the plant are utilized, among which the bark is the most extensively used. In Ayurveda, the traditional system of Indian medicine, the bark is used in various compound formulations. *Alstonia scholaris* is also an important component of the proprietary polyherbal preparation Ayush-64 **(Manjeshwar, 2011; Abhijit, 2011).** National Research Development Corporation (NRDC) and is marketed in India to treat malaria **(Manjeshwar, 2011; Abhijit, 2011)**. *Alstonia scholaris* leaves have potential in the treatment of breast cancer **(Surya *et al*., 2012)**.

In various traditions, the decoction prepared from the plant is bitter and used as a tonic, alternative, febrifuge, acrid, thermogenic, digestive, laxative, anthelmintic, astringen, febrifuge, anti-pyretic, depurative, galactogogue, stomachic, cardiotonic and tonic. It is useful in fever, malarial fever, abdominal disorders, diarrhoea, dysentery, dyspepsia, leprosy, skin diseases, pruritus, tumors, chronic and foul ulcers, asthma, bronchitis, cardiopathy, helminthiasis, agalactia and debility. It is given as postnatal conditions to mothers for increasing lactation, and to improve digestion and relieve post-delivery weakness. It is also useful against snake-bite. The systemic consumption of the decoction prepared from the barks is believed to prevent indigestion and dysentery, rectify liver disorders, decrease fever, asthma and lessen chronic cough. It is also an effective blood purifier and affords cardioprotective effects **(Manjeshwar, 2011)**. Its consumption is supposed to decrease post delivery weakness and increase lactation in mothers. The bark lepa (paste) is applied topically as a healing agent for chronic skin ulcers.

The latex is topically applied against inflammatory reactions, rheumatoid, as an antipyretic agent, muscular pains as well as to decrease blood pressure. It also increases digestive power and is also given in fever as an antipyretic agent. The ripe fruits of the plant are used in syphilis insanity and epilepsy. It is also used as a tonic, anti-periodic and anthelmintic agent. The milky juice of *Alstonia scholaris* has been applied to treat ulcers. Milky juice is applied to ulcers and to rheumatic pains; mixed with oil and dropped into ear to relieve ache **(Manjeshwar, 2011; Abhijit, 2011)**.

ii. Economic uses

The wood of this plant was used to make the writing slates for school children **(Komal *et al*., 2020)**. It is also cultivated in India, and Sri Lanka, South-East Asia, southern China, Malaysia and the northern part of Australia and Solomon Islands as an ornamental plant **(Manjeshwar, 2011)**.

I.1.1.4 Previous phytochemical studies of *Alstonia scholaris*

Phytochemically, *Alstonia scholaris* is one of the highly-investigated plants and nearly 400 compounds have been isolated and characterized **(Manjeshwar, 2011; Mangalore, 2012)**. The isolated compounds (alkaloids, iridoids, triterpenoids, flavanoids, coumarines, leucoanthocyanines, reducing sugars, simple phenolics, steroids, saponins and tannins) have been documented as the chief chemical constituents **(Mangalore, 2012)**. We are going to examine the previous pyhtochemical studies on some of these classes of compounds (alkaloids, triterpenes, steroids, flavonoids and iridoids) in the section below.

i. Alkaloids

Alkaloids are one of the major constituents of the species **(Abhijit, 2011)**. Approximately 169 alkaloids have been identified from the leaves, roots, stems, bark, fruits, and flowers of *Alstonia scholaris* and most of them belongs to monoterpene indole alkaloid (MIA) **(Komal *et al*., 2020).** MIAs are further classified into six subtypes after careful analysis of their structures such as Akuammiline, Vallesamine, Akuammicine (Strychnos family), Bisindole, Quinoline and Isoquinoline, and Miscellaneous **(Komal *et al*., 2020)**. Table 2 below gives the structures, names and references of some alkaloids isolated from *Alstonia scholaris.*

Table 2: Some alkaloids previously isolated from *Alstonia scholaris*

Structure/Name of compound	Plant part/Reference
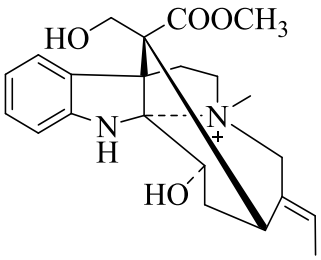 Echitamine **(2)**	Leaves/**Chaterjee *et al.*, *1*965**
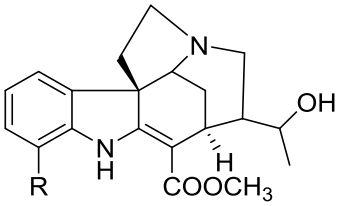 R = H: Etchitamine **(3)** R= OMe: scholarine **(4)**	Leaves/**Chaterjee *et al.*, *1*965** Leave/**Banerji *et al*., 1981** Fruits/**Wongseripipatana *et al*., 2004**
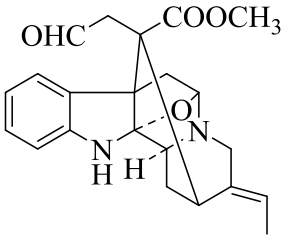 Picralinal **(5)**	Leaves/**Rastogi *et al*., 1970**
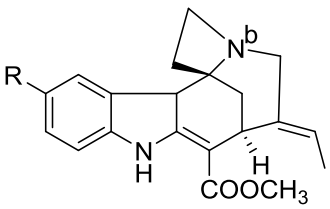 R= H: Akuammicine **(6)** R= H: N-oxide(Nb) $\xrightarrow{O)}$ akummicine-*N*b-oxide **(7)** R= OH: sewarine **(8)**	Bark/**Boonchuay *et al.*, 1976** Leave/**Banerji *et al*., 1981**
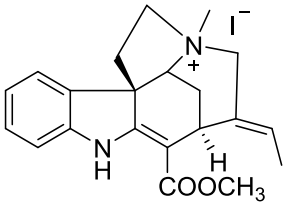 akummicine-Nb-methiodide **(9)**	Bark/**Boonchuay *et al.*, 1976**

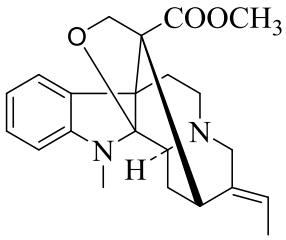 ψ-akuammigine **(10)**	Bark/**Boonchuay *et al.*, 1976**
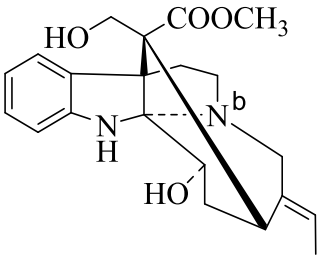 *Nb*demethylechitamine **(11)**	Bark/**Boonchuay *et al.*, 1976**
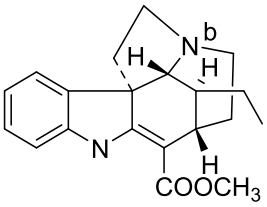 tubotaiwine **(12)**	Bark/**Boonchuay *et al.*, 1976** **Patrick *et al.*, 2005**
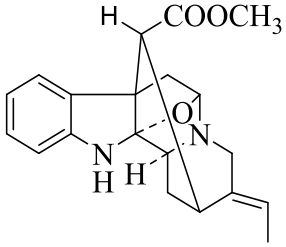 Picrinine **(13)** 19-*E*-picrinine **(14)**	Flower/**Dutta *et al.*, 1976** Fruits/**Wongseripipatana *et al.*, 2004**
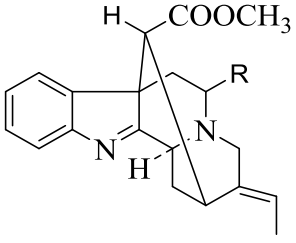 R= H strictamine **(15)** R= b-OCH_3 5-methoxystrictamine **(16)**	Flower/**Dutta *et al.*, 1976** Leaves/**Zhou *et al.*, 2005**
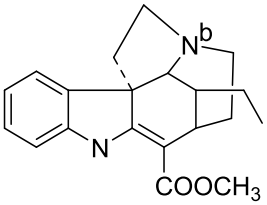 14,19-Dihydrocondylocarpine **(17)**	Leave/**Banerji *et al.*, 1981**

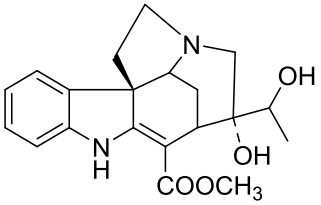 Alstovine **(18)**	Leave/**Banerji *et al.*, 1981**
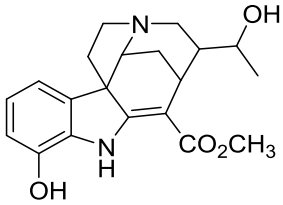 Scholaricine **(19)**	Leaves/**Rahman *et al.*, 1985**
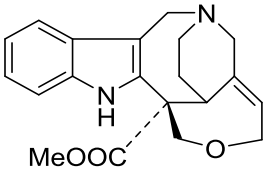 Alstonamine **(20)**	Leaves/**Rhaman *et al.*, 1987**
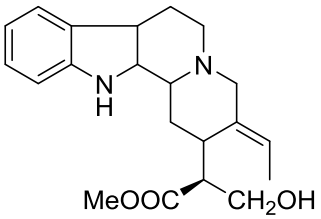 Rhazimanine **(21)**	Leaves/**Rhaman *et al.*, 1987**
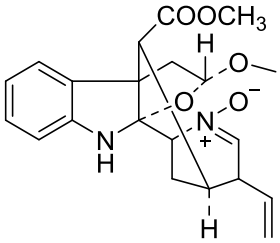 alschomine **(22)**	Leaves/**Abe *et al.*, 1989**
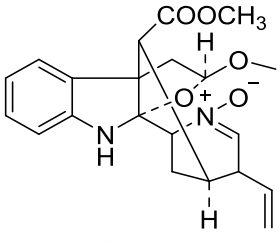 isoalschomine **(23)**	Leaves/**Abe *et al.*, 1989**

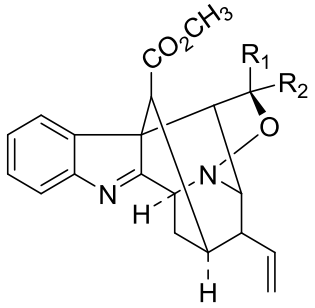 R_1= H, R_2= OH nareline **(24)** R_1= H, R_2= OEt nareline ethyl ether **(25)** R_1=OEt, R_2= H 5-epi-nareline ethyl ether **(26)**	Leaves/**Abe *et al.*, 1989** Leaves/**Kam *et al.*,1997**
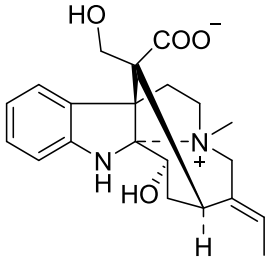 Echitaminic acid **(27)**	Trunk bark/**Salim *et al.*, 2004**
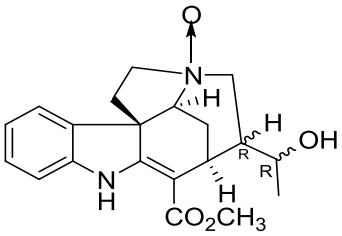 *N*^{b}-demethylalstogustine-*N*-oxide **(28)**	Trunk bark/**Salim *et al.*, 2004**
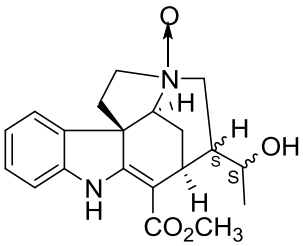 echitamidine-*N*-oxide **(29)**	Trunk bark/**Salim *et al.*, 2004**
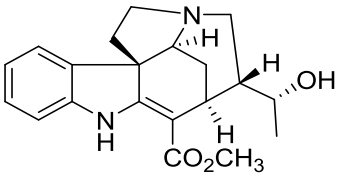 *Nb*-demethylalstogustine **(30)**	Trunk bark/**Salim *et al.*, 2004**

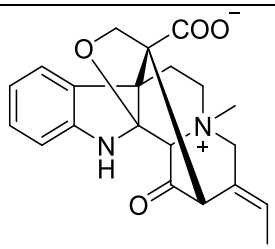 akuammiginone **(31)**	Trunk bark/**Salim *et al.*, 2004**
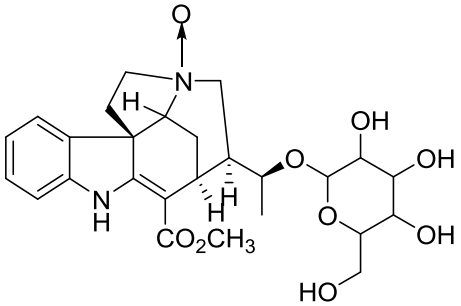 echitamidine-*N*-oxide-19-*O*-ß-D-glucopyranoside **(32)**	Trunk bark/**Salim *et al.*, 2004**
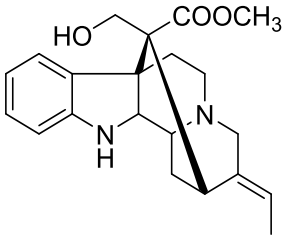 19-*E*-akuammidine **(33)**	Fruits/**Wongseripipatana *et al.*, 2004**
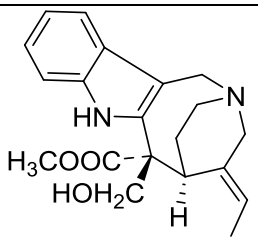 19-*E*vallesamine **(34)**	Fruits/**Wongseripipatana *et al.*, 2004**
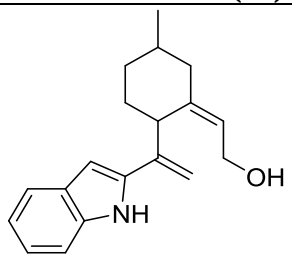 manilamine **(35)**	Leaves/**Patrick *et al.*, 2005**
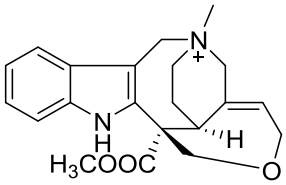 *N*4-methylangustilobine B **(36)**	Leaves/**Patrick *et al.*, 2005**

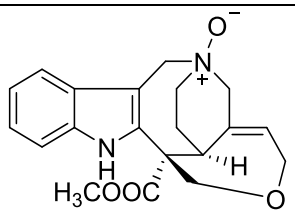 angustilobine-B-*N*4-oxide **(37)**	
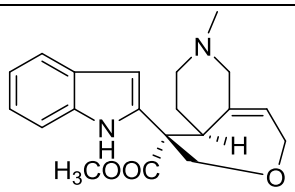 6,7-seco-angustilobine B **(38)**	
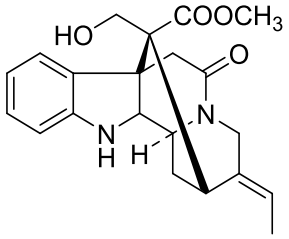 methyl (16R,19E)-1, 2-dihydro-16-(hydroxymethyl)-5-oxoakuammilan-17-oate **(39)**	Leaves/**Zhou *et al.*, 2005**
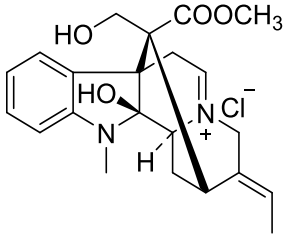 Methyl (2ß,16R,19E)-4,5-didehydro-1,2-dihydro-2-hydroxy-16-(hydroxymethyl)akuammilan-4-ium-17-oate chloride **(40)**	
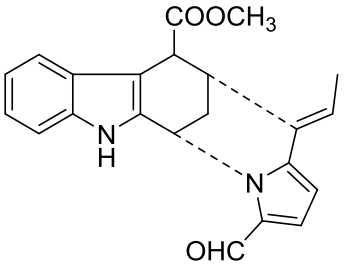 (19, 20) *E*-alstoscholarine **(41)**	Leaves/**Cai *et al.*, 2007**
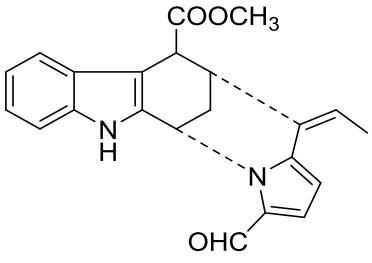 (19, 20) *Z*-alstoscholarine **(42)**	

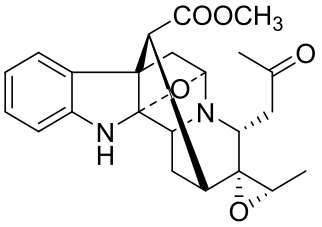 scholarisine B **(43)**	Bark/**Feng *et al.*, 2009**
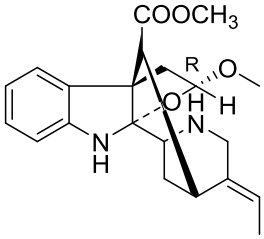 scholarisine C **(44)**	
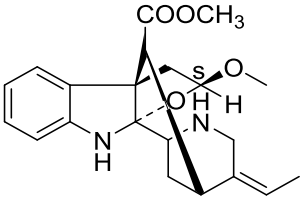 scholarisine D **(45)**	
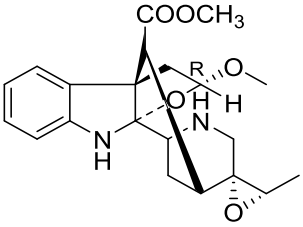 scholarisine E **(46)**	
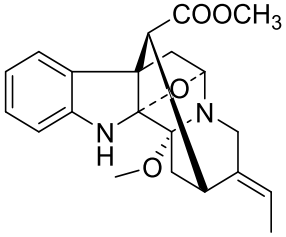 scholarisine F **(47)**	Bark/**Feng *et al.*, 2009**
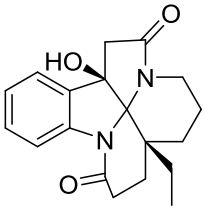 scholarisine G **(48)**	

ii. Terpenoids

Table 3 below gives structures and names of some terpenoids previouly isolated from *Alstonia scholaris.*

Table 3: Some terpenoids previouly isolated from *Alstonia scholaris*

Structure/Name of compound	Plant part/Reference
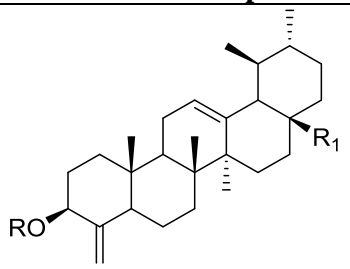 R=Ac R_1=CH_3 3β-acetate-24-nor-urs-4,12-diene ester triterpene **(49)** R=H R_1= 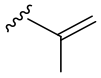 3β-hydroxy-24-nor-urs-4,12,28-triene triterpene **(50)**	Flowers/**Sultana and Saleem, 2010** Flowers/**Sultana *et al*., 2014**
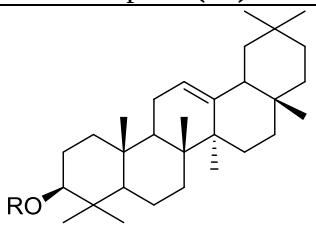 R= CH_3CO β-amyrin acetate **(51)** R=H β-amyrin **(52)**	Flowers/**Sultana and Saleem, 2010** Leaves/ **Chao-Min *et al*., 2017**
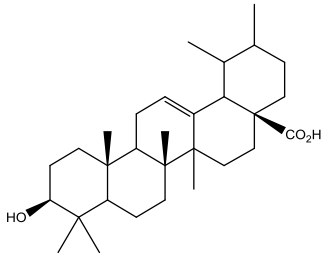 ursolic acid **(53)**	Flowers/**Sultana and Saleem, 2010** Leaves/ **Chao-Min *et al*., 2017**
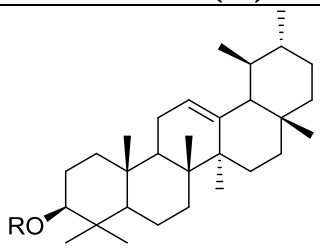 R=Ac α-amyrin acetate **(54)** R=H α-amyrin **(55)**	Flowers/**Sultana and Saleem, 2010** Flowers/**Sultana *et al*., 2014** Leaves/ **Chao-Min *et al*., 2017**

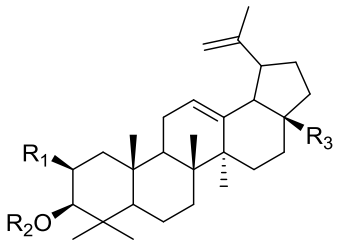 R_1=H R_2= H R_3=CH_3 Lupeol (**56**) R_1=H R_2= Ac R_3=CH_3 Lupeol acetate (**57**)	Flowers/**Sultana and Saleem, 2010** Leaves/ **Chao-Min *et al*., 2017** Flowers/**Sultana *et al*., 2014**
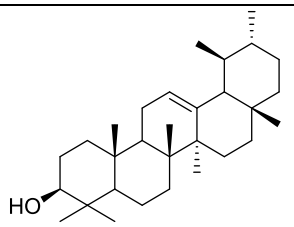 α-amyrin (**58**)	Flowers/**Sultana *et al*., 2014** Leaves/ **Chao-Min *et al*., 2017**
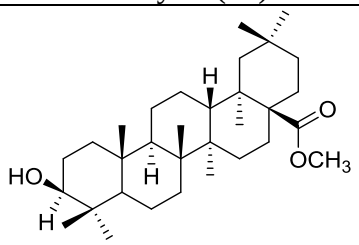 3--hydroxy-28--acetoxy-5-olea triterpene (**59**)	Flowers/**Sultana *et al*., 2014**
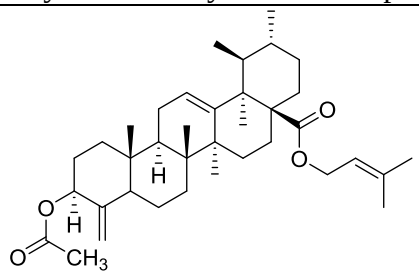 3-acetate-24-nor-urs-4,12,2'-triene ester triterpene (**60**)	Flowers/**Sultana *et al*., 2014**
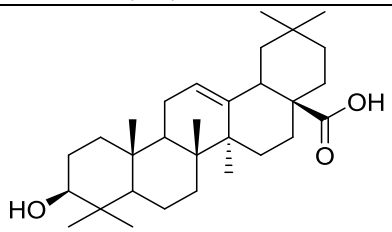 oleanolic acid (**61**)	Leaves/ **Chao-Min *et al*., 2017**
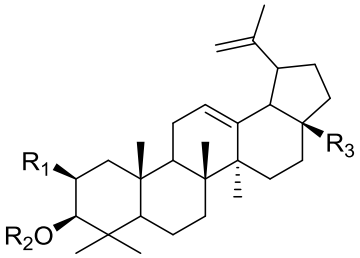 R_1=H R_2=H R_3=CH_2OH Betulin (**62**) R_1=H R_2=H R_3=COOH Betulinic acid (**63**) R_1=OH R_2=H R_3=CH_2OH 2B,3B,28-lup-20(29)-ene-triol (**64**)	Leaves/ **Chao-Min *et al*., 2017**

iii. Steroids

Table 4 below gives structures and names of some steroids previouly isolated from *Alstonia scholaris.*

Table 4: Some steroids previouly isolated from *Alstonia scholaris*.

Structure/Name of compound	Plant part/Reference
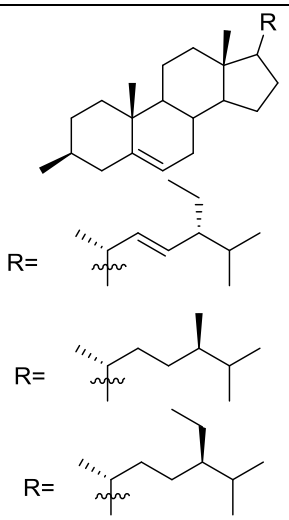 Poriferasterol **(65)** Epicampesterol **(66)** β-sitosterol **(67)**	Leaves/**Chao-Min *et al*., 2017**
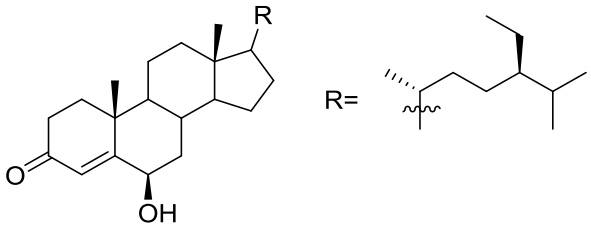 6β-hydroxy-4-stigmasten-3-one **(68)**	Leaves/**Chao-Min *et al*., 2017**
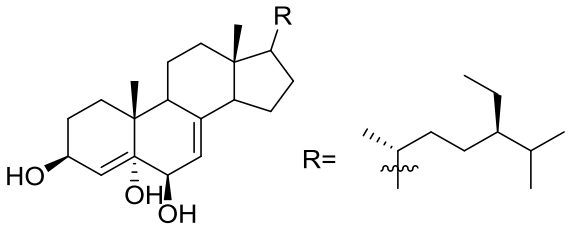 ergosta-7,22-diene-3β,5α,6β-triol **(69)**	Leaves/**Chao-Min *et al*., 2017**

iv. Flavonoids

Table 5 below gives structures and names of some flavonoids previouly isolated from *Alstonia scholaris.*

Table 5: Some flavonoids previouly isolated from *Alstonia scholaris*.

Structure/Name of compound	Plant part/Reference
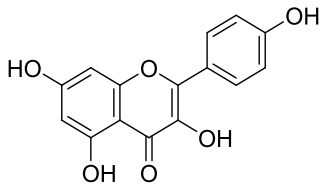 Kaempferol **(70)**	Leaves/**Tingting *et al*., 2009**
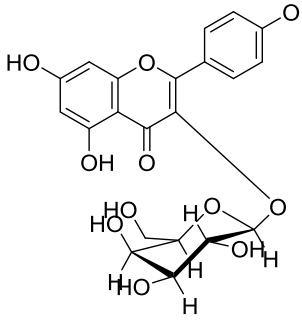 Kaempferol-3-O-*β*-*D*-galactopyranoside **(71)**	Leaves/**Tingting *et al*., 2009**
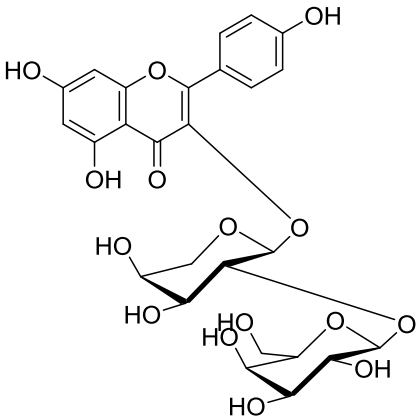 Kaempferol-3-O-*β*-*D*-xylopyranosyl-(2-1)-O-*β*-*D*-galactopyranoside **(72)**	Leaves/**Tingting *et al*., 2009**
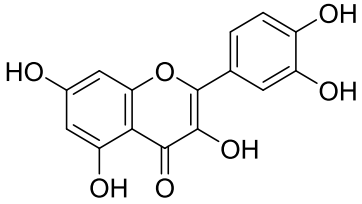 quercetin **(73)**	Leaves/**Tingting *et al*., 2009**

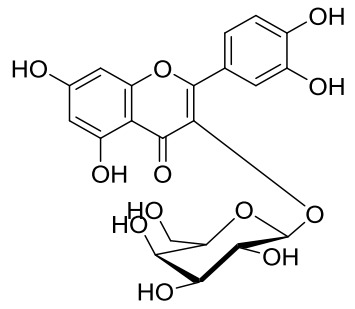 Quercetin-3-O-*β*-*D*-galactopyranoside **(74)**	Leaves/**Tingting *et al*., 2009**
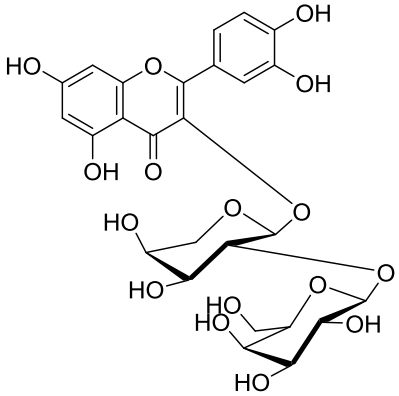 Quercetin-3-O-*β*-*D*-xylopyranosyl-(2-1)-O-*β*-*D*-galactopyranoside **(75)**	Leaves/**Tingting *et al*., 2009**
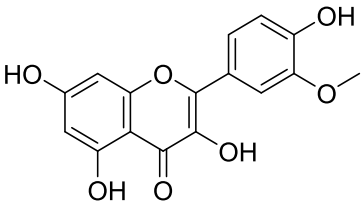 Isorhamnetin **(76)**	Leaves/**Tingting *et al*., 2009**
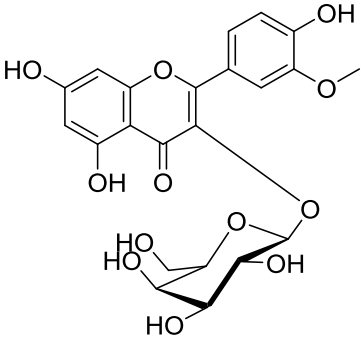 Isorhamnetin-3-O-*β*-*D*-galactopyranoside **(77)**	Leaves/**Tingting *et al*., 2009**

v. Iridoids

Table 6 below gives structures and names of some iridoids previouly isolated from *Alstonia scholaris.*

Table 6: Some iridoids previouly isolated from *Alstonia scholaris*

Structure/Name of compound	Plant part/Reference
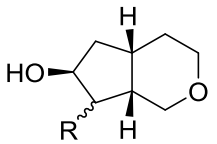 R= β-Me Scholareins A **(78)** R= α-Me Scholareins B **(79)**	Bark/**Tao *et al*., 2008**
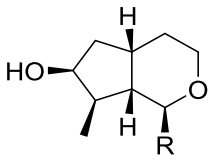 R= OH Scholareins C **(80)** R= MeO Scholareins D **(81)**	Bark/**Tao *et al*., 2008**
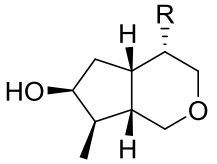 R= H Isoboonein **(82)** R= CH_2OH Alxialactone **(83)**	Bark/**Tao *et al*., 2008**
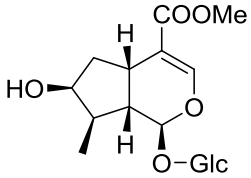 Loganin **(84)**	Bark/**Tao *et al*., 2008**

I.1.1.5 Previous biological studies of *Alstonia scholaris*

The plant has been reported for antimalarial, anticancer, anti-tussive, anti-asthmatic, antiinflammatory, hypoglycaemic, spasmolytic, analgesic, antipyretic, antipsychotic, antioxidant, antinociceptic, antidiabetic, antifertility, antiperiodic, anthelmintic, radioprotective, antiplasmodial, antileishmanial, antiparasitic, anti-hypertensive, aphrodisiac activities **(Dey, 2011).** Methanolic extract of leaf, stem, bark and root bark showed in-vitro antituberculosis (89% inhibition against *Mycobacterium tuberculosis* H37Rv at 50 µg/mL) using Micoplate Alamar or microBlue assay (MABA) **(Dey, 2011; Meena et *al*., 2011).**

The bark extract showed the skin carcinogenesis in swiss albino mice, while echitamine chloride, methanolic extract of root bark and the alkaloids fraction of *A. scholaris* showed cytotoxicity against HeLa, HepG2, HL60, KB and MCF-7 cancer cell lines in vitro and in mice bearing EAC Humen lung cancer cell lines, MOR-P (adenocarcinoma) and COR-L23 (large cell carcinoma), using the SRB assay **(Dey, 2011; Meena et *al.*, 2011)**. The ethanol extract of *A. scholaris* leaves induced pronounced bronchodilator activity in anaesthetized rats with the probable involvement of prostaglandins **(Maurya, 2014; Meena et *al.*, 2011).** The hepatoprotective effect of *A. scholaris* on liver injuries induced by carbon tetrachloride, β-D-galactosamine, acetaminophen and ethanol were investigated by means of serum-biochemical and histopathological examinations **(Maurya, 2014; Meena et *al.*, 2011).** The alkaloid fraction of *A. scholaris* leaf contain three main alkaloids, picrine, vallesamine and scholaricine and based on several in-vivo assay, these alkaloids produce the anti-inflammatory and analgesics effect peripherally, these alkaloids exhibited inhibition of inflammatory mediators (COX-1, COX-2 and 5-LOX), which is in accordance with the results on animal models **(Meena et *al.*, 2011)** Moreover, the main alkaloid, picrinine exhibited anti-tussive and anti-asthamatic activities in vivo **(Maurya, 2014; Meena et *al.*, 2011).** The aqueous and partially purified extracts of stem bark and leaf of *A. scholaris* possess molluscicidal as well as in vivo and in vitro anti-cholinesterase activity against the snail *Lymnea acuminta* **(Maurya, 2014; Meena et *al.*, 2011).**

I.1.2 Literature review on *Psorospermum guineense*

I.1.2.1 Hypericaceae family

Hypericaceae is a plant family in the order Malpighiales, comprising 6 to 9 genera and upto 700 species, and commonly known as the St. John's wort family. Members are found throughout the world apart from extremely cold or dry habitats. Most of the genera occur mostly in the tropical regions. Members of this family are annual or perennial herbs, subshrubs or shrubs. The leaves are simple and entire in opposite pairs; they are sometimes dotted with black or translucent glandular spots. The inflorescence consists of a branched, flat-topped cluster, each flower being radially symmetrical, with a superior ovary. Flowers have the following components: sepals, four or five, which tend to persist; petals four or five, usually yellow, sometimes dotted with black specks; stamens many, on long filaments; styles, three to five, often fused at filaments; styles, three to five, often fused at the base. The fruit

has a dehiscent capsule which splits open when ripe to release the fine black seed **(Angiosperm phylogeny group, 2009)**.At one time, this family was accepted as a subfamily of the family Clusiaceae. Now it has been elevated to full family status. In phytotaxa, six genera and around 590 species are listed, whereas 'The plant List' recognizes around 700 species.

Members of the family are found in temperate regions. Molecular data supports the monopoly of Hypericaceae. As a family, the cladogram of Hypericaceae would appear as shown in scheme 1 below.

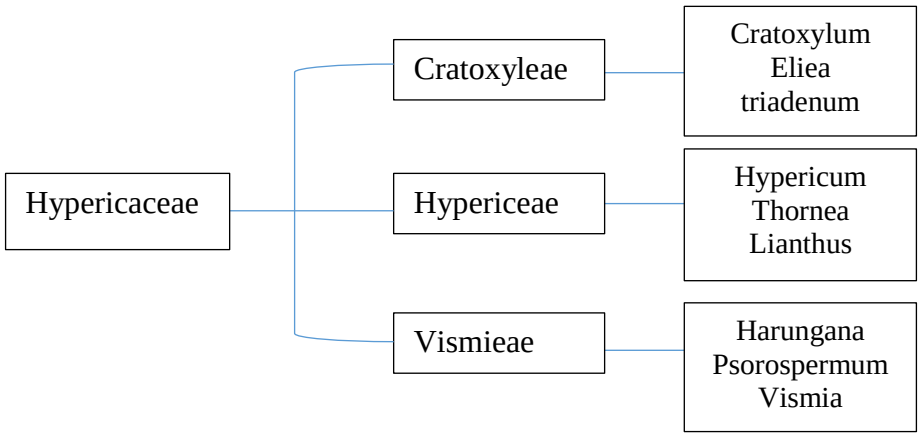

Scheme 1: Cladogram of Hypericacea family

Many members of this family contain the naphtodianthrone derivatives hypercin and pseudohypercin; these are contained in glandular tissues that appear as black, orange or translucent spots or lines on petals, leaves and other parts of the plant. These compounds are photosensitive and can cause reactions in grazing animals, such as blistering of the muzzle, as well as in people come in contact with the plant over prolonged periods. The genera of this family include, Asyrum, Cratolyx, Eliea, Haronga, Harungana, Hypericum, Lianthus, Psorospermum, Santomasia, Sarothra, Thomas, Triadenia, Triadenum and Vismia **(Wurdack and Davis, 2009)**.

I.1.2.2 *Psorospermum* genus

The genus Psorospermum Baker (tribe Vismieae, family Guttiferae, subfamily Hypericoideae) comprises 55 species, most of which are shrubs or small trees typically growing in the tropical regions of South America, Africa, and Madagascar. It is very similar in morphology to Vismia Vand, differing mainly in fruits. The main botanical features are given by opposite and petiolate leaves with an opaque lamina, dark-coloured glandular dots, mostly near the margin and brownish stellate hairs, particularly beneath; flowers grouped in a

terminal, cymose panicle and bisexual with 5 sepals and 5 petals, a 5-locular ovary with 1 or 2 ovulate loculi; fruits as berries with seeds having a fleshy, glandular-punctate heads. Most of the species of the genus Psorospermum have been used for a long time in the ethnomedical folk traditions of indigenous African populations as febrifugal, antidote against poisons (e.g. as a relief against bites of spiders and scorpions), purgative, stomachic, and as a remedy for the treatment of leprosy, skin diseases (like dermatitis, scabies, and eczemas), and subcutaneous wounds **(Epifiano *et al*., 2013)**.

The pool of secondary metabolites isolated from plants belonging to the title genus include alkaloids, simple and O- and C-prenylated anthraquinones, anthrones and bianthrones, vismiones, flavonoids, long chain alcohols, steroids, tannins, terpenes, and simple and O- and C-prenylated xanthones. The reported pharmacological activities of the above-mentioned natural compounds refer to antibacterial, anti-protozoal, anti-fungal, anti-viral, anticancer anti-oxidant, and neuroprotective effects **(Epifiano *et al*., 2013)**.

I.1.2.3 *Psorospermum guineense* species

I.1.2.3.1 Botanical aspect of *Psorospermum guineense*

It is a shrub **(Kuete *et al*., 2007)**.

Branches: They are clothed with a pale rusty-brown tomentum, deciduous on the upper surface of the leaves **(www.plants.jstor.org)**.

Leaves: They are opposite or alternate, elliptical or oblong-elliptical, subacute or obtusely apiculate, narrowed or rounded at the base but not cordate. They have broad petioles 2-3 lines **(www.plants.jstor.org)**.

Flowers: They are densely tomentous in axillary and terminal umbellate panicles shorter than the leaves or collected in terminal corymbose panicles a little exceeding the uppermost leaves **(www.plants.jstor.org)**.

Figure 3: Photo of *Psorospermum guineense* (www.inaturalist.org)

I.1.2.3.2 Taxonomical classification, Synonymns and Common names

i. Taxonomical classification of *Psorospermum guineense*

Kingdom	:	Plantae
Family	:	Hypericaceae
Genus	:	*Psorospermum*
Species	:	*Psorospermum guineense*

ii. Synonymns, Common names of *Psorospermum guineense*

Several synonyms are reported: *Psorospermum senegalense* Spach., *Hypericum guineense* L., *Vismia leonensis* Hook, *Vismia laurentii* De Wild., and *Vismia guineensis* (L.) Choisy. In particular, the last name seems to be the proper botanical terminology **(Bilia *et al*. 2004)**.

In Mali, French Guinea, Senegal, Tanzania, and Nigeria it is locally called "Karidjakouma" **(Wilcox *et al*., 2012**; **Bilia *et al*. 2004; Politi *et al*., 2004)**. In the North West region of Cameroon, the people of the Nso tribe call it 'Shijiy'. In the center Reion of Cameroon, it is known as ''atondo owse' **(Nguemeving *et al*., 2006)**.

I.1.2.3.3 Habitat and distribution of *Psorospermum guineense*

i. Habitat of *Psorospermum guineense*

It grows in the tropical and subtropical regions of the world **(Kuete *et al*., 2007)**.

ii. Distribution of *Psorospermum guineense*

It typically grows in French Guinea Mali, Senegal, Tanzania, and Nigeria **(Wilcox *et al*., 2012)**. It is also found in Cameroon and grows typically in the Center region **(Nguemeving *et al*., 2006)** and in the North West region of Cameron. The map below gives a representation of is distribution in Cameroon.

Regions where *Psorospermum guineense* is typically found in Cameroon (**Nguemeving, *et al*., 2006**)

Figure 4: Distribution of *Psorospermum guineense* in Cameroon

I.1.2.3.4 Uses of *Psorospermum guineense*

i. Ethnomedicinal or Traditional Uses

The leaves and twigs of the plant are used in Cameroon to treat breast cancer. In the regions where it is found, the local population use the roots, the twigs and the leaves to traditionally treat fever, dermatitis, leprosy, syphilis, herpes, scabies, eczemas and infected wounds (**Politi *et al*., 2004**; **Kuete *et al*., 2007; Wilcox *et al*., 2012**).

ii. Economic uses

In Mali, the plant is marketed as vaseline or karité butter ointments containing 1% Karidjakouma root (**Politi *et al*., 2004**). In Cameroon, the dry wood is lcally used as firewood.

I.1.2.3.5 Previous phytochemical studies of *Psorospermum guineense*

The ethobotanical uses of this plant have attracted many scientists to work on it isolating some secondary metabolites mainly of the classes, quinones, triterpenes, flavonoids and steroids. Some isolated compounds of these major groups are given below.

i. Quinones

The class of quinones mostly isolated from this plant is the anthraquinones class (they are compounds containing the anthracene nucleus with two carbonyl groups). The names, structures of some previously isolated quinones from this plant are given in Table 7 below alongside the plant part from which they were isolated.

Table 7: Quinones isolated from *Psorospermum guineense*

Structure/Name of compound	Plant part /Reference
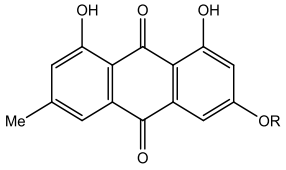 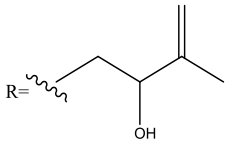 3-O-(2-hydroxy-3-methylbut-3-enyl)-emodin **(85)** 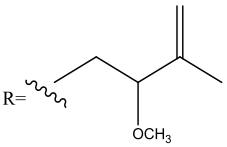 3-O-(2-methoxy-3-methylbut-3-enyl)-emodin **(86)** 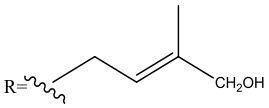 3-O-(E-3-hydroxymethylbut-2-enyl)-emodin **(87)** 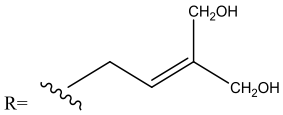 3-O-(3-hydroxymethyl-4-hydroxybut-2-enyl)-emodin **(88)** 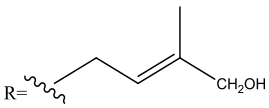 3-O-(E-3-hydroxymethylbut-2-enyl)-emodin **(89)**	Roots/**Bilia *et al*.,2000**
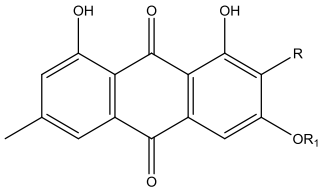 R= H R1=CH_3 Physcion (**90**) R= C_5H_9 R_1=H 2-isoPrenylemodin (**91**) R=H R_1=C_5H_9 Madagascin (**92**)	Leaves/**Politi *et al*., 2004** Roots/**Politi *et al*., 2004**
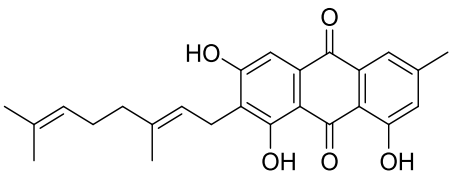 2-Geranylemodin **(93)**	Leaves and Roots/**Politi *et al*., 2004**
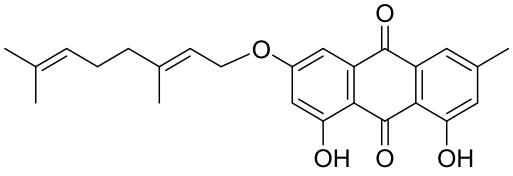 3-Geranyloxyemodin (**94)**	Leaves and Roots/**Politi *et al*., 2004 ;** Stembark/**Noungoue *et al*., 2009**

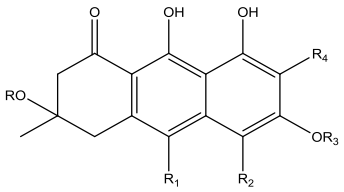 R=CH_3CO R_1= H R_2= H R_3= $C_{10}H_{17}$ R_4=H Acetylvismione D **(95)** R=CH_3CO R_1= H R_2= H R_3=H R_4=$C_{10}H_{17}$ Acetylvismione F **(96)** R=H R_1= H R_2= H R_3= $C_{10}H_{17}$ R_4=H Vismione D **(97)** R=H R_1= H R_2=H R_3= H R_4= $C_{10}H_{17}$ Vismione F **(98)** R=CH_3CO R_1= $C_{10}H_{17}$ R_2=H R_3= H R_4= H Vismione G **(99)** R=H R_1= H R_2=$C_{10}H_{17}$ R_3= H R_4= H Vismione L **(100)** R=H R_1= H R_2=H R_3= CH_3 R_4= $C_{10}H_{17}$ Vismione M **(101)**	Roots/**Politi *et al*., 2004**
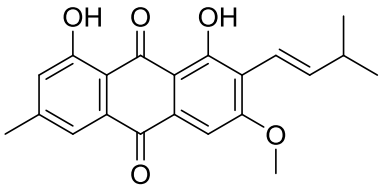 Vismiaquinone A **(102)**	Roots/**Nguemeving *et al*., 2006;** Seeds/**Tala et *al.*, 2013**
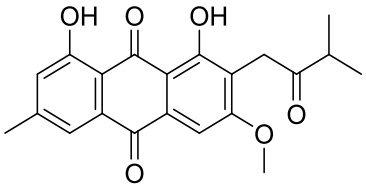 Vismiaquinone B **(103)**	Roots/**Nguemeving *et al*., 2006;** Stembark/**Noungoue *et al.*, 2009;** Seeds/**Tala et *al.*, 2013**
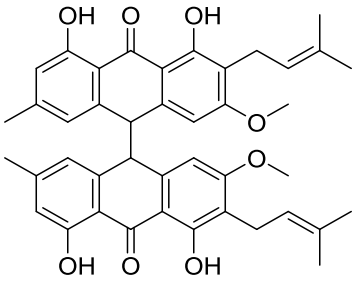 Bisvismiaquinone **(104)**	Roots/**Nguemeving *et al*., 2006** Stem bark/**Tala et *al.*, 2007** Fruits/**Noungoue *et al.*, 2008**
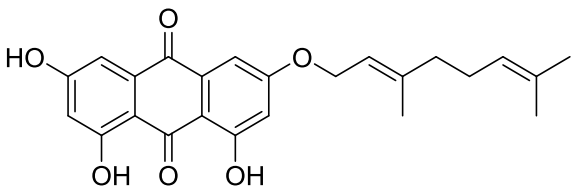 3-geranyloxy-6-methyl-1,8-dihydroxyanthraquinone **(105)**	Roots/**Nguemeving *et al*., 2006**

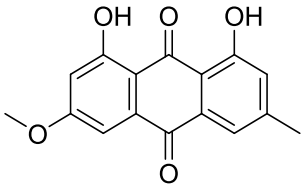 1,8-dihydroxy-6-methoxy-3-methylanthraquinone **(106)**	Roots/**Nguemeving *et al.*, 2006**
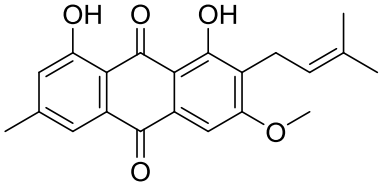 Vismiaquinone C **(107)**	Twigs/**Kuete *et al.*, 2007**
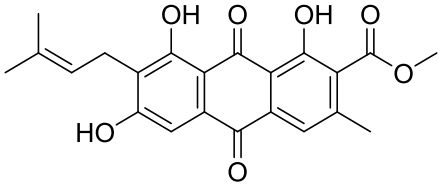 laurentiquinone A **(108)**	Fruits/**Noungoue *et al.*, 2008** Seeds/**Tala *et al.*, 2013**
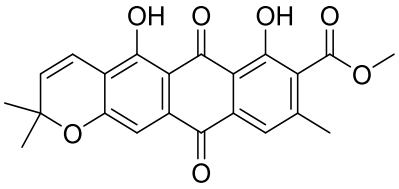 laurentiquinone B **(109)**	Fruits/**Noungoue *et al.*, 2008** Seeds/**Tala *et al.*, 2013**
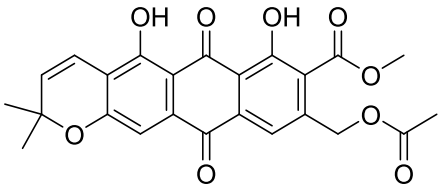 laurentiquinone C **(110)**	Fruits/**Noungoue *et al.*, 2008** Seeds/**Tala *et al.*, 2013**
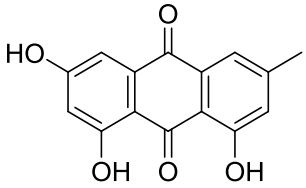 Emodin **(111)**	Fruits/**Noungoue *et al.*, 2008**
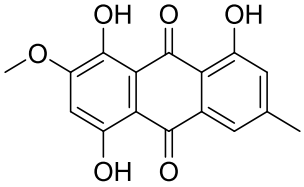 isoxanthorin **(112)**	Fruits/**Noungoue *et al.*, 2008**

ii. Triterpenes

The names and structures of some triterpenes previously isolated from *Psorospermum guineense* are given in Table 8 below alongside the plant part from which they were isolated.

Table 8: Triterpenes isolated from *Psorospermum guineense*

Structure/Name of compound	Plant part/Reference
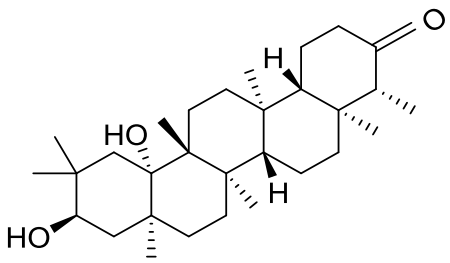 Friedelin **(113)**	Roots/**Nguemeving *et al*., 2006**
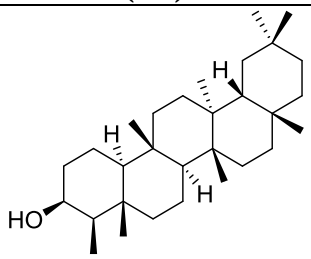 Epifriedelinol **(114)**	Stembark/**Noungoue *et al.*, 2009**

iii. Xanthones

The names and structures of some xanthones previously isolated from *Psorospermum guineense* are given in Table 9 below alongside the plant part from which they were isolated.

Table 9: Some xanthones previously isolated from *Psorospermum guineense*

Structure/Name of compound	Plant part/Reference
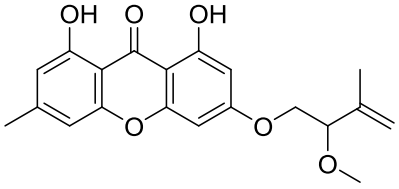 1,8-dihydroxy-3-(2-methoxy-3-methylbut-3-enyloxy)-6-methylxanthone **(115)**	Roots/**Bilia *et al*., 2000**
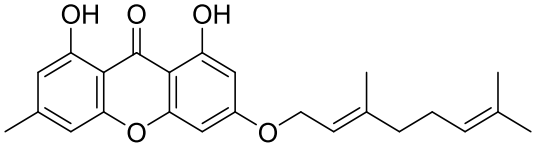 1,8-dihydroxy-3-geranyloxy-6-methylxanthone **(116)**	Roots/**Bilia *et al*., 2000**

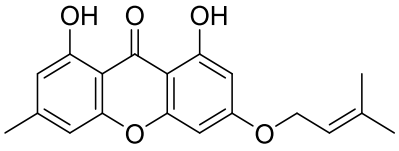 1,8-dihydroxy-3-isoprenyloxy-6-methylxanthone **(117)**	Roots/**Bilia *et al*., 2000**
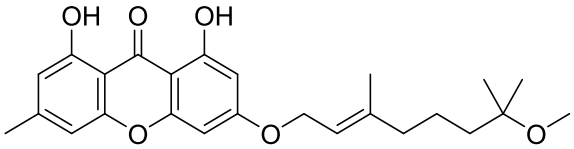 1,8-dihydroxy-3-(3,7-dimethyl-7-methoxyoct-2-enyloxy)-6-methylxanthone **(118)**	Roots/**Bilia *et al*., 2000**
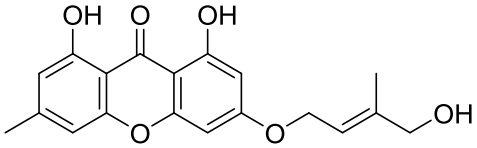 1,8-dihydroxy-3-(*E*-3-hydroxymethylbut-2-enyloxy)-6-methylxanthone **(119)**	Roots/**Bilia *et al*., 2000**
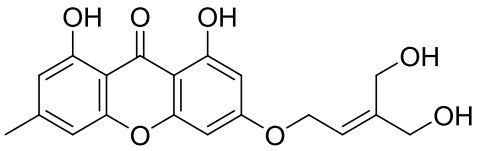 1,8-dihydroxy-3-(3-hydroxymethyl-4 hydroxybut-2-enyloxy)-6-methylxanthone **(120)**	Roots/**Bilia *et al*., 2000**
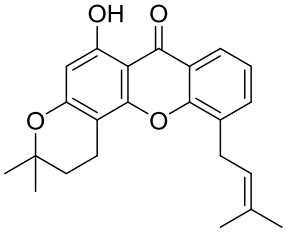 laurentixanthone A **(121)**	Roots/**Nguemeving *et al*., 2006**
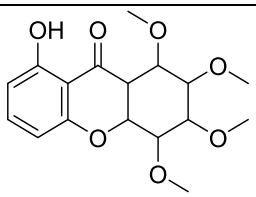 laurentixanthone B **(122)**	Roots/**Nguemeving *et al*., 2006**
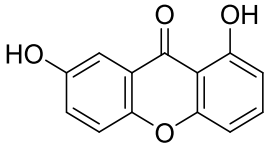 1,7-dihydroxyxanthone **(123)**	Roots/**Nguemeving *et al*., 2006**
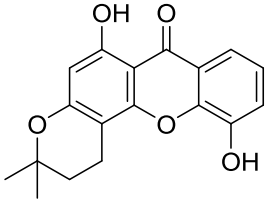 6-deoxyisojacareubin **(124)**	Roots/**Nguemeving *et al*., 2006** Roots/**Kuete *et al*., 2007**

iv. Flavonoids

The names and structures of some flavonoids previously isolated from *Psorospermum guineense* are given in the Table 10 below alongside the plant part from which they were isolated.

Table 10: Some flavonoids previously isolated from *Psorospermum guineense*

Structure/Name of compound	Plant part/Reference
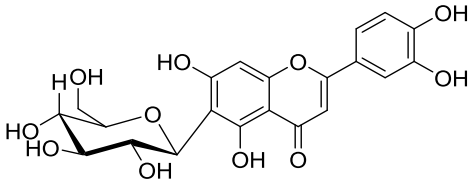 Iso-Orientin **(125)**	Leaves/**Politi *et al*., 2004**
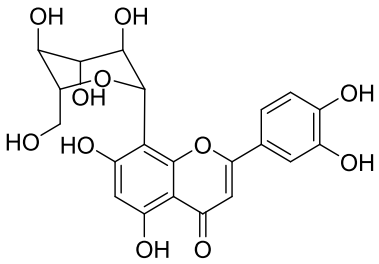 Orientin **(126)**	Leaves/**Politi *et al*., 2004**
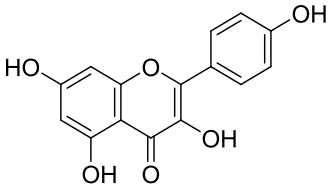 Kaempferol **(127)**	Roots/**Nguemeving *et al*., 2006**

v. Steroids

The names and structures of some steroids previously isolated from *Psorospermum guineense* are given in Table 11 below alongside the plant part from which they were isolated.

Table 11: Some steroids previously isolated from *Psorospermum guineense*

Structure/Name of compound	Plant part/Reference
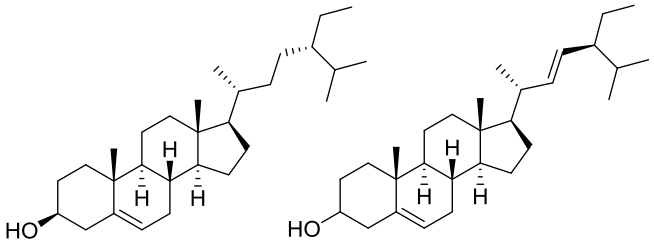 Mixture of β-sitosterol**(128)** and stigmastasterol **and 129)**	Seeds/**Tala *et al*., 2013**
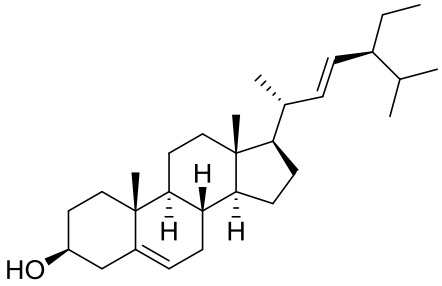 Stigmasterol **(129)**	Roots/**Nguemeving *et al*., 2006**
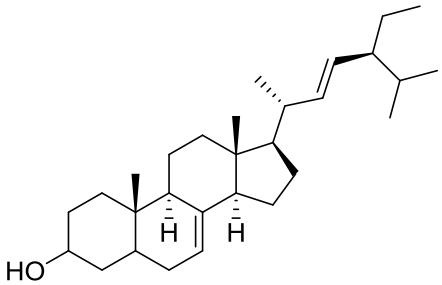 Stigmasta-7,22-dien-3-ol **(131)**	Stembark/**Noungoue *et al.*, 2009**
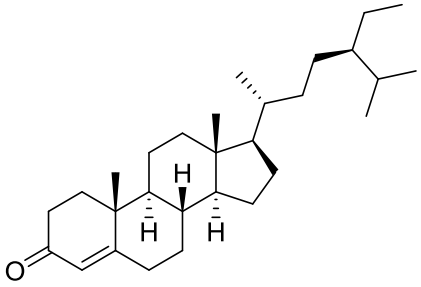 Stigmasta-4-en-3-one **(132)**	Seeds/**Tala *et al*., 2013**

I.1.2.4 Previous biological studies of *Psorospermum guineense*

Antimicrobial activities of the crude methanolic extracts and purified compounds are reported (**Kuete *et al.*, 2007**). The antimicrobial activity of root extract and isolated compounds is also reported by Nguemeving and collaborators (**Nguemeving *et al.*, 2006**). Antimalarial activity of the extract and compounds from the stembark of the plant are reported (**Noungoue *et al.*, 2009**). Crude extracts of hexane and EtOAc showed anti-plasmodial activity against the W2 strain of *Plasmodium falciparum* (**Ngouela *et al.*, 2007**).

The majority of compounds isolated from these two plants are mostly alkaloids, triterpenes and quinones. Herein, we shall discuss these classes in detail.

I.2 OVERVIEW ON ALKALOIDS, TRITERPENES AND QUINONES

I.2.1 Alkaloids

I.2.1.1 Definition of alkaloids

The word “alkaloid” was first coined by the German chemist Carl F. W. Meissner in 1819, derived from the Arabic name al-qali, which is associated to the plant from which soda was first sequestered (**Prasanta *et al.*, 2020**). Alkaloids are group of naturally occurring chemical compounds that mostly contain basic nitrogen atoms produced by a large variety of organisms including bacteria, fungi, plants, and animals (**Hamzat *et al.*, 2019**).

I.2.1.2 Classification of alkaloids

Here, we shall look at the classification established upon biogenesis and that established upon structure.

I.2.1.2.1 Classification established upon the biogenesis

Alkaloids illustrate large diversity not only in their botanical and biochemical origin but also in structure and pharmacological action. In this connection, various systems of classification are possible (**Prasanta *et al.*, 2020**). From a structural perception, alkaloids can be classified, based on their molecular precursor, structures, and origins or on the biological pathways used to obtain the molecule.

There are three central types of alkaloids: (1) true alkaloids, (2) protoalkaloids, and (3) pseudoalkaloids. True alkaloids and protoalkaloids are produced from amino acids, whereas pseudoalkaloids are not derived from these compounds (**Prasanta *et al.*, 2020**).

i. True alkaloids

These types of alkaloids are obtained from amino acids and they share a nitrogen-containing heterocyclic ring. They are highly reactive in nature and have potent biological activity. They form water-soluble salts, and many of them are crystalline in nature, which conjugates with acid and forms a salt. Almost all true alkaloids are bitter in taste and solid, except nicotine, which is a brown liquid. Their occurrence in plants occurs in three forms: (a) in Free-state, (b) as N-oxide, or (c) as salts. Various amino acids like L-phenylalanine/L-tyrosine, L-ornithine, L-histidine, L-lysine are the main sources of true alkaloids. Cocaine (**133**), quinine (**134**), morphine (**135**), are the common true alkaloids found in nature (**Prasanta *et al.*, 2020**).

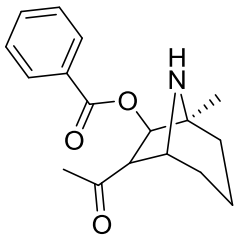

cocaine **133**

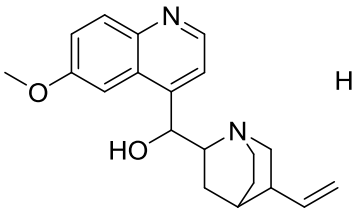

quinine **134**

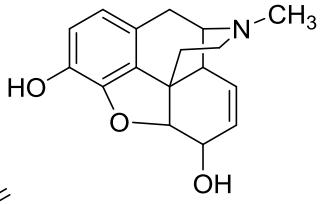

morphine **135**

ii. Protoalkaloids

This type of alkaloids contains a nitrogen atom, which is derived from an amino acid but is not part of the heterocyclic ring system. L-Tryptophan and L-tyrosine are the main precursors of this type of alkaloids. This minor group is structurally composed of simple alkaloids. Yohimbine (**136**), mescaline(**137**), and hordenine (**138**) are the main alkaloids of this type. They are used in various health disorders, including mental illness, pain, and neuralgia (**Prasanta *et al.*, 2020**).

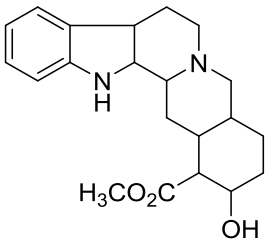

yohimbine **136**

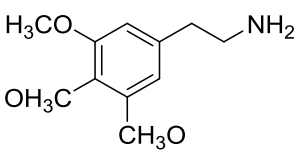

mescaline **137**

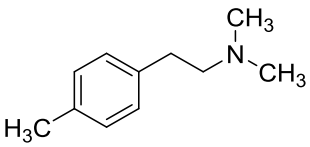

hordenine **138**

iii. Pseudoalkaloids

The basic carbon skeleton of pseudoalkaloids is not directly derived from amino acids; instead, they are connected with amino acid pathways where they are derived from by amination or transamination reaction from forerunners or postcursors of amino acid (**Prasanta *et al.*, 2020**). Nonamino-acid precursors can also produce pseudoalkaloids. They can be phenylalanine or acetate derived. Capsaicin (**139)**, caffeine (**140)**, ephedrine (**141)** are very common examples of pseudoalkaloids.

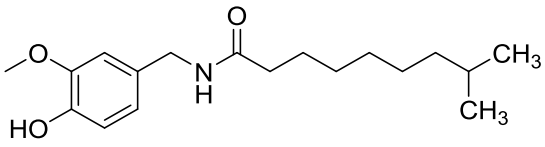

capsaicin **139**

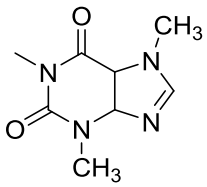

caffeine **140**

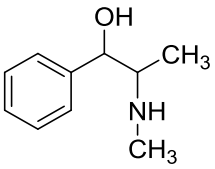

ephedine **141**

I.2.1.2.2 Classification established upon the ring structure

This is the most comprehensively established classification, based on the presence of a basic heterocyclic nucleus in their structure. Based on this we have ten different classes of alkaloids and their base structures are represented in scheme 2 below.

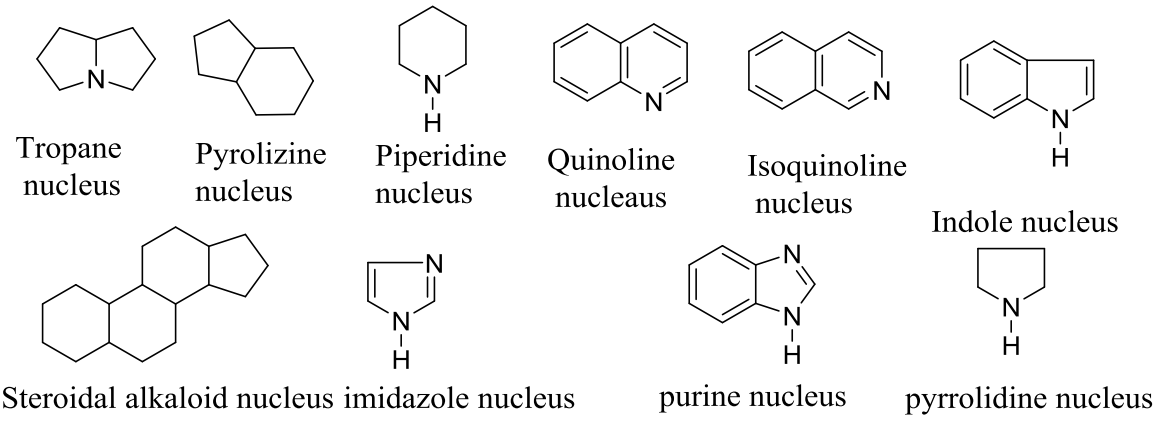

scheme 2: Basic nuclei of various ring structures for the classification of alkaloids established on ring structure (**Prasanta *et al.*, 2020**)

i. Tropane alkaloid

This category of alkaloids has tropane (C4N skeleton) nucleus. They are abundantly found in the Solanaceae family. They are derived from ornithine and acetoacetate. Structurally, pyrrolines are the precursor of these type of alkaloids. Maximum of them are

esters of mono, di, trihydroxytropane, having a wide range of hydroxylation arrangements (**Prasanta *et al.*, 2020**).Nicotine and scopolamine are some examples of this class of alkaloids.

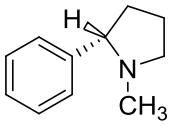

nicotine **142**

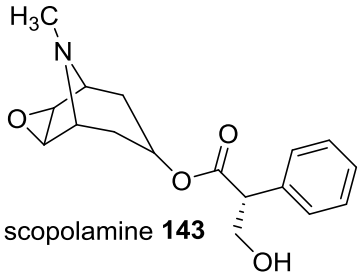

scopolamine **143**

ii. Pyrrolizidine alkaloids

The pyrrolizidine nucleus is distinctive of this group of alkaloids. Majority of pyrrolizidine alkaloids occur in the plants as N-oxides, whose role being lost during the isolation process. Senecionine (**144**) is the popular alkaloid of this type (**Prasanta *et al.*, 2020**).

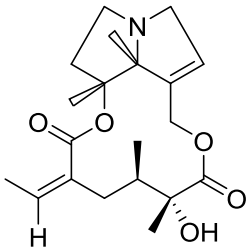

senecionine **144**

iii. Piperidine alkaloids

Piperidine nucleus is the basic ring system of this group of alkaloids. Monocycle compounds with the C5N nucleus is the important feature of true piperidine alkaloids. Presence of odor is the common feature of piperidine alkaloids. They exert chronic neurotoxicity. Many of them are originated from plants. Although piperidine itself is a lysine-derived alkaloid, some of the piperidine alkaloids also derived from acetate, acetoacetate, in an analogous fashion to the simple pyrrolidine alkaloids. Lobeline (**145**) is one of the important alkaloids in this group (**Prasanta *et al.*, 2020**).

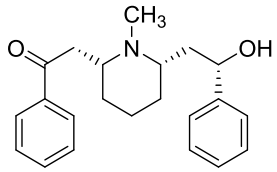

lobeline **145**

iv. Quinoline alkaloids

This type of quinolone-nucleus-containing alkaloid is achieved exclusively from the bark of the Cinchona plant. But a variety of simple heteroaromatic quinolines are also isolated from various marine sources (4,8-quinolinediol from cephalopod ink and 2-heptyl-4-hydroxyquinoline from a marine pseudomonad). The major alkaloid of this specific group is cinchonine (**146**), cinchonidine(**147**), quinine(**148**), and quinidine(**149**) (**Prasanta *et al.*, 2020**).

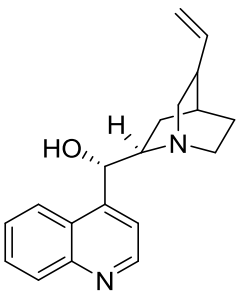

Cinchonine **146**

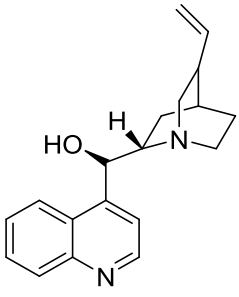

Cinchodinine **147**

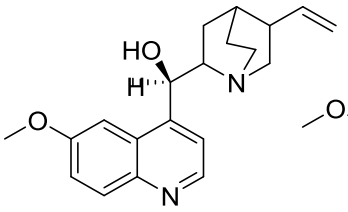

Quinine **148**

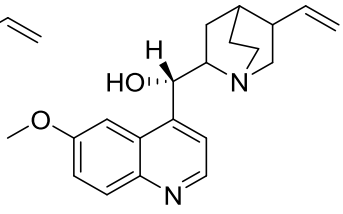

Quinidine **149**

v. Isoquinoline alkaloids

Isoquinoline alkaloids are an extremely large group of alkaloids mostly occurring in higher plants, but few groups are also isoquinolinoid marine alkaloids. Isoquinoline nucleus is the basic structural feature. These groups of alkaloids have huge types of medicinal properties like antiviral, antifungal, anticancer, antioxidant, antispasmodic, and an enzyme inhibitor. Morphine (**135**) and codeine (**150**) are the major and widely studied isoquinoline alkaloids. They are derived from tyrosine or phenylalanine. They are made from a predecessor of dopamine (3,4-dihydroxytryptamine) associated with a ketone or aldehyde. This group of alkaloids is further classified as follows: Simple isoquinoline alkaloids (e.g., salsoline(**151**), mimosamycin (**152**)),benzylisoquinoline alkaloids (e.g., reticuline(**153**), imbricatine(**154**)), bisbenzylisoquinoline alkaloids (e.g., fumaricine(**155**)), manzamine alkaloids (e.g., manzamine A(**156**)), pseudobenzylisoquinoline alkaloids (e.g., polycarpine(**157**), ledecorine(**158**)), secobisbenzylisoquinoline alkaloids (e.g., baluchistanamine(**159**)),

isbenzylisoquinoline alkaloids containing one ether link (e.g., dauricine(**160**)), bisbenzylisoquinoline alkaloids containing two ether links (e.g., berbamine(**161**)), bisbenzylisoquinoline alkaloids containing aryl links only (e.g., pisopowetine(**162**)), bisbenzylisoquinoline alkaloids containing one aromatic link and one or two ether links (e.g., rodiasine(**163**)) (**Prasanta *et al.*, 2020**).

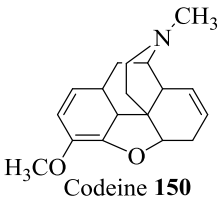
Codeine **150**

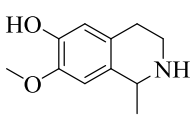
Salsoline **151**

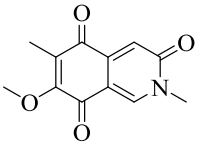
Mimosamycin **152**

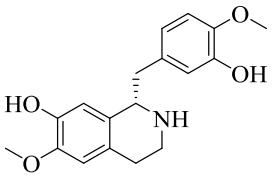
Reticuline **153**

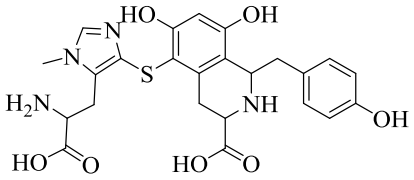
Imbricatine **154**

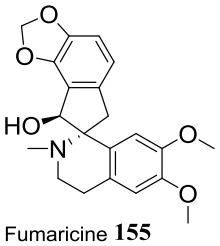
Fumaricine **155**

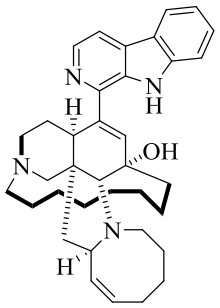
Manzamine A **156**

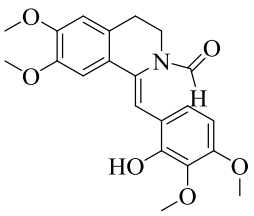
Polycarpine **157**

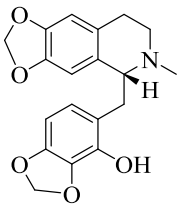
Ledecorine **158**

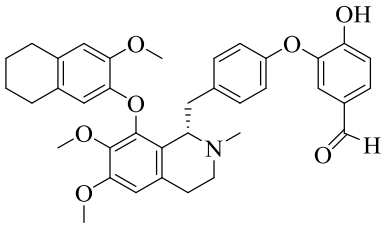
Baluchistanamine **159**

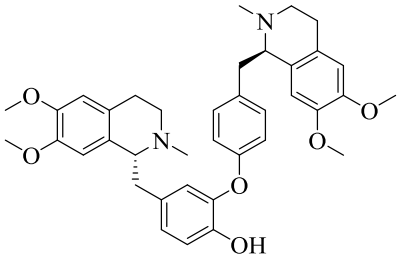
Dauricine **160**

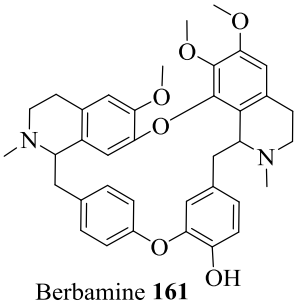
Berbamine **161**

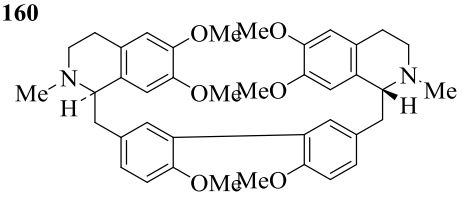
Pisopowetine **162**

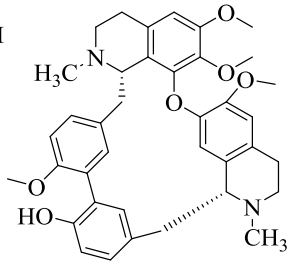
Rodiasine **163**

vi. Indole alkaloids

This is the largest and most interesting alkaloid group derived from tryptophan. The important alkaloids from this group include simple tryptamine derivatives, carbazoles (where the ethanamine chain has been lost), a diversity of alkaloids where one or more prenyl residues are combined with tryptamine, and others where integration of regular monoterpenoid or diterpenoid units occurred. Although structural diversity varies according to the terrestrial and marine source, classical research studies have been carried out on alkaloids from both origins and the fungal source. Polyhalogenation is a common feature of these alkaloids. They are further classified as follows: simple indole alkaloids (e.g., Aplysinopsin (**164**)), bisindoles (e.g., Indirubin (**165**)), simple tryptamine alkaloids (e.g., Tryptamine (**166**)), cyclotryptamine alkaloids (e.g., Physostigmine (**167**)), quinazolinocarbazole alkaloids (e.g., Rutaecarpine (**168**)), β-carboline alkaloids (e.g., Harman(**169**)), carbazole alkaloids (e.g., Ekeberginine (**170**)), indolonaphthyridine alkaloids (e.g., Canthin-6-one (**171**)), ergot alkaloids (e.g., ergotamine (**172**)) (**Prasanta *et al.*, 2020**). (See base structure in scheme 2.)

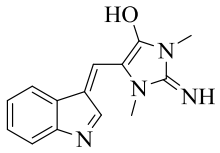

Aplysinopsin **164**

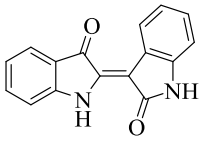

Indirubin **165**

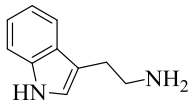

Tryptamine **166**

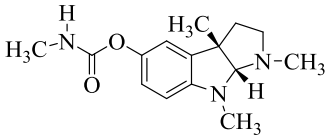

physostigmine **167**

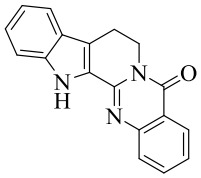

Rutecarpine **168**

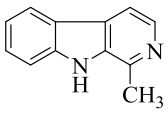

Harman **169**

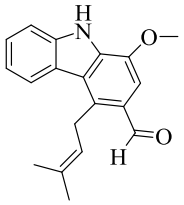

Ekeberginine **170**

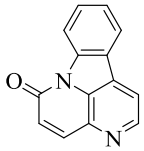

Cathin-6-one **171**

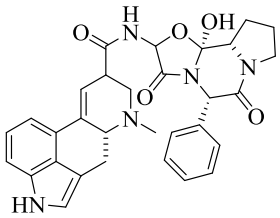

Ergotamine **172**

vii. Steroidal alkaloids

1,2-Cyclopentane phenanthrene ring system is the characteristic of this type of alkaloids. They are typically originated from higher plants, which belong to Liliaceae, Solanaceae, Apocynaceae, Buxaceae families, but some are also isolated from amphibians too. These alkaloids are divided into various other subtypes, among them various types of aminopregnanes are the simplest type. The others types of steroidal alkaloids are Salamandra type (e.g., cycloneosamandione (**173**)), jerveratrum type (e.g., jervine(**174**)), spirosolane type (e.g., soladulcidine (**175**)), solanidine type (e.g., rubijervine(**176**)), cerveratrum type (e.g., 3,6-cevanediol(**177**)), conanine type (e.g., didymeline(**178**)), Buxus type (e.g., cyclobuxine(**179**)), pregnane type (e.g., 20α-dimethylamino-3β-senecioylamino-16β-hydroxy-pregn-5-ene(**180**)), cephalostatins/ritterazines (e.g., ritterazines(**181**)), miscellaneous steroidal alkaloids (e.g., bufotoxin(**182**)) (**Prasanta *et al.*, 2020**). (See base structure in scheme 2.)

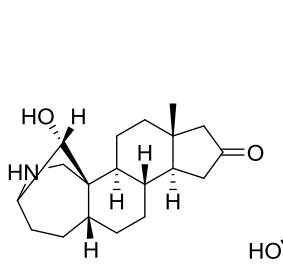

cycloneosamandione **173**

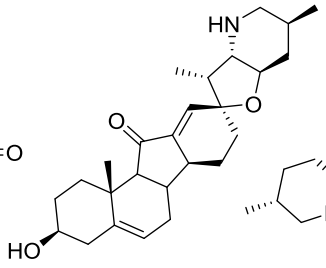

Jervine **174**

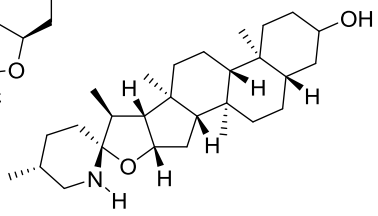

soladulcidine **175**

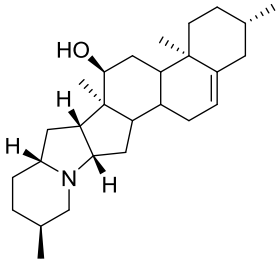

Rubijervine **176**

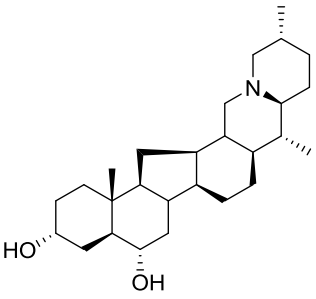

3,6-cevanediol **177**

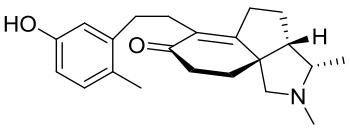

Didymeline **178**

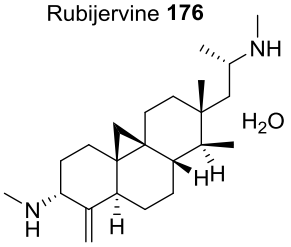

Cyclobuxine **179**

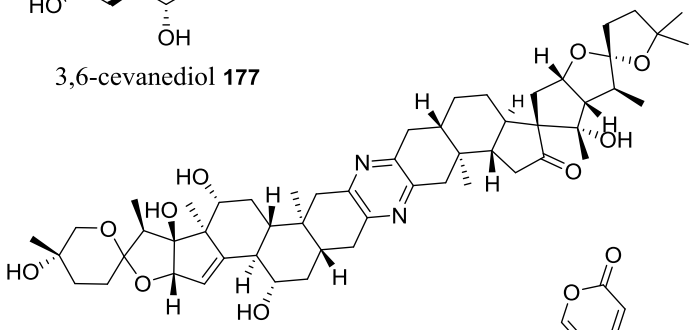

Ritterazines A **180**

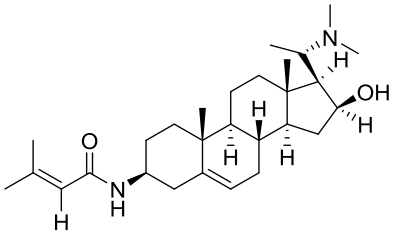

20-α-dimethylamino-3β-senecioylamino-16β-hydroxy-pregn-5-ene **181**

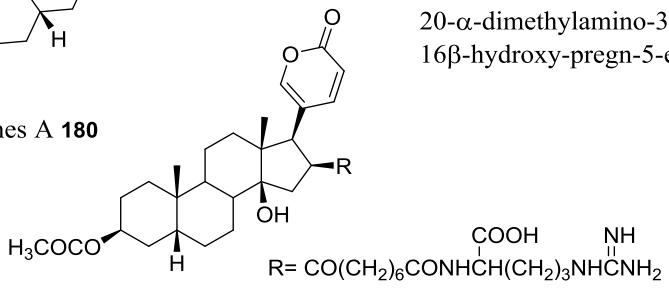

bufotoxin **182**

viii. Imidazole alkaloid

The imidazole ring structure is the characteristic of this type of alkaloid. The imidazole ring of these alkaloids is previously made at the stage of the precursor, so they are an exemption in the ransformation procedure of structures. This type of alkaloids contains numerous structurally different examples, particularly among marine and microbial alkaloids. They display a wide array of biological activities and significant pharmaceutical potential. Pilocarpine (**183**) is the most pharmaceutically significant imidazole alkaloid (**Prasanta *et al.*, 2020**). (See base structure in scheme 2.)

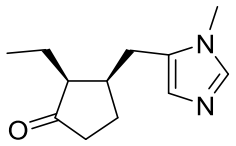

Pilocarpine **183**

ix. Purine alkaloids

Purine is the nitrogenous base of nucleotide (building block of DNA and RNA), which consist of purine ring and pentose sugar along with another base pyrimidine. Caffeine, Theophylline and Theobromine are typical examples of purine alkaloids. They are popular as plant alkaloids, but they can be also originated in marine organisms with substituted purines (e.g., Phidolopin (**184**)) and a variety of terpenoid-purine alkaloids, such as the age lines and others (**Prasanta *et al.*, 2020**). (See base structure in scheme 2.)

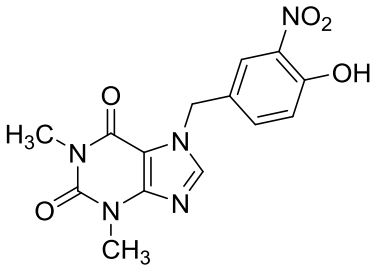

Phidolopine **184**

x. Pyrrolidine alkaloids

Pyrrolidine nucleus constitutes the basic nucleus of pyrrolidine alkaloids. Many pyrrolidine alkaloids are known from plants. Hygrine (**185**) (biosynthesized from ornithine), ficine (**186**) (where the pyrrolidine ring is involved to a flavone nucleus), and brevicolline (**187**) (wherein it is attached to a β-carboline unit) are some examples of this type of alkaloids (**Prasanta *et al.*, 2020**). (See base structure in scheme.)

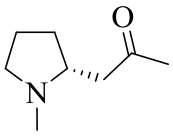

Hygrine **185**

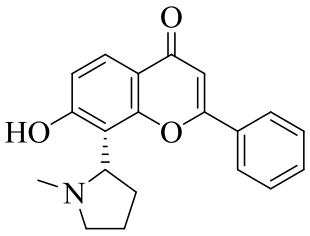

Ficine **186**

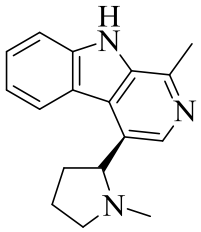

Brevicoline **187**

I.2.1.3 Test for alkaloids

Here, we would describe some three methods used by by scientists to test for the presence of alkaloids. These are: Wagner's test, Hager's test and Dragendorff's test.

Wagner's test: The plant extract is added in test tube. Few drops of Wagner's reagent were added to the test tube. A yellow or reddish-brown precipitate is formed indicating the presence of alkaloids **(Mistry *et al*., 2016; Suryawanshi and Vidyasagar, 2016)**.

Dragendorff's test: The sample is mixed with few drops of acetic acid followed by Dragendorff's reagent. Orange red precipitate is formed indicating the presence of alkaloids (**Mistry *et al*., 2016)**.

Hager's test: To 2 mg of the extract taken in a test tube, a few drops of Hager's reagent were added. Formation of a yellow precipitate confirmed the presence of alkaloids (**Suryawanshi and Vidyasagar, 2016)**.

I.2.1.4 Biosynthesis of Monoterpenes Indole Alkaloids (MIAs)

Here, we are going to look at a proposed general schematic of biosynthesis of MIA (Monoterpene indole alkaloids) and biosynthetic pathway for akuammiline and akuammicine class of alkaloids. The proposed general Scheme of biosynthesis of MIA is described in the figure below **(Koma *et al*., 2020).** .

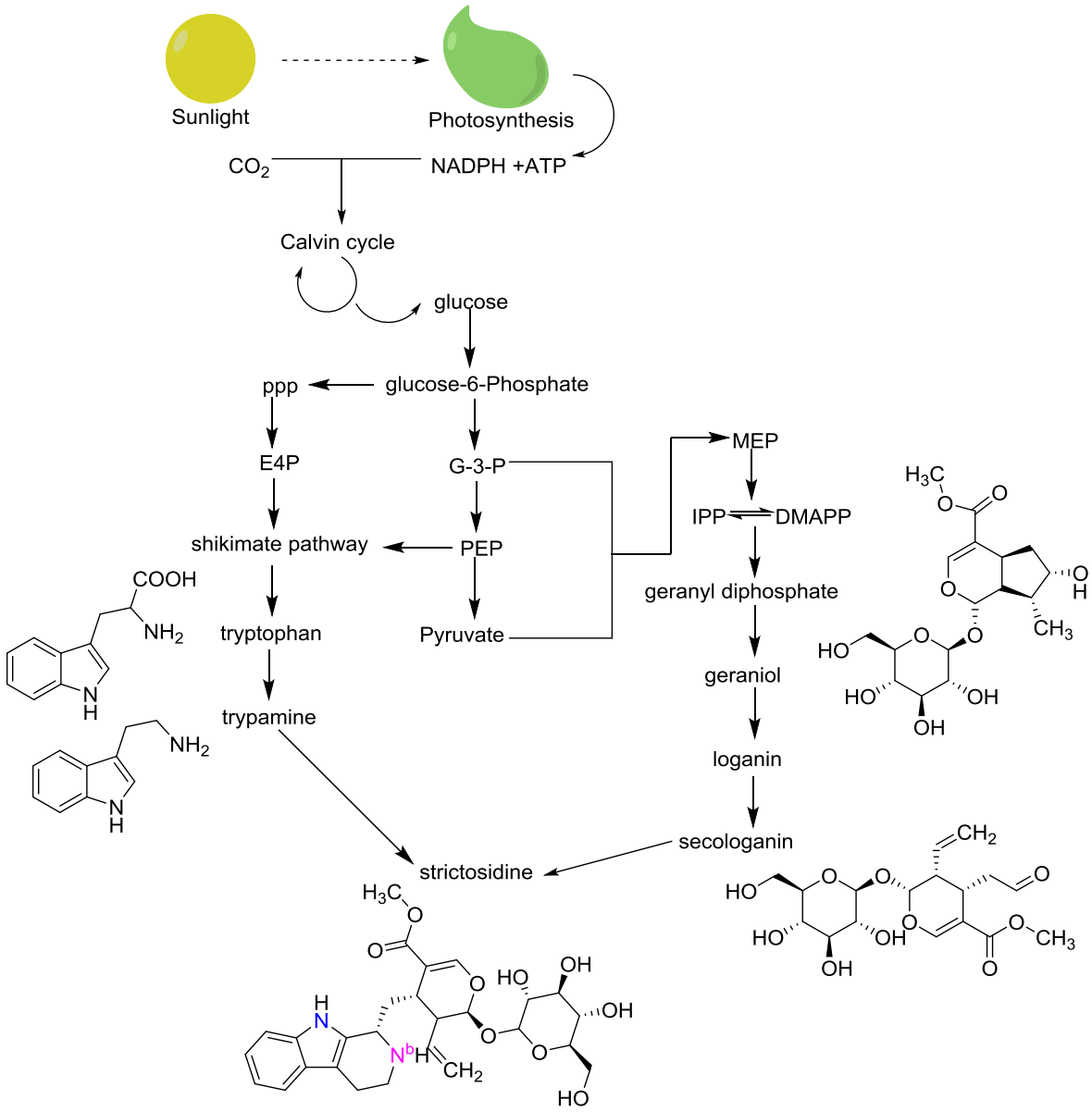

Scheme 3: Proposed biosynthetic pathway for monoterpenoid indole alkaloids (MIAs) synthesis (Koma *et al*., 2020)

The biosynthesis of akuammiline includes cyclization of strictosidine and reduction of iminium ion resulted into geissoschizine (corynanthe alkaloids). Further, C_7–C_{16} bond in akuammiline alkaloids has been formed by the secondary cyclization

involving oxidative dearomatization of the indole ring with an intramolecular attack of the 1,3-dicarbonyl group.

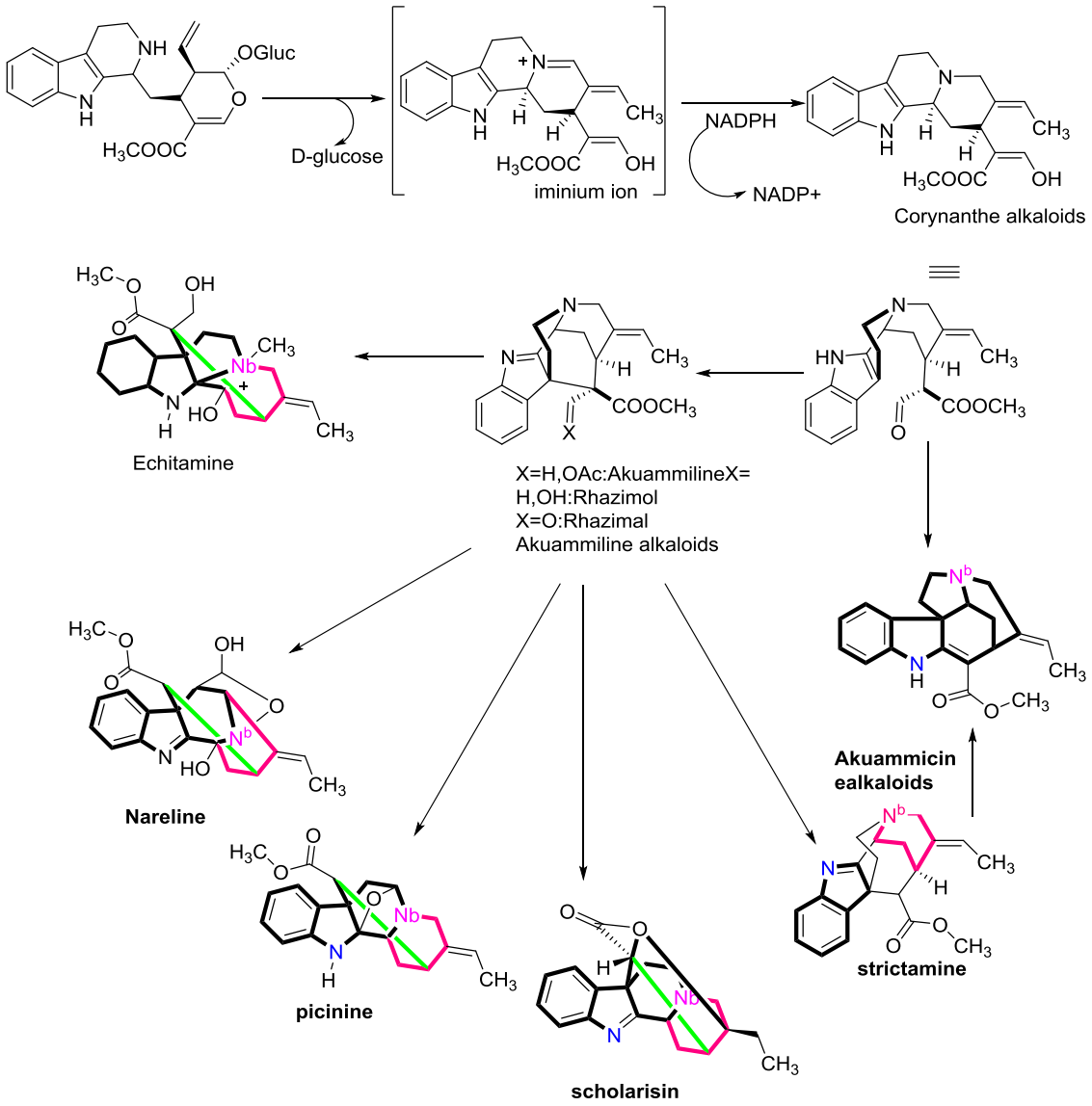

Scheme 4: Proposed biosynthetic pathway for akuammiline and akuammicine class of alkaloids (Koma *et al.*, 2020)

I.2.1.5 Structure elucidation techniques of alkaloids

On the UV spectra of alkaloids, we observe various characteristic peaks which varry from one class of alkaloids to another for example, the uv spectrum of an indole alkaloid like scholaricine presents λ_{max}^{MeOH}: 210, 235, 285 and 335 nm; on addition of base the maxima shift to λ_{max}^{MeOH}: 217, 247, 299 and 358 nm characteristic of an anilino-acrylate

chromophore (This suggests the presence of aphenolic OH group in the molecule) (**Atta-Ur-Rahman *et al.* 1985**). The IR spectrum of some alkaloids gives absorptions at 3500 cm^{-1} (OH), 3400 cm^{-1} (NH) and 1660 cm^{-1} (α,β unsaturated ester, C=O). The NH proton appears as a singlet at about δ 8.5 (**Atta-Ur-Rahman *et al.* 1985**).

I.2.2 Triterpenes

I.2.2.1 Definition and basics of triterpenes

Terpenoids or isoprenoids constitute one of the richest classes of natural products with a great diversity in structure even though all are constructed from the same 5-carbon compound called isoprene. More than 30,000 terpenoids have been isolated from plants, both marine and terrestrial with new compound being discovered yearly. Terpenoids include terpenes and steroids which is gradually gaining the status of a class of its own accord. The different terpenoids could be acyclic, mono-, di-/bi-, tetra- or penta-cyclic structures which frequently carries a functional group (**Adenot, 2000**). Terpenoids are common in living organisms where they could be found in the free form, as esters or glycosides. Mono- and sesqui-terpenes are common in essential oils of plants, di-, sesqui-, and triterpenes are found in balsam, resins and higher plants.

The majority of triterpenoids are 6-6-6-5 tetracycles, 6-6-6-6-5 pentacycles, or 6-6-6-6-6 pentacycles types.

I.2.2.2 Classification of triterpenes

The pentacyclic triterpenes are classified in several structural groups and are made up of rings generally noted A, B, C, D, and E. Certain groups consist of five rings with six carbon atoms in each of the rings, others have rings with five or seven carbon atoms in their skeleton (**Mahato and Kundu, 1994**). Glycosylation can take place on each one of these structural groups. When this occurs, the natural products formed are called saponins. Triterpene skeleton always have at the beginning a hydroxyl group fixed on C-3 carbon. This hydroxyl group can serve as the point of linkage between triterpenic and osidic skeletons (**Mahato and Kundu, 1994**). The table below gives some structural groups of pentacyclic triterpenoids.

i. Classification of pentacyclic triterpenes

The classification of pentacyclic triterpenes is based on the structure of the carbon skeleton of the saturated hydrocarbon from which it is derived. Amongst the pentacyclic triterpenes, we have the symmetric (cycle A, B, C, B', A') and non-symmetric triterpenes (cycle A, B, C, D, E).

a) Symetric**:** (Rings A, B, C, B', A')

- Ring C opened
- Ring C closed

b) Asymmetric**:** (Rings A, B, C, D, E)

- Ring E with 5 corners.
- Ring Ewith 6 corners :
- Methyl groups 29 and 30 attached on carbon 20.
- Methyl groups 29 and 30 attached on carbons 19 and 20 respectively.

ii. Differents structural groups of triterpenes

The schemes 7, 8 and 9 represent the diffferent structural groups of pentacyclic triterpenes.

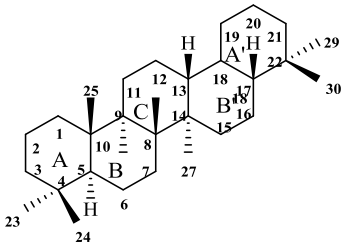

Gammacérane (**188**)

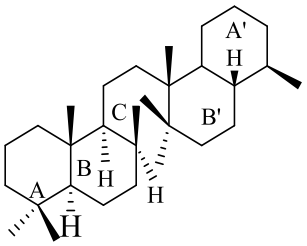

Lanostane (**189**)

Scheme 5: Pentacyclic triterpenes with ring B closed: Gammacerane (188) and ring C opened: lanostane (189) (Mahato and Kundu, 1994)

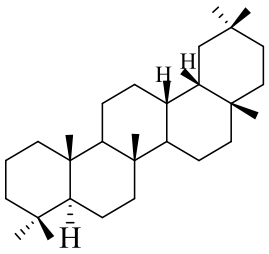

Oleanane (**190**)

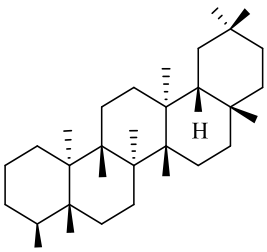

Friedelane (**191**)

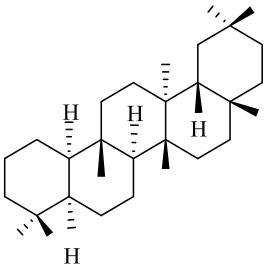

Glutinane (**192**)

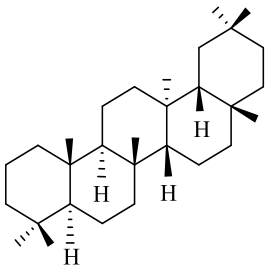

Taraxerane (**193**)

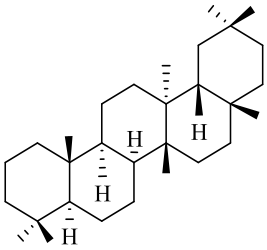

Multiflorane (**194**)

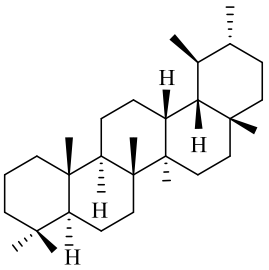

Ursane (**195**)

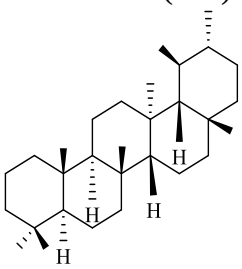

Friedoursane (**195**)

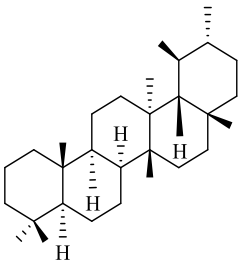

Bauerane (**196**)

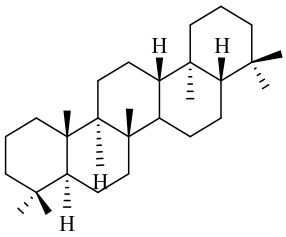

Serratane (**197**)

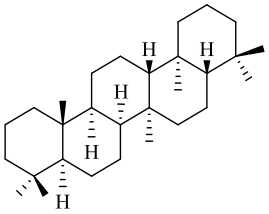

Friedogammacerane (**198**)

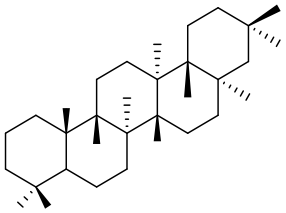

Stitane (**199**)

Scheme 6: Different structural groups of pentacyclic triterpenes with ring E having 6 carbons (Mahato and Kundu, 1994)

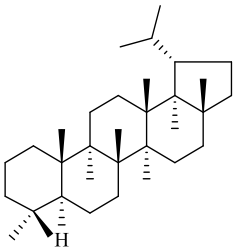
Lupane (**200**)

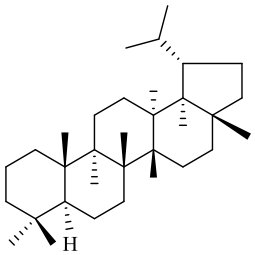
Friedolupane (**201**)

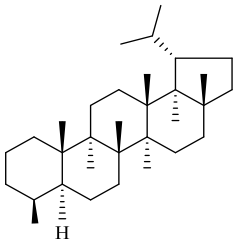
Friedolupane(A) (**202**)

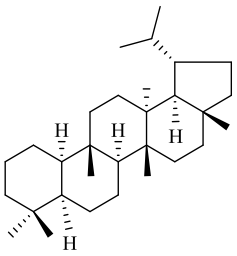
Friedolupane (B) (**203**)

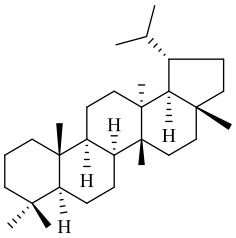
Friedolupane (C) (**204**)

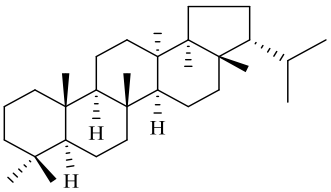
lupane (**205**)

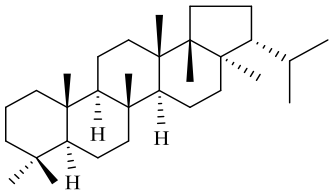
Neolupane (**206**)

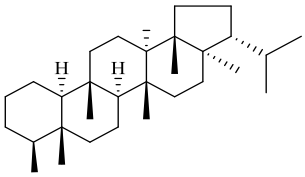
Filicane (**207**)

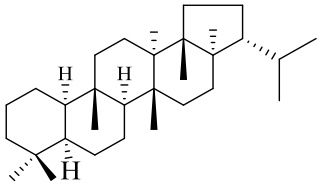
Adianane (**208**)

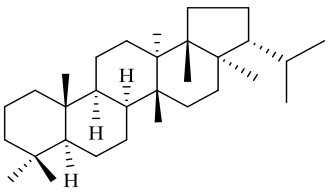
Fernane (**209**)

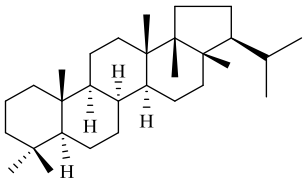
Arborane (**210**)

Scheme 7: Different structural groups of pentacyclic triterpenes with ring E having 6 carbons (Mahato and Kundu, 1994)

I.2.2.3 Biosynthesis of triterpenes

i. Synthesis of IPP and DMAPP

Mevalonate-route triterpene biosynthesis begins with a Claisen condensation reaction between two molecules of acetyl-CoA molecules catalyzed by acetoacetyl CoA-thiolase to give acetoacetyl-CoA (Hung-wen, 2010). A second aldolique condensation reaction with a third acetyl-CoA molecule then results in a compound of six-carbon, (*S*)-hydroxy-3-methylglutaryl coenzyme A (HMGCoA). HMG-CoA is then reduced to mevalonate by HMGR (HMG-CoA reductase). Mevalonate is then converted to phosphomevalonate and then to diphosphomevalonate via two consecutive phosphorylation reactions involving the hydrolysis of adenosine-5'-triphosphate (ATP), the first of which is catalyzed by mevalonate kinase and the second by phosphomevalonate kinase **(Hung-wen, 2010; Tarek, 2012)**.

Diphosphomevalonate is then converted to isopentenyl diphosphate (IPP) by diphosphomevalonate decarboxylase. In this step, the CO_2 release of diphosphomevalonate occurs in conjunction with the hydrolysis of ATP to adenosine 5'diphosphate (ADP). Finally, IPP is converted into its isomer dimethylallyl diphosphate (DMAPP) by the action of IPP isomerase **(Hung-wen, 2010; Tarek, 2012)**. The sequence thus described is illustrated by **(Scheme 10)** below.

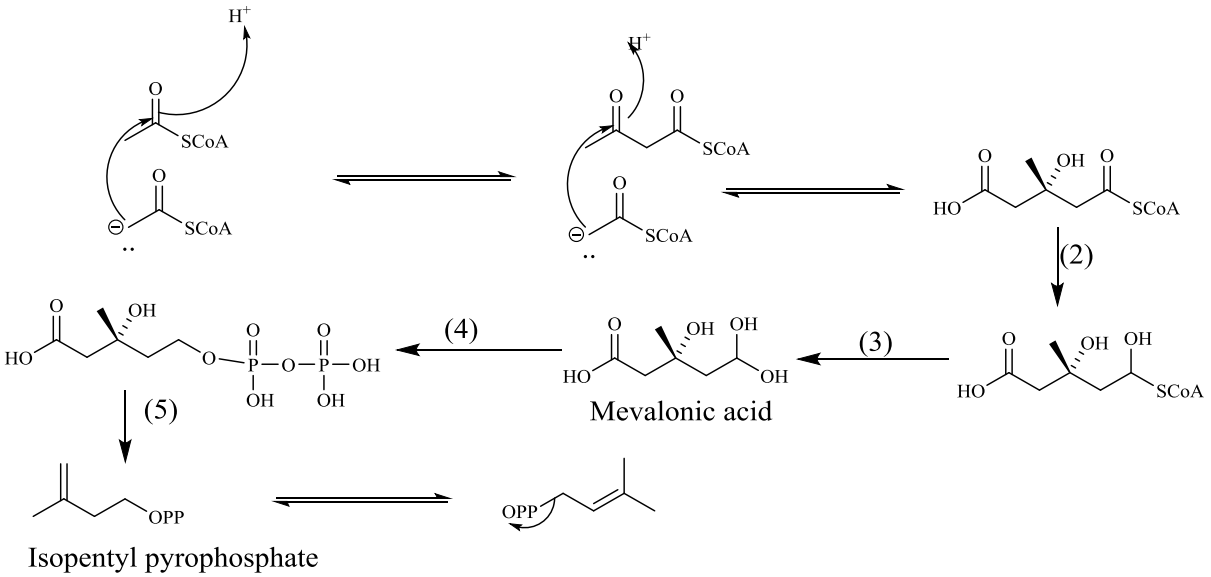

Scheme 8: Biosynthesis of isopentenyldiphosphate (Hung-wen, 2010)

ii. Biosynthesis of squalene

After isomerization of IPP to DMAPP, the two isomers will undergo head-tail condensation to form geranyl pyrophosphate (GPP) precursors of monoterpene (C10). Head-tail condensation of this same compound with IPP leads to farnesyl pyrophosphate (FPP). This molecule is the precursor of sesquiterpenes (C15). The addition of a IPP molecule on the FPP gives geranyl-geranyl-pyrophosphate (GGPP), precursor of diterpenes (C20); Then the IPP is added to the GGPP to give geranylfarnesyl pyrophosphate (GFPP), precursor of sesterterpenes (C25). Although all these isoprene units are connected head to tail, the formation of squalene involves a tail-to-tail condensation of two FPP molecules as well as the formation of tetraterpenes by condensation of two GGPP molecules **(Bruneton, 1999; Tarek, 2012)**.

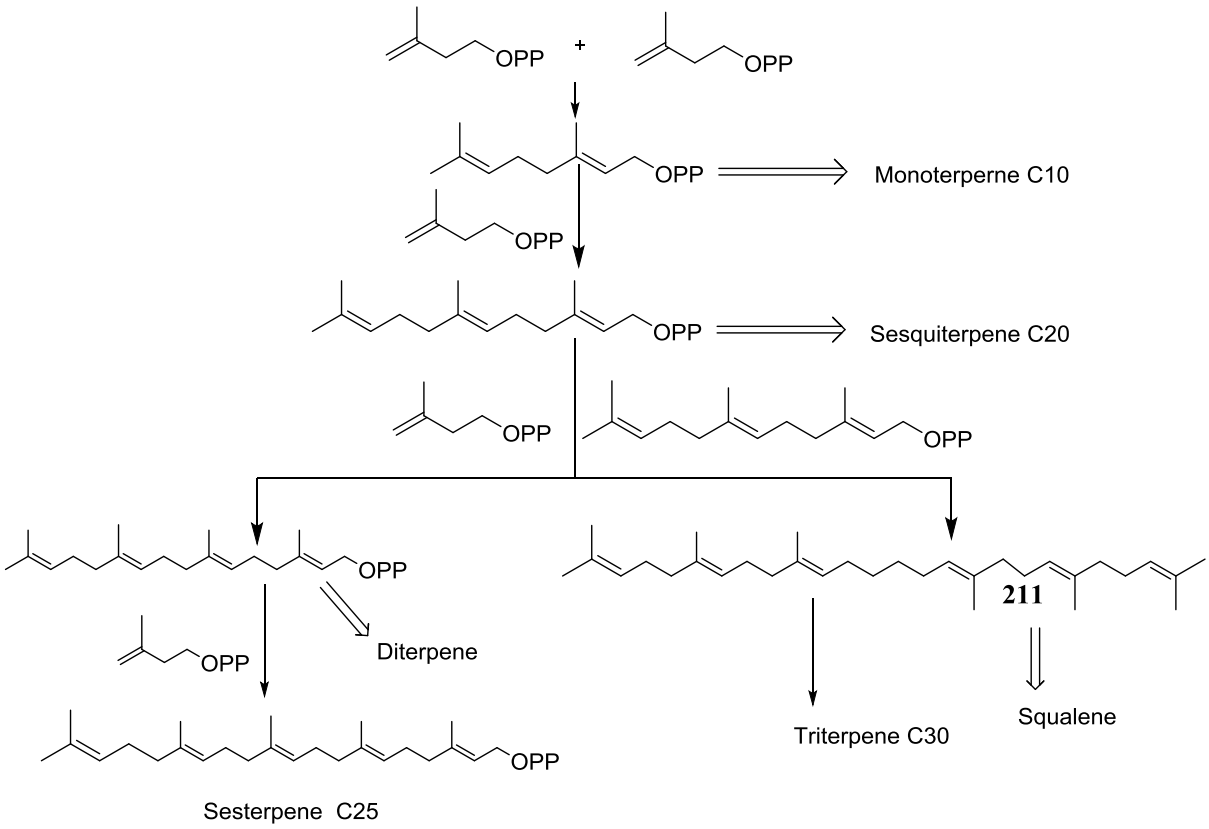

Scheme 9: Squalene formation (Bruneton, 1999; Tarek, 2012)

iii. Squalene cyclization

Before starting cyclization, the squalene undergoes oxidation to give epoxy-2,3-squalene **(Scheme 10)**. The opening of this epoxide initiates cyclization. The enzyme responsible for this cyclization stabilizes the conformation of the polyisoprene in such a way that stereoelectronic requirements are met **(Bruneton, 1999)**.

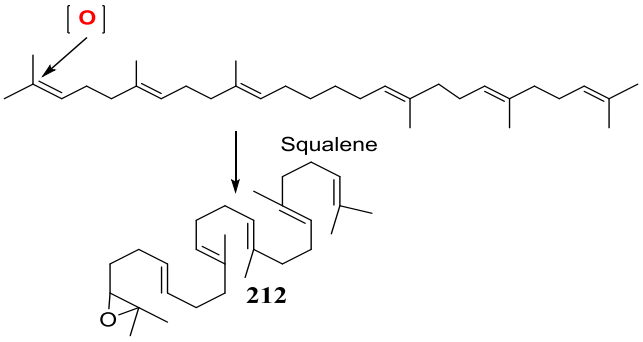

Scheme 10: Formation of epoxysqualene (Bruneton, 1999)

It is on the initial conformation of epoxysqualene (**168**) on the surface of the enzyme that the orientation of biosynthesis towards tetra- and pentacyclic triterpenes as well as steroids depends **(Bruneton, 1999)**.

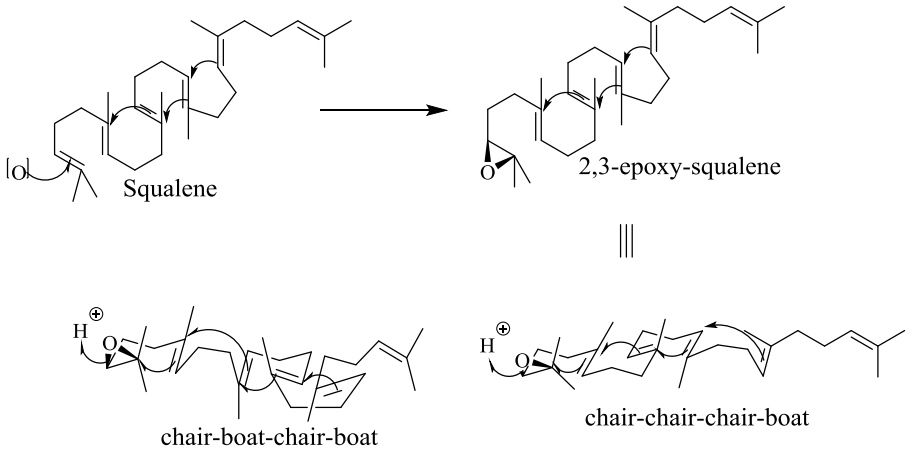

Scheme 11: Cyclization of squalene (Bruneton, 1999)

If epoxysqualene adopts the conformation chair-chair-chair-boat, cyclization results in another cation called dammaranyl cation which leads to pentacyclic triterpenes of type lupane, ursane, oleanane etc **(Bruneton, 1999)**.

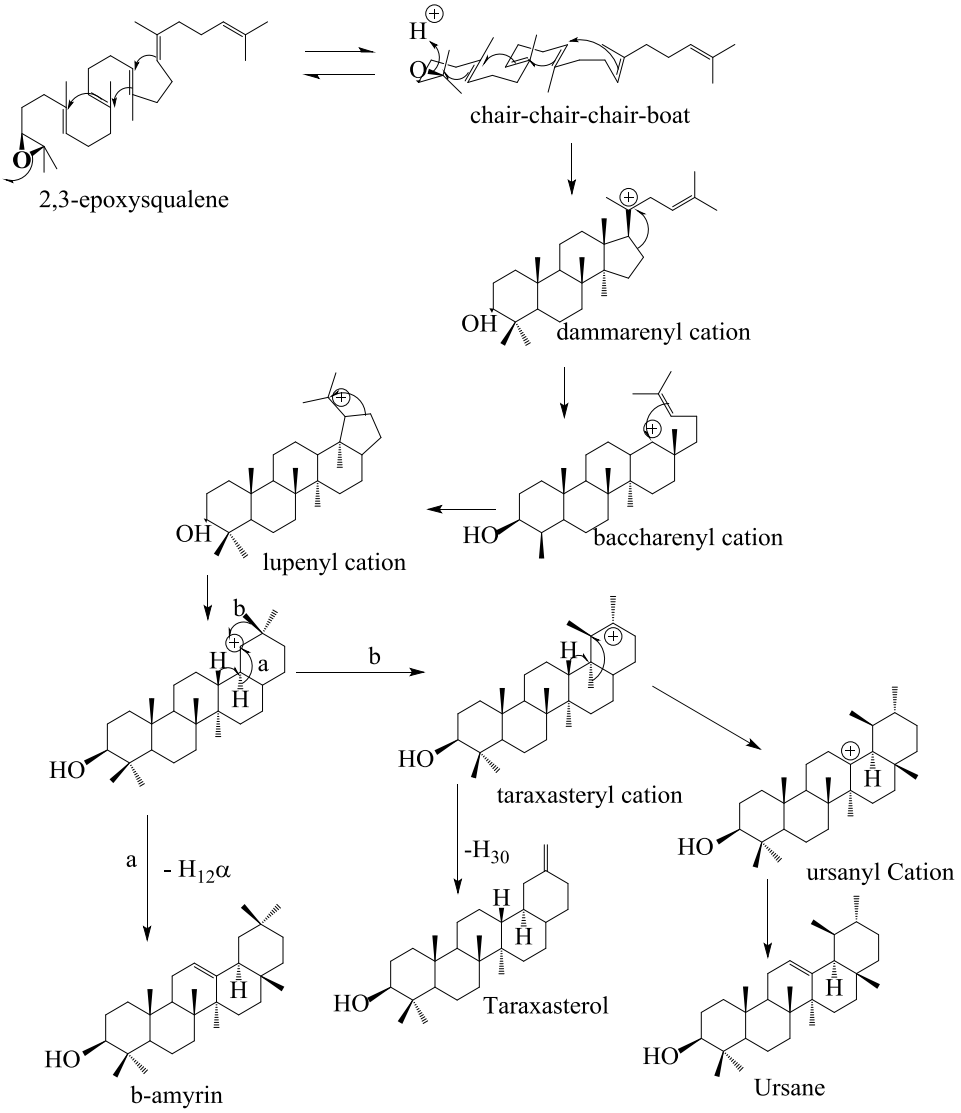

Scheme 12: Cyclisation of 2,3-eposysqualene to pentacyclic triterpenoid (Bruneton, 1999)

I.2.2.4 Test for triterpenes

Two ypes of tests can be used to test for the presence of triterpenes namely: Liebermann - Burchard's test and Salkowaski's test.

Liebermann-Burchard's test: 2 mg of dry extract is dissolved in acetic anhydride, heated to boiling, cooled and then 1 ml of concentrated sulphuric acid is added along the sides of the test tube. Formation of a violet colored ring indicates the presence of triterpenoids (**Suryawanshi and Vidyasagar, 2016**).

Salkowaski test: A few drops of concentrated sulphuric acid are added to the test solution, shaken and allowed to stand, lower layer turns yellow indicating the presence of triterpenoids (**Suryawanshi and Vidyasagar, 2016**).

I.2.2.5 Structure elucidation techniques of triterpenes

Mass spectroscopy is used to establish the molecular weight of the compound under analysis. Soft ionisation techniques such as ESI, FAB, MALDI, direct ionization and chemical ionization are commonly used to establish the mass of steroids, triterpenoids and their saponins from pseudomolecular ion peaks on the spectrum (**Yang *et al* 2014; Bonfill *et al.*, 2005**). EI is also frequently used to get the molecular mass directly from the molecular ion peak and information concerning the structure of a molecule is provided by fragmentation patterns observed on the EI-MS. The most prominent fragmentation pattern shown by pentacyclic triterpenoids is that due to a RDA reaction common in tritepenoids with a double bond. This usually leads to a base peak at m/z 218 and a prominent peak at m/z 203 on simple unsubstituted triterpenoids like α and β-amyrin. It is thus possible to get more information about the structure of a substituted triterpenoid by making deductions from the distinctive peaks, oleanolic and ursolic acid show base peak at m/z 203 and other prominent peaks at m/z 203 + COOH and 218 + COOH (**Ogunkoya, 1981**).

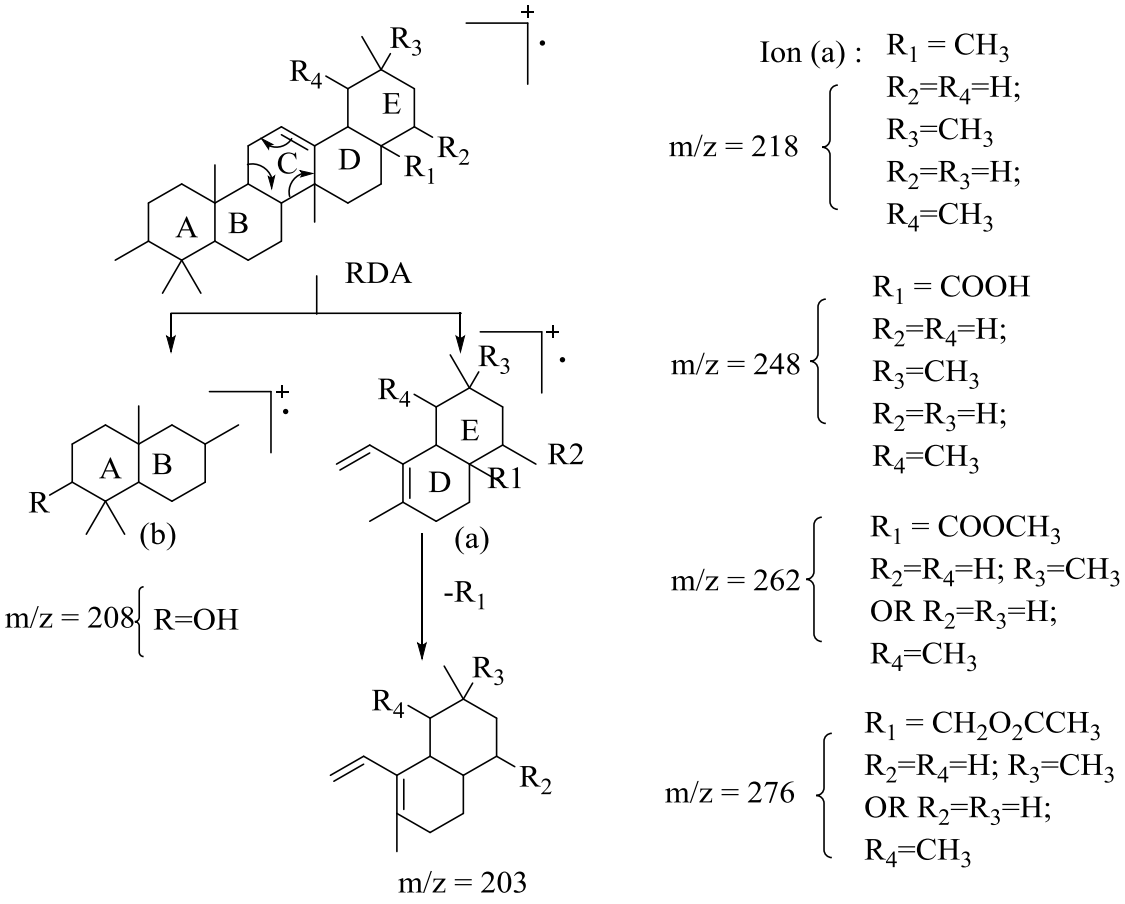

Scheme 13: Retro-Diels-Alder fragmentation pattern for Oleanane and Ursane type triterpenoids (Ogunkoya, 1981)

By simple inspection of the mass spectrum of an unknown triterpenoid, it is possible to decide whether the compound belongs to the oleanane and ursane-type (Δ^{12}) or otherwise (Δ^{14}, Δ^{18}). The RDA reaction usually occurs in the ring which bears a double bond. For the Δ^{12} triterpenoids it occurs in ring C, leading to base peak at 218 or 203, and diagnostic peaks at m/z between 200 and 300 as shown in the chart above. Δ14 triterpenoids like taraxerol undertake a ring D RDA reaction in which rings A, B, and C are retained, leading to base peak at m/z 302, 300 for taraxerol and taraxerone respectively with prominent peaks at 204 (**Djerassi, 1964**). However, oleanane and ursane-type triterpenoids cannot be distinguished by mass spectrometry, since they show identical fragmentation process- the RDA reaction involving the Δ^{12} double bond.

NMR methods have indisputably become the single most important spectroscopic techniques for the identification and structure elucidation of most organic compounds including triterpenoids. Several 1D and 2D NMR experiments are now commonly used for

the characterisation of pentacyclic triterpenes. These methods include ^{1}H- and ^{13}C-NMR, APT, DEPT, COSY, HMQC, HMBC and TOCSY. Notwithstanding, other spectroscopic techniques such as IR, UV, and especially mass spectrometry are still frequently useful. Triterpenoids are easily identified on the ^{1}H NMR by the appearance of between four and eight very intense peaks in the 0.50 to 2.00 ppm region, each integrating for three protons. These readily discernable peaks are the angular methyls on the triterpenoid structure. Most triterpenoids are hydroxylated at position 3 of the triterpenoids structure, hence the oxymethine proton appear between 3.00 and 4.00 ppm. But if the proton attached to the oxygen is substituted by an ester or ether bond, then the oxymethine proton will appear further downfield after 4.00 ppm. Protons attached to any other oxygenated carbon appear downfield after 3.00 ppm; meanwhile protons attached to unsaturated carbons appear further up-field after 5.00 ppm. In the ^{1}H NMR spectrum of oleanane-type triterpenoids, H-18 appears around δ_H 2.20 as a doublet of doublet whereas it appears as a doublet around δ_H 2.50 in ursane-type triterpenoids. When the methyl C-17 is oxidized to carboxylic acid, the proton H-18 undergoes an attractor effect of the acid which then moves it downfield to about δ_H 2.84 for oleanane-type molecules and δ_H 2.40 for ursane-type.

The proton NMR spectrum must be corroborated by other NMR experiments. The ^{13}C NMR experiment is the finger print of any molecule; it is different even for two very close molecules. Triterpenoids show 30 signals on their broad band proton decoupled ^{13}C NMR spectrum, except in cases where more than one carbon atoms possess same magnetic environment and hence the same chemical shift value, reducing the number of signals or when other molecules add up to triterpenoids, increasing the number of signals. Some triterpenoids are said to be “Oleanane-type” or “Ursane-type” and “Lupane-type” (**Mahato and Kundu, 1994**). These model compounds are quickly distinguished on their ^{13}C NMR spectrum by the appearance of some unique signals pertaining to the olefinic carbons at C-12 and C-13: Olean-12-enes have signals approximately at δC 122 and 145 ppm respectively; Urs-12-enes have signals at δC 124 and δC 139 ppm; and lup-20(29)-enes have signals at δC 109 and 150 ppm for C-20 and C-29 respectively. Evidently these resonances are affected by the introduction of substituents (Mahato and Kundu, 1994). The ^{13}C DEPT experiments, especially DEPT 135 help in the differentiation of CH, CH_2 and CH_3 in the molecule. In addition to the above, 2D NMR experiments; HMQC, HMBC, NOESY and TOSY experiments are important tools for the unambiguous elucidation of the structures of unknown molecules. The HMQC or HSQC permits attribution of protons to particular carbon-atoms,

the HMBC allows for connectivity between protons and the carbon atoms adjacent to the one bearing the proton usually up to 2 or 3 bonds apart (^{2}J, ^{3}J), but sometimes ^{4}J occurs. The HMBC is very important in establishing a link between parts of the same molecule (**Mahato and Kundu, 1994**). The proton on C-18 is very useful in that it connects easily to other carbons of the molecule on HMBC, thus indicating the position of olefinic carbons and usually the carbonyl function at C-28. NOESY helps in the attribution of the relative stereochemistry around stereogenic centres. TOCSY is very useful in the elucidation of the structure of saponins. Literature study is indispensible for the elucidation of the structures of triterpenoids. It is relatively easier nowadays to identify an unknown triterpenoid molecule from its spectroscopic and physical data than it was two decades now. This is possible due to the presence of tables that compile some outstanding features of triterpenoids, permitting quick comparison with new NMR data (**Mahato and Kundu, 1994**). In this compilation, pentacyclic triterpenoids are further classified into different classes based on their carbon-skeleton. Oleanane type and Ursane type triterpenoids, based on the way methyl groups are attached on position 19 and 20 of the pentacyclic skeleton. Oleanane when two methyls are attached to position 20 and Ursane when one methyl is attached to each of the positions. The above arrangement has a remarkable impact on the ^{1}H NMR spectrum, appearance of two doublet methyl doublets on the spectrum of an ursane type molecule whose protons at 19 and 20 have not been oxidised (**Mahato and Kundo, 1994**).

I.2.3 Quinones

I.2.3.1 Definition of quinones

Quinones are conjugated cyclic diketones. They are molecules comprised of a basic benzoquinone chromophore, which is an unsaturated cyclic structure with two carbonyl groups **(John and Marjorie, 2023)**.

I.2.3.2 Classification of quinones

They can be classified into three main classes: benzoquinones, naphthoquinones, and anthraquinones.

i. Benzoquinones

As previously described, the benzoquinone-type structure forms the basic unit of quinones. Therefore, benzoquinones serve as an important building block in quinone

biosynthesis. In nature, benzoquinones are found in flowering plants, fungi, lichens, and insects **(Gorman *et al*., 2003)**. (See base structure in scheme 14.)

ii. Naphtoquinones

Naphthoquinones are molecules structurally related to naphthalene. Naphthoquinone structure consists of a benzene ring linked to conjugated cyclic diketone, with the two carbonyl groups arranged in the *para* orientation (1,4-naphthoquinones) and rarely in the *ortho* orientation (1,2-naphthoquinones) **(Gorman *et al*., 2003)**. It has been reported that 1,4-naphthoquinones can act as electrophiles in Michael-type additions due to the presence of a highly electron-deficient double bond in their structure. Considering that the tautomeric forms of 1,4-naphthoquinones (named 1,4-naphthohydroquinones or 1,4-dihydroxynaphthalenes) can act as nucleophiles and couple with their corresponding naphthoquinones, dimeric naphthoquinones can also be found in nature **(Gorman *et al*., 2003)**. Naphthoquinones are biosynthesized by a wide variety of organisms, including plants and fungi. (See base structure in scheme 14.)

iii. Anthraquinones

The third class of quinones is anthraquinones, which are compounds derived from anthracene. The structure of anthraquinones is comprised of a planar three-ring aromatic system, with two carbonyl groups in the central ring. Thus, the basic structure of these molecules is known as 9,10-anthracenedione or 9,10-dioxoanthracene **(Moss, 1973)**. Anthraquinone derivatives include hydroanthraquinones (compounds obtained by the reduction of double bonds in the benzene ring), anthrols (analogs with one –OH group in the central ring), anthrones derivatives with one carbonyl group in the central ring), dimeric anthraquinones, and naphthodianthrones **(Moss, 1973)**. (See base structure in scheme 14.)

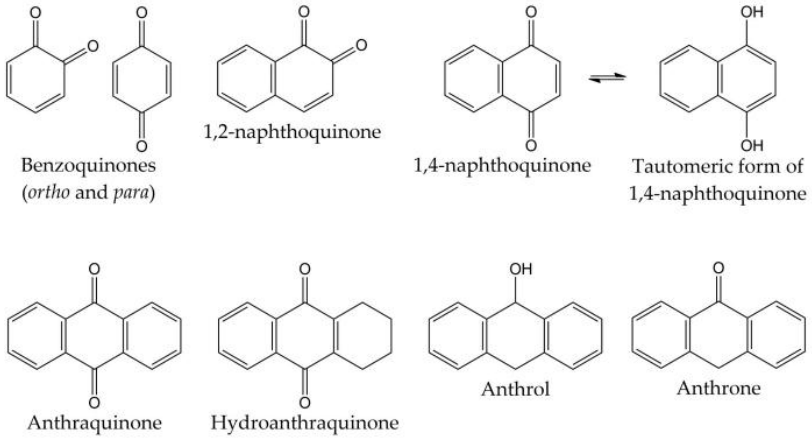

Scheme 14: Chemical structures of the different types of quinones (Abegaz, 2002)

I.2.3.3 Biosynthesis of quinones

We distinguish two biosynthesis pathways for quinones namely: the acetate/malonate pathway and the shikimic acid pathway.

i. The acetate/malonate pathway

Quinones result from the condensation of acetyle-Coenzyme A, which itself is derived from acetic acid in the presence of Coenzyme A (CoA). Firstly, two units of acetyl coenzyme A condense to produce acetoacetyl-CoA followed by the formation of a polyketide chain which when modified through reduction and cyclisation would produce fatty acids and polyphenols. This route passes inevitably through the formation of β-acetoacetyl-CoA polymers. The scheme of this biosynthesis is as follows:

Scheme 15: Biosynthesis of poly-β-acetoacetylCoA through the acetate/malonate pathway (Herbert, 1989)

The condensation of these polyketides of β-acetoacetyl-CoA generally gives diversed types of quinones through the scheme shown below.

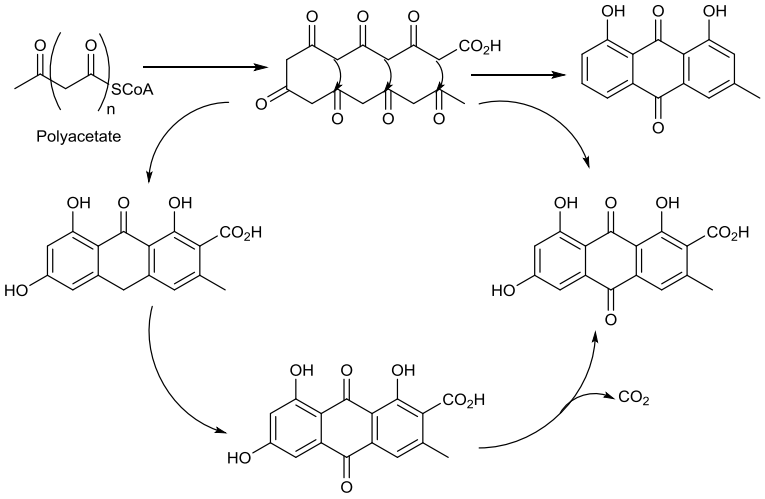

Scheme 16: Formation of quinones through the β-acetoacetyl-CoA polymers (Herbert, 1989)

ii. The shikimic acid pathway

Many of compounds which present the C_6-C_3 linkage come drom shikimic acid. The biosynthesis through the shikimic acid pathway of 1-hydroxy-2-methoxy-9,10-dioxoanthracene illustrated below, passes through the condensation of phosphoenolitic pyruvate with a tetrose (D-Erythrose-4-phosphate) to give 3-deoxy-D-arabinoheptulosanic-7-phosphate (DAHP), a sugar of seven carbons. The biosynthesis scheme is presented in the figure below.

I.2.3.4 Test for quinones

Borntrager Test: Powdered sample is mixed with ether, which is filtered, and to the filtrate add caustic soda and aqueous ammonia. Red, pink or violet colour produced indicates the presence of anthraquinone.

I.2.3.5 Structure elucidation techniques of quinones

i. Spectrometric methods

a. Ultraviolet

Most, if not all, quinones are colored compounds (yellow powder, yellow needles, yellow, orange, dark purple, purple, red, etc. crystal pigments) and absorb strongly when viewed on a UV lamp. This is due to the presence of carbonyl-olefinic chromophores.

- **Benzoquinones**

The spectrum of p-benzoquinone is characterized by an intense absorption near 240 nm (εmax 26,000), an average band of around 285 nm (εmax ~ 300) attributed to an electron transfer (ET) transition and to much lower absorptions (n → π *) from the visible region **(Thomson, 1971; Singh and Singh, 1986)**.

O-Benzoquinones are rare; therefore, relatively few o-benzoquinone spectra have been recorded **(Thomson, 1971)**. They exhibit triple absorption peaks and are easily distinguished from para isomers by relatively low intensity and intensified bathochromic shifts.

- **Naphthoquinones**

Their spectra are inevitably more complex than those of benzoquinones because both benzenoid and quinoid absorptions are involved, and one or both rings may be substituted. The spectra can be further complicated depending on the substituents. However,

naphthoquinones exhibit two major absorption maxima **(Singh and Singh, 1986)**. The spectrum of the parent 1,4-naphthoquinones includes intense benzenoid and quinonoid electron transfer absorption in the region of 240-290 nm and a medium intensity benzenoid band at 335 nm.

- **Anthraquinones**

Anthraquinones exhibit three to four major absorption maxima: intense absorption of benzenes at 250 nm and average absorption at 322 nm; Strong quinonoid electron transfer bands are observed at 263 and 272 nm and a weak quinonoid absorption band at 405 nm. These absorption zones are characteristic of quinones and the pattern in the ultraviolet region is not seriously affected by the substitution **(Thomson, 1971; Singh and Singh, 1986).**

b. Mass spectrometry

Common features in the mass spectra of all quinones are peaks corresponding to the loss of one or two carbon dioxide molecules. Benzos and naphthoquinones also remove ethylene (--C=C--) and acetylenic (O=C--C=C--) fragments **(Gorman *et al*., 2003; Thomson, 1971)**.

ii. Spectroscopy methods

a. Infra-red spectroscopy

Infrared spectral studies of quinones provide relatively little structural information compared to other spectral techniques. Carbonyl absorptions are most useful for elucidating the structure of quinones. The carbonyl absorption of p-benzoquinone occurs at 1669 cm^{-1}, corresponding to an α,β-di-unsubstituted ketone, and the frequency increases with increasing number of condensed linear rings (1675cm^{-1}). 1 for 1,4-naphthoquinones, 1678 cm^{-1} for 9,10-anthraquinones and 1682 cm^{-1} for naphthacene-5,12-quinones). The carbonyl frequency is lowered by hydrogen bonding, by substitution either in the quinonoid ring or in an adjacent benzenoid ring with the +I or +M groups **(Thomson, 1971; Singh and Singh, 1986)**.

b. Nuclear Magnetic Resonance Spectroscopy (^{1}H and ^{13}C NMR)

The quinonoid protons in p-benzoquinone resonate at 6.72 ppm and in 1,4-naphthoquinones at 6.97 ppm. Chelated α-hydroxyl groups are easily recognizable because their protons resonate at very low fields (~12-13 ppm), while unchelated hydroxyl groups

appear upstream. Likewise, periaromatic protons with carbonyl functions appear from 8 ppm **(Thomson, 1971)**.

The carbon spectrum generally shows peaks at 175-180 ppm characteristic of the carbonyl groups of quinones. The 1,4-naphthoquinones have closed peaks between 110 and 130 ppm corresponding to benzylic protons.

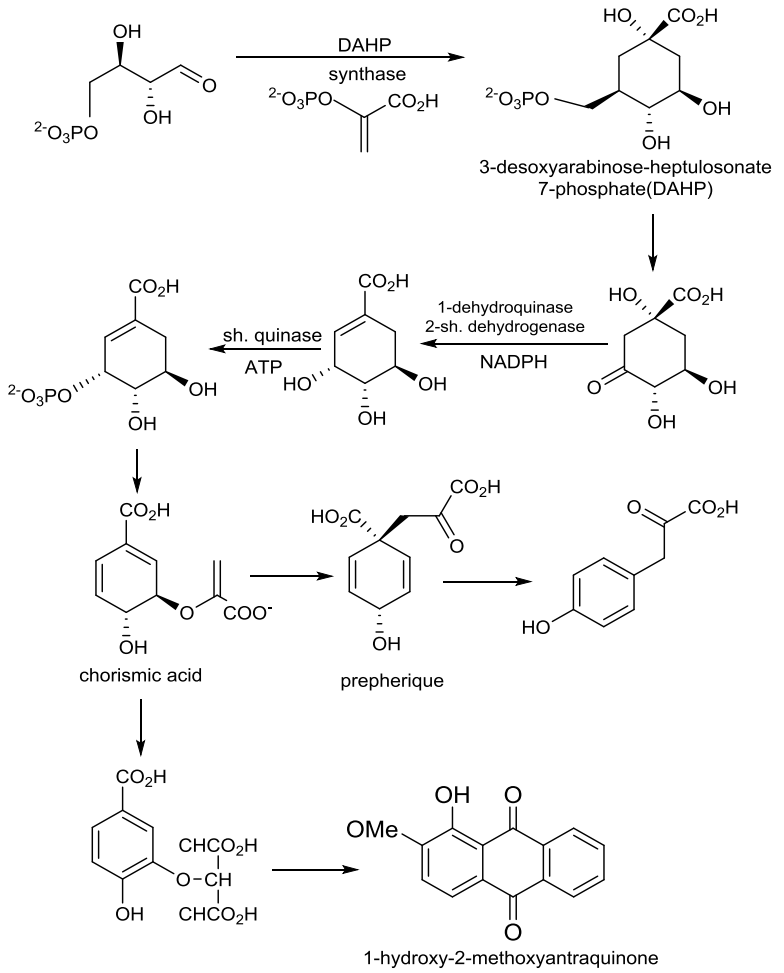

Scheme 17: The shikimic acid pathway (Bruneton, 1999)

I.3 CANCER: EMPHASIS ON BREAST CANCER

Our research was directed towards the particular cancer type, breast cancer. Thus, in this section, we focus our literature on breast cancer.

I.3.1 Definition

Cancer is the proliferation of malignant cells. We have various types of cancers named with respect to the organ in which the cancer started such as lung cancer in the case where the proliferation occurs at the lungs, prostate cancer when the proliferation occurs at the prostate and breast cancer when the proliferation occurs at the breast, amongst others **(Kathryn *et al*., 2011)**.

Breast cancer is the second most common cancer in women and a leading cause of death due to cancer. It starts as a localized tumor, but can metastasize to distant sites and cause mortality. Breast cancers are heterogeneous and pose challenges for diagnosis and treatment. Especially challenging are so-called triple negative breast cancers, or those in which the tumor does not express the three types of receptors most closely associated with breast cancer growth–estrogen, progesterone, and HER-2/neu and which do not respond to any hormonal therapies **(Kathryn *et al*., 2011)**.

I.3.2 Prevalence of breast cancer and epidemiology

Worldwide, breast cancer becomes the most commonly diagnosed malignance among women, accounting for 30% of all new cancer diagnoses in 2019. Despite important advances in early detection and research development, breast cancer remains a major health problem affecting women. In 2019, breast cancer alone accounts for 15% of all cancer deaths, inferior to lung and bronchus1, and the disease burden becomes more severe in young women aged < 45 years old **(Chang Bao *et al*., 2019)**. 18.1 million new cancer cases and 9.6 million deaths reported in 2021 **(WHO, 2021)** meanwhile, 6000 Cameroonian women died of cancer and the breast is the most affected with 2625 new cases recorded between 2010 and 2015 **(Zingue *et al*., 2021)**.

I.3.3 Types of breast cancers

Breast cancer is a heterogeneous disease comprising of clinically and molecularly distinct subtypes **(Karen *et al*., 2016)**. Clinically, breast cancer can be divided into distinct subtypes that have prognostic and therapeutic implications. Breast cancer patients routinely

have the expression of estrogen receptor (ER), progesterone receptor (PR), and amplification of HER-2/Neu evaluated. These markers allow classification of breast cancer tumors as hormone receptor positive tumors, HER-2/Neu amplified tumors, and those tumors which do not express ER, PR, and do not have HER-2/Neu amplification. The latter group is referred to as triple-negative breast cancer (TNBC) based on the lack of these three molecular markers **(Kathryn *et al.*, 2011)**.

Comprehensive gene expression profiling has identified 4 major molecular subtypes of breast cancer, including luminal A, luminal B, HER2 positive and TNBC, which are characterized by specific biological properties, morphological patterns and, more importantly, distinct clinical process and prognosis **(Chang Bao *et al.*, 2019)**.

- **Emphasis on tripple negative breast cancer**

TNBC is characterized by the lack of estrogen receptor (ER) and progesterone receptor (PR) expression and human epidermal growth factor receptor 2 (HER2) amplification. TNBCs are associated with advanced stage at diagnosis and poorer outcome compared to other breast cancer subtypes **(Nathan *el al.*, 2017)**. Characteristic TNBC clinical features include a peak in recurrence risk within the first 3 years, a weak relationship between the tumor size and lymph node metastasis, and a peak of cancer-related death in the first 5 years. At the molecular level, TNBC has significant overlap with the basal-like subtype as approximately 80% of TNBCs are classified as basal-like **(Nathan *el al.*, 2017)**.

I.3.4 Treatment of breast cancer

Generally, hormone receptor expressing breast cancers have a more favorable prognosis than either those with HER-2/Neu amplification or those that are triple-negative. While all breast tumor types may be treated with chemotherapy, therapeutic options in both early and late stage breast cancer are affected significantly by the expression of these three markers. Tumors that express ER and PR are treated with agents that interfere with hormone production or action **(Kathryn *et al.*, 2011)**. Tumors that have amplified HER-2/Neu are treated with agents that inhibit HER-2/Neu. These targeted therapies are the mainstay of the successful outcomes seen in hormone receptor positive and HER2/Neu amplified tumors. Both early stage and advanced TNBC tumors are treated with predominantly chemotherapy **(Kathryn *et al.*, 2011)**. Doxorubicin (DOX) is widely used for chemotherapy as it kills rapidly proliferating cancer cells by targeting topoisomerase II **(Jeonghun *et al.*, 2019)**.

The most aggressive subtype is TNBC, lacking of estrogen receptor (ER), progesterone receptor (PR) and human epidermal growth factor receptor 2 (HER2), accounting for 15–20% of all breast cancers5. Unfortunately, due to the devoid of early detection biomarkers and clear therapeutic targets, TNBC patients are often diagnosed late with a high histological grade, and do not benefit from hormonal or targeted therapies6. As a result, patients with TNBC usually suffer high risks of metastasis and distal recurrence, and have poor prognosis with shortened disease-free survival (DFS) and overall survival (OS). Hence, as a serious clinical challenge, TNBC calls for urgent needs of developing novel prognostic biomarkers and therapeutic targets **(Chang Bao *et al*., 2019)**.

Interestingly, the incidence of TNBC in African American women is two to three times higher than other ethnic groups, although the reason for this has not been elucidated. Given the lack of validated molecular targets and the poor outcome in patients with TNBC, there is a clear need for a greater understanding of TNBC at all levels and for the development of better therapies **(Kathryn *et al*., 2011)**. TNBC has no known therapeutic targets to date, and as chemotherapy and radiotherapy are the standard clinical therapies for TNBC, tolerance to chemotherapy severely affects the prognosis of the patient **(Jeonghun *et al*., 2019)**. Given that limited treatment options exist for patients with TNBC besides classical chemotherapy, novel treatment regimens e.g.by development of novel chemotherapeutics, are urgently needed to improve the prognosis of these patients **(Karen *et al*., 2016)**. Among breast cancers, the triple-negative breast cancer (TNBC) subtype has the worst prognosis with no approved targeted therapies and only standard chemotherapy as the backbone of systemic therapy **(Nathan *et al*., 2017)**. TNBC accounts for 15 – 20 % of invasive breast cancers. TNBC is characterized by the lack of estrogen receptor (ER) and progesterone receptor (PR) expression and human epidermal growth factor receptor 2 (HER2) amplification. TNBCs are associated with advanced stage at diagnosis and poorer outcome compared to other breast cancer subtypes **(Nathan *et al*., 2017)**. TNBC is a highly heterogeneous disease at the molecular level, and this heterogeneity likely underlies the variable treatment responses in patients. Recent studies involving comprehensive gene expression analysis revealed extensive molecular heterogeneity within TNBC cases and identified four to six distinct molecular TNBC subtypes **(Nathan *et al*., 2017)**. Understanding metabolic profiles and drug responses may prove valuable in targeting TNBC subtypes and identifying therapeutic susceptibilities in TNBC patients **(Nathan *et al*., 2017)**.

I.3.5 Causes of treatment failure: emphasis on chemo resistance

The unfavorable prognosis of triple-negative breast cancer (TNBC) stems in part from a lack of effective targeted therapies and heterogeneity in clinical response to standard chemotherapy. There is an urgent unmet need to identify features of TNBC that can predict response to current standard cytotoxic treatment and facilitate the development of new targeted therapies for this disease. Towards filling this need, significant efforts have been made to define the molecular heterogeneity of TNBC and to correlate these molecular signatures with clinical outcome and therapeutic effectiveness **(Jose *et al*., 2020)**. Let us look at the factor of chemoresistance and acquired resistance. Chemoresistance is a major cause of treatment failure in a variety of carcinomas and can be divided into primary resistance and acquired resistance. Primary resistance is a *de novo* lack of therapeutic response, whereas acquired resistance arises during the course of chemotherapy. The mechanisms of acquired resistance vary depending on the type of chemotherapeutic agent and patient, making it difficult to predict **(Jeonghun *et al*., 2019)**.

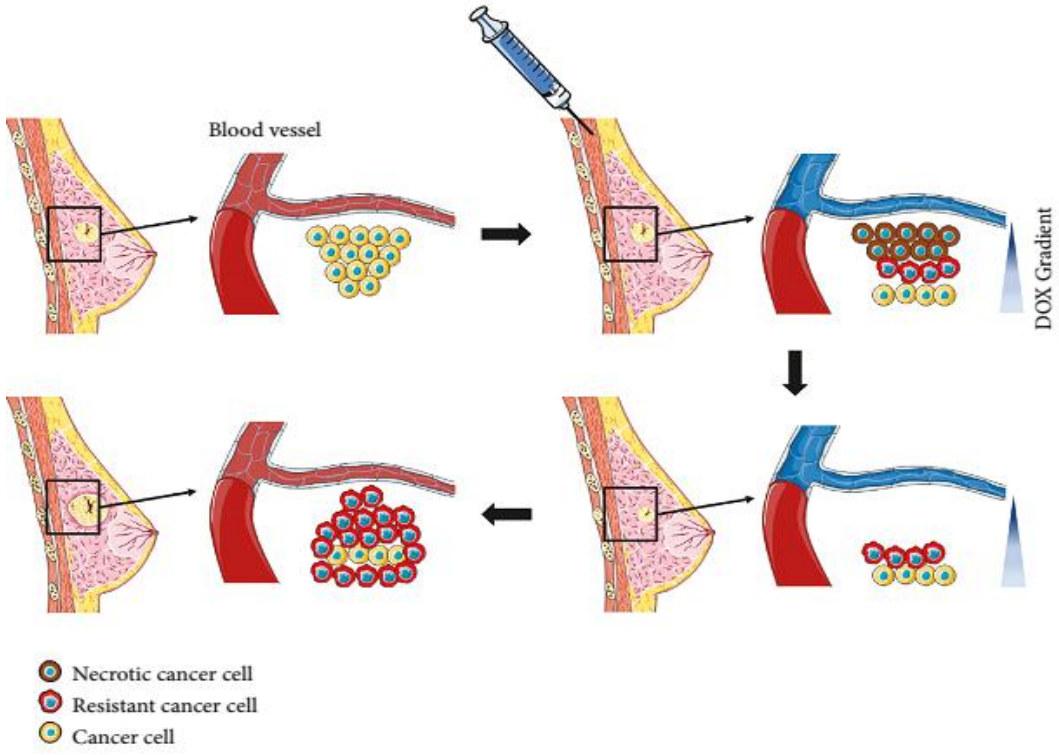

Figure 5: A schematic representation of the breast cancer patient's situation against chemotherapy corresponding to the acquisition of drug resistance derived from the CDRA concentration gradient chip (Jeonghun *et al.*, 2019*)*.

I.3.6 Breast cancer cell lines

Cancer cell lines have proved useful in laboratory and preclinical investigations since the first cell line was established more than 50 years ago **(Kathryn *et al.*, 2011)**. Cancer cell lines were initially derived from tumors and cultured in a two-dimensional environment. Due to the merit of cell culture, they have been widely used as models to study cancer biology and test drug candidates. However, the fact that many drugs with promising preclinical evidence fail in the clinic urges the reinvestigation of cell lines as tumor models. The differences between cell lines and tumors have raised the critical question to what extent cell lines recapitulate the biology of tumor samples **(Ke *et al.*, 2019)**. We have various types of cell lines and it will be interesting to understand their nomenclature.

I.3.6.1 Nomenclature of breast cancer cell lines

Cell line naming does not, in general, reflect its phenotypical association, but rather how they are established regarding, e. g. whether they are derived from the same laboratory, the same patient, isolated by serial subculture from the same initial population, or cultured using the same approach. For instance, 'HCC series' cell lines, as represented by their names, were isolated at Hamon Cancer Centre; 'MDA series' were established from M. D. Anderson Hospital and Tumor Institute **(Xiaofeng *et al.*, 2017)**. As cell lines are typically named by the scientist who derived them, there is no rule on how each cell line is named especially for those do not belong to any series. It is until recently that standardization on cell line nomenclature has been proposed, which helps regularize the naming of newly established cell lines and ultimately improvement in cell line annotation and scientific reproducibility **(Xiaofeng *et al.*, 2017)**.

I.3.6.2 Molecular classification of breast cancer cell lines

The original algorithm that classified triple-negative breast cancer (TNBC) into six subtypes has recently been revised. The revised algorithm (TNBCtype-IM) classifies TNBC

into five subtypes and a modifier based on immunological (IM) signatures. The molecular signature may differ between cancer cells in vitro and their respective tumor xenografts. We identified cell lines with concordant molecular subtypes regardless of classification algorithm or analysis of cells in vitro or in vivo, to establish a panel of clinically relevant molecularly stable TNBC models for translational research **(Jose *et al.*, 2020)**. Gene expression profiling has been widely applied to catalogue breast cancer cell lines, with diverse number of clusters being matched into various schemes. In 2017, Xiaofeng and collaborators did the characterisation of 84 cell lines based on the status of three important receptors conventionally used for breast cancer subtyping, i. e. , estrogen receptor (ER), progesterone receptor (PR), and human epithelial receptor 2 (HER2), and classified them using the same nomenclature, i. e. , luminal A, luminal B, HER2 positive, and triple negative subtypes, with triple negative cells being further divided into A and B to capture its heterogeneity and provide an easy link to the widely used names, i. e. , basal A and B. The figure 2 below shows the comparison of the current subtyping schemes between breast cancer cell lines and tumors.

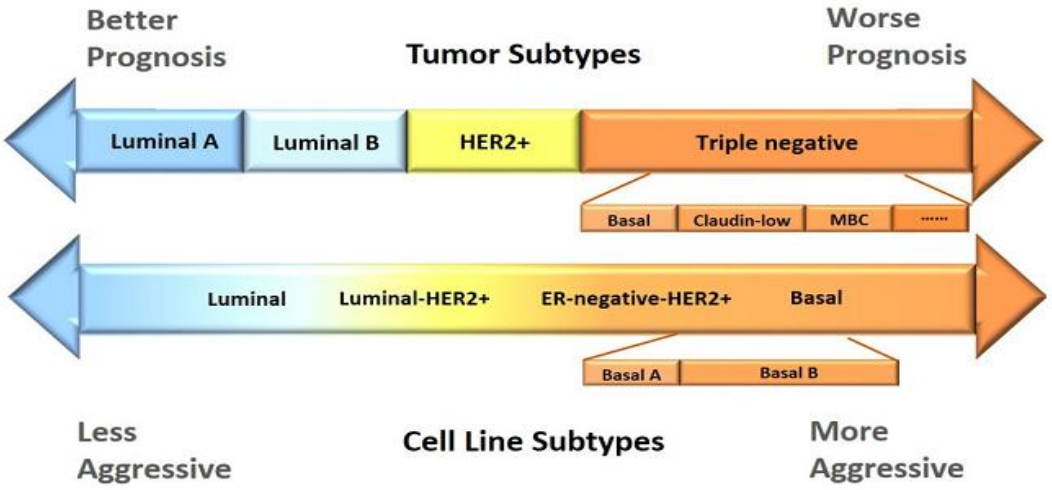

Figure 6: Comparison of the current subtyping schemes between breast cancer cell lines and tumors (Xiaofeng *et al.*, 2017).

Triple negative cell lines, as represented by the name, are featured by low or no expression of all three markers, i.e., ER-PR-HER2-. It is the most heterogeneous among all subtypes and referred to as basal A and basal B cell lines in many literatures.

I.3.6.3 Emphasis on triple negative breast cancer cell lines

There are numerous types of human TNBC cell lines amongst which we have; MDA-MB-157, MDA-MB-231, MDA-MB-435, MDA-MB-436, MDA-MB-468, HCC 3153, HS578T, SUM52PE, SUM102PT, SUM149PT, SUM159PT, SUM185PE, SUM229PE, MCF10A, MCF12A, etc **(Kathryn *et al*., 2011)**.

I.3.7 Risk factors

Here, we have two categories of risk factors and they are: Risk factors which a person cannot change and risk factors which a person can change **(www.cdc.gov).** It's worth noting that having a risk factor does not mean you will get the disease, and not all risk factors have the same effect. Most women have some risk factors, but most women do not get breast cancer. It's recommended for a person to talk with your doctor about ways through which one can lower the risk and about screening for breast cancer. We would move on to discuss the factors one after the other in the two categories mentioned above.

I.3.7.1 Risk Factors which a person can Change

These include the following:

- Getting older. The risk for breast cancer increases with age. Most breast cancers are diagnosed after age 50.
- Genetic mutations. Women who have inherited changes (mutations) to certain genes, such as BRCA1 and BRCA2, are at higher risk of breast and ovarian cancer.
- Reproductive history. Starting menstrual periods before age 12 and starting menopause after age 55 expose women to hormones longer, raising their risk of getting breast cancer.
- Having dense breasts. Dense breasts have more connective tissue than fatty tissue, which can sometimes make it hard to see tumors on a mammogram. Women with dense breasts are more likely to get breast cancer.
- Personal history of breast cancer or certain non-cancerous breast diseases. Women who have had breast cancer are more likely to get breast cancer a second time. Some non-cancerous breast diseases such as atypical ductal hyperplasia or lobular carcinoma in situ are associated with a higher risk of getting breast cancer.
- Family history of breast or ovarian cancer. A woman's risk for breast cancer is higher if she has a mother, sister, or daughter (first-degree relative) or multiple family members on

either her mother's or father's side of the family who have had breast or ovarian cancer. Having a first-degree male relative with breast cancer also raises a woman's risk.

- Previous treatment using radiation therapy. Women who had radiation therapy to the chest or breasts (for instance, treatment of Hodgkin's lymphoma) before age 30 have a higher risk of getting breast cancer later in life.
- Exposure to the drug diethylstilbestrol (DES). DES was given to some pregnant women in the United States between 1940 and 1971 to prevent miscarriage. Women who took DES have a higher risk of getting breast cancer. Women whose mothers took DES while pregnant with them also may have higher risk of getting breast cancer **(www.cdc.gov).**

I.3.7.2 Risk Factors which a person cannot Change

These include the following:

- Not being physically active. Women who are not physically active have higher risk of getting breast cancer.
- Being overweight or having obesity after menopause. Older women who are overweight or have obesity have a higher risk of getting breast cancer than those at a healthy weight.
- Taking hormones. Some forms of hormone replacement therapy (those that include both estrogen and progesterone) taken during menopause can raise risk for breast cancer when taken for more than five years. Certain oral contraceptives (birth control pills) also have been found to raise breast cancer risk.
- Reproductive history. Having the first pregnancy after age 30, not breastfeeding, and never having a full-term pregnancy can raise breast cancer risk.
- Drinking alcohol. Studies show that a woman's risk for breast cancer increases with the more alcohol she drinks.
- Research suggests that other factors such as smoking, being exposed to chemicals that can cause cancer, and changes in other hormones due to night shift working also may increase breast cancer risk **(www.cdc.gov).**

We shall now move on to look at a brief review on lipoxygenase, definition, types and relationship with cancer.

I.4 LIPOXYGENASE

I.4.1 Definition and functioning principle

Lipoxygenases (LOXs) are dioxygenases that catalyze the formation of corresponding hydroperoxides from polyunsaturated fatty acids such as linoleic acid and arachidonic acid in the presence of molecular oxygen **(Ryuichi *et al*., 2015; Neha *et al*., 2018)**. Lipoxygenases are a group of oxidative enzymes with a non-heme iron atom in their active site, which are involved in the regulation of inflammatory responses by generation of pro-inflammatory mediators known as leukotrienes or anti-inflammatory mediators known as lipoxins. These enzymes catalyze the insertion of oxygen (O_2) into poly-unsaturated fatty acids (PUFAs) such as arachidonic acid and linoleic acid **(Rosalina and Frank, 2014)**. It has been described that the catalytic reaction of lipoxygenases involves a single electron oxidation by the active site iron atom which switches between Fe^{2+} and Fe^{3+} redox states. In the catalytic reaction, $Fe^{3+}$is reduced to Fe^{2+} with concomitant oxidation of the lipid substrate by hydrogen abstraction from a bis-allylic methylene to give a pentadienyl radical, which is re-arranged to provide a 1-cis,3-trans-conjugated diene moiety. Subsequently, a stereo-specific insertion of oxygen at the pentadienyl radical takes place to form an oxygen centered fatty acid hydroperoxide radical. The intermediate hydroperoxide radical is reduced to the corresponding anion with concomitant re-oxidation of iron to Fe^{3+} see scheme below **(Rosalina and Frank, 2014).**

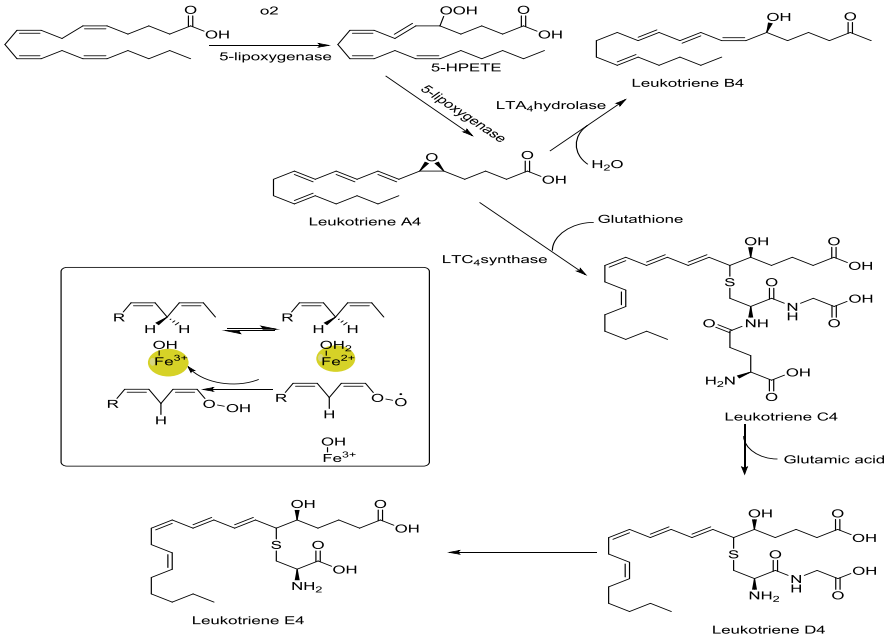

Scheme 18: Oxidation reactions of lipoxygenases in the leukotriene (LT) biosynthesis pathways

Lipoxygenases catalyze the formation of hydroperoxy eicosatetraenoic acids (HPETEs) from arachidonic acid. These HPETEs are subsequently reduced and transformed to form so called eicosanoids, which are signaling molecules that play an important regulatory role in the immune responses and other physiological processes **(Rosalina and Frank, 2014)**.

I.4.2 Types of lipoxygenases

In general, lipoxygenases are classified as 5-, 8-, 12, and 15-lipoxygenases according to their selectivity to oxygenate fatty acids in a specific position **(Rosalina and Frank, 2014)**.

In the humans and mice, six LOX isoforms have been known **(Ryuichi *et al*., 2015, Neha *et al*., 2018)** and they are listed below:

- 15-LOX, a prototypical enzyme originally found in reticulocytes shares the similarity of amino acid sequence as well as the biochemical property to plant LOX enzymes.
- 15-LOX-2, which is expressed in epithelial cells and leukocytes, has different substrate specificity in the humans and mice, therefore, the role of them in mammals has not been established.
- 12-LOX is an isoform expressed in epithelial cells and myeloid cells including platelets. Many mutations in this isoform are found in epithelial cancers, suggesting a potential link between 12-LOX and tumorigenesis.
- 12R-LOX can be found in the epithelial cells of the skin. Defects in this gene result in ichthyosis, a cutaneous disorder characterized by pathophysiologically dried skin due to abnormal loss of water from its epithelial cell layer.
- eLOX-3 is also expressed in the skin epithelial cells acting downstream 12R-LOX, is another causative factor for ichthyosis.
- 5-LOX is a distinct isoform playing an important role in asthma and inflammation.

Table 12 below presents some human lipoxygenases and their most important substrate, products and functions.

Table 12: Human lipoxygenases and their most important substrates, products, and functions (Rosalina and Frank, 2014)

Lipoxygenase type	Substrate	Product	Physiological function
5-lipoxygenase *(5-LOX)*	arachidonic acid	5(*S*)-HPETE, Leukotriene A4	Pro-inflammatory mediator
	γ-linoleic acid	Dihomo-γ-linoleic acid (DGLA)	Inhibition of arachidonic acid Conversion
	Eicosapentaenoic acid (EPA)	Leukotriene A5	Anti-inflammatory mediator/inhibitor LTA4 hydrolase
Platelet 12-lipoxygenase (p12-LOX)	arachidonic acid	12(*S*)-HPETE	Modulation of platelet aggregation
	Dihomo-γ-linoleic acid (DGLA)	12(*S*)-HPETrE	
	Eicosapentaenoic acid (EPA)	12(*S*)-HPEPE	
	α-linoleic	acid 12(*S*)-HPOTrE	
12R-lipoxygenase (12*R*-LOX)	arachidonic acid	12(*R*)-HPETE	Epidermal barrier acquisition
	Linoleyl-ω-hydroxy ceramide	9(*R*)-hydroperoxyllinoleoyl-ω-hydroxy ceramide	
epidermis LOX3 (eLOX3)	9(R)-hydroperoxyllinoleoyl-ω- hydroxy ceramide	9(*R*)-10(*R*)-trans-epoxy-11E-13(*R*)-hydroxylinoleoyl-ω-hydroxy ceramide	Epidermal barrier acquisition
15-lipoxygenase-1 (15-LOX1)	linoleic acid	13(*S*)-HPODE	modulation of MAP kinase signaling pathways
	arachidonic acid	15(*S*)-HPETE	modulation of leukotriene B4, proinflammatory mediators
15-lipoxygenase-2 (15-LOX2)	arachidonic acid	15(*S*)-HPETE	negative cell cycle regulator and tumor suppressor

I.4.3 Relationship between lipoxygenase and cancer

Lipoxygenase (LO)-catalyzed products have a profound influence on the development and progression of human cancers **(Vernon *et al*., 1999)**. Compared with normal tissues, significantly elevated levels of LO metabolites have been found in lung, prostate, breast, colon, and skin cancer cells, as well as in cells from patients with both acute and chronic leukemias **(Rosalina and Frank, 2014)**. LO-mediated products elicit diverse biological activities needed for neoplastic cell growth, influencing growth factor and transcription factor activation, oncogene induction, stimulation of tumor cell adhesion, and regulation of apoptotic cell death. **(Vernon *et al*., 1999)**.

Lipoxygenases and their catalysis products are associated with carcinogenic processes such as tumor cell proliferation, differentiation, and apoptosis **(Rosalina and Frank, 2014)**. Several lines of evidence have proven the crucial role of lipoxygenases in cancer. In human prostate cancer cells, the overexpression of platelet 12-lipoxygenase (p12-LOX) has been observed, which is a trigger for angiogenesis and tumor growth **(Rosalina and Frank, 2014)**. The increased expression of the 5-LOX enzyme and the LTB4 receptors were observed in pancreatic cancer. In addition, 5-LOX expression levels were suggested as indicator for early neoplastic lesions. Leukotriene LTB4 is a potential stimulator for cancer cell growth and also plays a role in the formation of ROS in response to hypoxia. It has also been shown that the 5-LOX metabolite LTB4 is capable of activating the transcription factor NF-κB in cancer cells, which suggest a tumor promoting role via this route. The roles of 15-LOX-1 metabolites are reported in the development of breast cancer by promoting the invasion of tumor cells into the lymphatic vessels and the formation of lymph node metastasis **(Rosalina and Frank, 2014)**.

Agents that block LO-catalyzed activity may be effective in preventing cancer by interfering with signaling events needed for tumor growth. In fact, in a few studies, LO inhibitors have prevented carcinogen-induced lung adenomas and rat mammary gland cancers **(Vernon *et al*., 1999)**. Considering the potent pro-inflammatory properties of lipoxygenases and their products, the modulation of the lipoxygenase pathways using small molecule inhibitors should provide new therapeutic approaches for numerous inflammatory diseases and cancer **(Rosalina and Frank, 2014)**.

We shall now move on to look at a brief review on anti-oxiidants; definition, their types and their relationship with cancer.

I.5 ANTI-OXIDANTS

I.5.1 Definition and functioning principle

Antioxidants are natural substances or synthetic that can help to delay cell damage or prevent (**Kunming, 2022)**. Free radicals are molecules produced when your body breaks down food or while you're exposed to tobacco smoke or radiation. Antioxidants, consisting of nutrients C and E and carotenoids, may help protect cells from damage caused by free radicals. Other naturally occurring antioxidants include tannins, flavonoids, lignans and phenols (**Kunming, 2022)**. An antioxidant is a molecule stable enough to donate an electron to a rampaging free radical and neutralize it, thus reducing its capacity to damage (**Lobo *et al*., 2010**). These antioxidants are substances that could defend your cells against free radicals, which may play a role in heart disorder, cancer and different sicknesses (**Kunming, 2022)**. These antioxidants delay or inhibit cellular damage mainly through their free radical scavenging property. These low-molecular-weight antioxidants can safely interact with free radicals and terminate the chain reaction before vital molecules are damaged. Some of such antioxidants, including glutathione, ubiquinol, and uric acid, are produced during normal metabolism in the body. Other lighter antioxidants are found in the diet. Although there are several enzymes system within the body that scavenge free radicals, the principle micronutrient (vitamins) antioxidants are vitamin E (α-tocopherol), vitamin C (ascorbic acid), and β-carotene. The body cannot manufacture these micronutrients, so they must be supplied in the diet (**Lobo *et al*., 2010**).

It may be important to note that plant-based foods are the best sources. These include whole grains, vegetables, fruits, seeds, nuts, spices, herbs and even cocoa. As an advantage fruits, vegetables and whole grains are high in antioxidants and are also typically high in fiber, low in saturated fat and cholesterol, and good sources of vitamins and minerals. Glutathione is the most effective among the antioxidants our body produces. It's a mixture of 3 amino acids; it tackles ageing through the intestines and circulatory system. It has strong anti-ageing properties, it protects cells, tissues and organs of the body and it continues to keep them young.

Two principle mechanisms of action have been proposed for antioxidants. The frst is a chain- breaking mechanism by which the primary antioxidant donates an electron to the free radical present in the systems. The second mechanism involves removal of ROS/reactive nitrogen species initiators (secondary antioxidants) by quenching chain-initiating catalyst.

Antioxidants may exert their effect on biological systems by different mechanisms including electron donation, metal ion chelation, co-antioxidants, or by gene expression regulation.

The antioxidants acting in the defense systems act at different levels such as preventive, radical scavenging, repair and de novo, and the fourth line of defense, i.e., the adaptation (**Lobo *et al*., 2010**).

The frst line of defense is the preventive antioxidants, which suppress the formation of free radicals. Although the precise mechanism and site of radical formation *in vivo* are not well elucidated yet, the metal-induced decompositions of hydroperoxides and hydrogen peroxide must be one of the important sources (**Lobo *et al*., 2010**).

The second line of defense is the antioxidants that scavenge the active radicals to suppress chain initiation and/or break the chain propagation reactions. Various endogenous radical-scavenging antioxidants are known: some are hydrophilic and others are lipophilic. Vitamin C, uric acid, bilirubin, albumin, and thiols are hydrophilic, radical-scavenging antioxidants, while vitamin E and ubiquinol are lipophilic radical-scavenging antioxidants. Vitamin E is accepted as the most potent radical-scavenging lipophilic antioxidant (**Lobo *et al*., 2010**).

The third line of defense is the repair and *de novo* antioxidants. The proteolytic enzymes, proteinases, proteases, and peptidases, present in the cytosol and in the mitochondria of mammalian cells, recognize, degrade, and remove oxidatively modified proteins and prevent the accumulation of oxidized proteins (**Lobo *et al*., 2010**).

The DNA repair systems also play an important role in the total defense system against oxidative damage. Various kinds of enzymes such as glycosylases and nucleases, which repair the damaged DNA, are known. There is another important function called adaptation where the signal for the production and reactions of free radicals induces formation and transport of the appropriate antioxidant to the right site.

I.5.2 Types of anti-oxidants

Antioxidants by their mechanism are divided into three types; primary antioxidants, secondary antioxidants and tertiary antioxidants.

- Primary antioxidants: These essentially function as free radical terminators. They are important antioxidant enzymes certainly produced by our body. These internal antioxidant enzymes serve as our body's most potent defense against free radicals and harmful inflammatory reactions. There are only 3 primary-antioxidants: Catalase (CAT), Glutathione Peroxidase (GPx) and SOD (**Kunming, 2022)**.

- Secondary antioxidants: These function by retarding chain initiation and it is also important preventive antioxidants. They frequently known as hydro peroxide decomposers, act to convert hydro peroxides into nonradical, nonreactive and thermally stable products. To yield synergistic stabilization effects they are often used in combination with primary antioxidants. Glucose-6-phosphate dehydrogenase, Glutathione reductase, ubiquinone and glutathione-s-transferase, are the secondary antioxidants. Iron, copper, zinc, manganese and selenium also increase the antioxidant enzyme activities (**Kunming, 2022)**.
- Tertiary oxidants: Tertiary oxidants by repairing the oxidized molecules and there function takes place (some enzymes of DNA, proteolytic enzymes, etc.) through sources like consecutive antioxidants or dietary (**Kunming, 2022)**.

I.5.3 Relationship between anti-oxidants and cancer

Antioxidants can decrease oxidative stress induced carcinogenesis by a direct scavenging of ROS and/or by inhibiting cell proliferation secondary to the protein phosphorylation. β-carotene may be protective against cancer through its antioxidant function, because oxidative products can cause genetic damage. Thus, the photo protective properties of B-carotene may protect against UV induced carcinogenesis. Immunoenhancement of B-carotene may contribute to cancer protection. B-carotene may also have anticarcinogenic effect by altering the liver metabolism effects of carcinogens. Vitamin C may be helpful in preventing cancer. The possible mechanisms by which vitamin C may affect carcinogenesis include antioxidant effects, blocking of formation of nitrosanimes, enhancement of the immune response, and acceleration of detoxifcation of liver enzymes. Vitamin E, an important antioxidant, plays a role in immunocompetence by increasing humoral antibody protection, resistance to bacterial infections, cell-mediated immunity, the T-lymphocytes tumor necrosis factor production, inhibition of mutagen formation, repair of membranes in DNA, and blocking micro cell line formation. Hence vitamin E may be useful in cancer prevention and inhibit carcinogenesis by the stimulation of the immune system. The administration of a mixture of the above three antioxidant reveled the highest reduction in risk of developing cardiac cancer (**Lobo *et al*., 2010**).

We shall now move on to look at a brief review on urease; its definition and relationship with cancer.

I.6 UREASE

I.6.1 Definition

Urease, is a dinickel enzyme that is responsible for the formation of carbamic acid (H_2NCOOH) as a byproduct of the breakdown of urea into carbonic acid (H_2CO_3) and ammonia (NH_3) (**Mbachu *et al.*, 2023**; **Khan *et al.*, 2011**). In aqueous solutions, ammonium (NH_4^+) and bicarbonate ions (HCO_3^-) are in equilibrium with NH_3 and carbonic acid, respectively.

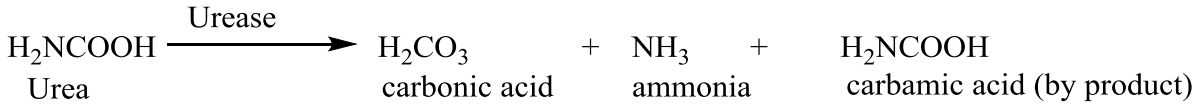

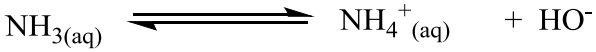

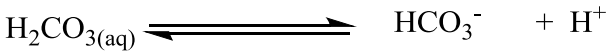

I.6.2 Relationship between urease and cancer

A wide variety of organisms, including bacteria, fungi, plants, and invertebrates, may make urease enzymes. Surprisingly, the active site and the essential structure of urease are identical among all species (**Mbachu *et al.*, 2023**). The consequences of urease-induced urea hydrolysis and the increase in pH caused by the formation of NH_3 are widespread. As a result, they are significant in a variety of different ways (**Mbachu *et al.*, 2023**). Particularly, *Helicobacter pylori* (*H. pylori*) releases urease enzyme in humans, which neutralizes the acidic environment and increases the pH of the environment from 6.5 to 9, resulting in hydrolysis of urea which helps them to colonize in the stomach wall and thus can cause duodenal, peptic ulcers, and gastric cancer (**Ata *et al,* 2023**) as well as damaged urea and urease (**Mbachu *et al.*, 2023**). Urease contains two Ni^{2+} ions, covalently bound to a hydroxy group, and a carbamylated lysine at the active site. A rapid increase in environmental pH due to enzymatic activity negatively affects human health (**Mbachu *et al.*, 2023**). Relating urease and cancer from another view point, one could say that ureases could cause oxidative stress or inflammation; under oxidative stress, reactive oxygen species (ROS), such as HO·, O_2·-, NO, H_2O_2, and ONO_2, are produced and their role is like a double-edged sword (**Ata *et aL.*, 2023**). While serving as secondary messengers in numerous major physiological occurrences, they

induce pathologic or degenerative roles like coronary heart disease, aging, neurodegenerative disorders, cancer, Alzheimer's disease, inflammation, atherosclerosis, and cataracts (**Ata *et al.*, 2023**). Summarily, urease, could play a role in carcinoma development. Therefore, urease inhibitors can be employed to fight against the activity of ureases hence interfering the role played by urease in carcinoma development. The scheme below gives some examples of urease inhibitors.

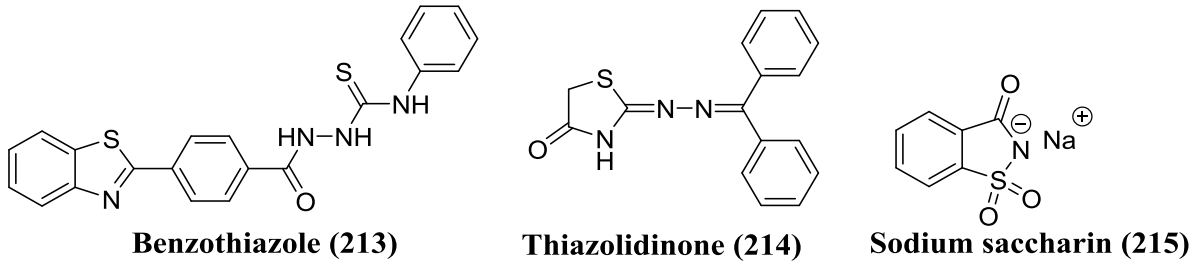

Benzothiazole (213) **Thiazolidinone (214)** **Sodium saccharin (215)**

Scheme 19: Some urease inhibitors *(*Ata *et al.*, 2023*)*

We shall now move on to look at a brief review on molecular docking; definition, basic principle and theory, approaches, types, importance, advantages and limitations of molecular docking.

I.7 MOLECULAR DOCKING

I.7.1 Definition

Molecular docking is a kind of bioinformatic modelling which involves the interaction of two or more molecules to give the stable adduct. Depending upon binding properties of ligand and target, it predicts the three-dimensional structure of any complex. Molecular docking generates different possible adduct structures that are ranked and grouped together using scoring function in the software. The information obtained from the docking technique can be used to suggest the binding energy, free energy and stability of complexes. Docking simulations predict optimized docked conformer based upon total energy of the system **(Shweta and Ranjana, 2016)**.

Molecular docking is a kind of computational modeling, which facilitates the prediction of preferred binding orientation of one molecule (eg. ligand) to another (eg. Receptor), when both interact each other in order to form a stable complex. Information gained from the preferred orientation of bound molecules may be employed to predict the energy profiling (such as binding free energy), strength and stability (like binding affinity and binding constant) of complexes. This can be done using scoring function of molecular docking. Nowadays, molecular docking is often utilized to forecast the binding orientation of small molecules (drug candidates) to their biomolecular target (such as protein, carbohydrate and nucleic acid) with the aim to determine their tentative binding parameters. This establishes raw data for the rational drug designing (structure-based-drug development) of new agents with better efficacy and more specificity **(Shweta and Ranjana, 2016)**. Presently, there are more than thirty docking programs available to carry out molecular docking. The most frequent ones include: AutoDock, GOLD, FlexX, and DOCK. They enable us to screen a vast number of a library of compounds. The program is usally based on specific algorithms and the protocol is made up of two steps: docking and scoring **(Ayaz and Shafia, 2017)**.

I.7.2 Basic principle and theory of docking

I.6.1.1 Basic principle

Molecular dockng is based on drug-enzyme complex

$$[\ \text{Drug}\ ] + [\ \text{Receptor}\ ] \underset{K_2}{\overset{K_1}{\rightleftharpoons}} [\ \text{Drug - Receptor}\ ]$$

Rate 1 = K_1 [Drug][Receptor]

Rate 2 = K_2 [Drug-Receptor]

At equilibrium, Rate 1 = Rate 2

Which implies that, K_1[Drug][Receptor]=K_2[Drug-Receptor]

$$\frac{K_2}{K_1} = K_d = \frac{[Drug][Receptor]}{[Drug - Receptor]}$$

If [Drug-Receptor] is high or K_d is small, it implies that the compound binds significantly to the receptor hence; there is activity. ΔG= -RTln K_d that is, the smaller the small ΔG, the higher the activity.

I.6.1.2 Theory of docking

Molecular docking is an attractive scaffold to understand drug-biomolecular interactions for the rational drug design and discovery, as well as in mechanistic study. This is done by placing a molecule (ligand) into the preferred binding site of the target specific region of the DNA/protein (receptor) mainly in a non-covalent fashion to form a stable complex of potential efficacy and more specificity**.** At present, docking technique is utilized to predict the tentative binding parameters of ligand-receptor complex beforehand **(Ayaz and Shafia, 2017)**. It has become an important common component of the drug discovery toolbox, and its relative low-cost implications and perceived simplicity of use has stimulated an even increasing popularity within academic communities. It **is** an indispensable ultra-HTS technique, and is making an impact on drug discovery and development. This is in part due to increasing numbers of X-ray structures of proteins, in particular ligand-bound proteins, and in part due to well-annotated databases such as PubChem, ChEMBL, ZINC, and Drug Bank, which provide public access to the structures and biological activities of millions of chemicals**.**

The first docking tools obeyed the “lock and key” hypothesis where the ligand (key) is complementary at the geometric level to the active site of the receptor (lock). Nowadays,

docking can be related to an optimization problem according to a numerical value which would account for a more or less favorable conformation of two entities (the total free energy of the protein-ligand system for example). Hence, molecular docking takes place in two complementary stages. The first step is to find and generate all the possible conformations. That is the conformations of the ligand capable of establishing ideal interactions with the receptor in order to find the overall minimum energy. The second step is the so-called score function making it possible to evaluate these conformations by a rapid calculation of the total free energy of the protein-ligand system formed. The ability of a program to do this is usually judged by the root-mean-square deviation (RMSD) of the model designed by the software with respect to the crystal structure. The accepted ratio is a maximum difference of 2Å beyond which the prediction is considered irrelevant **(Ayaz and Shafia, 2017; Shweta and Ranjana, 2016)**.

I.7.3 Approaches of Molecular Docking

I.7.3.1 Simulation approach

Here the ligand and target is being separated by physical distance and then ligand is allowed to bind into groove of target after "definite times of moves" in its conformational space. The moves involve variations to the structure of ligand either internally (torsional angle rotations) or externally (rotations and translations). The ligand in every move in the conformational limit releases energy, as "Total Energy". This approach is advantageous in the sense that it is more compatible to accept ligand flexibility. In addition, it is more real to assess the molecular recognition between ligand and target. Nevertheless, this approach takes longer duration to estimate optimal docked conformer due to the large energy dissipating for each conformation **(Ayaz and Shafia, 2017; Shweta and Ranjana, 2016)**.

I.7.3.2 Shape complementarity approach

This approach employs ligand and target as surface structural feature that provides their molecular interaction. Here the surface of the target is shown with respect to its solvent-accessible surface area while the ligand's molecular surface is shown in terms of matching surface illustration. The complementarity between two surfaces based on shape matching illustration helps in searching the complementary groove for ligand on target surface. This

approach is rather quick and involves the rapid scanning of numerous thousands of ligands in a few seconds to find out the possible binding properties of ligand on target molecular surface **(Ayaz and Shafia, 2017; Shweta and Ranjana, 2016)**.

I.7.4 Importance of docking in new drug development

Ligand-protein docking is an optimization of problem based on predicting the position of aligand with the lowest binding energy in the active site of the receptor. The net predicted binding free energy (ΔG_{bind}) is revealed in terms of various parameters: Hydrogen bond (ΔG_{hbond}), electrostatic (ΔG_{elec}), Torsional free energy (ΔG_{tor}), Dispersion and repulsion (ΔG_{vdw}), Desolvation (ΔG_{desolv}), Total internal energy (ΔG_{total}) and Unbound system's energy (ΔG_{unb}). Molecular docking is a kind of bioinformatic modeling which involves the interaction of two or more molecules to give the stable adduct. Depending upon binding properties of ligand and target, it predicts the three-dimensional structure of any complex. At present, docking technique is utilized to predict the tentative binding parameters of ligandreceptor complex beforehand. Molecular docking generates different possible adduct structures that are ranked and grouped together using scoring function in the software. Molecular docking of small molecules to a target includes a pre-defined sampling of possible conformation of ligand in the particular groove of target in an order to establish the optimized conformation of the complex (**Nagaraju *et al.*, 2017**). This can be made possible using scoring function of software. Since the infrared spectroscopy, X –ray crystallography and Nuclear Magnetic Resonance (NMR) spectroscopy are the techniques for the investigation and establishment of three-dimensional structures of any organic molecule/ bio-molecular targets. A new multi-objective strategy for molecular docking, named as MoDock, is presented to further improve the docking accuracy with available scoring functions. Tests of MoDock against the GOLD test data set reveal the multiobjective strategy improves the docking accuracy over the individual scoring functions. Meanwhile, a 70% ratio of the good docking solutions with the RMSD (simply root-meansquare deviation) value below 1.0 A^o outperforms other six commonly used docking programs, even with a flexible receptor docking program included (**Nagaraju *et al.*, 2017**).

I.7.5 Advantages of docking

The application of docking in a targeted drug delivery system is a huge benefit. One can study the size, shape, charge distribution, polarity, hydrogen bonding, and hydrophobic interactions of both ligand (drug) and receptor (target site). Molecular docking helps in the identification of target sites of the ligand and the receptor molecule (**Nagaraju *et al*., 2017**). Docking also helps in understanding of different enzymes and their mechanism of action. The "scoring" feature in docking helps in selecting the best fit or the best drug from an array of options. Not everything can be proved experimentally as traditional experimental methods for drug discovery take a long time. Molecular docking helps in moving the process of computer-aided drug designing faster and also provides every conformation possible based on the receptor and ligand molecule. Docking has a huge advantage when it comes to the study of protein interactions. There are millions of compound, ligands, drugs, and receptors, the 3D structure of which has been crystallized. Virtual screening of these compounds can be made (**Nagaraju *et al*., 2017**).

I.7.6 Limitations of docking

The scoring functions used in docking, almost all of them, do not take into account the role played by covalently bound inhibitors or ions. The methodology and research in protein–protein docking have to be greatly increased as the success in this field is greatly hampered by many false positives and false negatives (**Nagaraju *et al*., 2017**).

Haven done a review of the literature on various aspects of the work done, we shall now move on to present the results of our research project and findings in chapter II below.

CHAPTER II: RESULTS AND DISCUSSIONS

II.1 EXTRACTION AND ISOLATION OF SECONDARY METABOLITES

II.1.1 Extraction and isolation of secondary metabolites from *Alstonia scholaris*

The air-dried and powdered leaves of *A. scholaris* (25 Kg) were successively extracted with ethanol (3 × 20 L × 120 h) by maceration at room temperature. The extract was concentrated *in vacuo* to obtain 637 g of dark coloured ethanol extract. Water (500 mL) was added to the extract then, acidified with 20.5 mL of 1.5 N H_2SO_4 and extracted with CH_2Cl_2. The organic phase was concentrated to afford 260 g of the non-alkaloid extract. The aqueous phase was basified with 500 mL of 3 N Na_2CO_3 to release the alkaloids which were then extracted with CH_2Cl_2. Concentration of the resulting organic phase afforded 9.33g of the alkaloidal extract, while the aqueous fraction upon treatment with n-butanol afforded 40 g of the n-butanol fraction. The non-alkaloid extract was subjected to column chromatography (CC) eluting with mixtures of n-hexane-EtOAc to afford 9 series F_1-F_9. Series F_1 (3.55 g) was infused in 3-4 % hex/EtOAc for about 9 hours to produce 0.5 g of a white substance. The resulting white substance was filtered and washed with hexane and then attributed the code AS_1. The F_2 series (5 g) was purified by soaking it in hexane to give 0.3 g of AS_2. CC of series F_3 (8g) using hexane-EtOAc as eluent afforded 20 mg of an inseparable mixture AS_3 & AS_4. Another CC of fraction F_4 (8.9g) using hexane-EtOAc as eluent afforded 18 mg of AS_5. CC of fraction F_5 (20g) using hexane-EtOAc as eluent afforded 20 mg of AS_6, 10 mg of AS_7 and 10 mg of AS_8. Finally, CC of 6.9 g of the alkaloid extract using DCM-MeOH as eluent afforded 9.8 mg of AS_9.

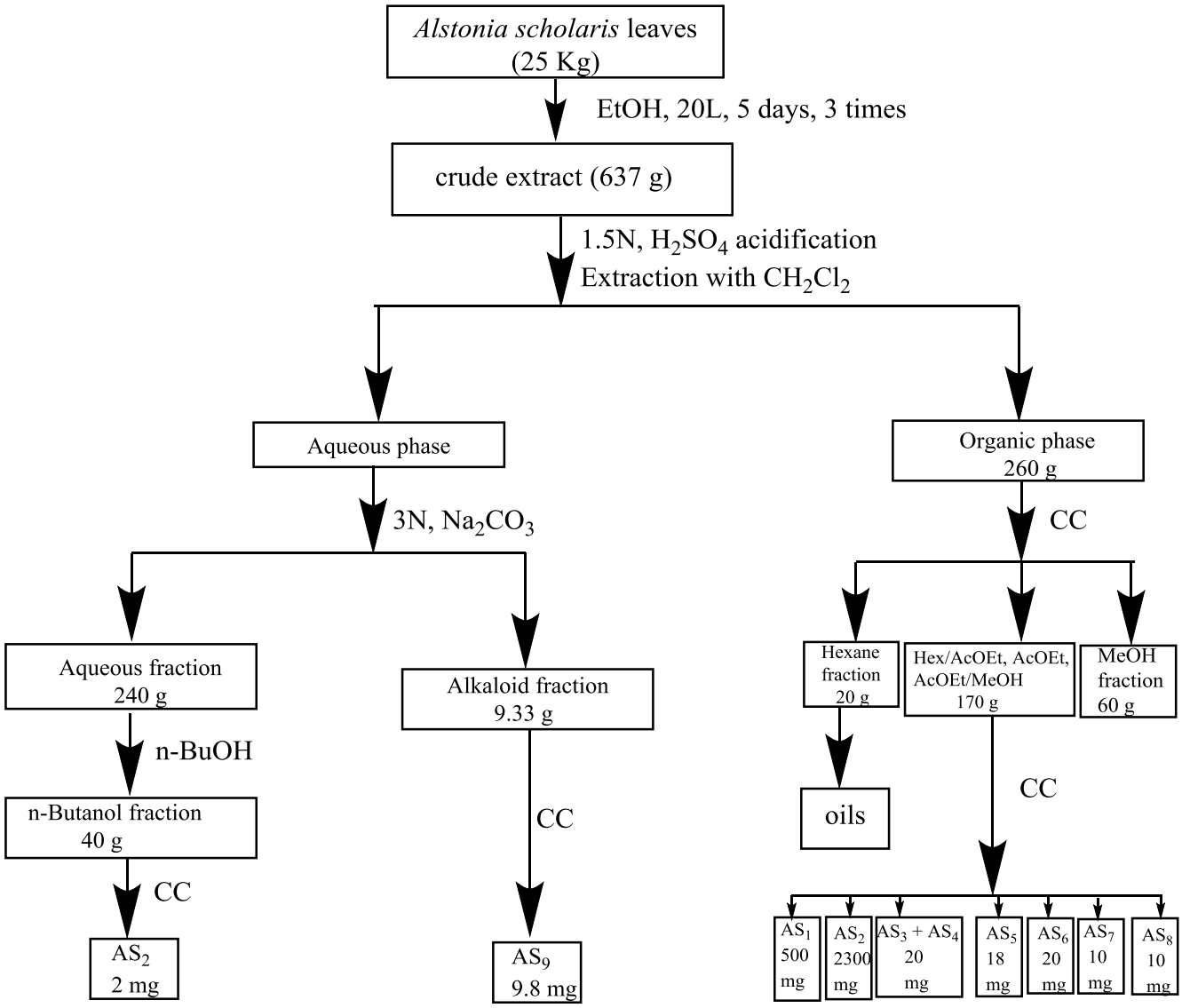

Scheme 20: Protocol for the extraction and purification of the leaves of *Alstonia scholaris*

II.1.2 Extraction and isolation of secondary metabolites from *Psorospermum guineense*

Powdered twigs (1.5 Kg) were extracted by sonication in MeOH/CH_2Cl_2 (1:1 v/v) at room temperature. The filtrates were concentrated on a rotary evaporator under reduce pressure to yield 300 g of crude extract. A portion of the crude extract (150 g) was subjected to fractionation using hexane, EtOAc and n-BuOH to afford hexane (30g), EtOAc (25g) and n-BuOH (20g) fractions. The LCMS analyses of the various extracts indicated that the hexane and EtOAc extractss were rich in secondary metabolites. These fractions were each subjected

to silica gel 60 (0.063 – 0.200 mm) using hexane, hexane-EtOAc gradient systems and EtOAc. Fractions (150) of 150 mL each were collected and concentrated under vacuum. The hexane fraction afforded four compounds coded; PG_1 (100 mg), PG_2 (10 mg), PG_3 (100 mg) and PG_4 (75 mg). The EtOAc fraction afforded PG_1 (200 mg), PG_3 (200 mg), PG_4 (150 mg), PG_5 (25 mg), PG_6 (250mg), PG_7 (250 mg). The n-butanol fraction afforded PG_8 (100mg).

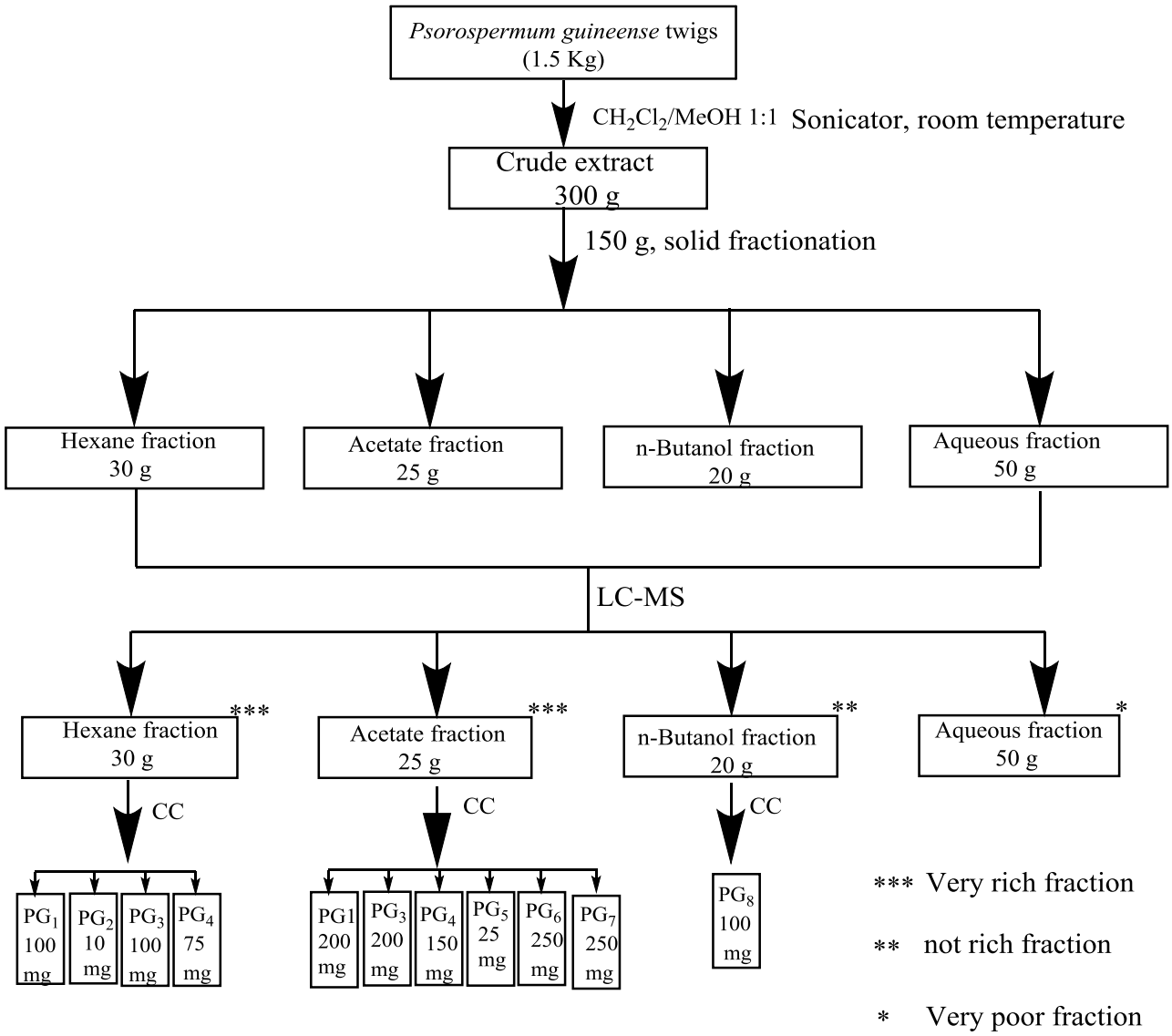

Scheme 21: Protocol for extraction and purification of the twigs of *Psorpspermum guineense*

II.2 IDENTIFICATION OF COMPOUNDS

Phytochemical studies carried out on the species *A. scholaris* and *P. guineense* have led to the isolation of several secondary metabolites which belong to the classes of triterpenes, quinones, alkaloids and phenylpropanoid. The structures of all these compounds were elucidated on the basis of spectroscopic and chemical evidence (IR, UV, MS, 1D and 2D NMR spectroscopy).

II.2.1 Identification of terpenoïds

II.2.1.1 Identification of compound AS_1

AS_1 was obtained as white powder from Hexane-Ethyl acetate 20% (m.p. 284 °C) and gave a positive result (purple) to the Libermann-Buchard test characteristic of triterpenes. Its EIMS (**Figure 7**) showed a molecular ion peak $[M]^+$ at *m/z* 442.3 compatible with the molecular formula $C_{30}H_{50}O_2$ corresponding to six degrees of unsaturations. Its ^1H NMR spectrum (**Figure 8**) exhibited:

- Five singlets of three protons each between δ 0.60 and 0.90 attributable to five angular methyl groups of lupane triterpènes
- One singlet of three protons at δ 1.77 attributable to proton H-30
- One multiplet of one proton at δ 3.21 attributable to the oxymethine proton H-3
- Two multiplets of one proton each at δ 3.71 and 3.32 attributable to the oxy methylene protons H-28
- Two doublets of two protons each at δ 4.60 and 4.61 characteristic of proton H-29 of the lup-20(29)-ene
- A multiplet of one proton at δ 2.84 attributable to proton H-19

The ^1H-^1H COSY spectrum (**Figure 9**) shows the correlation between the two olefinic protons at position 28.

These physical and spectroscopic data were in agreement with those previously reported for betulin **(62)** (**Gurupriya and Cathrine, 2021**).

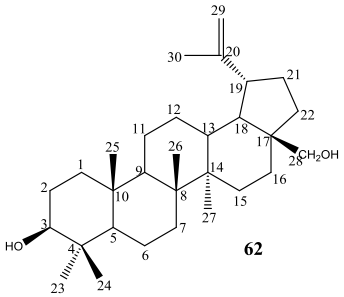

62

Table 13: ^{1}H NMR data of AS_1 and the litterature

	AS_1	Betulin (Gurupriya *et* Cathrine, 2021)
N_o	**^{1}H (nH , m, *J* in Hz)**	**^{1}H (nH , m)**
3	3.21 (1H, m)	3.18 (1H, dd)
20	-	-
23	0.91 (3H, s)	0.96 (3H, s)
24	0.75 (3H, s)	0.75 (3H, s)
25	0.86 (3H, s)	0.80 (3H, s)
26	0.95 (3H, s)	0.97 (3H, s)
27	0.99 (3H, s)	0.99 (3H, s)
28	3.32 - 3.71 (2H, m)	3.33-3.79 (2H, d)
29	4.60- 4.61 (2H, d, *J* = 1.5Hz)	4.58-4.70 (2H, d)
30	1.77 (3H, s)	1.67 (3H, s)

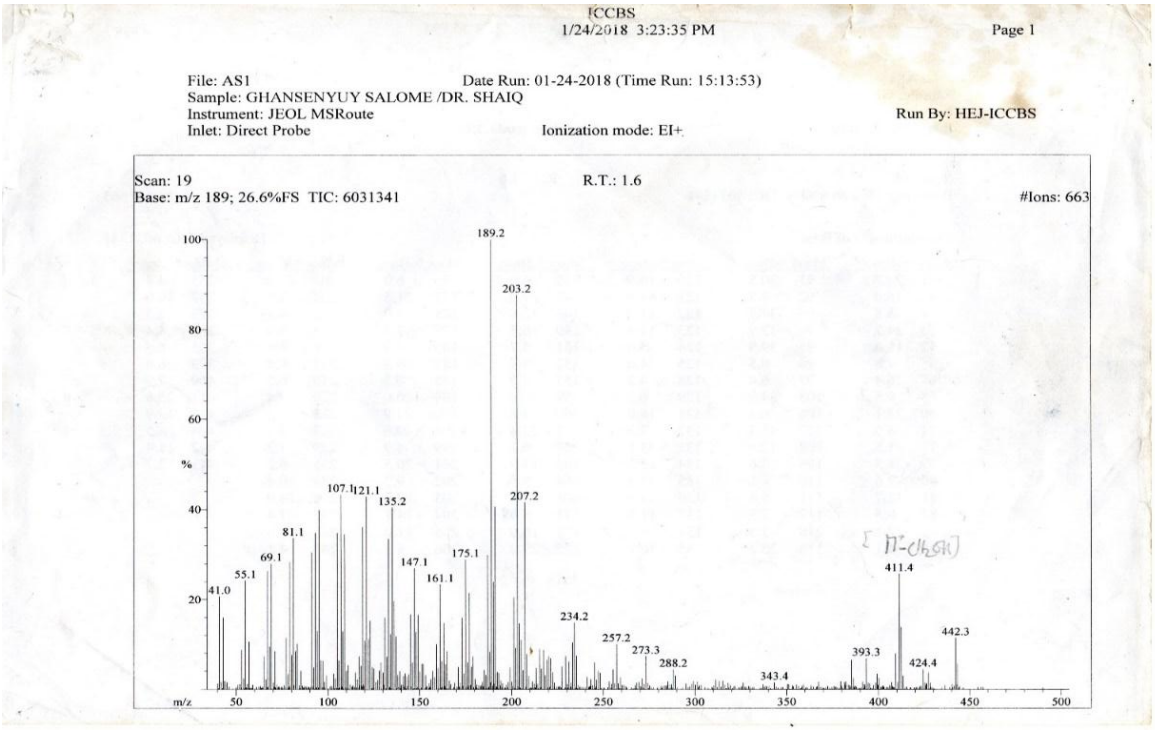

Figure 7: EI-Mass spectrum of Compound 62

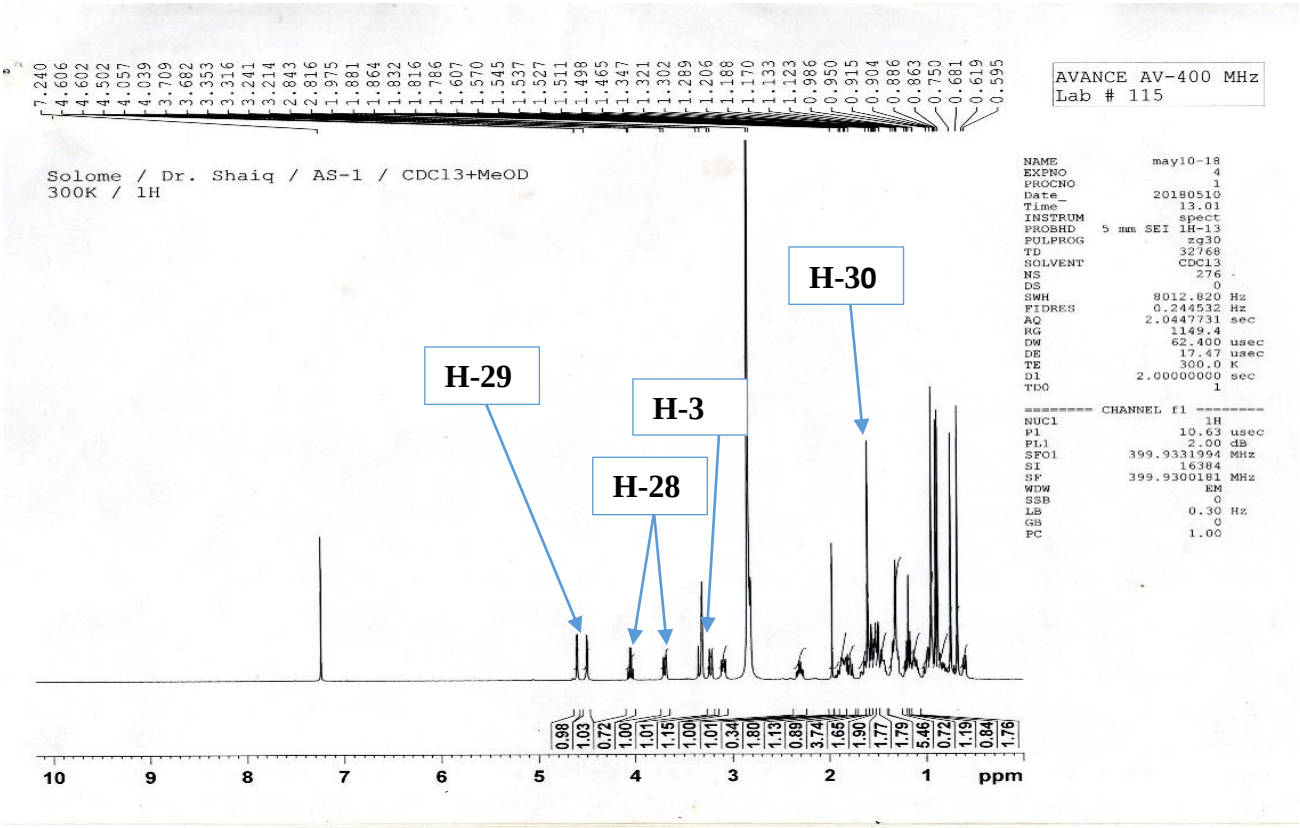

Figure 8: ^{1}H-NMR of Compound 62 ($CDCl_3$/CD_3OD, 400 MHz)

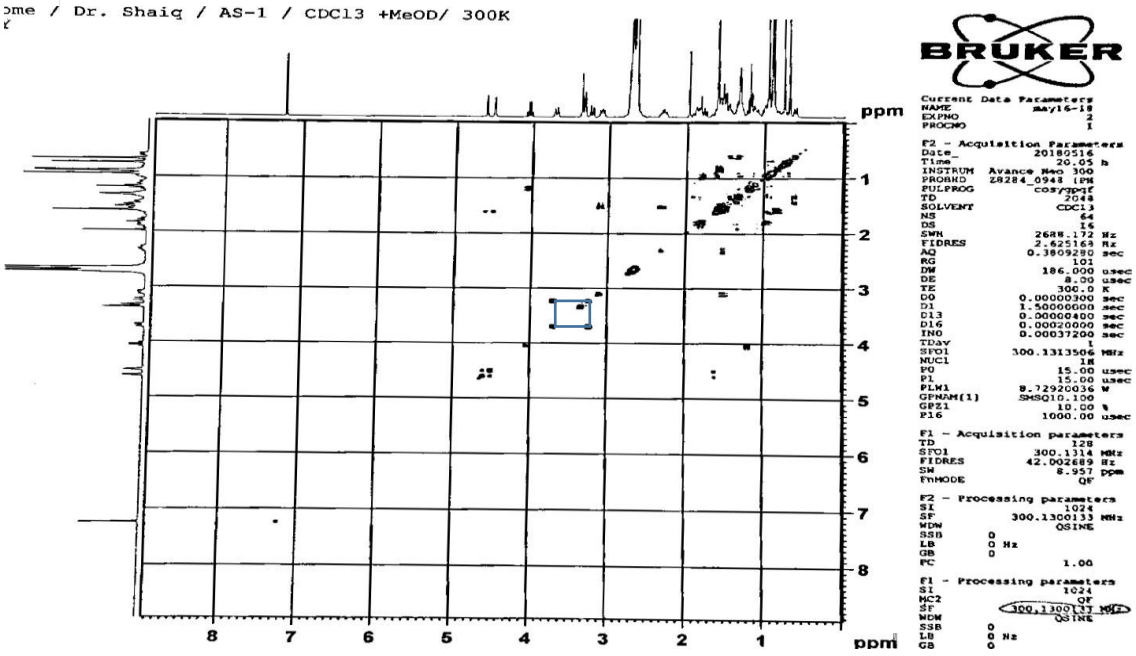

Figure 9: ^{1}H-^{1}H COSY spectrum of compound 62

II.2.1.2 Identification of compound AS_2

AS_2 was obtained as white powder from Hexane 100 % (m.p. 186 °C) and gave a positive result (purple) to the Libermann-Buchard test characteristic of triterpenes. Its EIMS (**Figure 10**) showed a molecular ion peak $[M]^+$ at *m/z* 468.3 compatible with the molecular formula $C_{32}H_{52}O_2$ corresponding to seven degrees of unsaturations. Its ^1H NMR spectrum exhibited:

- Two signals of three protons each at δ 0.88 and at δ 0.74 attributable to H-30 and H-29 of the ursane triterpene skeleton,
- A multiplet of one proton at δ 5.01 attributable to the olefinic proton H-12,
- A doublet of one proton at δ 4.44 attibutable to h-3 deshielded by the electron withdrawing effects of the acetyl group,
- One singlet of three protons at δ 2.00 attributable to the h-2' of the acetyl group,
- Six singlets of three protons at δ 1.02, 0.96, 0.93, 0.83, 0.82, 0.75 attributable to H-27, 26, 25, 24, 23, 28 respectively.

The ^1H-^1H COSY spectrum (**Figure 12**) shows the correlation between the olefinic protons at δ 5.01 (H-12) and δ1.87 (H-11) and also correlaytion between the proton at δ 4.44 (H-3) and δ 1.52 (H-2).

The HMBC spectrum (**Figure 13**) shows the correlation between the proton at δ 2.00 (H-2') and the carbon at δ 172.0 (C-1') and also the correlation between the proton at δ 4.44 H-3) and the carbon at δ 172.0 (C-1').

These physical and spectroscopic data were in agreement with those previously reported for alpha amyrin acetate **(54)** (**Okoye *et al.*, 2014**).

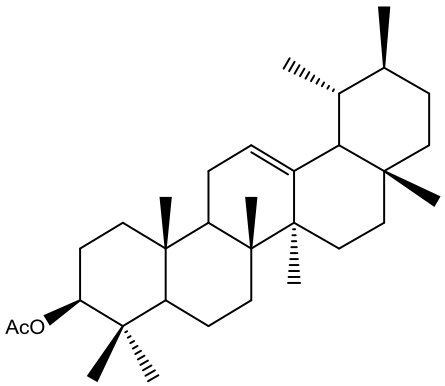

(54)

Table 14: ^{1}H NMR data of AS_2 and the litterature

AS_2		α-amyrin acetate (Okoye et *al.*, 2014)
N_o	**^{1}H (nH , m)**	**^{1}H (nH , m)**
3	4.44 (1H, d)	4.48 (1H, dd)
12	5.01 (1H, m)	5.10 (1H, t)
23	0.82 (3H, s)	0.83 (3H, s)
24	0.83 (3H, s)	0.84 (3H, s)
25	0.93 (3H, s)	0.96 (3H, s)
26	0.96 (3H, s)	0.98 (3H, s)
27	1.02 (3H, s)	1.04 (3H, s)
28	0.75 (3H, s)	0.78 (3H, s)
29	0.74 (3H, dd)	0.77 (3H, dd)
30	0.88 (3H, dd)	0.83 (3H, dd)
1'	-	-
2'	2.00 (3H, s)	2.02 (3H, s)

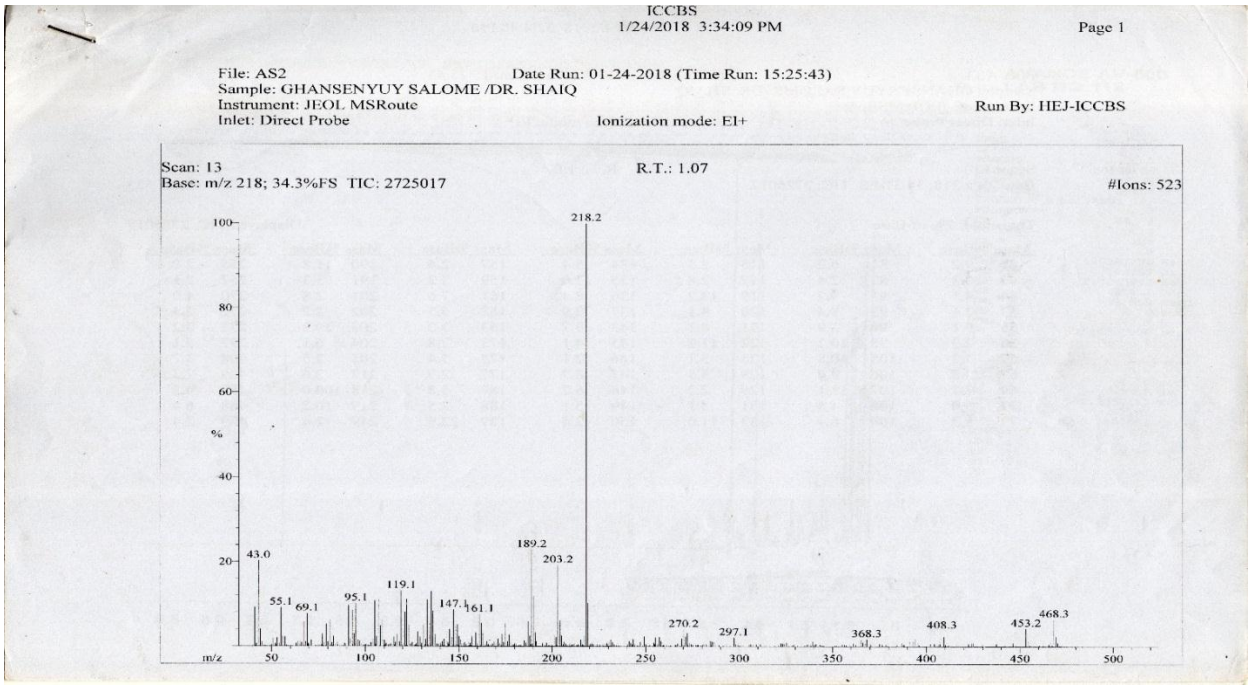

Figure 10: EI-Mass spectrum of compound 54

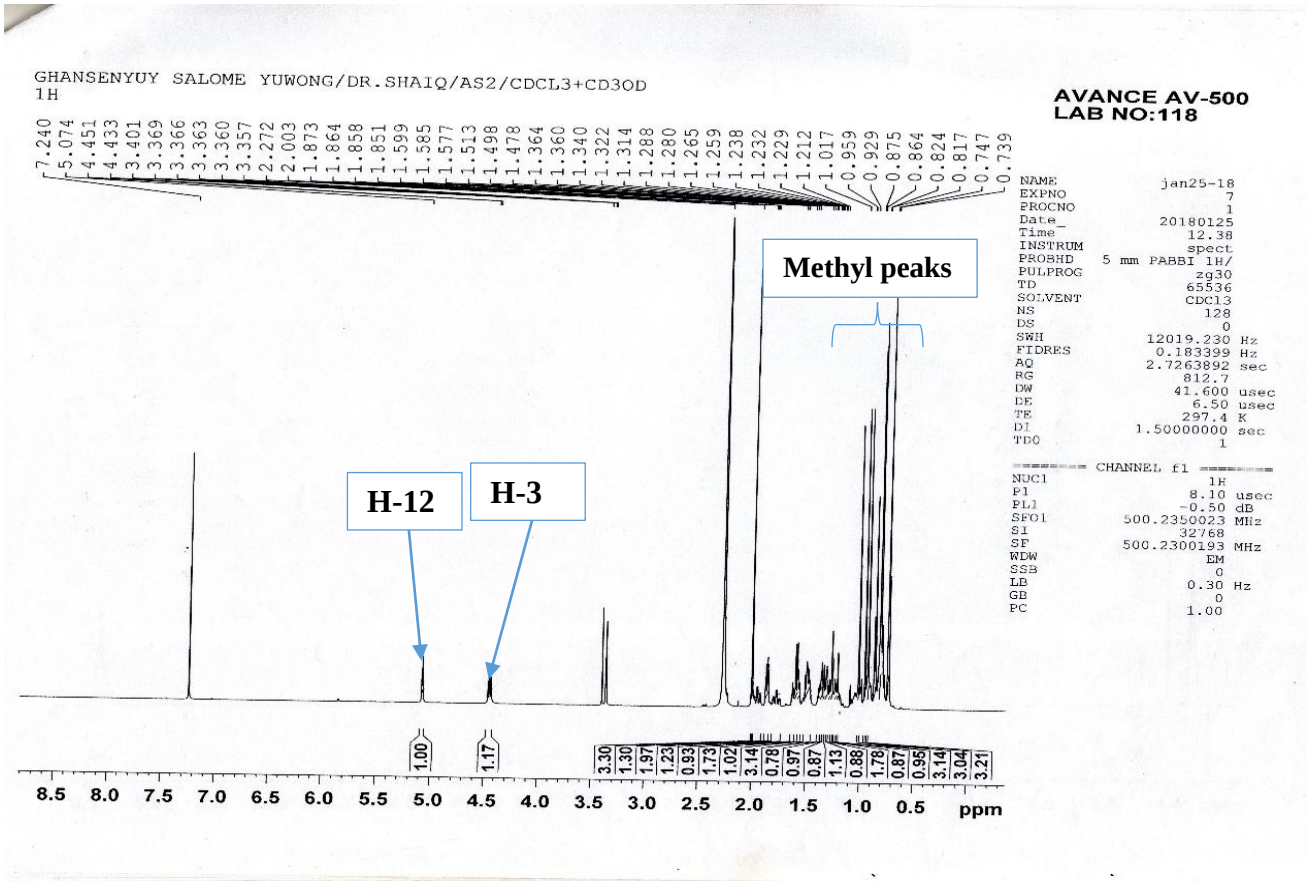

Figure 11: ^{1}H-NMR of Compound 54 ($CDCl_3$, 500 MHz)

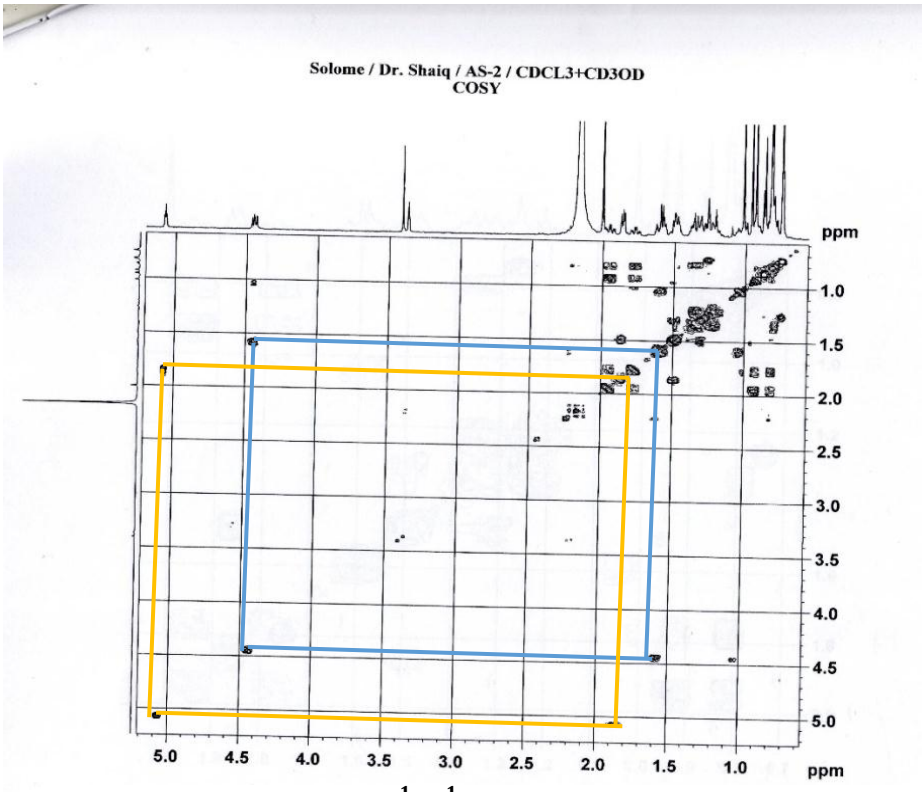

Figure 12: ^{1}H-^{1}H COSY of compound 54

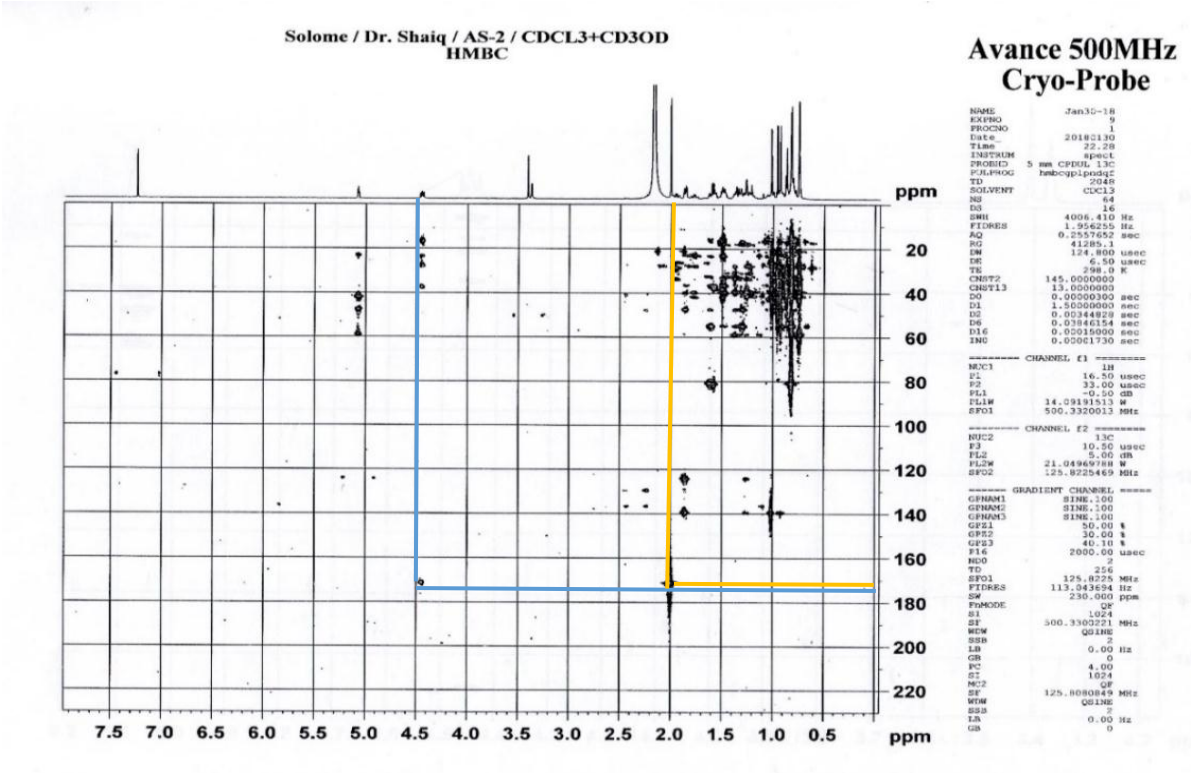

Figure 13: HMBC of compound 54

II.2.1.3 Identification of compound AS_6 =PG_7

AS_6 was obtained as white powder from DCM/MeOH 1% (m.p. 287 °C) and gave a positive result (purple coloration) to the Libermann-Buchard test characteristic of triterpenes. Its EIMS **(Figure 14)** showed a molecular ion peak $[M]^+$ at *m/z* 456.2 compatible with the molecular formula $C_{30}H_{40}O_3$ corresponding to seven degrees of unsaturations.

Its ^{1}H NMR spectrum **(Figure 15)** exhibited:

- A broad singlet of one proton at δ 5.50 attributable to the olefinic proton H-12
- A doublet of doublet at δ 3.44 attributable to the oxymethine proton H-3
- A doublet of three protons at δ 1.03 and a broad singlet of three protons at δ 3.88 attributable to protons H-29 and H-30 respectively
- Five singlets of three protons each at δ1.05, 1.02, 1.01, 0.94, 0.89, (each 3H, s H-27, 26, 25), (each 3H, s, H-24, 23)

These physical and spectroscopic data were in agreement with those previously reported for ursolic acid (**53)** (**Werna *et al.*, 2003**).

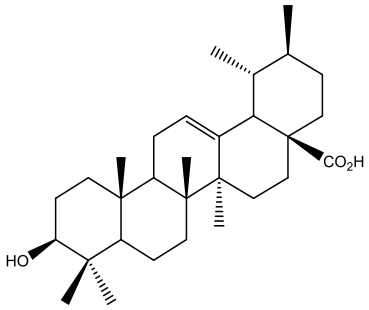

(53)

Table 15: ^{1}H NMR data of AS_6 = PG_7 and the literature

	AS_6	Ursolic acid (Seebacher et *al.*, 2003)
N_o	**^{1}H (nH , m)**	**^{1}H (nH , m)**
3	3.47 (1H, m)	3.44 (1H, dd)
12	5.49 (1H, s)	5.49 (1H, s)
23	1.24 (3H, s)	1.24 (3H, s)
24	1.05 (3H, s)	1.02 (3H, s)
25	0.93 (3H, s)	0.92 (3H, s)
26	1.05 (3H, s)	1.06 (3H, s)
27	1.24 (3H, s)	1.24 (3H, s)
28	-	-
29	1.02 (3H, d)	1.02 (3H, d)
30	0.99 (3H, brs)	0.97 (3H, d)

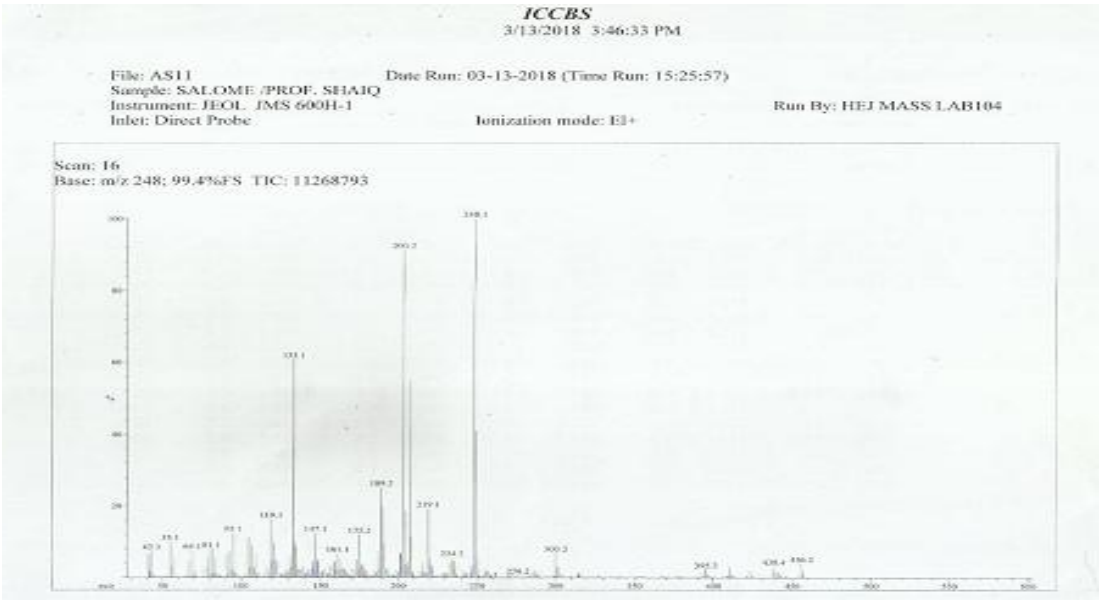

Figure 14: EI-Mass spectrum of compound 53

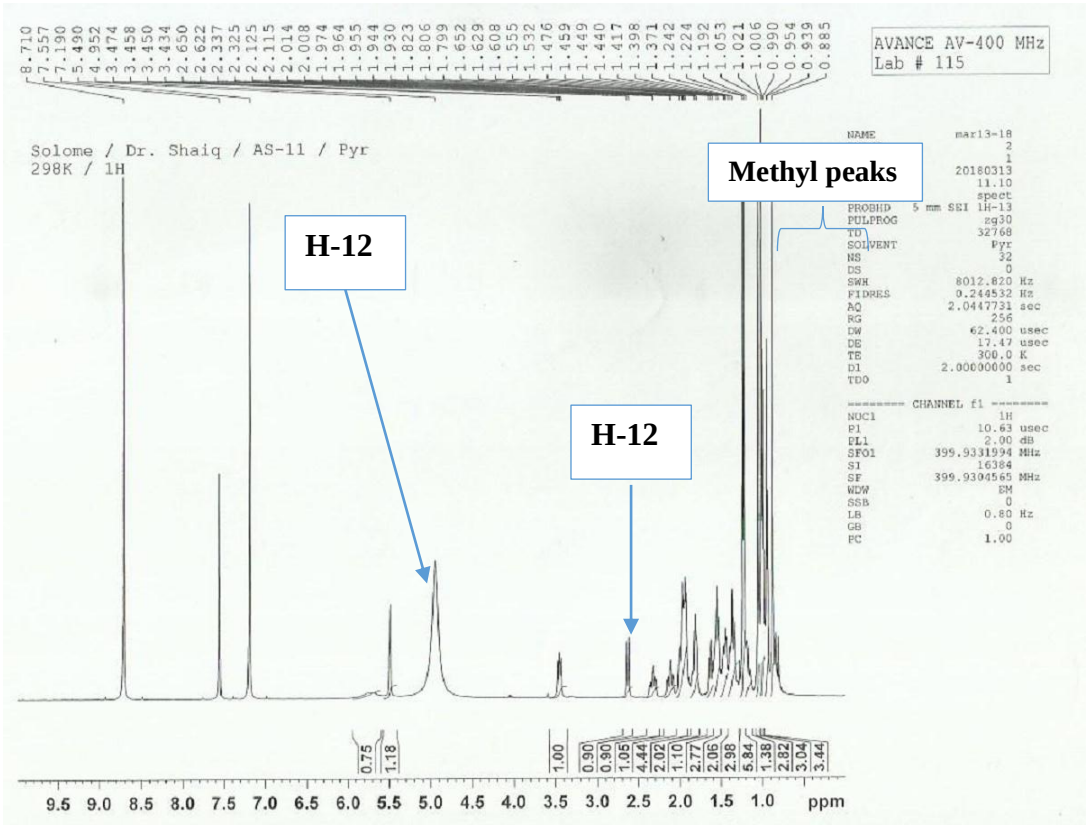

Figure 15: ^{1}H-NMR spectrum of compound 53 ($CDCl_3$, 400 MHz)

II.2.1.4 Identification of compound PG_2

PG_2 was obtained as white powder from Hexane-Ethyl acetate 5 % (m.p. 160 °C) and gave a positive result (purple coloration) to the Libermann-Buchard test characteristic of triterpenes. Analysis of the ^{1}H NMR **(Figure 16)** spectrum displayed resonances due to:

- an oxymethine proton at δ_H 3.50 (*brs*, 1H) ppm.
- methyl protons at δ_H 0.97 (s, H-24), 1.11 (d, H-23), 0.93 (s, H-25), 0.97 (s, H-26), 1.01 (s, H-27), 1.00 (s, H-30), 1.17 (s, H-28) and 0.89 (s, H-29) ppm.

Analysis of the ^{13}C NMR spectrum **(Figure 17)** displayed signals of:

- C-4 at δ_C 49.2
- C-3 at δ_C 72.8
- C-10 at δ_C 61.3

Analysis of its DEPT 135 NMR spectrum **(Figure 18)** displayed;

- eleven signals on the negative phase corresponding to eleven methylene carbon

- thirteen signals on the positive phase corresponding to thirteen methyl and methine groups.

The ^{1}H and ^{13}C NMR spectra data showed complete agreement with those reported in the literature **(Kemboi *et al.*, 2022; Islam et *al.*, 2014).**

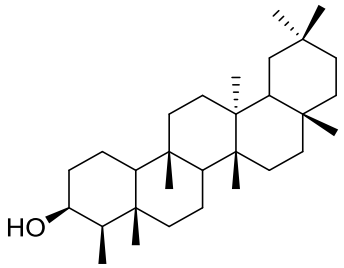

(219)

Table 16: ^{1}H NMR data of PG_2 and the literature

	PG_2		**3β-fridelanol (Islam et *al.*, 2014)**	
N_o	**^{1}H (nH , m, *J* in Hz)**	**^{13}C**	**^{1}H (nH , m, *J* in Hz)**	**^{13}C**
3	3.75 (1H, brs)	72.8	3.74 (1H, brs)	71.3
23	0.93 (3H, d, *J* = 6.8 Hz)	16.4	0.93 (3H, d, *J* = 6.8 Hz)	16.8
24	0.96 (3H, s)	11.7	0.96 (3H, s)	14.7
25	0.86 (3H, s)	18.3	0.86 (3H, s)	18.3
26	0.97 (3H, s)	18.7	0.98 (3H, s)	18.7
27	1.00 (3H, s)	20.1	1.00 (3H, s)	20.3
28	1.18 (3H, s)	32.1	1.18 (3H, s)	32.1
29	0.94 (3H, s)	31.8	0.94 (3H, s)	31.8
30	0.98 (3H, s)	35.1	0.99 (3H, s)	35.0

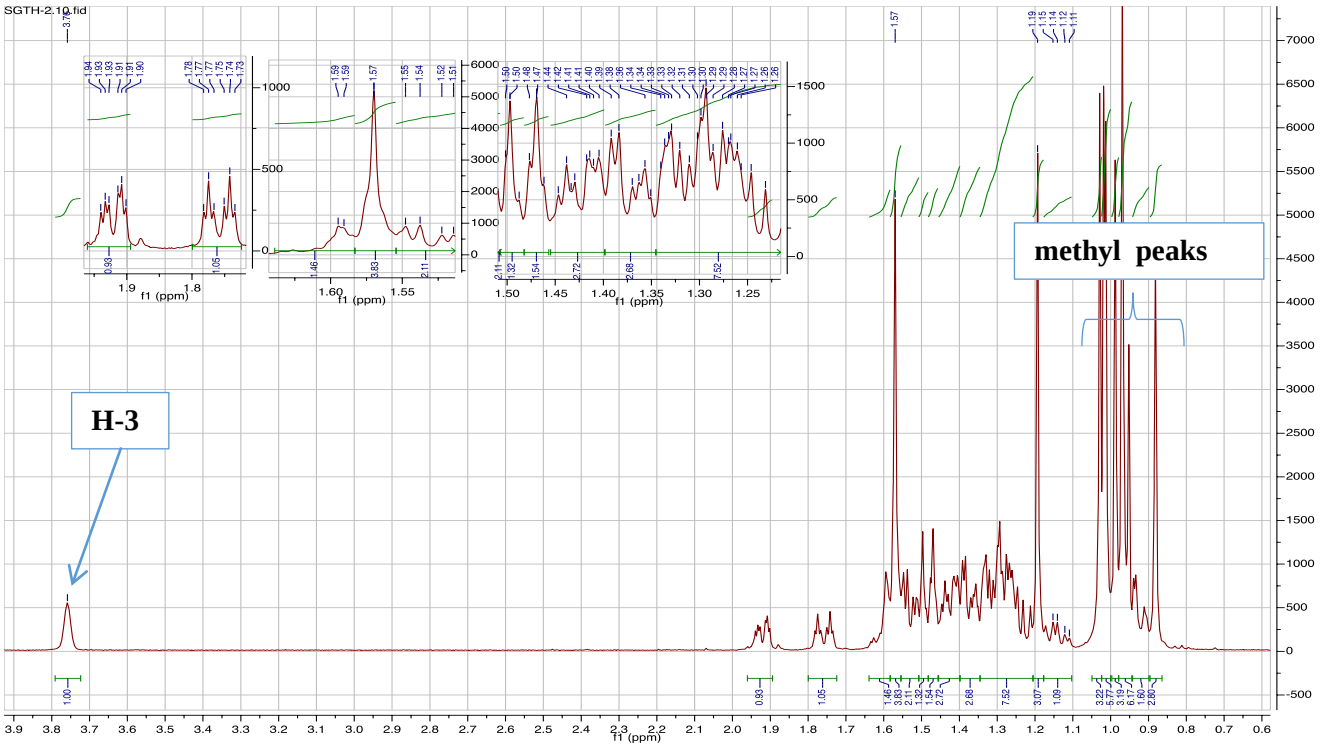

Figure 16: ^{1}H NMR spectrum of compound 219 ($CDCl_3$, 400 MHz)

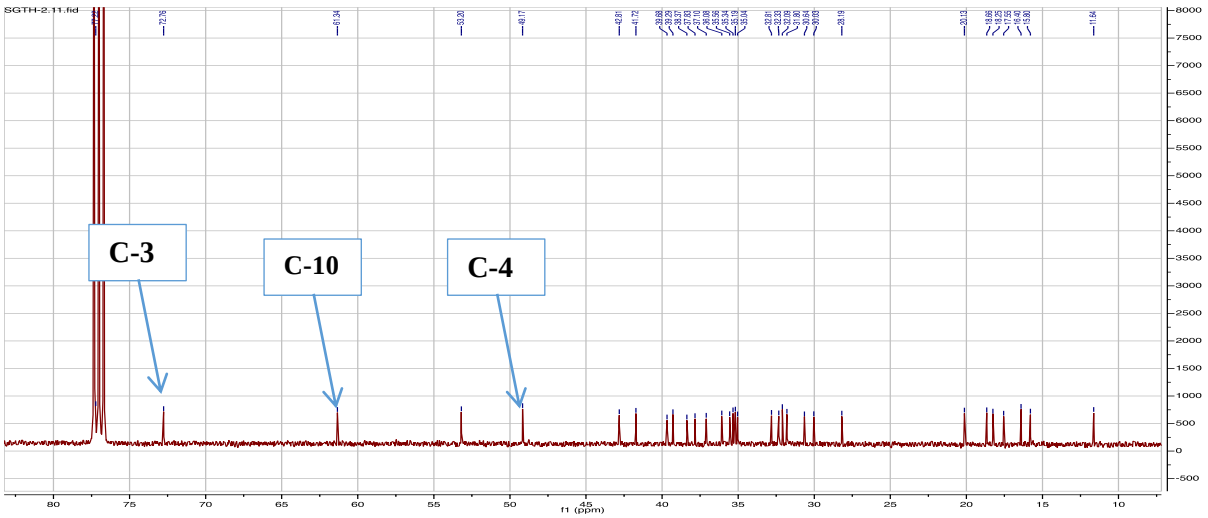

Figure 17: ^{13}C NMR spectrum of compound 219 ($CDCl_3$, 100 MHz)

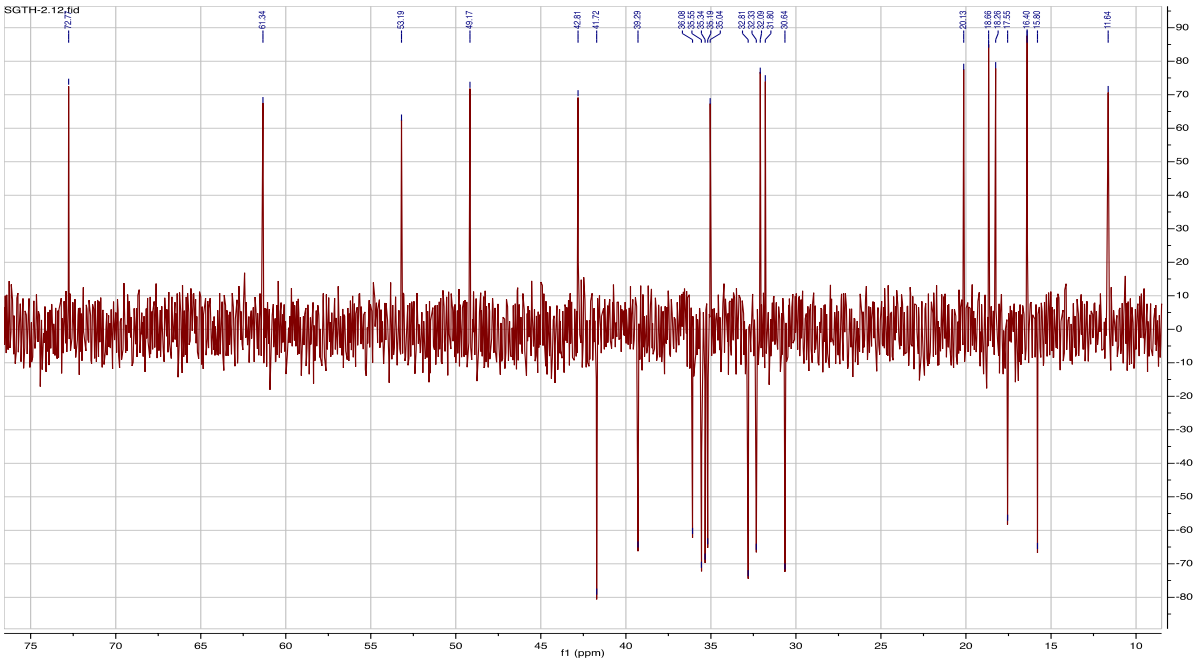

Figure 18: DEPT 135 NMR spectrum of compound 219 ($CDCl_3$, 100 MHz)

II.2.1.5 Identification of compound PG_6

PG_6 was obtained as white powder from Hexane-Ethyl acetate 25-27% (m.p. 288 °C) and gave a positive result (purple) to the Libermann-Buchard test characteristic of triterpenes. Its LC-MS (**Figure 19**) showed showed a retention time of 10.2 minutes and we observed a molecular ion peak $[M-H]^+$ at *m/z* 455.20 compartible with the molecular formula $C_{30}H_{47}O_3$ corresponding to seven degrees of unsaturations. Its ^1H NMR spectrum exhibited:

- Five singlets of three protons each between δ 0.60 and 1.10 attributable to five angular methyl groups of lupane triterpenes
- One singlet of three protons at δ 1.77 attributable to proton H-30
- One multiplet of one proton at δ 3.21 attributable to the oxymethine proton H-3
- Two doublets of two protons each at δ 4.60 and 4.61 characteristic of proton H-29 of the lup-20(29)-ene
- A multiplet of one proton at δ 2.84 attributable to proton H-19

The ^{13}C NMR (**Figure 21**) and DEPT-135 (**Figure 22**) spectroscopic data disclosed the presence of one carbonyl carbon (δ178.8), six quaternary carbons (one of which is an sp^2 carbon at δ 150.6), eleven methylene carbons (one of which is an sp^2 at δ 108.7), six methine carbons (one of which is an oxymethine at δ 78.25), and six methyl carbons.

These physical and spectroscopic data were in agreement with those previously reported for betulinic acid (**63**) **(Yemback *et al.*, 2023)**.

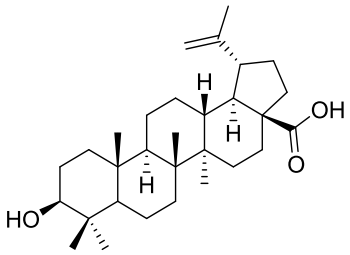

(63)

Table 17: ^{1}H NMR et ^{13}C NMR data of PG_6 and the literature

	PG_6		Betulinic acid (Yemback et *al.*, 2023)	
N_o	**^{1}H (nH , m)**	**^{13}C**	**^{1}H (nH , m)**	**^{13}C**
3	3,21 (1H, m)	78.3	3.01 (1H, m)	77.2
19	2.84 (1H, m)	48.1	2.80 (1H, m)	48.3
20	-	150.6	-	150.8
24	1.09 (3H, s)	21.0	1.09 (3H, s)	21.0
27	0,93 (3H, s)	14.3	0.95 (3H, s)	14.6
28	-	178.8	-	177.7
29	4.60 – 4.61 (2H, *brs*)	108.7	4.54 – 4.65 (2H, *brs*)	110.2
30	1.77 (3H, s)	19.2	1.69 (3H, s)	19.3

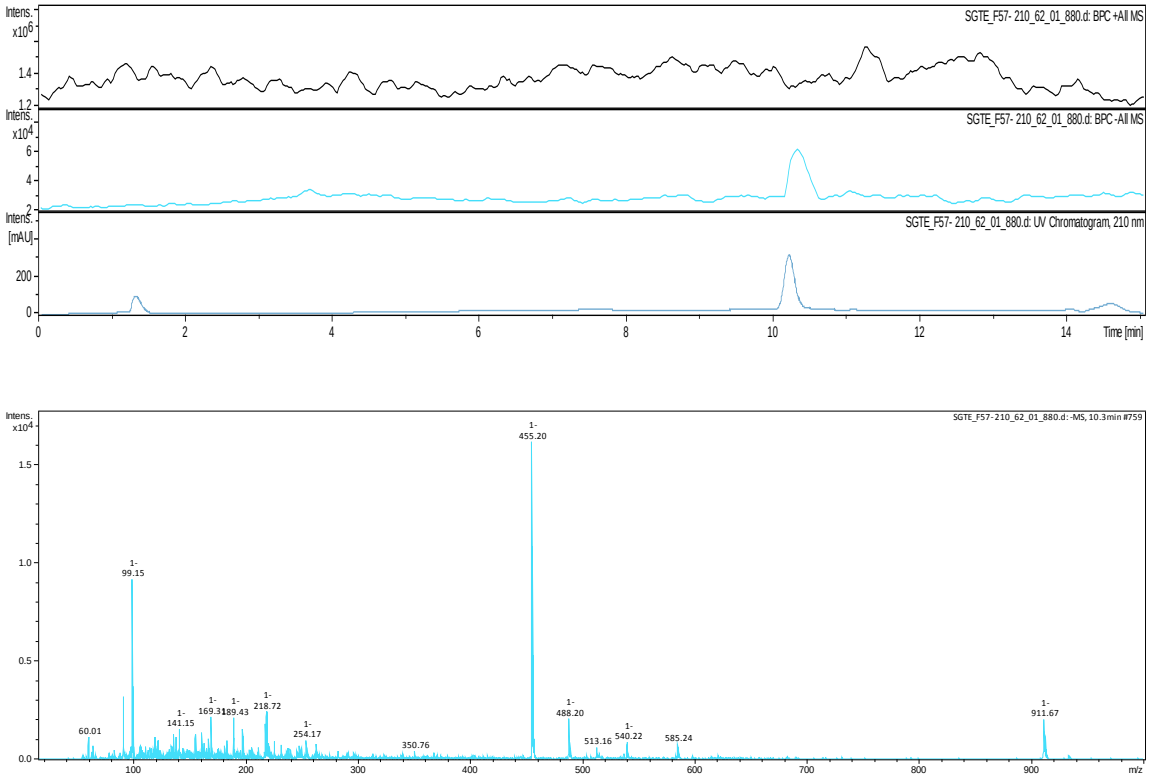

Figure 19: LC-MS Spectrum of compound 63

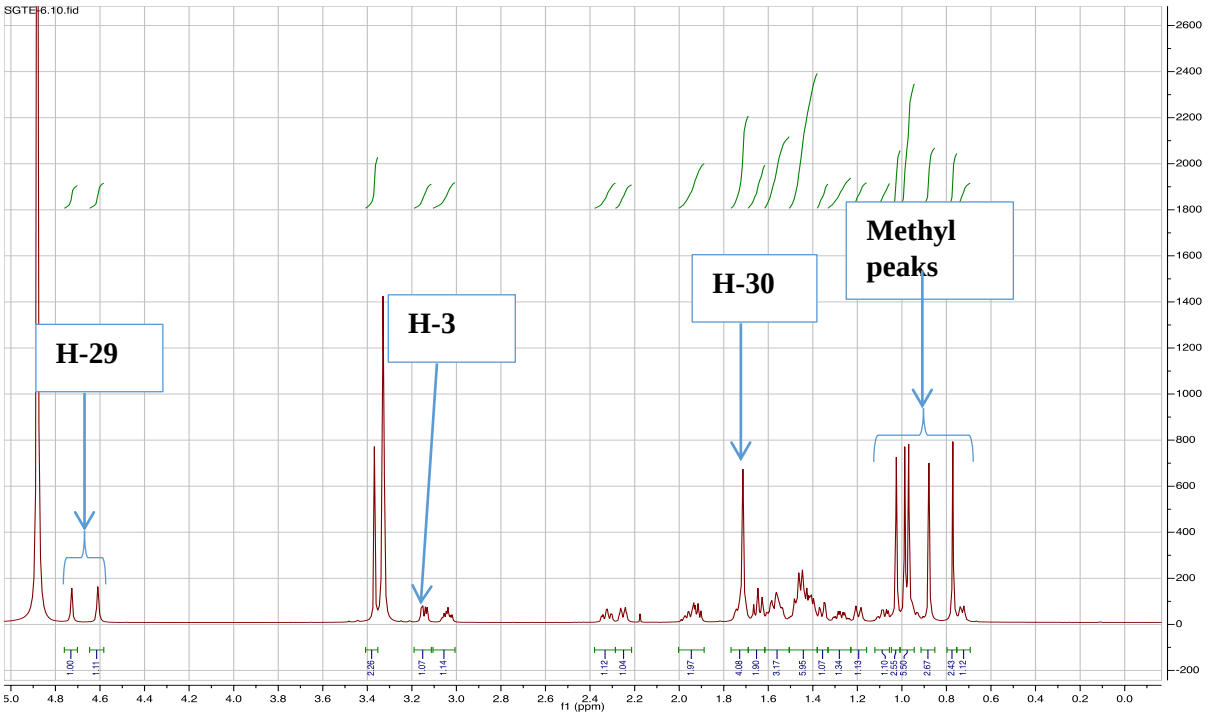

Figure 20: ^{1}H NMR spectrum of compound 63 (CD_3OD, 400 MHz)

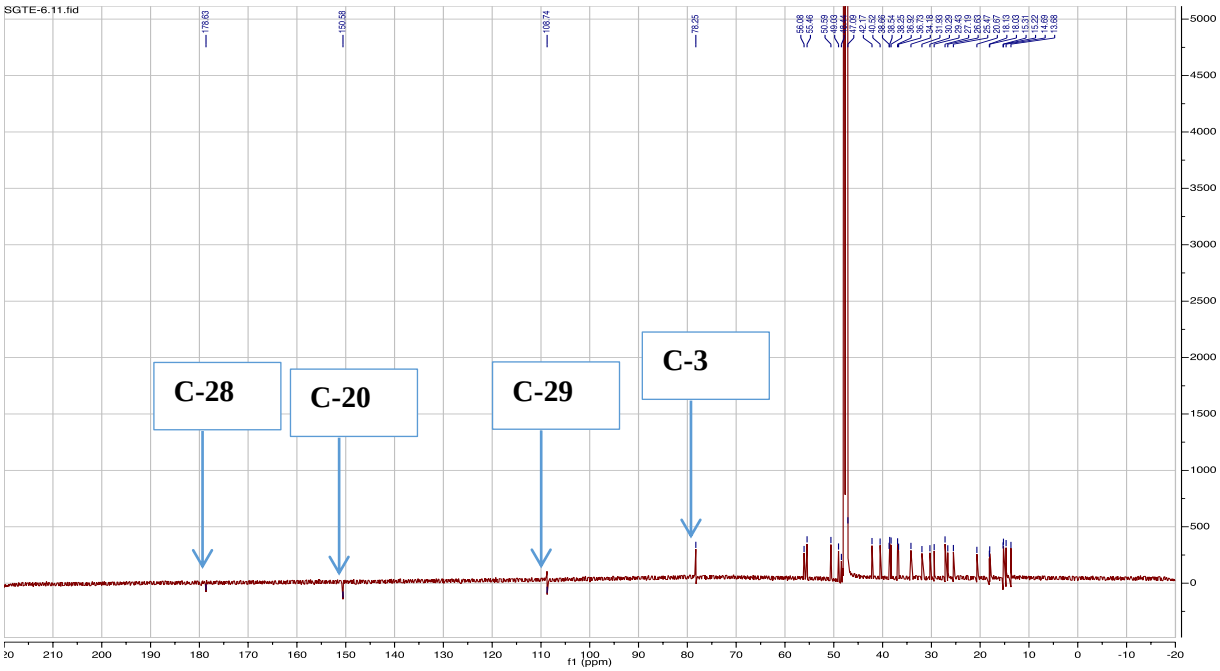

Figure 21: ^{13}C NMR spectrum of compound 63 (CD_3OD, 100 MHz)

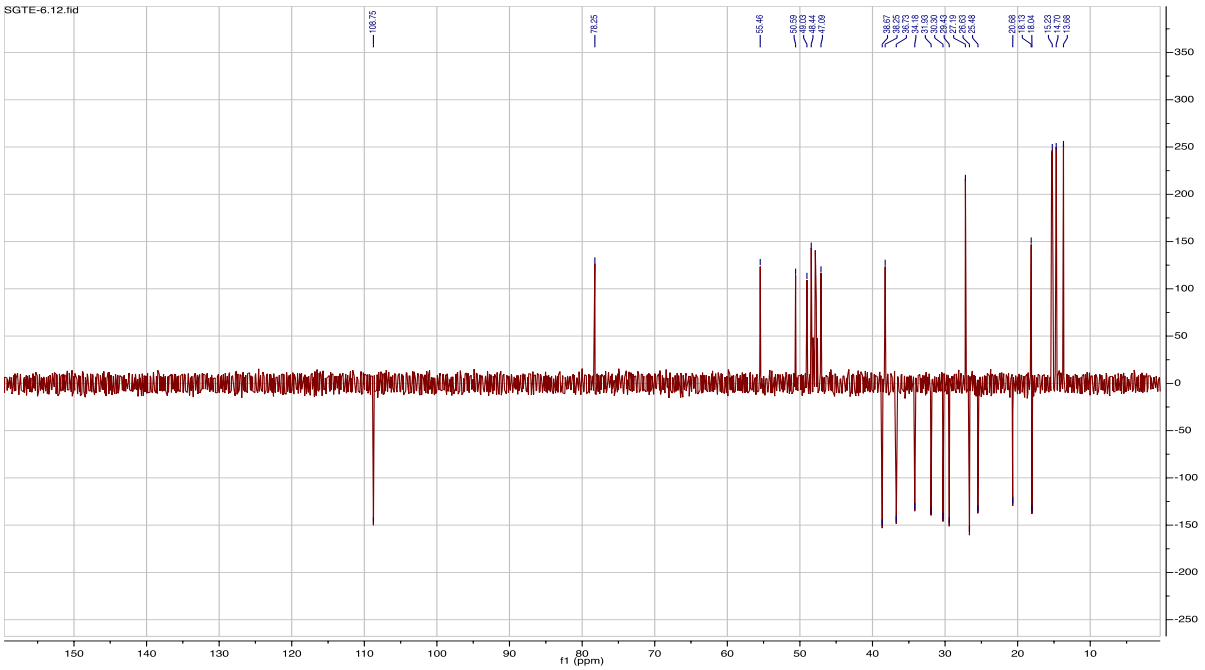

Figure 22: DEPT 135 NMR spectrum of compound 63 (CD_3OD, 100 MHz)

II.2.1.6 Identification of compounds AS_3 & AS_4

The mixture of AS_3 & AS_4 was obtained as white powder from *n*-hexane/EtOAc 4 % and gave bluish-green coloration to the Liebermann Buchard test characteristic of steroids. The EIMS spectrum **(Figure 23)** showed a peak at *m/z*: 414.3 corresponding to $C_{29}H_{50}O/C_{29}H_{48}O$. Its ^1H NMR spectrum showed a peak at δ 5.3 indicative of β-sitosterol and two broad peaks at δ 5.10 characteristic of stigmasterol.

It was identified as a mixture of *β*-sitosterol and stigmasterol by comparative TLC with authentic sample available in our laboratory and by comparison of its physical and spectroscopic data with those reported in the literature (**Luhata *et* Munkombwe, 2013**).

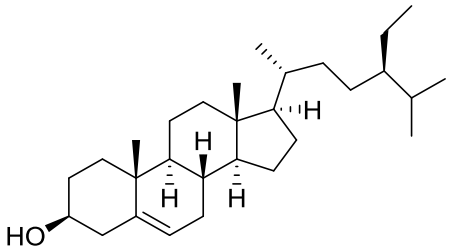

(128)

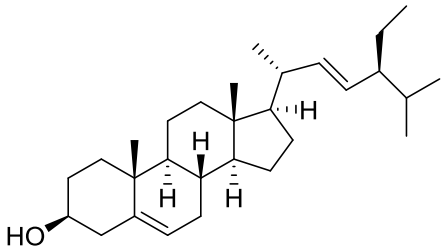

(129)

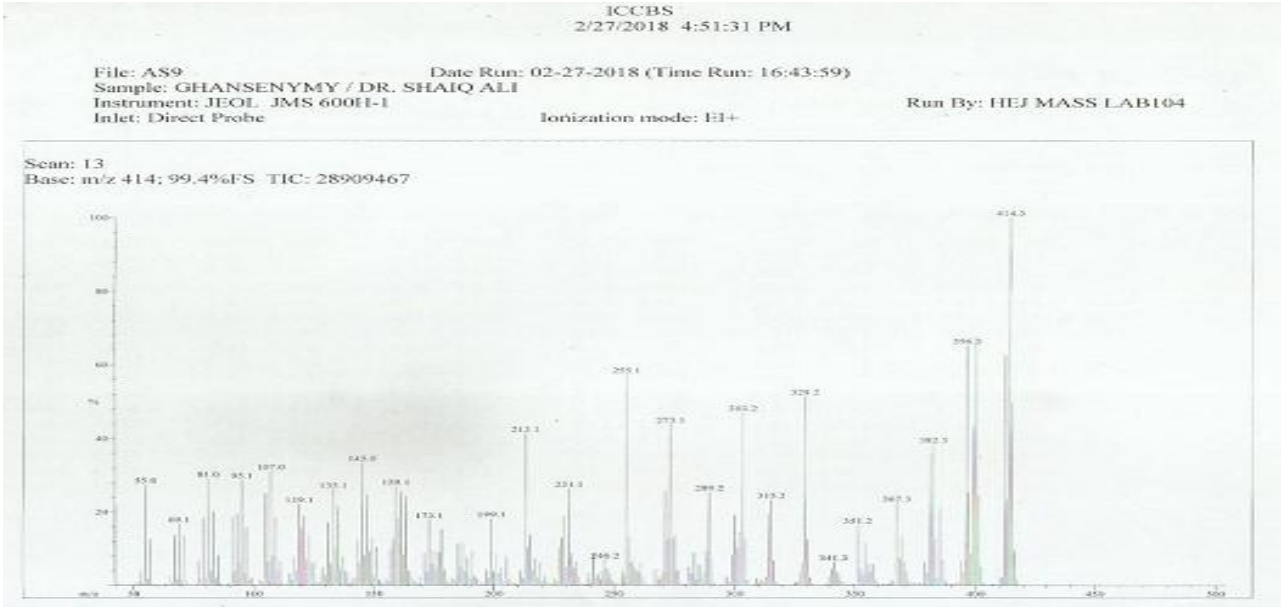

Figure 23: EI-Mass spectrum of compounds 128 and 129

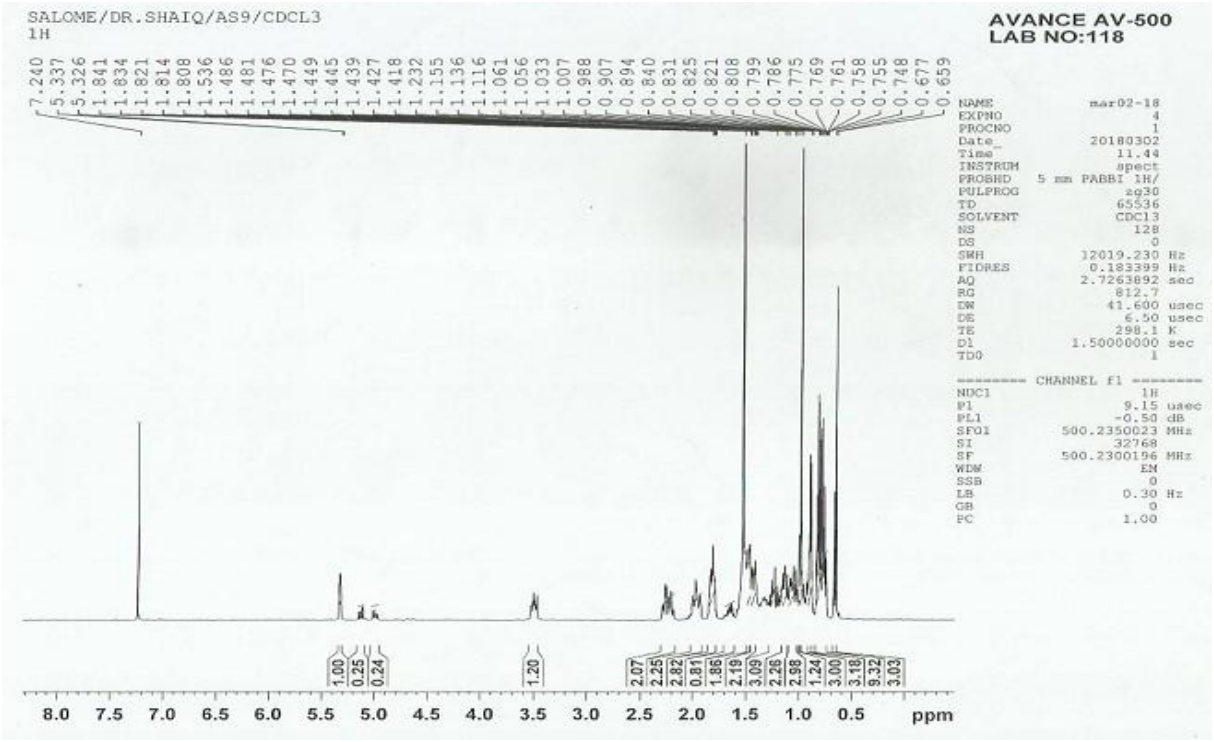

Figure 24: ^{1}H-NMR spectrum of compounds 128 and 129 ($CDCl_3$, 500 MHz)

II.2.1.7 Identification of compound AS_8

AS_8 was obtained as brownish-black powder from DCM/MeOH 5% and gave bluish-green coloration to the Liebermann Buchard test. It's HR-EI-MS spectrum **(Figure 25)** showed a molecular ion peak at *m/z*: 576.8 compatible with the molecular formula $C_{35}H_{60}O_6$. It was identified as β-sitosterol-3-O-ß-D-glucopyranoside **(218)** by comparative-TLC with authentic sample available in our laboratory and by comparison of its physical and spectroscopic data with those reported in the literature.

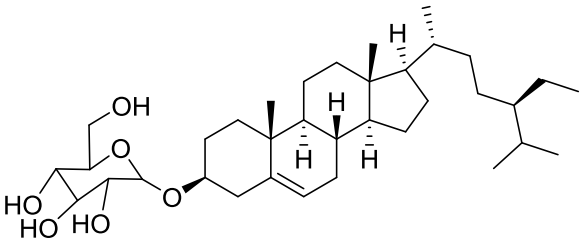

(218)

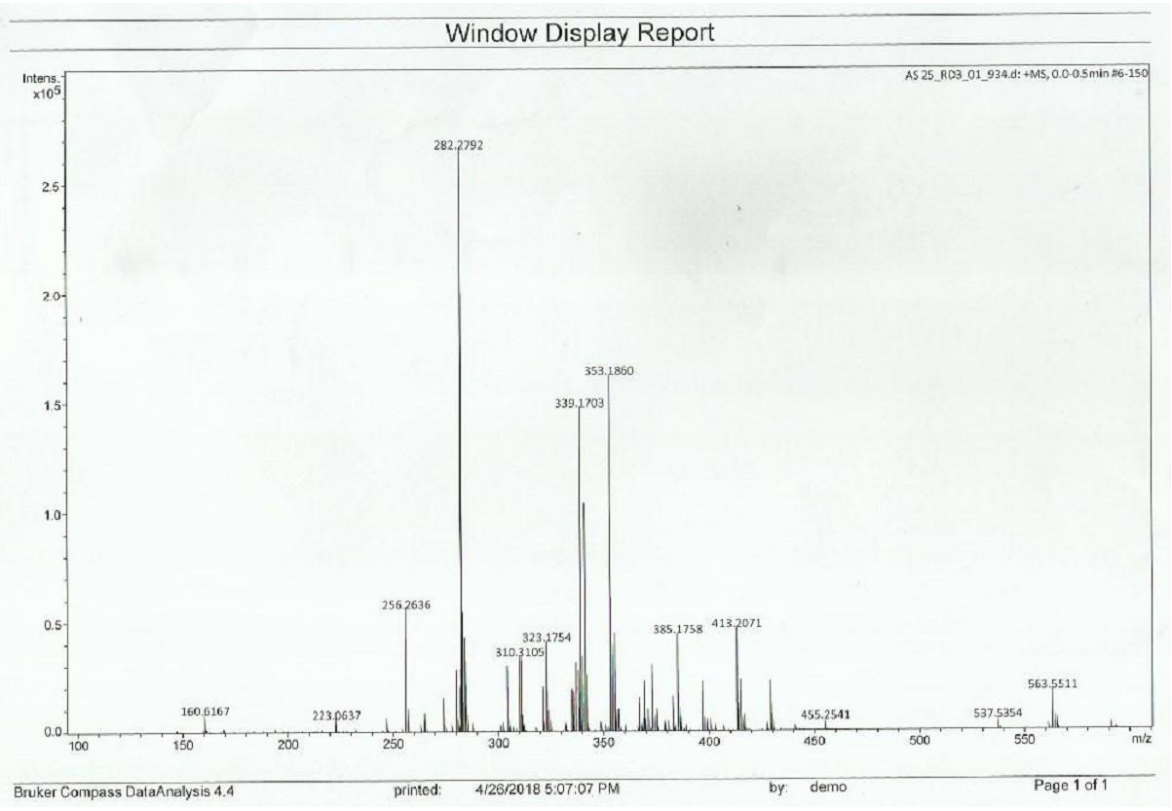

Figure 25: HR-EI-Mass spectrum of compound 218

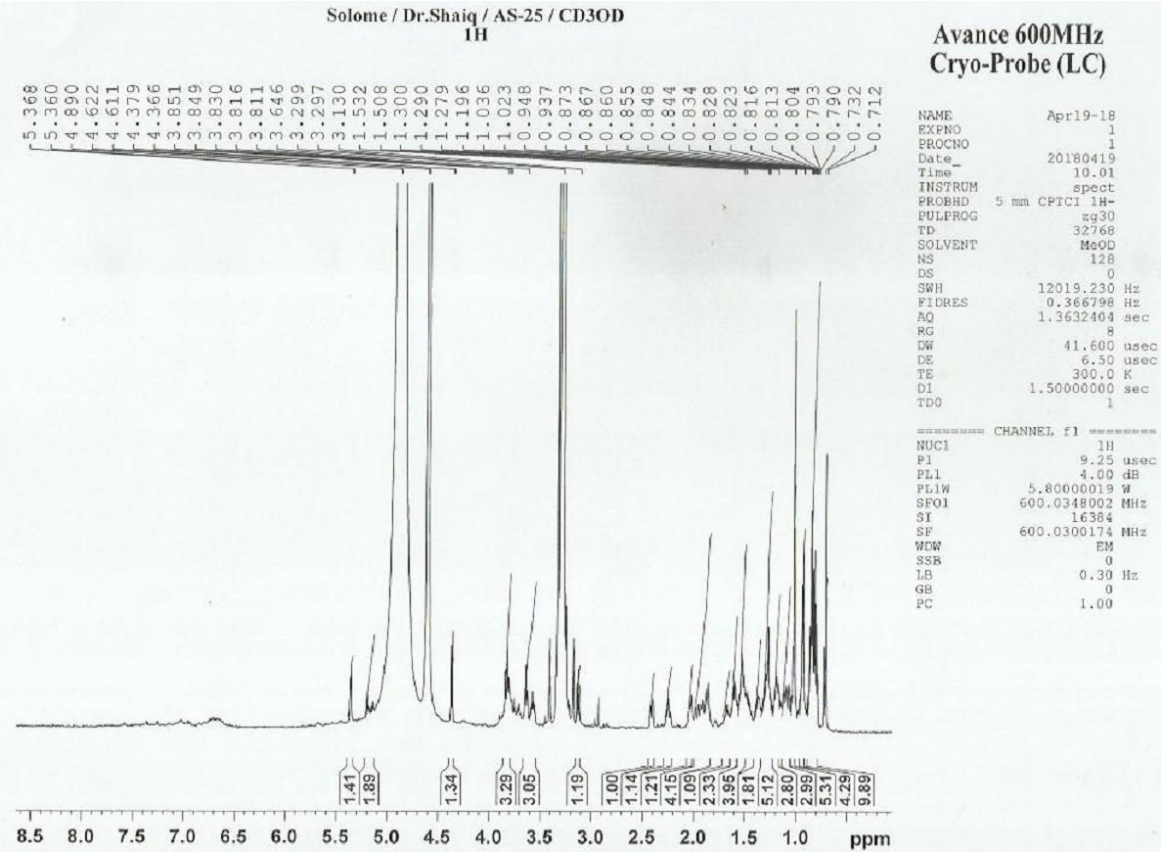

Figure 26: ^{1}H-NMR spectrum of compound 218 (CD_3OD, 600 MHz)

II.2.2 Characterisation of quinones

II.2.2.1 Identification of compound PG_1

PG_1 was obtained as orange powder from Hexane-Ethyl acetate 4 % (m.p. 120 °C) and gave a positive result to the Borntrager test characteristic of anthraquinones. Its LC-MS **(Figure 28)** showed a molecular ion peak *m/z*: 406.03 (with retention time at 12.80 min) compatible with the molecular formula $C_{25}H_{26}O_5$, corresponding to thirteen degrees of unsaturations. We also observed a retention time of 12.5 minutes. The analysis of its NMR data [^{1}H, ^{13}C NMR and DEPT 135] enabled us to assign structure **(219)**.

The ^{1}H NMR spectrum **(Figure 29)** exhibited:

- Four singlets of one proton each at δ 7.60 (1H, s, H-2), 7.40 (1H, s, H-5), 7.10 (1H, s, H-4) and 6.70 (1H, s, H-7) attributable to aromatic protons of tetra substituted anthraquinones. H-4 and H-5 are called peri protons and are characteristic of anthraquinone derivatives and nornally resonate as from 8.00 ppm.
- A deshielded singlet of three protons at δ 2.49 indicating the presence of a methyl on the aromatic ring.

- Two singlets of one proton each corresponding to two chelated hydroxyl groups (δ 12.4 and δ 12.2).
- A group of singlets and multiplets at δ 1.65 (3H, s, H-10'), 1.70 (3H, s, H-8'), 1.80 (3H, s, H-9'), 2.20 (4H, m, H-4', H-5'), 4.70 (2H, m, H-1'), 5.15 (1H, m, H-6') and 5.50 (1H, m, H-2') indicative of a geranyl moiety .

The ^{13}C NMR (**Figure 30**) and DEPT (**Figure 31**) spectroscopic data disclosed the presence of :

- two carbonyl carbons (δ 190.7 and δ182.1)
- ten sp^2 quaternary carbons (three of which were oxygen-bearing δ 166.9, 166.1, 162.5)
- six sp^2 methines (δ 107.5, 108.8, 117.9, 121.2, 123.6, 124.5)
- three sp^3 methylenes (δ 26.2, 39.5, 65.8)
- four methyl carbons (δ 16.8, 17.7, 22.2, 25.7).

These physical and spectroscopic data were in agreement with those previously reported for emodin **(Botta *et al.*, 1983)**.

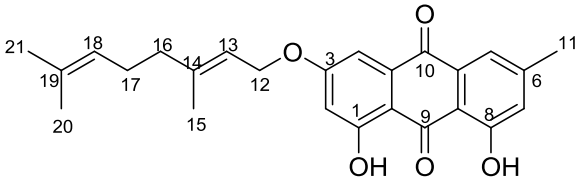

(94)

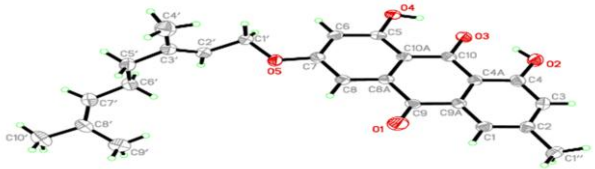

Figure 27: Single crystal X-ray structure of 3-geranyloxy Emodin 94

Table 18: ^{1}H NMR and ^{13}C NMR data of PG_1 and the litterature

	PG_1		**3-geranyloxy Emodin (Botta *et al.*, 1983)**	
N_o	**^{1}H (nH , m, *J* in Hz)**	**^{13}C**	**^{1}H (nH , m, *J* in Hz)**	**^{13}C**
1	-	165.1	-	163.6
2	6.60 (1H, br)	107.5	6.60 (1H, d, *J* = 2.5 Hz)	109.2
3	-	165.9	-	166.7
4	7.40 (1H, br)	108.8	7.25 (1H, br d, *J* = 2.4 Hz)	110.6
4a	-	135.2	-	131.9
4b	-	133.2	-	133.0
5	7.55 (1H, br)	121.2	7.50 (1H, br d, *J* = 1.8 Hz)	121.8
6	-	148.4	-	149.6
7	7.20 (1H, br)	123.6	7.00 (1H, br d, *J* = 1.8 Hz)	125.2
8	-	162.5	-	163.6
8a	-	113.7	-	113.9

8b	-	110.1	-	108.6
9	-	182.1	-	183.4
10	-	190.7	-	191.7
11	2.48 (3H, s)	22.2	2.40 (3H, s)	22.1
12	4.63 (2H, d, br)	65.8	4.60 (2H, d, *J* = 7 Hz)	65.2
13	5.50 (1H, t, *J* = 7.1 Hz)	117.9	5.43 (1H, t, *J* = 7 Hz)	119.1
14	-	142.8	-	139.5
15	1.65 (3H, s)	16.8	1.67 (3H, s)	16.4
16	2.12 (4H, m)	39.5	2.10 (4H, m)	39.7
17		26.2		26.4
18	5.10 (1H, br)	124.5	5.05 (1H, br)	123.5
19	-	132.0	-	132.0
20	1.58 (3H, s)	18.6	1.60 (3H, s)	18.6
21	1.75 (3H, s)	25.7	1.77 (3H, s)	24.6

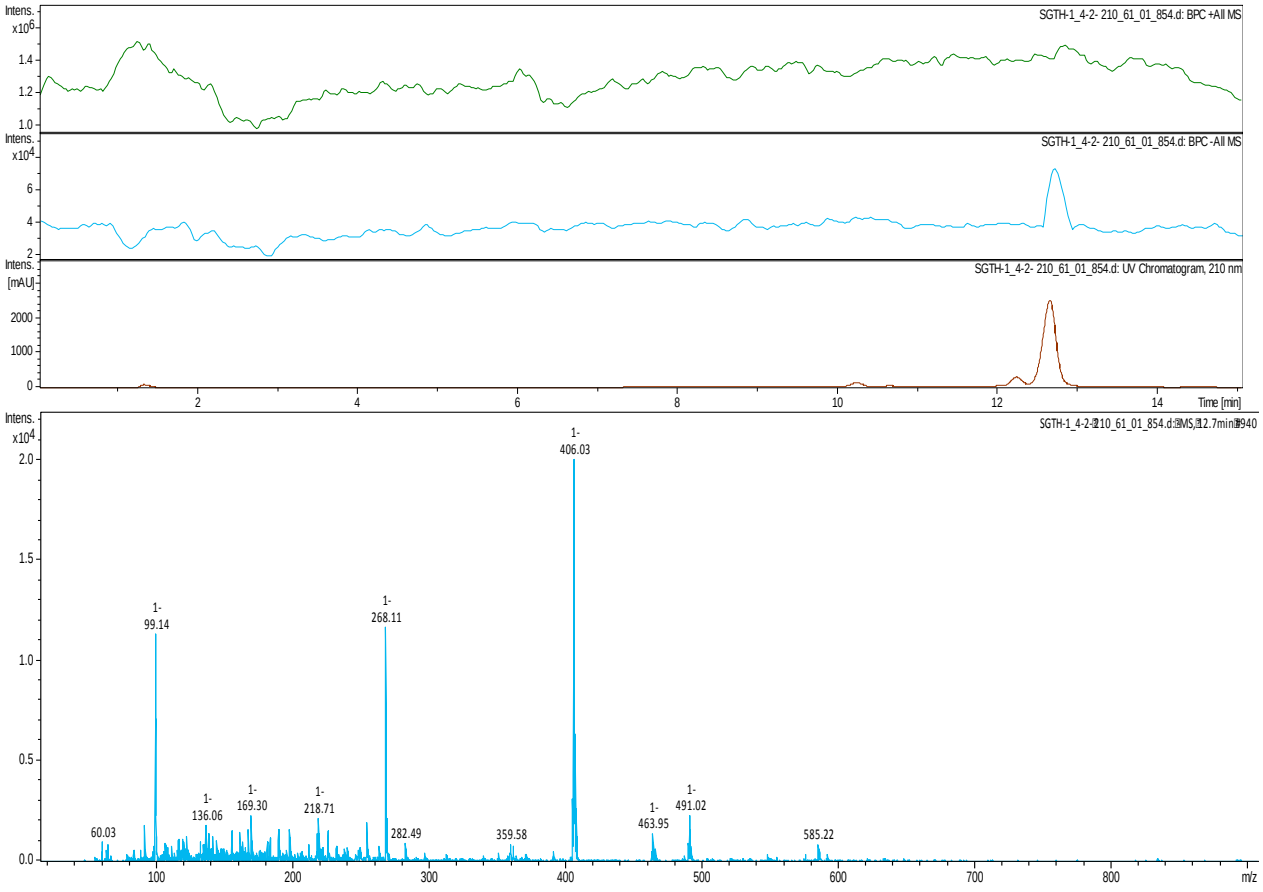

Figure 28: LC-MS spectrum of compound 94

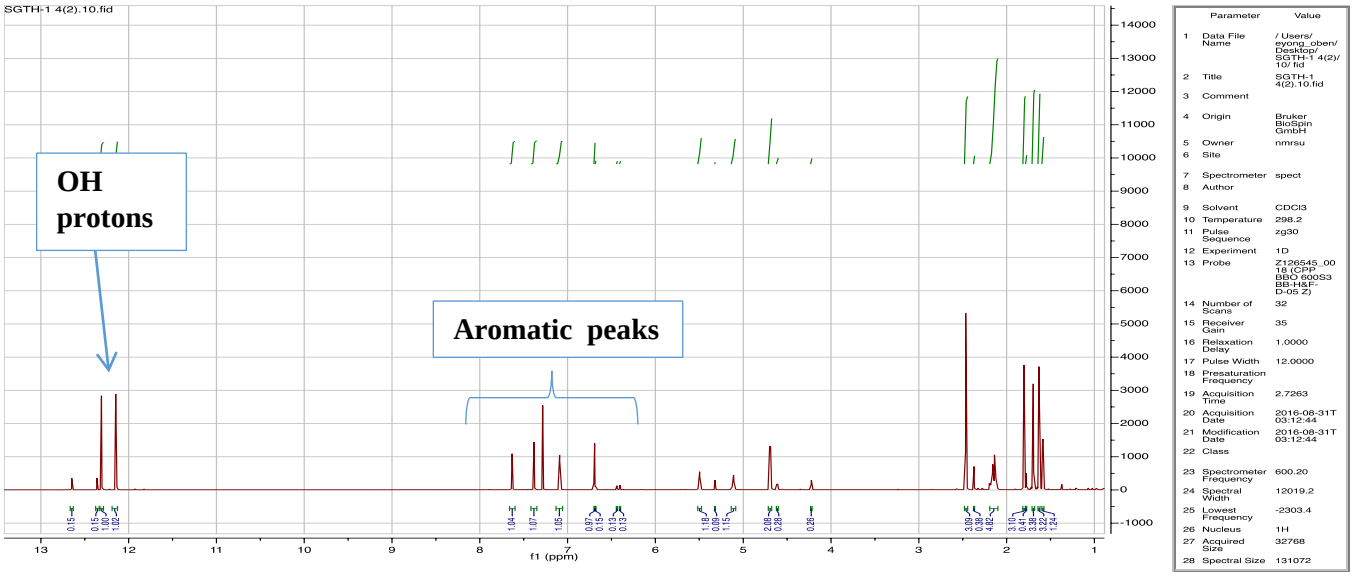

Figure 29: ^{1}H NMR of compound 94 ($CDCl_3$, 400 MHz)

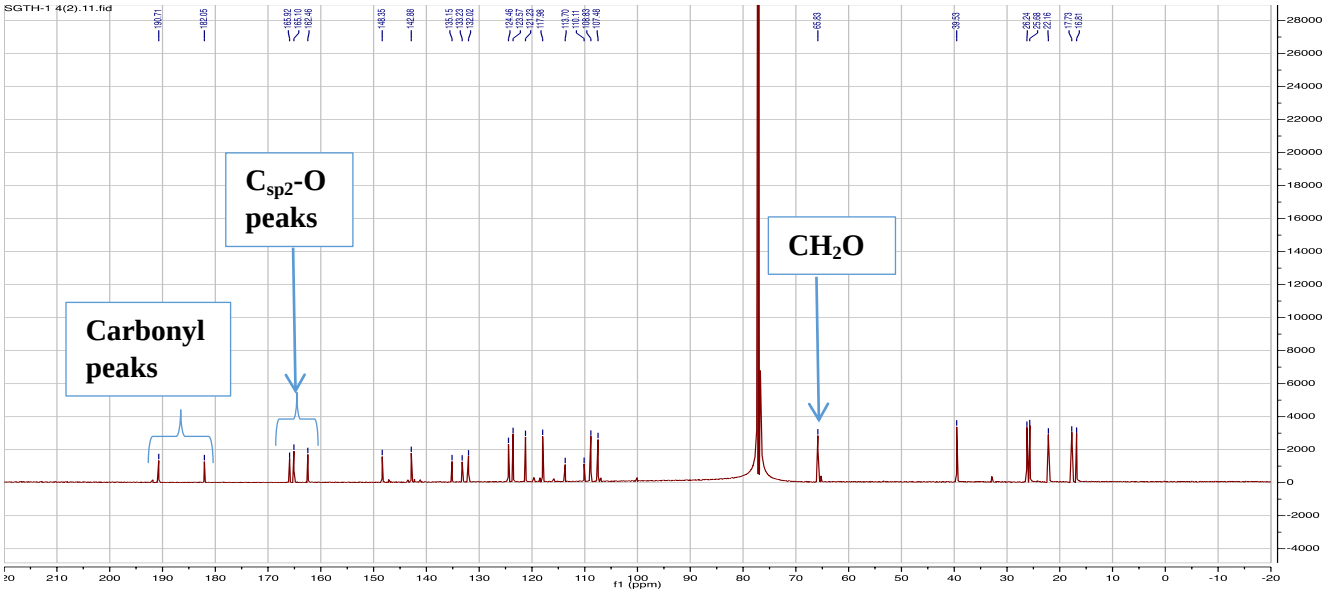

Figure 30: ^{13}C NMR spectrum of compound 94 ($CDCl_3$, 100 MHz)

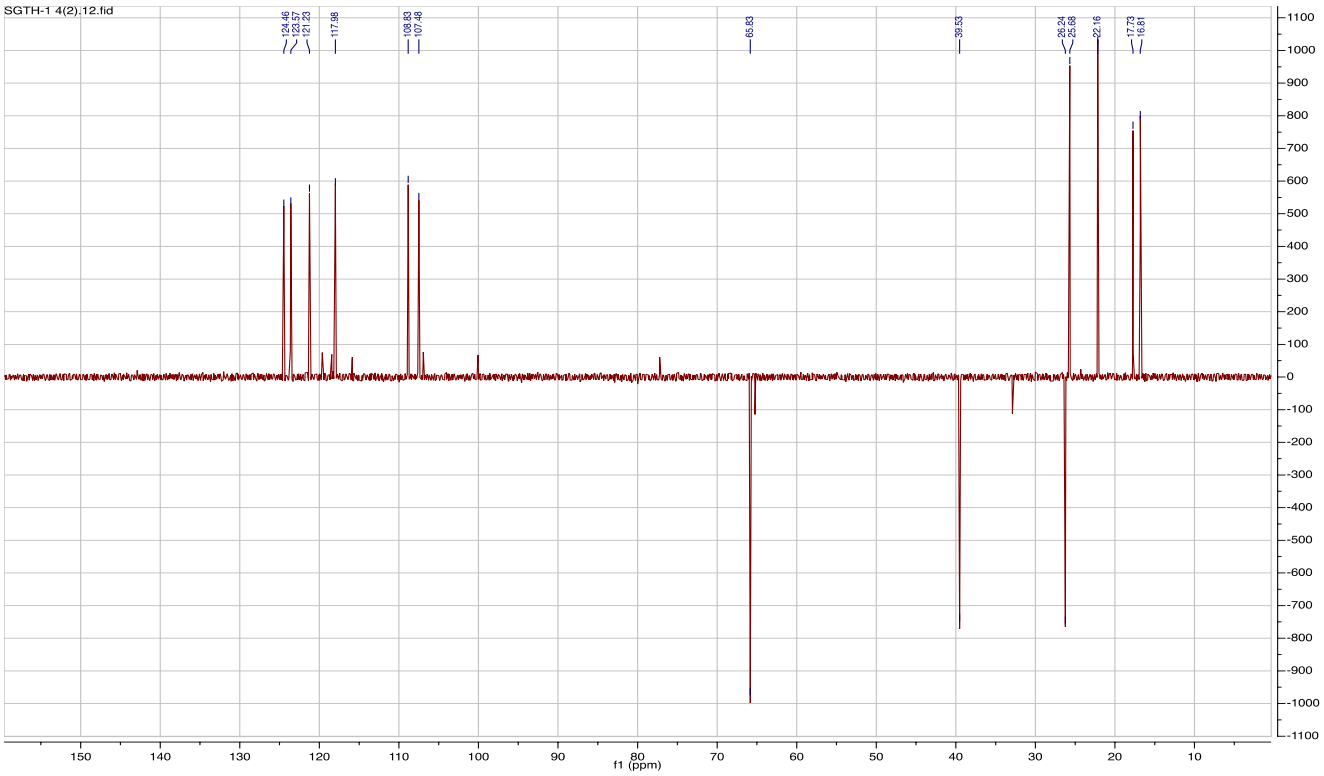

Figure 31: DEPT-135 NMR spectrum of compound 94 ($CDCl_3$, 100 MHz)

II.2.2.2 Identification of compound PG_3

PG_3 was obtained as yellow powder from Hexane-Ethyl acetate 6 % (m.p. 118 °C) and gave a positive result to the Borntrager test characteristic of anthraquinones. Its LC-MS **(Figure 32)** showed a molecular ion peak *m/z*: 392.07 (with retention time at 12.45 min) compatible with the molecular formula $C_{25}H_{28}O_4$, corresponding to twelve degrees of unsaturations. Comparison of its ^{1}H NMR spectrum **(Figure 33)** with that of PG_1 shows the appearance of two methylene protons at δ 4.20 (H-10). Also, comparison of its ^{13}C NMR **(Figure 34)** and APT spectra **(Figure 35)** with those of PG_1 shows the disappearance of one carbonyl group and the appearance of an additional methylene carbon (δ 32.9).

All these physical and spectroscopic data enabled us to identify the compound as 3-geranyloxyemodin anthrone **(219)**, previously isolated by Lenta and collaborators in 2008. **(Lenta *et al*., 2008)**.

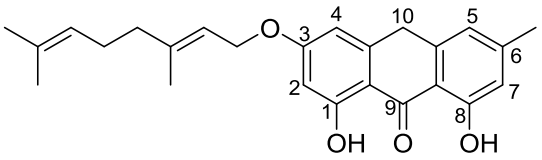

(219)

Table 19: ^{1}H NMR and ^{13}C NMR data of PG_3

PG_3		
N_o	**^{1}H (nH , m, *J* in Hz)**	**^{13}C**
1	-	165.1
2	6.40 (1H, s)	100.1
3	-	165.4
4	6.49 (1H, s)	107.0
4a	-	142.3
4b	-	141.2
5	6.80 (1H, s)	118.4
6	-	147.2
7	6.75 (1H, s)	123.6
8	-	162.7
8a	-	113.5
8b	-	109.9
9	-	191.9
10	4.35 (2H, brs)	32.9
11	2.48 (3H, s)	22.1
12	4.63 (2H, d, br)	65.2
13	5.50 (1H, t, *J* = 7.0 Hz)	116.0
14	-	143.5
15	1.65 (3H, s)	16.8
16	2.20 (4H, m)	39.5
17		26.3
18	5.20 (1H, br)	119.6
19	-	132.0
20	1.58 (3H, s)	17.7
21	2.40 (3H, s)	25.7

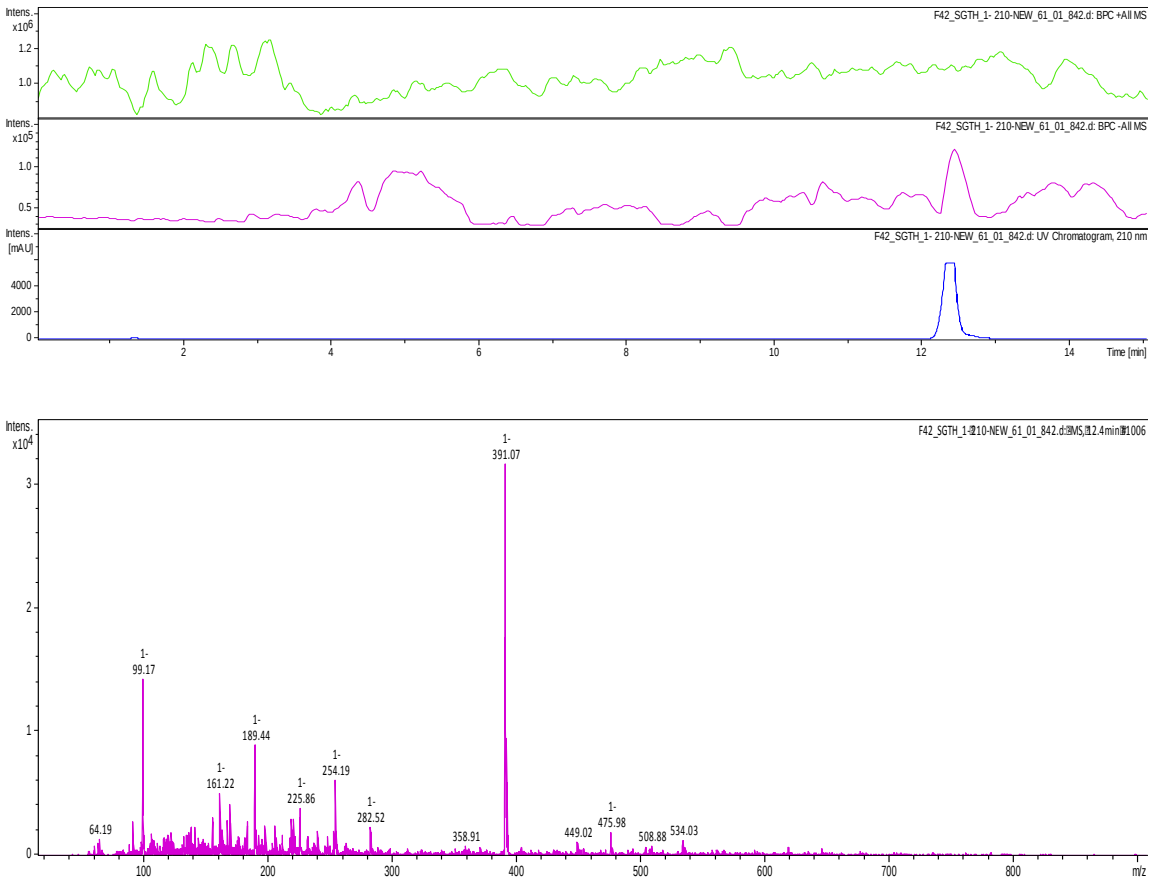

Figure 32: LC-MS spectrum of compound 219

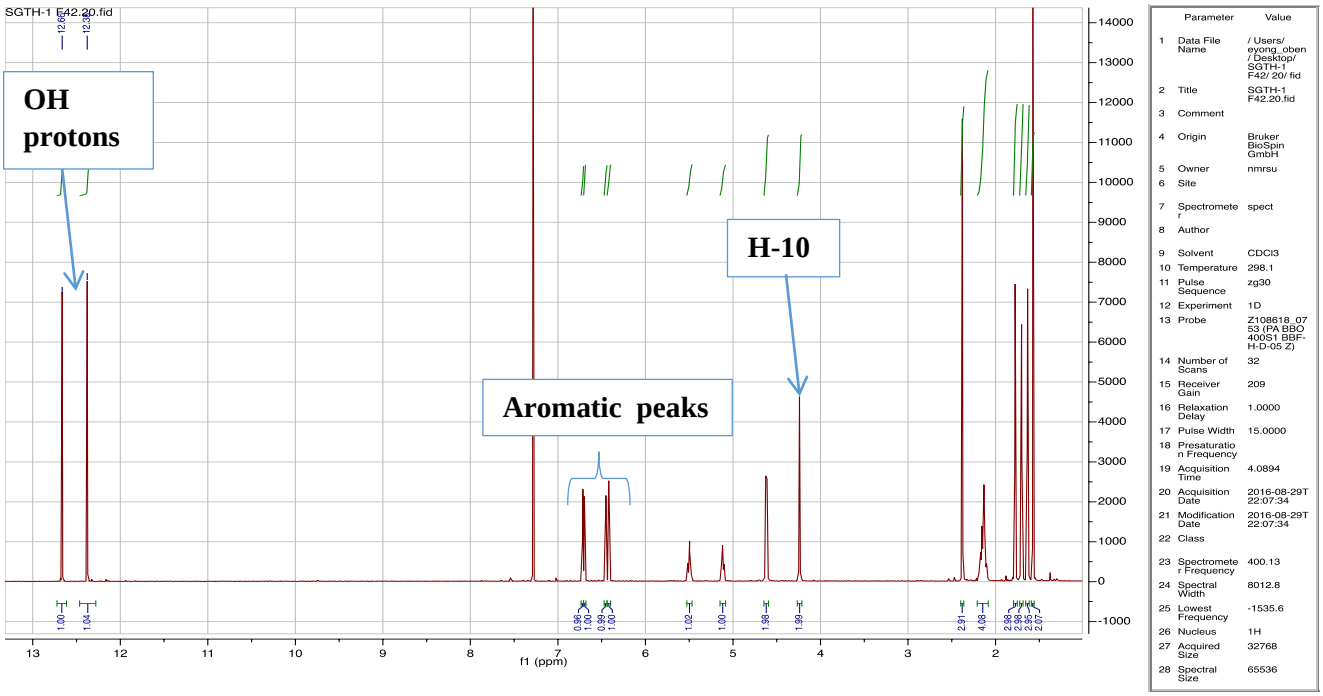

Figure 33: ^{1}H NMR spectrum of compound 219 ($CDCl_3$, 400 MHz)

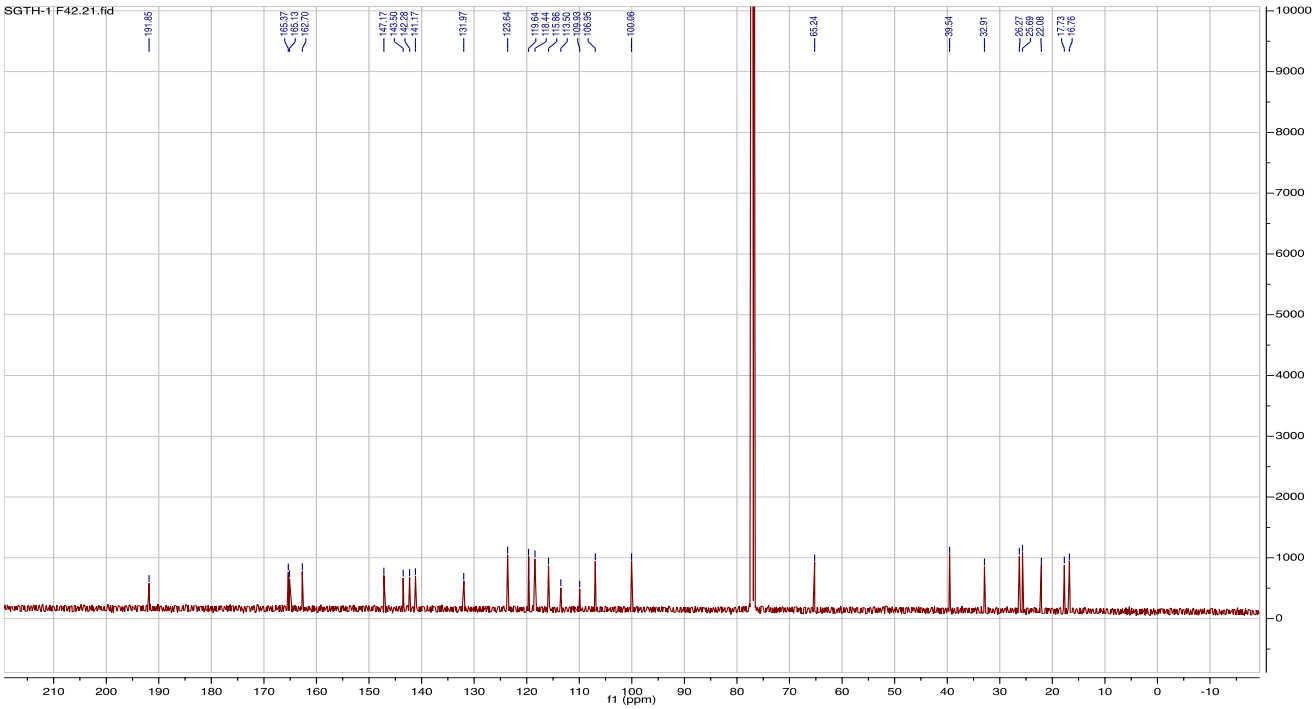

Figure 34: ^{13}C NMR spectrum of compound 219 ($CDCl_3$, 100 MHz)

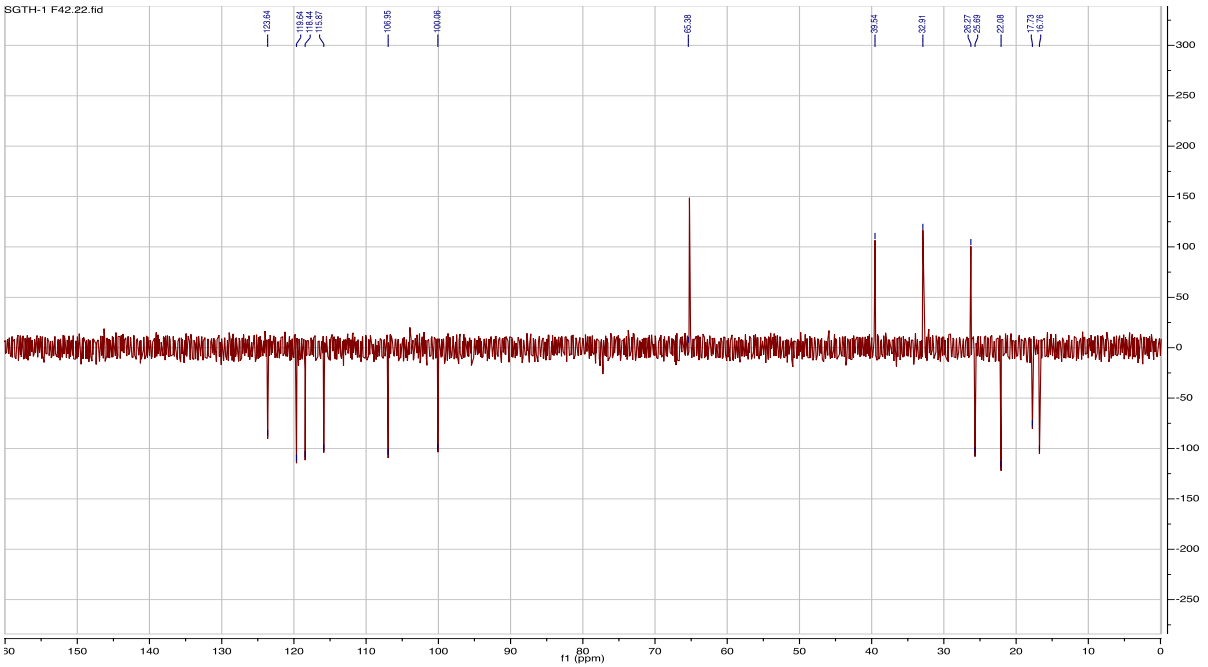

Figure 35: APT spectrum of compound 219 ($CDCl_3$, 100 MHz)

II.2.2.3 Identification of compound PG_4

PG_4 was obtained as yellow powder from Hexane-Ethyl acetate 6 % (m.p. 78-80 °C) and gave a positive result to the Borntrager test characteristic of anthraquinones. Its LC-MS **(Figure 36)** showed a molecular ion peak *m/z*: 406.02 (with retention time at 9.80 min) compatible with the molecular formula $C_{25}H_{26}O_{5,}$ corresponding to thirteen degrees of unsaturations. Comparison of its ^{1}H NMR spectrum **(Figure 37)** with that of PG_1 shows the disappearance of one of the aromatic methane protons and the appearance of a non-chelated hydroxyl group linked to a benzene ring at δ 11.28 suggesting that the gernaly group is no more bonded to the oxygen atom but to a carbon atom of one of the benzene rings. Also, comparison of its ^{13}C NMR spectra **(Figure 38 and Figure 39)** with those of PG_1 shows an additional sp^2 quartenary carbon (eleven quartenary carbon atoms instead of ten).

All these physical and spectroscopic data enabled us to identify the compound as 2-geranylemodin **(93)**, previously isolated by Lenta and collaborators in 2008. **(Lenta *et al.*, 2008)**.

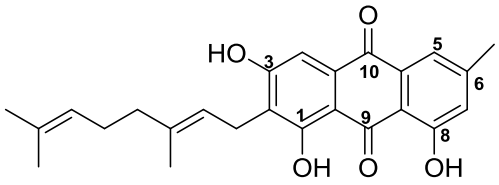

(93)

Table 20: ^{1}H NMR and ^{13}C NMR data of PG_4

PG_4		
N_o	**^{1}H (nH , m)**	**^{13}C**
1	-	163.2
2	-	108.5
3	-	161.8
4	7.20 (1H, br)	109.8
4a	-	133.2
4b	-	132.5
5	7.48 (1H, br)	121.2
6	-	148.6
7	7.24 (1H, br)	123.6
8	-	162.4
8a	-	113.7
8b	-	110.1
9	-	181.6
10	-	190.4
13	5.23 (1H, br)	117.9
14	-	135.7
16	2.40 (4H, m)	40.5
17		26.6
18	5.01 (1H, br)	124.5
19	-	131.1

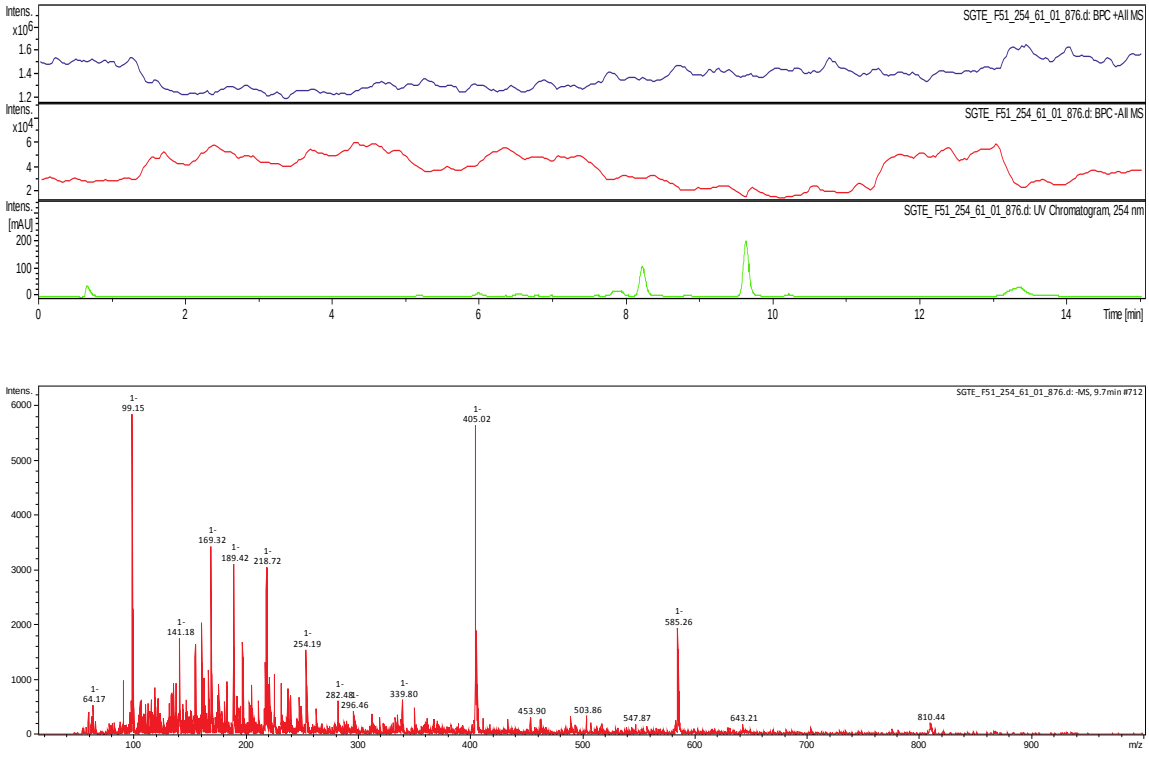

Figure 36: LC-MS spectrum of compound 93

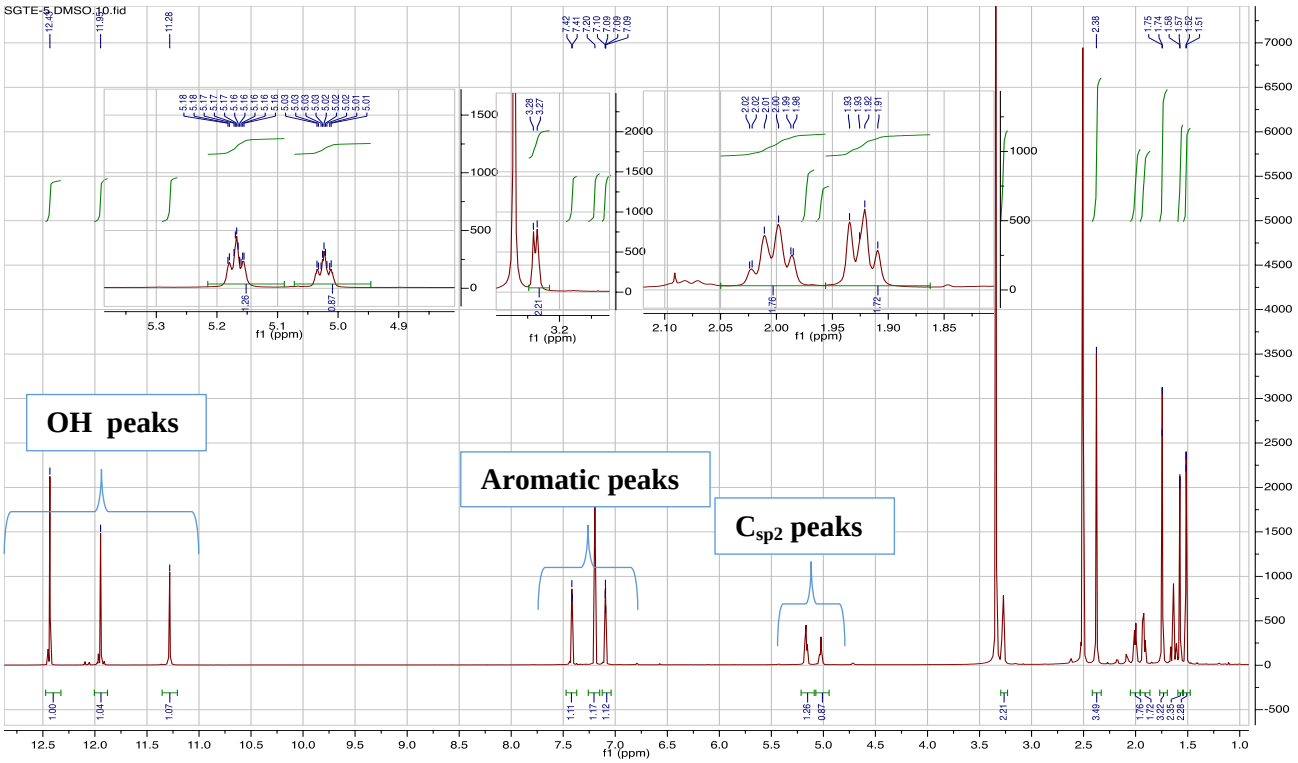

Figure 37: ^{1}H NMR Spectrum of compound 93 (CD_3OD, 400 MHz)

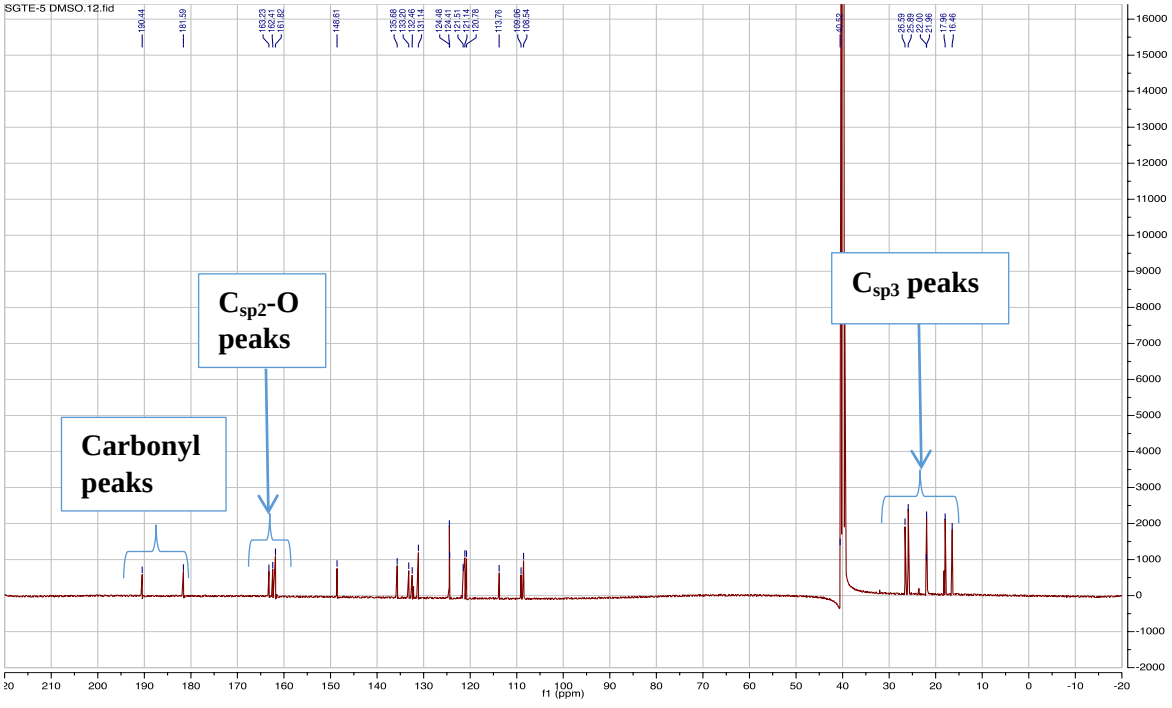

Figure 38: ^{13}C NMR spectrum of compound 93 (CD_3OD, 100 MHz)

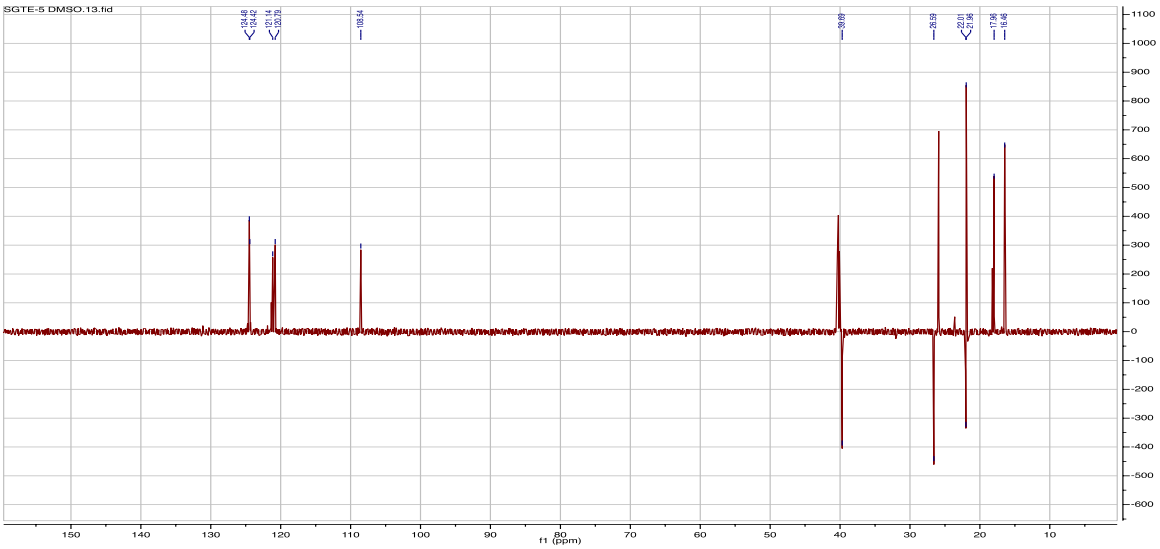

Figure 39: DEPT 135 NMR spectrum of compound 93 CD_3OD, 100 MHz)

II.2.2.4 Identification of compound PG_5

PG_5 was obtained as yellow powder from Hexane-Ethyl acetate 15 % (m.p. 216 °C) and gave a positive result to the Borntrager test characteristic of anthraquinones. Its LC-MS **(Figure 40)** showed a molecular ion peak *m/z*: 452.05 (with retention time at 9.35 min) compatible with the molecular formula $C_{27}H_{32}O_6$, corresponding to thirteen degrees of unsaturations.

The analysis of its NMR data (^{1}H, ^{13}C-NMR and DEPT 135) enabled us to assign structure **100**. The ^{1}H-NMR spectrum **(Figure 41)** exhibited:

- One chelated hydroxyl group (δ 15.99) and one unchelated hydroxyl group bonded to a benzene ring (δ 9.80).
- Three singlets of one proton each at δ 6.80 (1H, s, H-2), 6.51 (1H, s, H-4), 6.50 (1H, s, H-10) attributable to aromatic protons of vismiones.
- A singlet of three protons at δ 1.90 attributable to the methyl group of an acetyl group. Moreover on the ^{1}H-NMR spectrum, we observe the presence of a methyl group (δ 1.40) on the cyclohexenone ring of vismione bonded to the same carbon atom with an acetyl group.
- A group of singlets and multiplets at δ 1.66 (3H, s, H-15), 1.63 (3H, s, H-21), 1.58 (3H, s, H-20), 2.23 (4H, m, H-16, H-17), 4.63 (2H, m, H-12), 5.15 (1H, m, H-18) and 5.50 (1H, m, H-13) indicative of a geranyl moiety.

The ^{13}C NMR **(Figure 42)** and APT **(Figure 43)** spectroscopic data disclosed the presence of:

- Two carbonyl carbon (δ 200.6 and δ 170.4
- nine sp^2 quaternary carbons (three of which were oxygen-bearing δ 165.7, 163.0, 159.7)
- five sp^2 methines (δ 100.8, 101.6, 117.5, 118.9, 123.7)
- three sp^3 methylenes (δ 26.3, 39.6, 65.2)
- five methyl carbons (δ 16.8, 17.7, 22.1, 24.5, 25.7).

These physical and spectroscopic data were in agreement with those previously reported for acetylvismione D **(Giuliano *et al*., 1987)**.

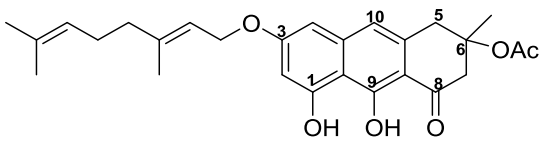

(95)

Table 21: ^{1}H NMR and ^{13}C NMR data of PG_5 and the litterature

PG_5			Acetylvismione D (Botta et *al.*, 1986)	
N_o	**^{1}H (nH, m, *J* in Hz)**	**^{13}C**	**^{1}H (nH, m, *J* in Hz)**	**^{13}C**
1	-	163.0	-	161.8
2	6.50 (lH, br s)	100.8	6.30 (1H, d, *J* = 2 Hz)	99.3
3	-	159.7	-	160.6
4	6.54 (lH, br s)	101.6	6.55 (lH, d, *J* = 2 Hz)	102.3
4a	-	140.9	-	139.1
4b	-	134.5	-	137.2
5	3.10-3.63 (2H, m)	39.6	3.00-3.60 (2H, m)	44.1
6	-	80.7	-	83.6
7	2.87-3.21 (2H, m)	49.2	2.87-3.21 (2H, m)	46.5
8	-	200.6	-	202.3
8a	-	108.1	-	111.0
8b	-	107.9	-	108.4
9	-	165.7	-	164.4
10	6.80 (lH, br s)	117.5	6.77 (lH, br s)	117.1
11	1.74 (3H, s)	24.5	1.75 (3H, s)	23.4
12	4.63 (2H, d, br)	65.1	4.60 (2H, d, *J* = 7 Hz)	65.2
13	5.50 (1H, br s)	118.8	5.45 (1H, t, *J* = 7 Hz)	119.1
14	-	141.9	-	139.5
15	1.65 (3H, s)	16.8	1.65 (3H, s)	16.4
16	2.23 (4H, m)	39.5	1.90-2.30 (4H, m)	39.7
17		26.3		26.4
18	5.15 (1H, br)	123.7	5.08 (1H, m)	123.5
19	-	131.9	-	132.0
20	1.58 (3H, s)	17.7	1.60 (3H, s)	18.6
21	1.63 (3H, s)	25.7	1.63 (3H, s)	24.6
$COO\underline{CH_3}$	1.75 (3H, s)	22.1	1.75 (3H, s)	21.3
$\underline{CO}OCH_3$	-	170.4	-	170.2

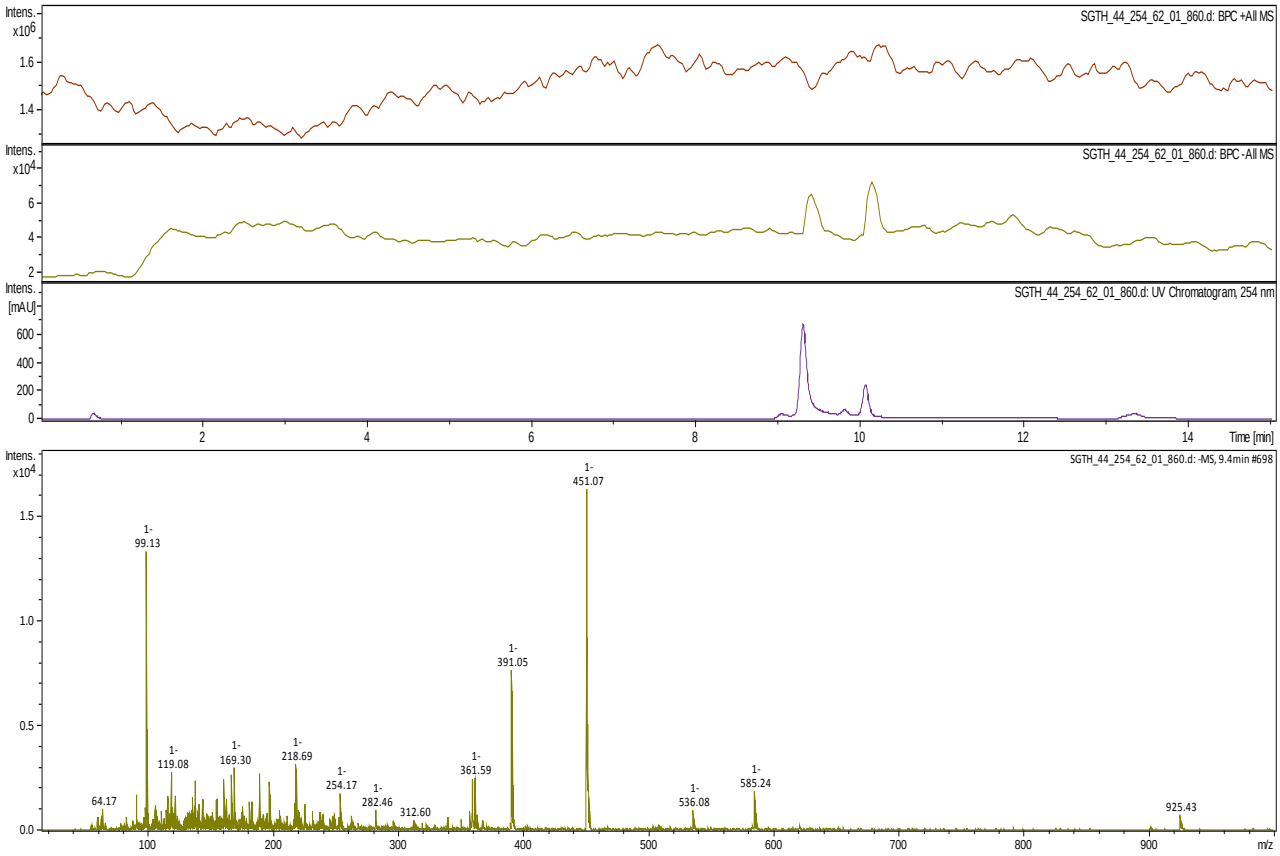

Figure 40: LC-MS spectrum of compound 95

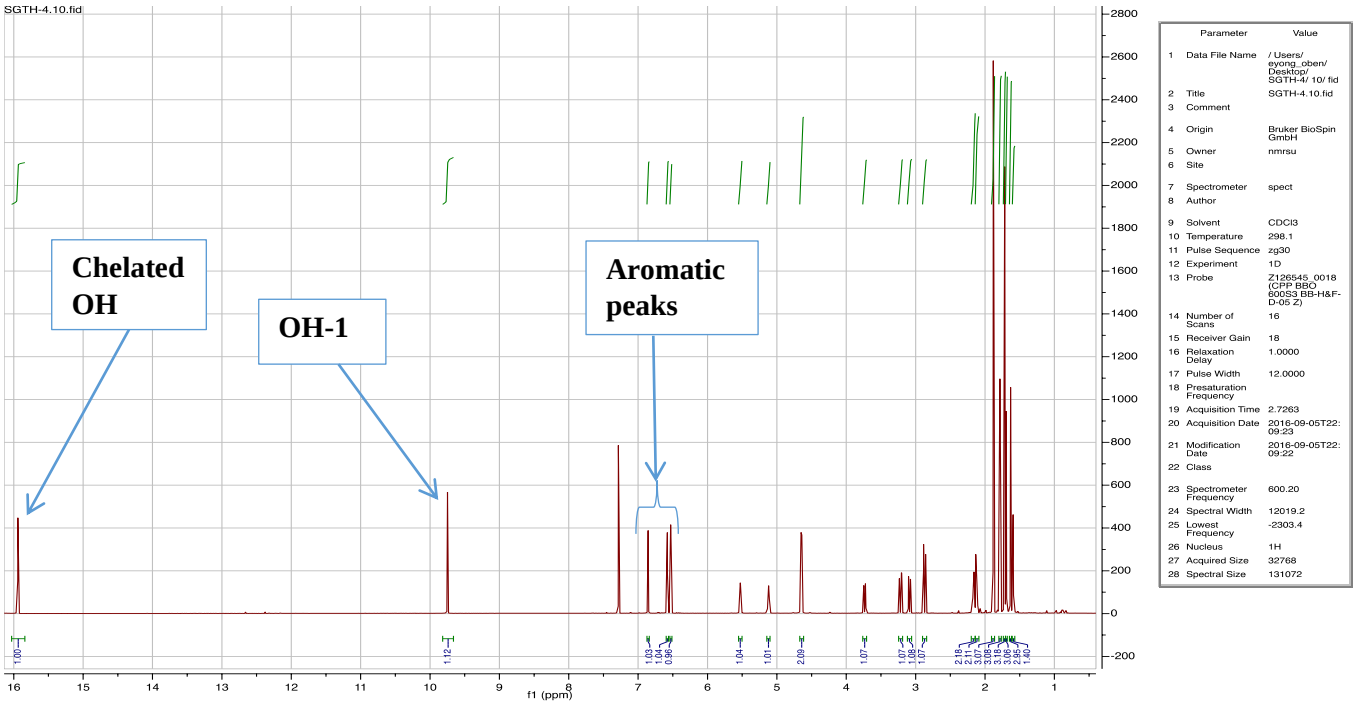

Figure 41: ^{1}H NMR Spectrum of compound 95 ($CDCl_3$, 400 MHz)

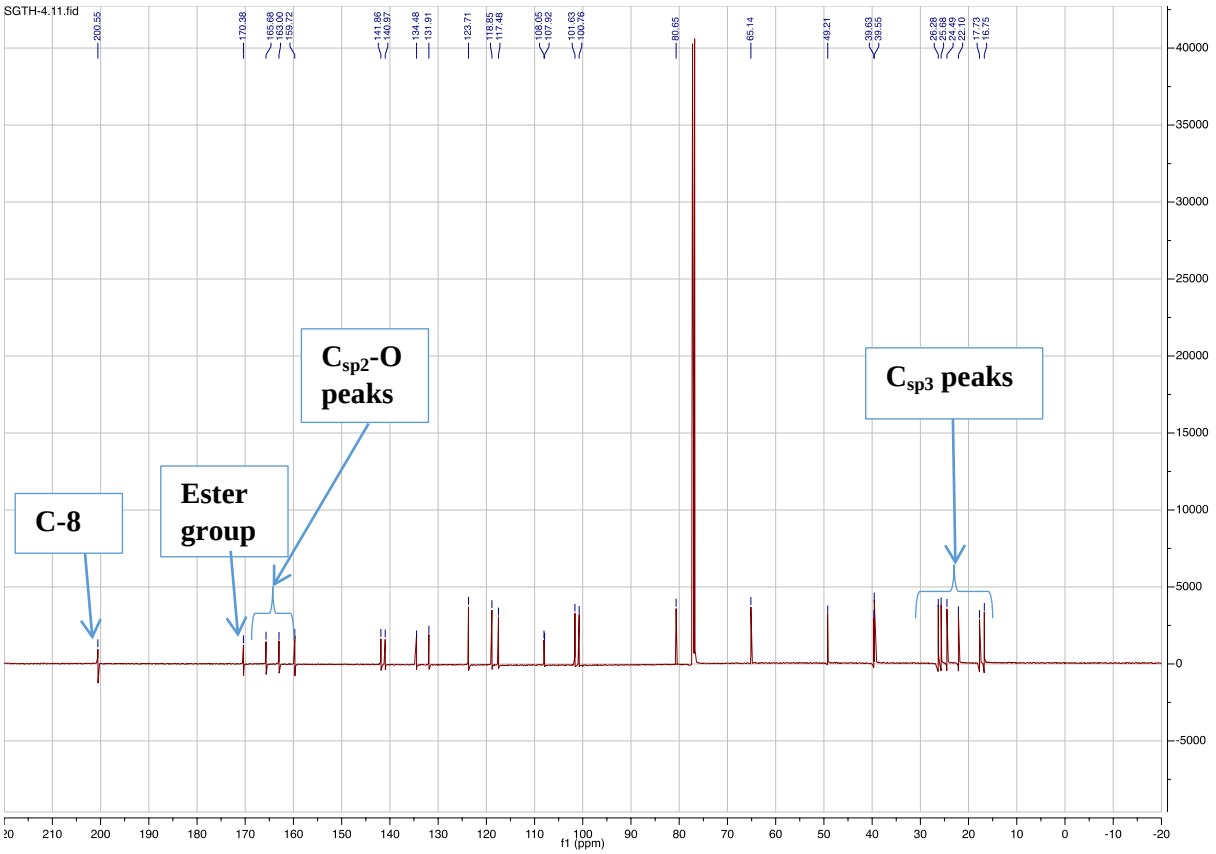

Figure 42: ^{13}C NMR spectrum of compound 95 ($CDCl_3$, 100 MHz)

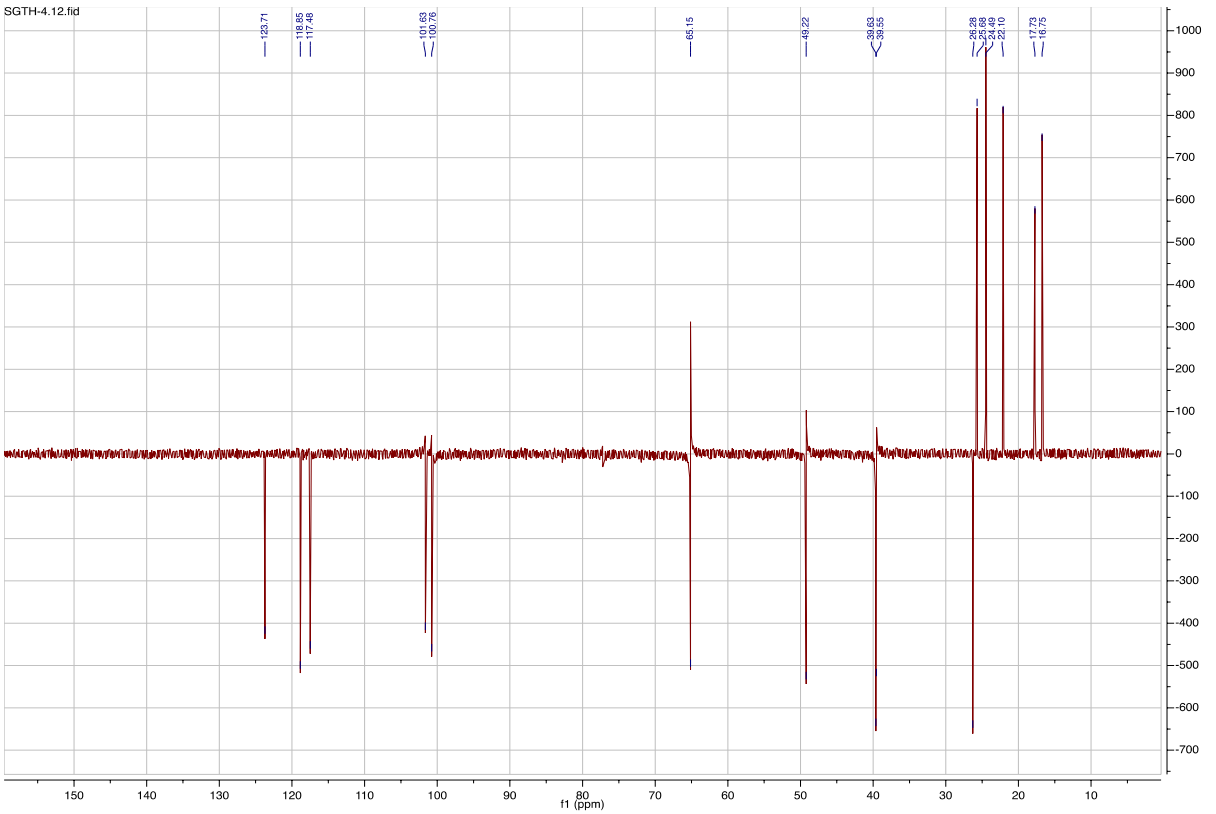

Figure 43: APT spectrum of compound 95 ($CDCl_3$, 100 MHz)

II.2.2.5 Identification of compound PG_8

PG_8 was obtained as yellow powder from Hexane-Ethyl acetate 20 % (m.p. 240 °C) and gave a positive result to the Borntrager test characteristic of anthraquinones. Its HR-TOF-MS ESI **(Figure 44)** showed a molecular ion peak *m/z*: 270.0450 compatible with the molecular formula $C_{15}H_{10}O_5$ corresponding to eleven degrees of unsaturations. The analysis of its NMR data [^{1}H, ^{13}C-NMR and DEPT 135] enabled us to assign structure **111**. The ^{1}H-NMR spectrum **(Figure 45)** exhibited:

- four singlets of one proton each at δ 7.53 (1H, s, H-2), 7.15 (1H, s, H-5), 7.07 (1H, s, H-4) and 6.54 (1H, s, H-7) attributable to aromatic protons of tetra substituted anthraquinones.
- A shielded singlet of three protons at δ 2.43 indicating the presence of a methyl group attached to an aromatic ring.

The ^{13}C-NMR spectrum **(Figure 46)** showed characteristic carbon signals of anthraquinones at δ 190.5 (C-9), 181.9 (C-10), 135.6 (C-14) and 133.4 (C-11). The presence of the methyl group was further confirmed by the carbon signal at δ 20.8.

These physical and spectroscopic data were in agreement with those previously reported for emodin **(Wells *et al.*, 1975; Toma *et al.*, 1975; Dewi et *al.*, 2008)**.

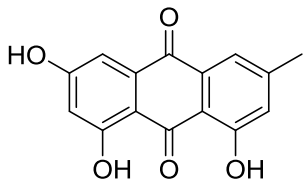

(111)

Table 22: ^{1}H NMR and ^{13}C NMR data of PG_8 and the litterature

	PG_8		Emodin (Dewi et *al.*, 2008)	
N_o	^{1}H (nH, m)	^{13}C	^{1}H (nH, m)	^{13}C
1	-	165.4	-	163.6
2	6.54 (1H, s)	107.9	6.53 (1H, d)	109.2
3	-	166.5	-	166.7
4	7.15 (1H, s)	109.1	7.17 (1H, d)	110.6
4a	-	135.6	-	136.9
5	7.53 (1H, s)	120.5	7.56 (1H, d)	121.8
6	-	148.3	-	149.6
7	7.05 (1H, s)	123.9	7.09 (1H, d	125.2
8	-	162.3	-	163.6
8a	-	113.6	-	115.0
9	-	181.9	-	183.4
9a	-	113.6	-	114.9
10	-	190.5	-	191.7
10a	-	133.4	-	143.7
11	2.43 (3H, s)	20.8	2.43 (3H, s)	22.1

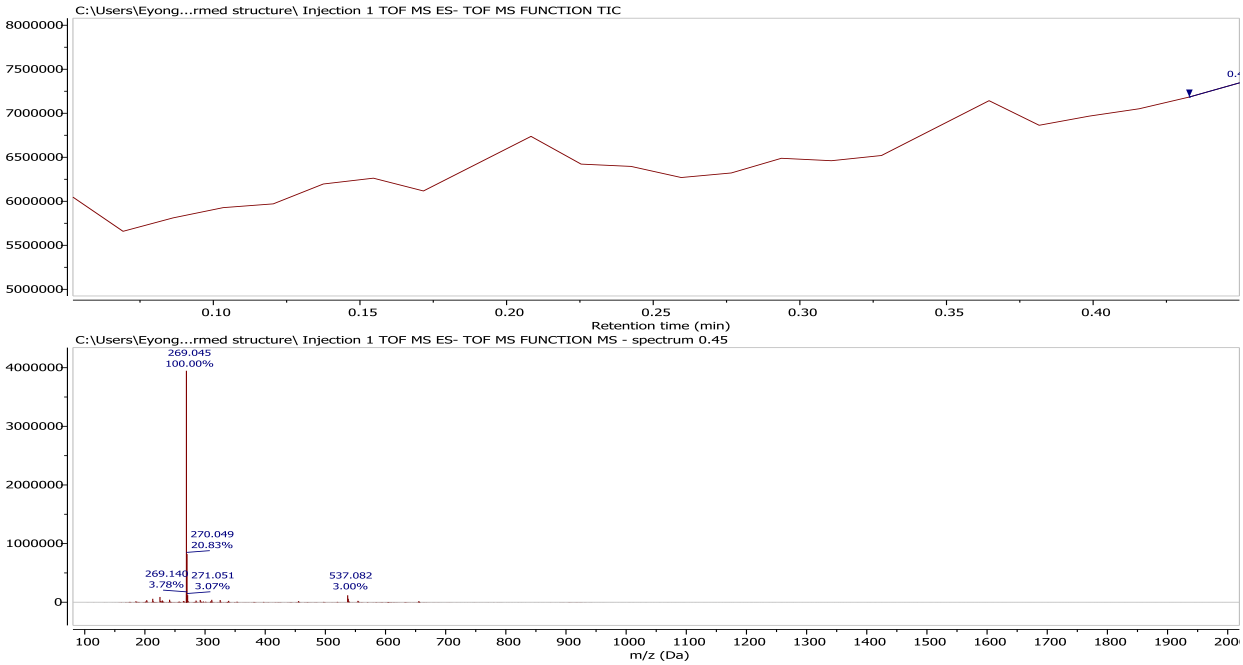

Figure 44: HR-ESI-TOF-MS spectrum of compound 111

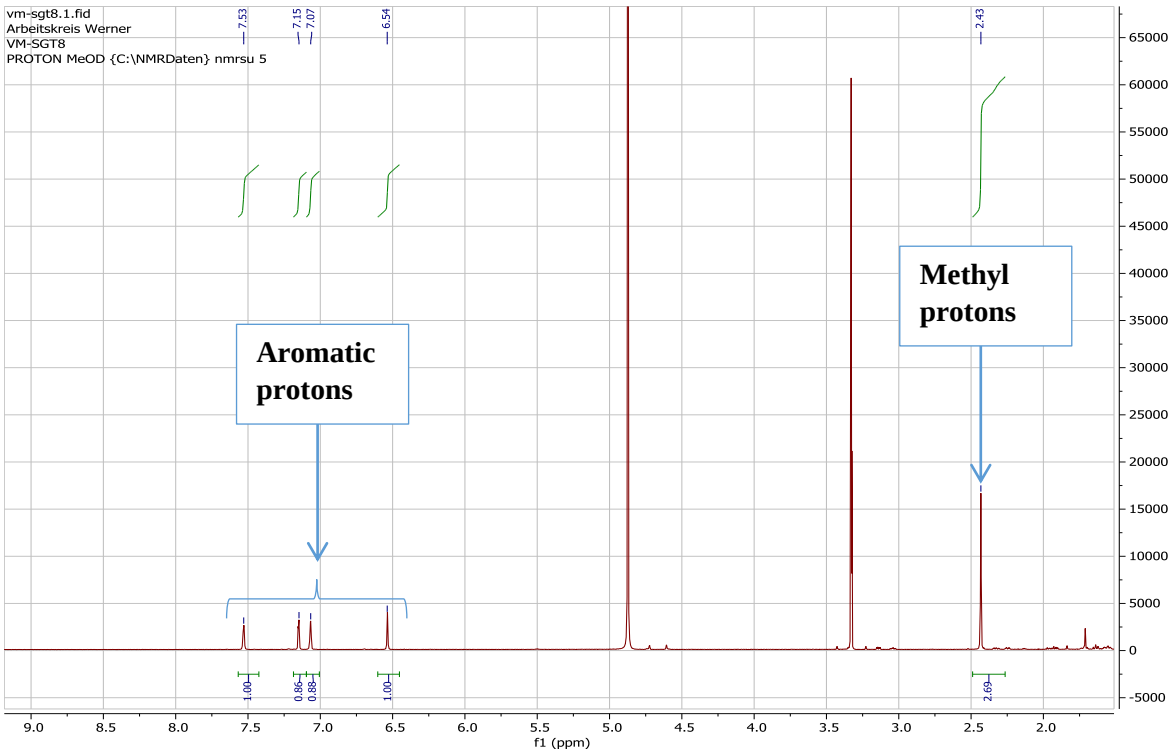

Figure 45: ^{1}H NMR spectrum of compound 111 (CD_3OD, 400 MHz)

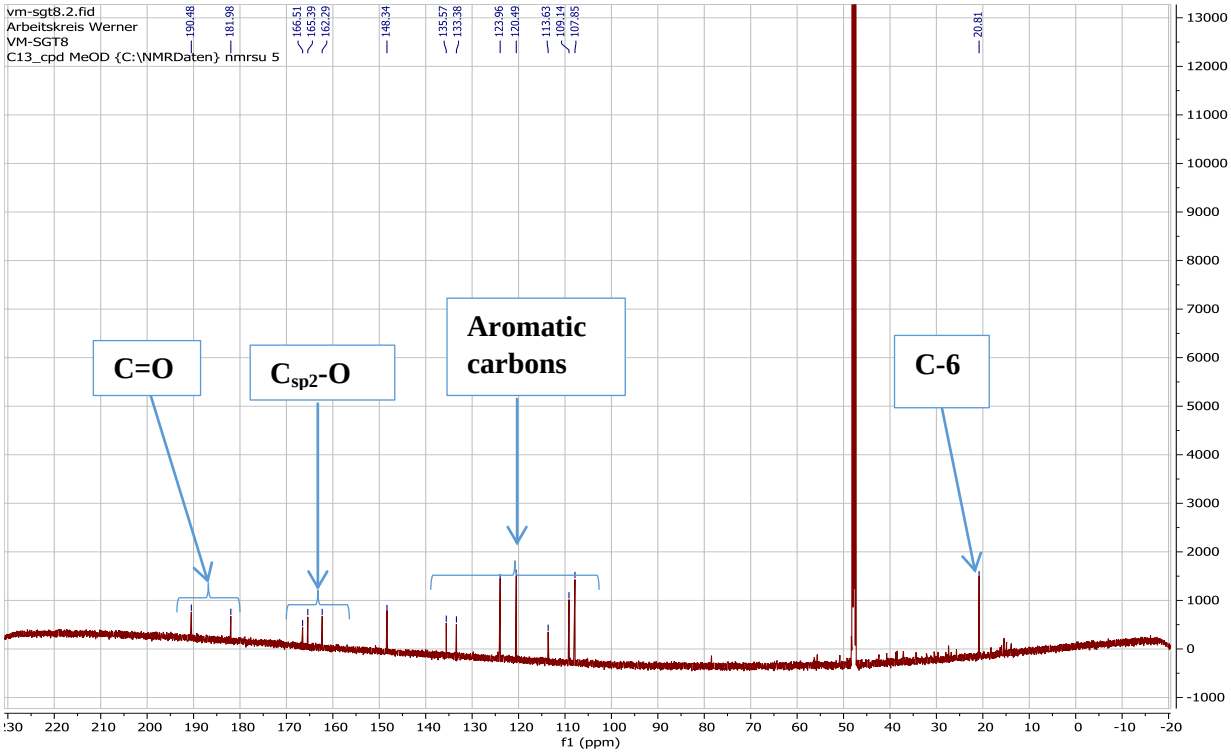

Figure 46: ^{13}C NMR spectrum of compound 111 (CD_3OD, 100 MHz)

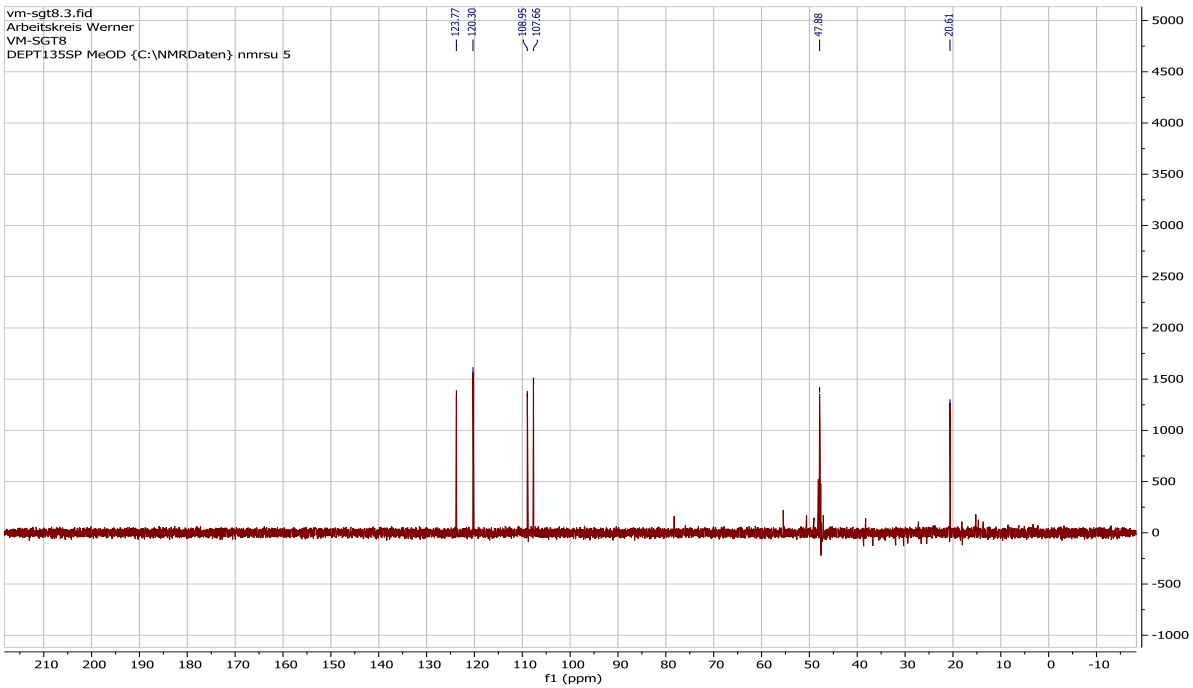

Figure 47: DEPT 135 NMR spectrum of compound 111 (CD_3OD, 100 MHz)

II.2.3 Identification of alkaloids

II.2.3.1 Identification of compound AS_7

AS_7 was obtained as a greenish brown powder, from DCM/MeOH 2% (m. p. 519.5 ^{0}C); its EI showed a molecular ion peak at *m/z*: 338.2 compatibles to the molecular formula $C_{20}H_{22}N_2O_3$.

Its ^{1}H NMR spectrum **(Figure 51)** exhibited:

- A multiplet of four protons at δ 7.05–6.65 attributable to the protons, H-9, 10,11, 12,
- A singlet of one proton at δ 6.74 attributable to the NH of an indole type alkaloid,
- A multiplet of one proton at δ 5.23 attributable to the olefin proton H-18,
- A doublet of one proton at δ 4.69 attributable to H-5,
- A singlet of three protons at δ 3.50 attributable to a methoxy group of the acetate,
- A doublet of three protons at δ 1.46 attributable to the methyl group at position 17.

Analysis of the ^{13}C **(Figure 52)** and DEPT (90 and 135) NMR spectra gave twenty signals corresponding to twenty carbon atoms. We observed:

- Six quartenary carbon atoms amongst which, carbonyl of an ester at δ 178.7, two aromatic carbons at δ 136.6 (C-8) and 149.7 (C-13), olefinic carbon at δ136.4 (C-19)
- Nine methine carbons amongst which an oxymethine carbon atom at δ 88.1
- Two methylene carbons
- Two methyl carbons

The ^{1}H-^{1}H COSY spectrum **(Figure 54)** showed correlations between the aromatic protons at δ 7.05–6.65.

The HMBC spectrum **(Figure 55)** showed correlations between the aromatic protons at δ 7.05–6.65 and the aromatic carbons at δ 136.6 (C-8) and 149.7 (C-13).

The HSQC spectrum **(Figure 56)** showed correlations between the aromatic protons at δ δ 7.05–6.65 and the aromatic carbons at δ 111.0 -125.4.

These physical and spectroscopic data were in agreement with those previously reported for picralstonine **(217)** (**Atta-ur-Rahman *et al.*, 1986**).

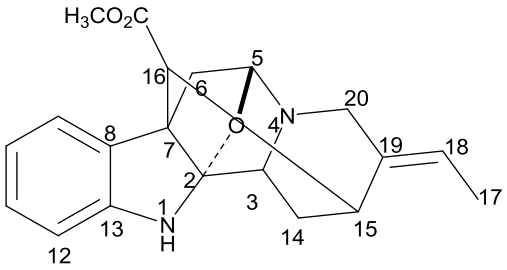

(217)

Table 23: ^{13}C NMR data of AS_7 and the literature

N_o	AS_7	picralstonine (Atta-ur-Rahman et *al.*, 1986)
	^{13}C	^{13}C
3	53.0	51.9
5	88.1	87.4
6	41.0	40.5
7	52.0	52.1
8	125.0	125.0
9	125.4	125.1
10	122.1	120.0
11	129.0	127.9
12	111.0	110.6
13	149.7	144.6
14	26.6	26.0
15	32.2	31.2
16	53.2	52.1
17	13.2	12.7
18	120.9	120.9
19	136.4	136.3
20	49.8	46.4
$COCH_3$	46.7	51.3
$COOCH_2$	173.9	172.0

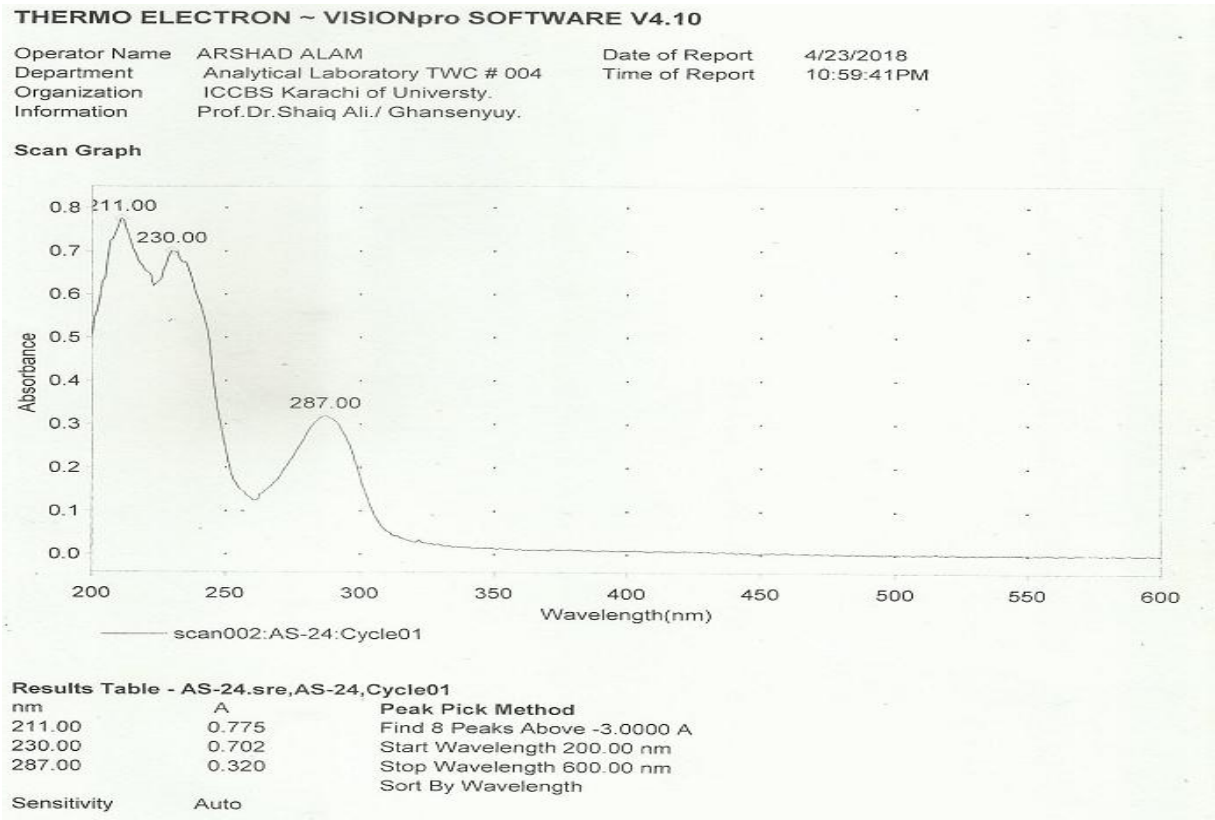

Figure 48: UV spectrum of compound 217

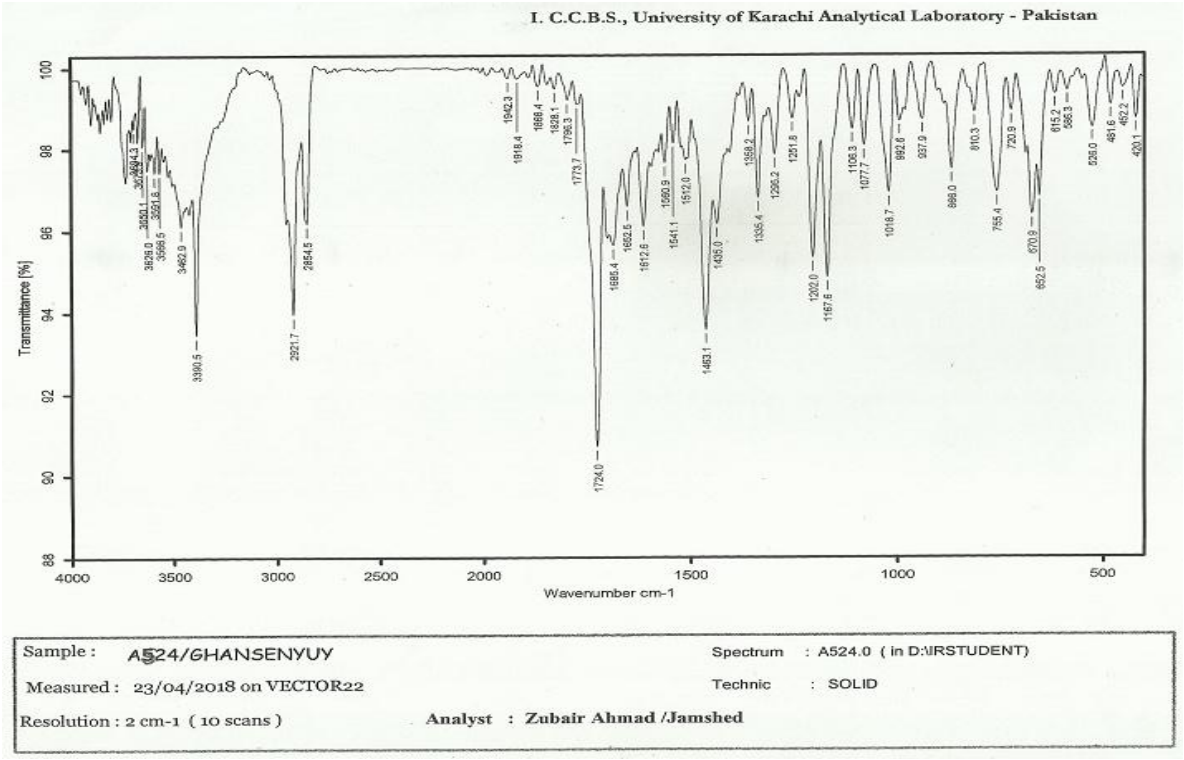

Figure 49: IR spectrum of compound 217

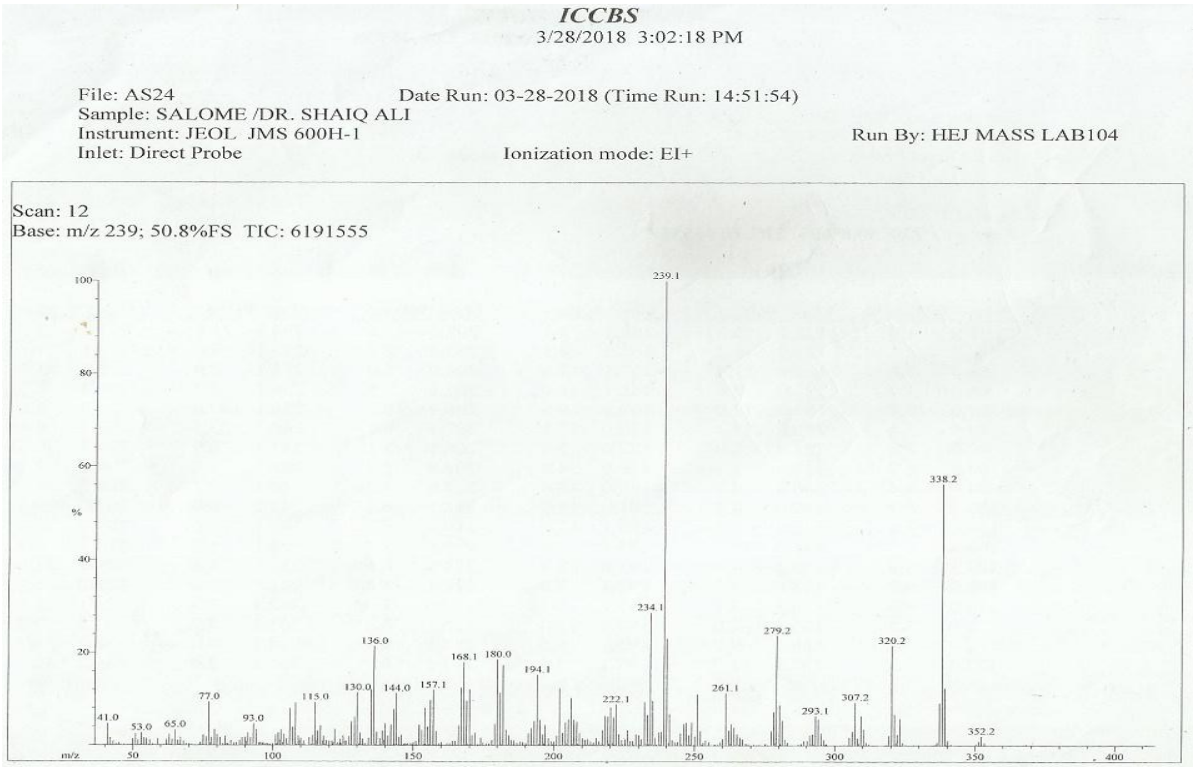

Figure 50: EI-Mass spectrum of compound 217

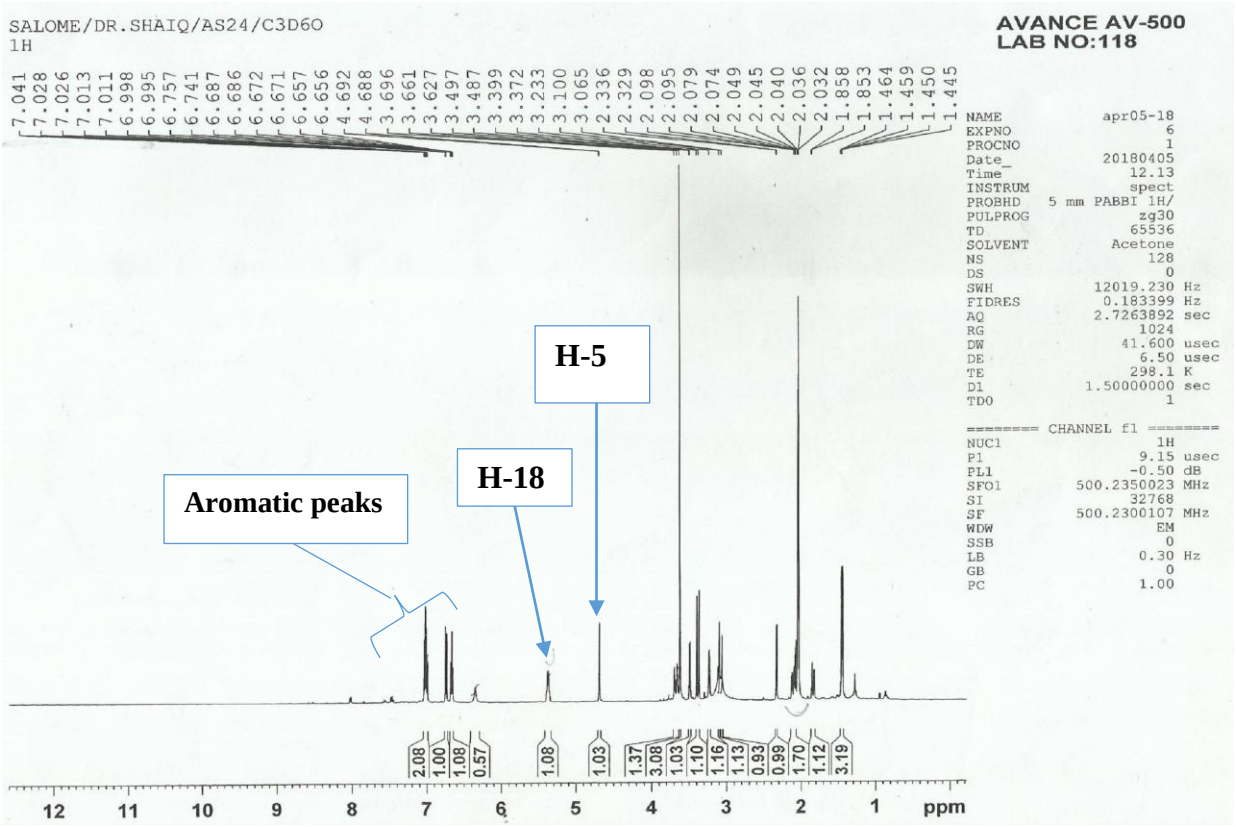

Figure 51: ^{1}H-NMR spectrum of compound 217 ($C3D_6O$, 500 MHz)

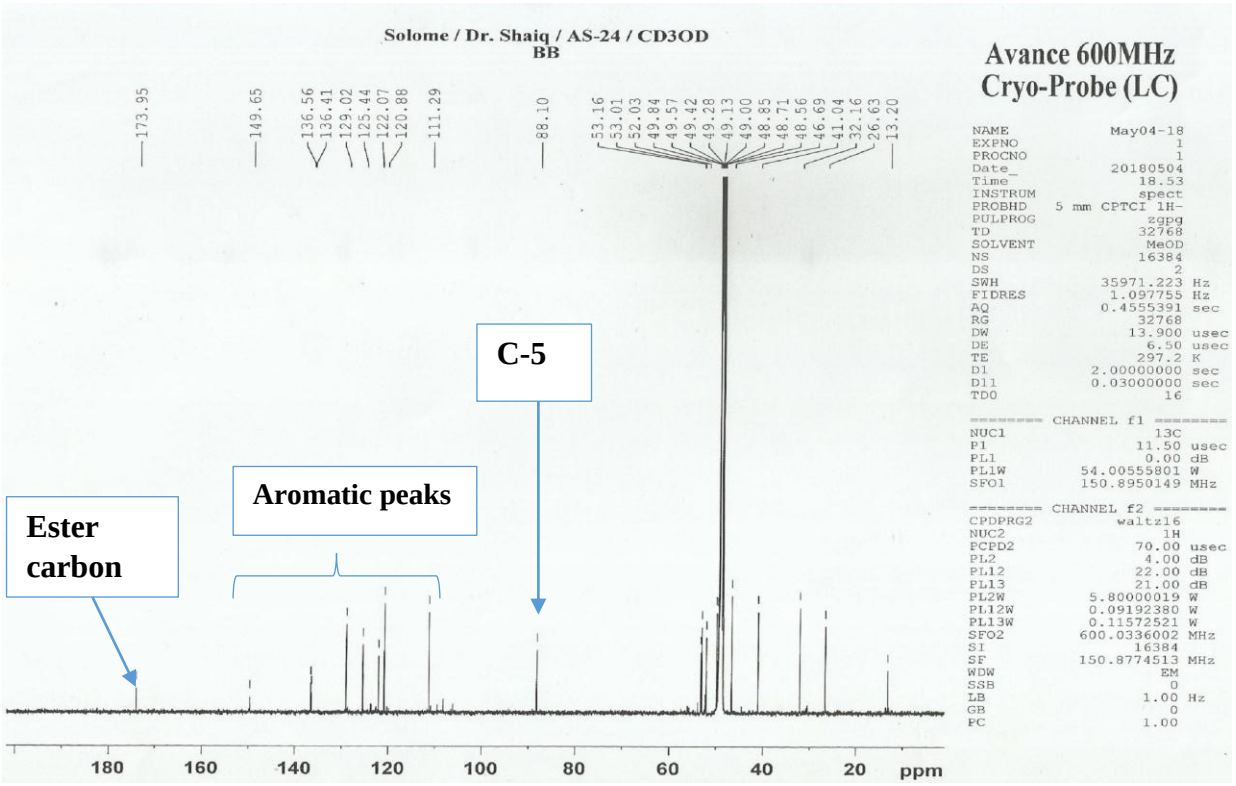

Figure 52: ^{13}C-NMR spectrum of compound 217 (CD_3OD, 150 MHz)

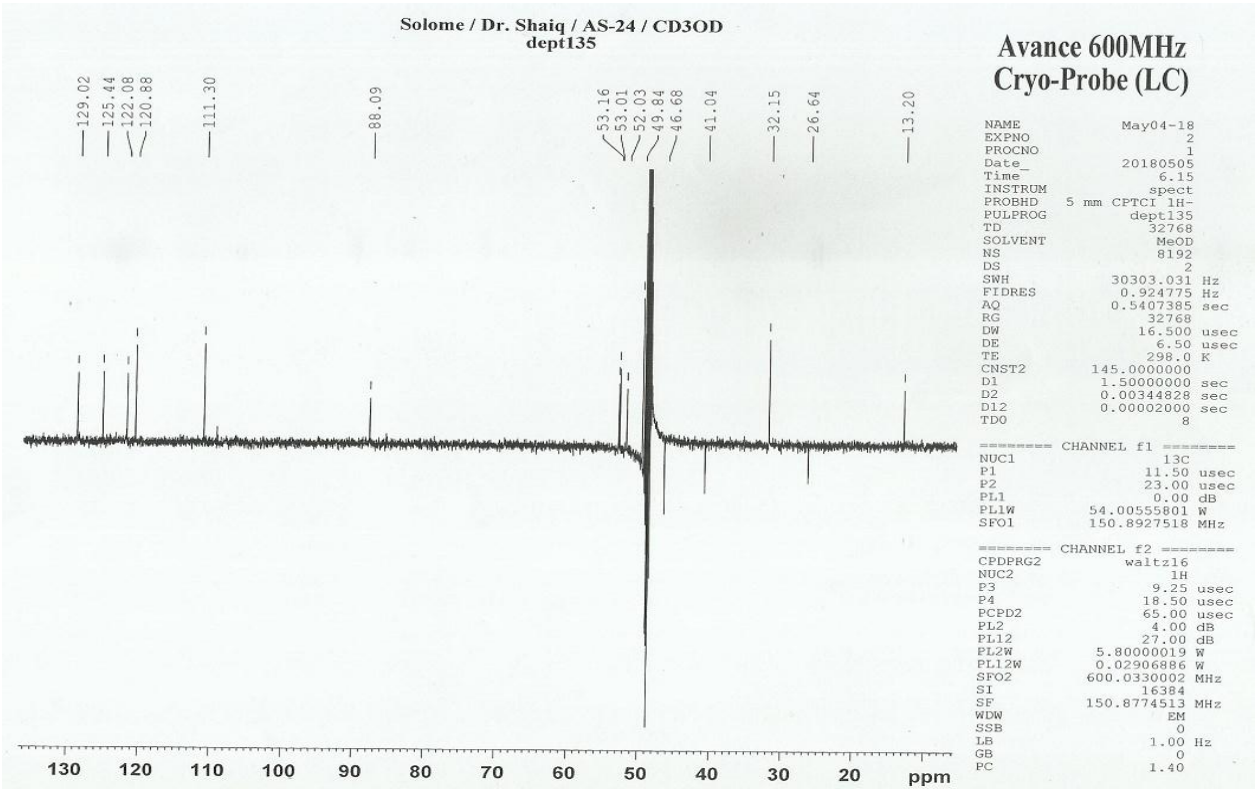

Figure 53: DEPT 135 spectrum of compound (217) (CD_3OD, 150 MHz)

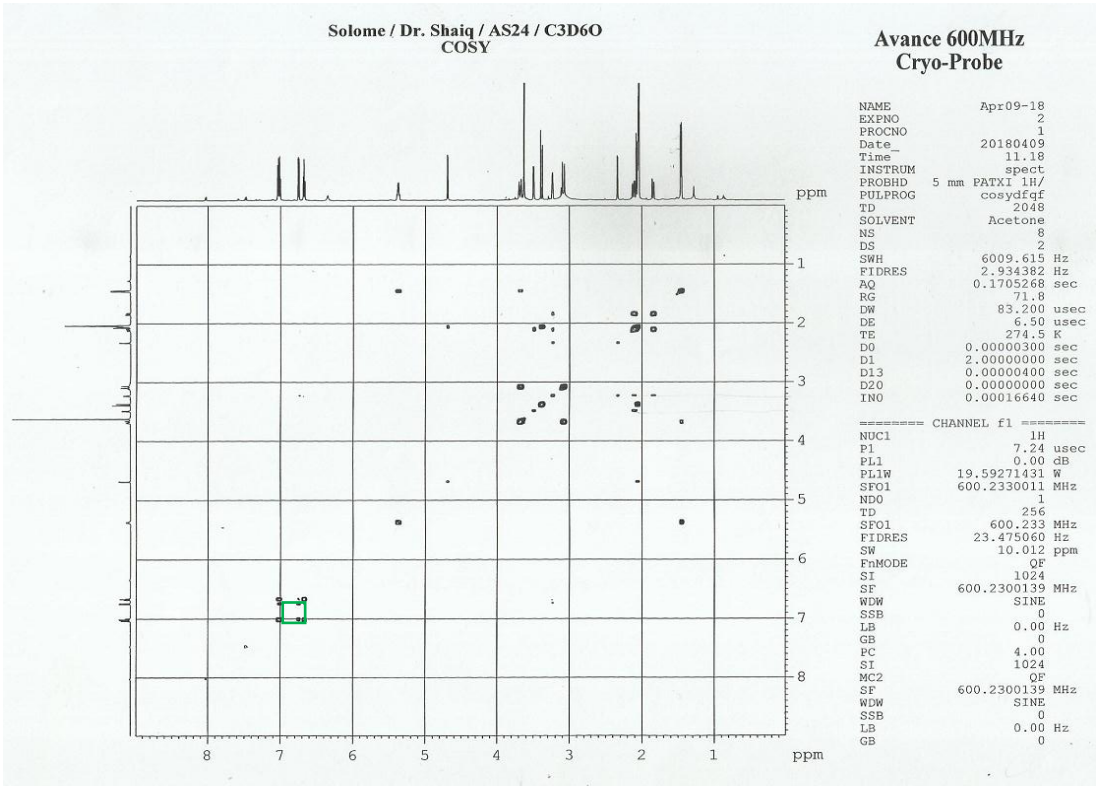

Figure 54: ^{1}H-^{1}H COSY spectrum of compound 217

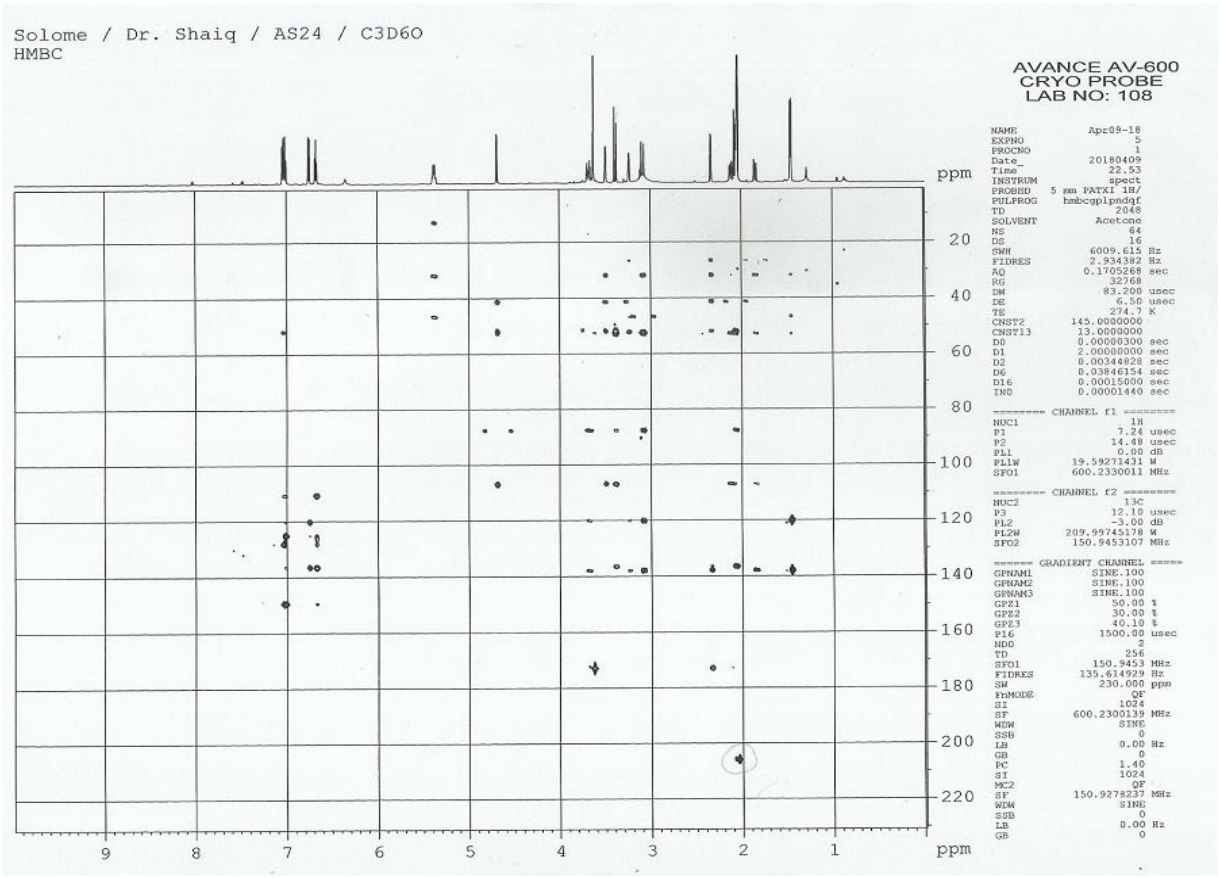

Figure 55: HMBC spectrum of compound 217

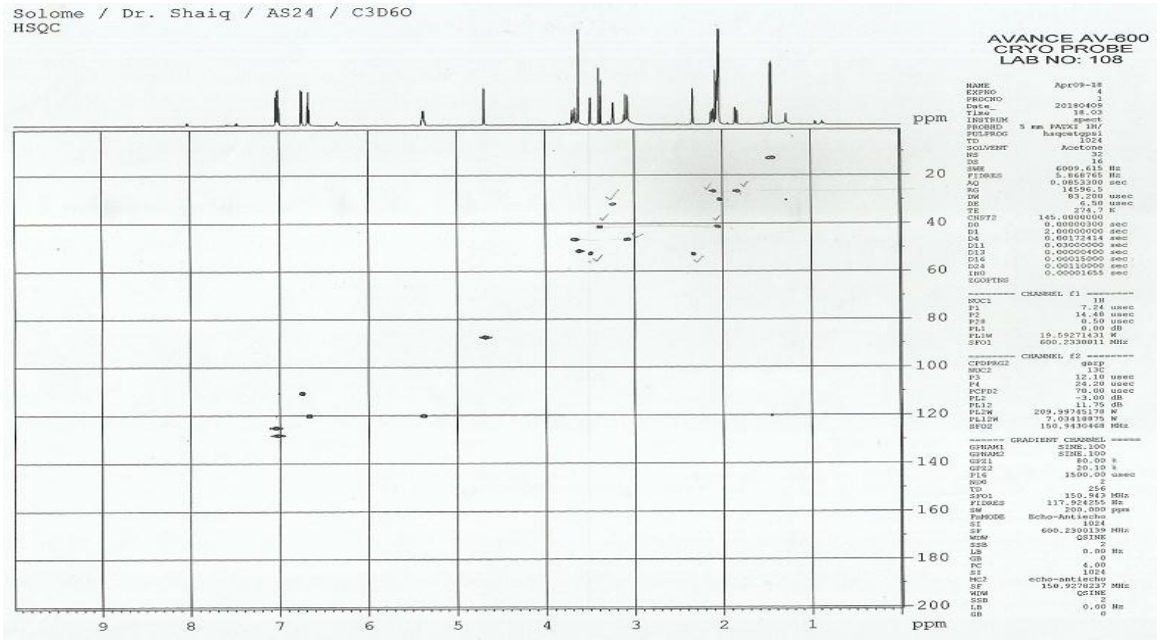

Figure 56: HSQC spectrum of compound 217

II.2.3.2 Identification of compound AS_9

AS_9 was obtained as a white powder from ethyl acetate 100 % (m.p. 180 ^{0}C); its EI spectrum **(Figure 60)** showed a molecular ion peak at *m/z*: 356.2 compatible with the molecular formula $C_{20}H_{24}N_2O_4$.

The UV spectrum of scholaricine was characteristic of an anilino-acrylate chromophore **(Atta-Ur-Rhamman, 1985)**, λ_{max} (MeOH): 214, 230, 286 and 338 nm. The IR spectrum gave absorptions at 3425 cm^{-1} (OH), 3425 cm^{-1} (NH) and 1668 cm^{-1} (α,β unsaturated ester, C=O).

Its ^{1}H NMR spectrum **(Figure 61)** exhibited:

- a multiplet of three protons within δ 6.69 – 6.90 attributable to the protons 9,10,11
- a singlet of three protons at δ 3.87 attributable to a methoxy group of an acetate
- a doublet of one proton at δ 3.40 attributable to H-19,
- a doublet of of three protons at δ 1.15 attributable to H-18

Analysis of the ^{13}C and DEPT (90 and 135) NMR spectra gave twenty signals corresponding to twenty carbon atoms. We observed:

- seven quartenary carbon atoms amongst which, carbonyl of an ester at δ 172.3, two aromatic carbons at δ 132.4 (C-8) and δ 142.9 (C-13), two olefinic carbon at δ170.8 (C-2) and δ 138 (C-16)
- seven methine carbons amongst which an oxymethine carbon atom at δ 69.3
- four methylene carbons
- two methyl carbons

The ^{1}H-^{1}H COSY spectrum **(Figure 64)** showed correlations between the aromatic protons at δ 6.85–6.87.

The HMBC spectrum **(Figure 65)** showed correlations between the aromatic protons at δ 6.85–6.87 and the aromatic carbons at δ 132.4 (C-8) and 142.9 (C-13).

The HSQC spectrum **(Figure 66)** showed correlations between the aromatic protons at δ δ 6.85–6.87 and the aromatic carbons at δ 112.2 -123.7.

These physical and spectroscopic data were in agreement with those previously reported for scholaricine (**19)** (**Atta-ur-Rahman *et al.*, 1985**).

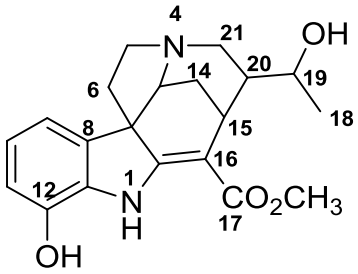

(19)

Table 24: ^{13}C NMR data of AS_9 and the litterature

AS_9		**scholaricine (Atta-ur-Rahman et *al.*, 1985)**
N_o	**^{13}C**	**^{13}C**
2	172.3	169.1
3	62.3	60.2
5	54.2	53.9
6	43.7	43.4
7	58.2	57.9
8	132.4	132.2
9	112.2	111.3
10	123.7	122.4
11	116.6	115.1
12	138.0	136.9
13	142.9	141.8
14	31.6	31.0
15	29.8	28.9
16	97.9	96.7
17	170.8	172.2
18	20.2	19.7
19	69.3	68.5
20	46.7	45.9
21	48.6	48.2
COO$\underline{CH_3}$	52.4	51.8

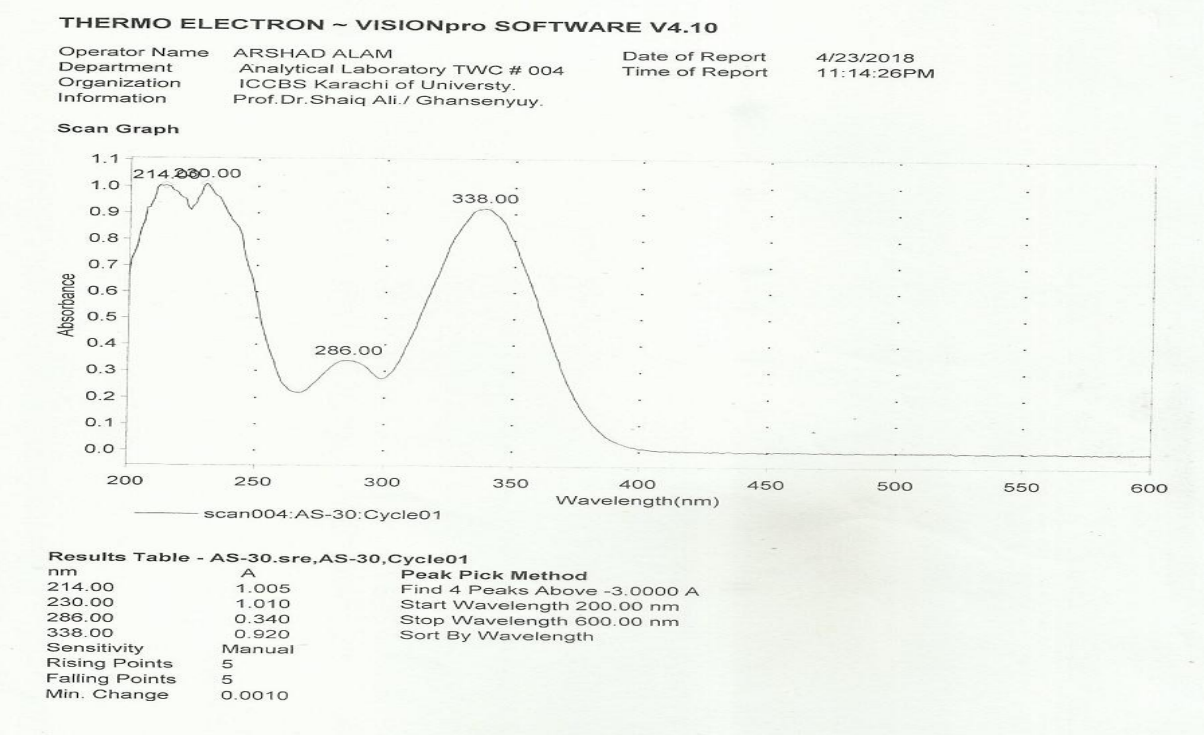

Figure 57: UV spectrum (MeOH) of compound 19

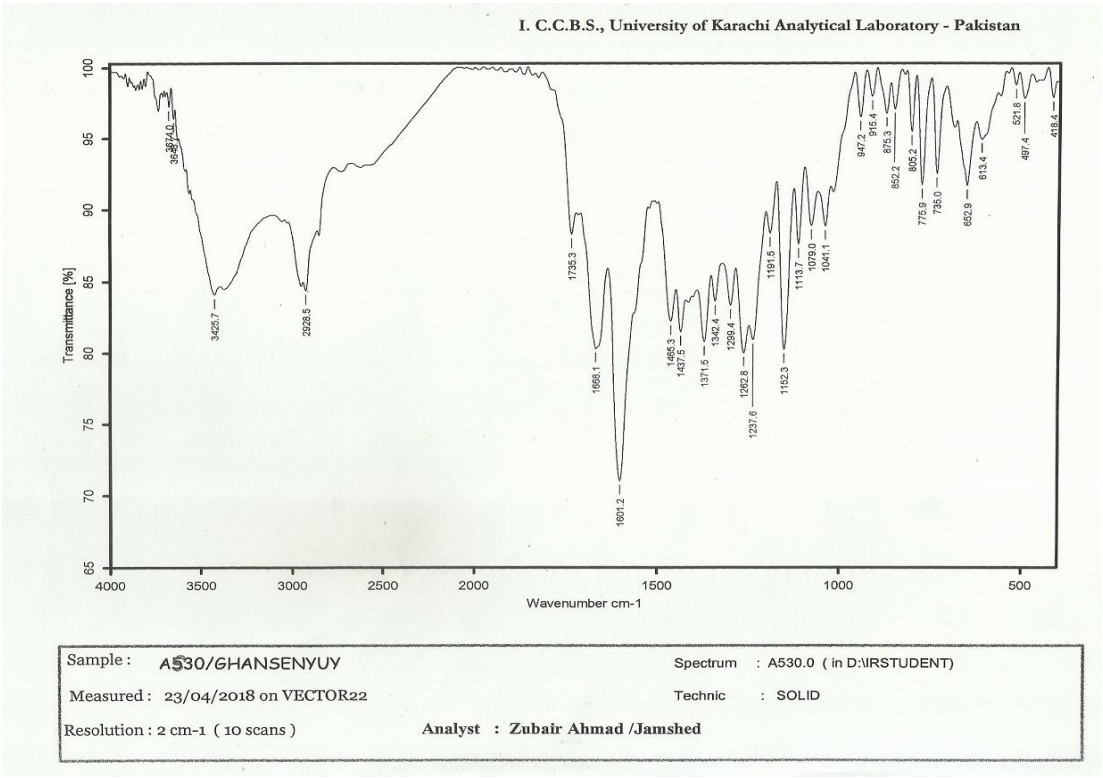

Figure 58: IR spectrum (KBr) of compound 19

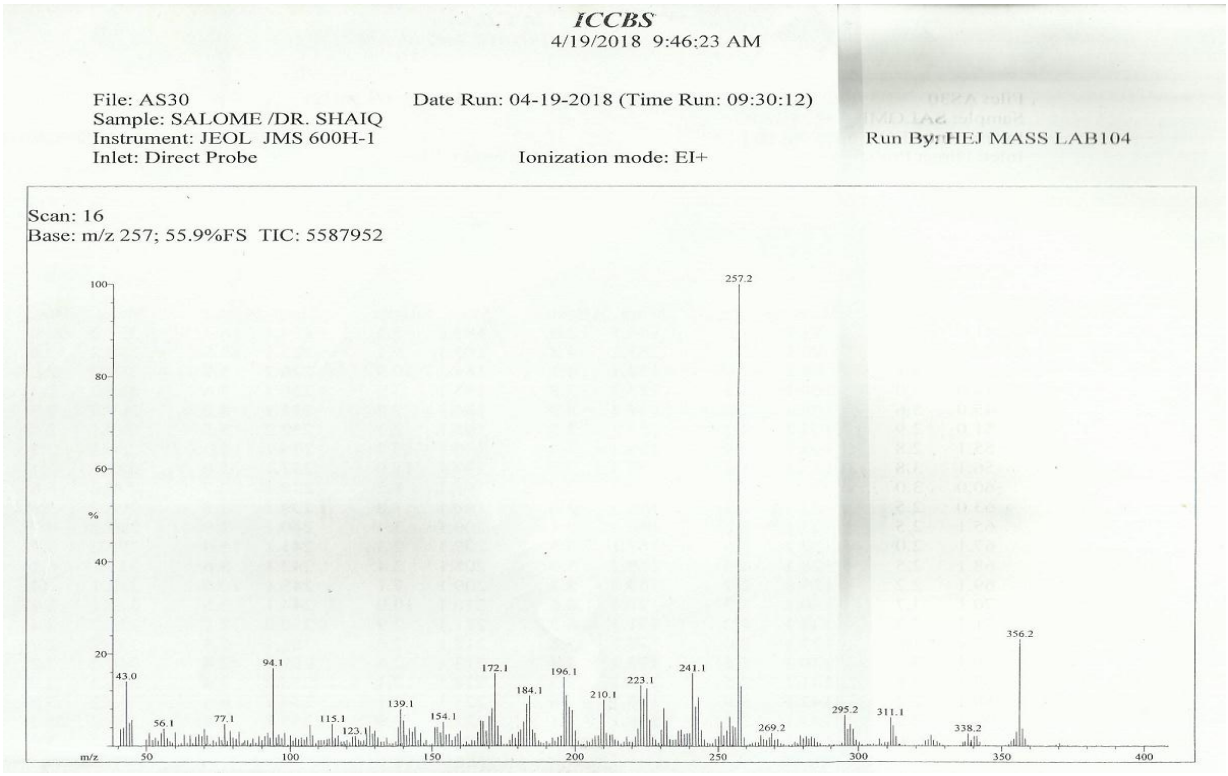

Figure 59: EI-Mass spectrum of compound 19

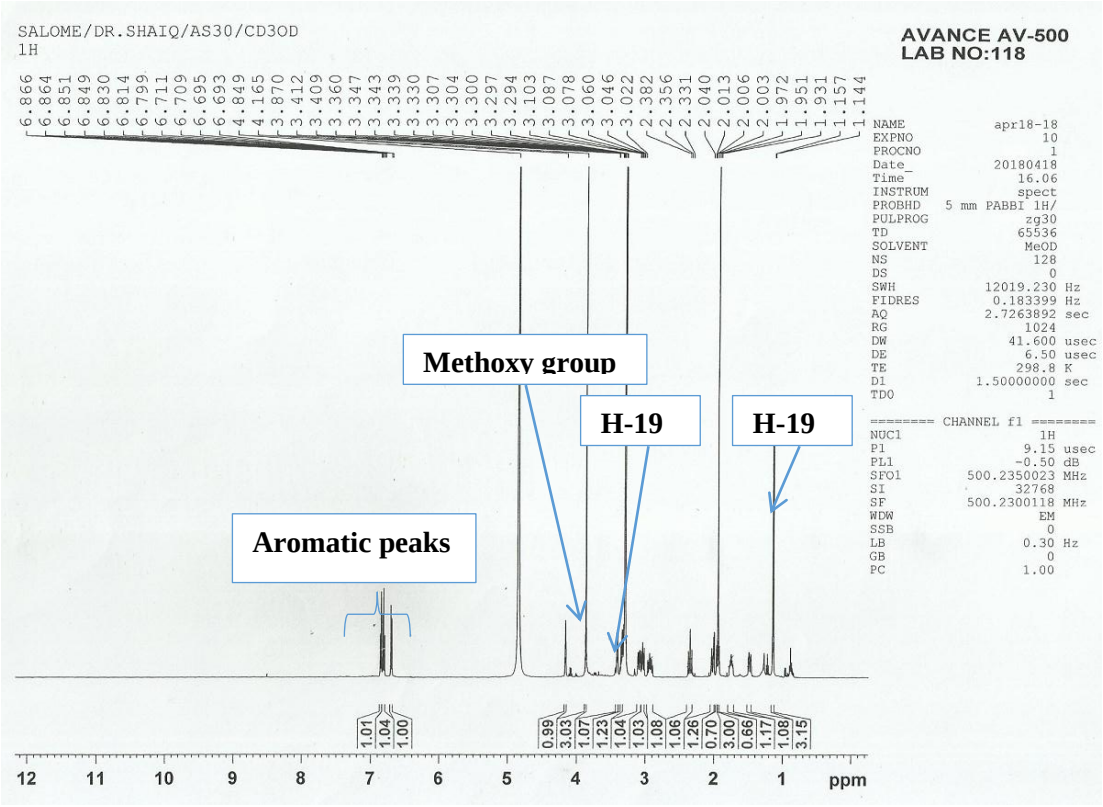

Figure 60: ^{1}H-NMR spectrum of compound 19 (CD_3OD, 500 MHz)

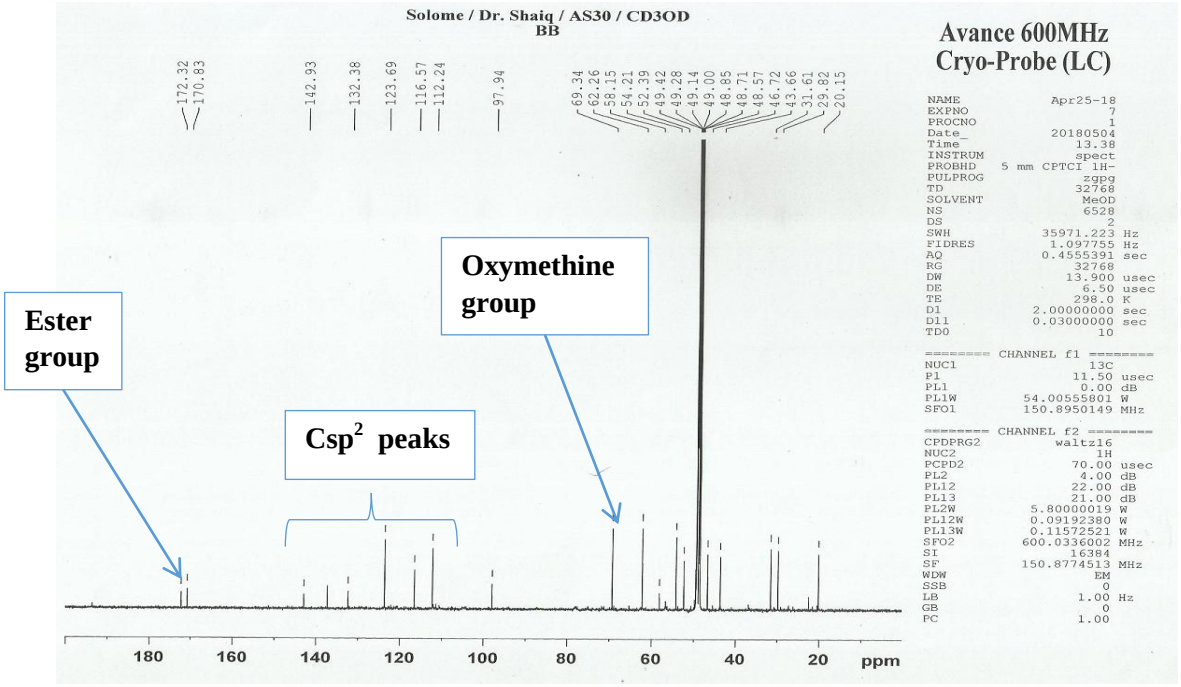

Figure 61: ^{13}C NMR spectrum of compound 19 (CD_3OD, 150 MHz)

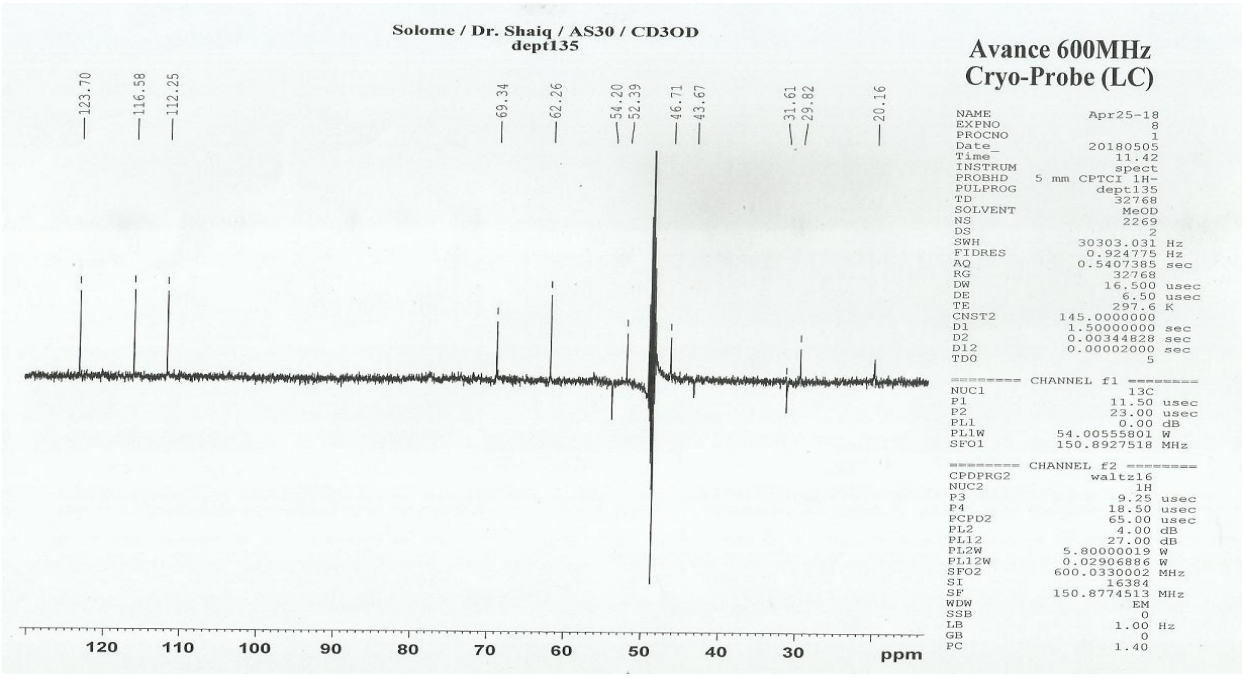

Figure 62: DEPT 135 spectrum of compound 19 (CD_3OD, 150 MHz)

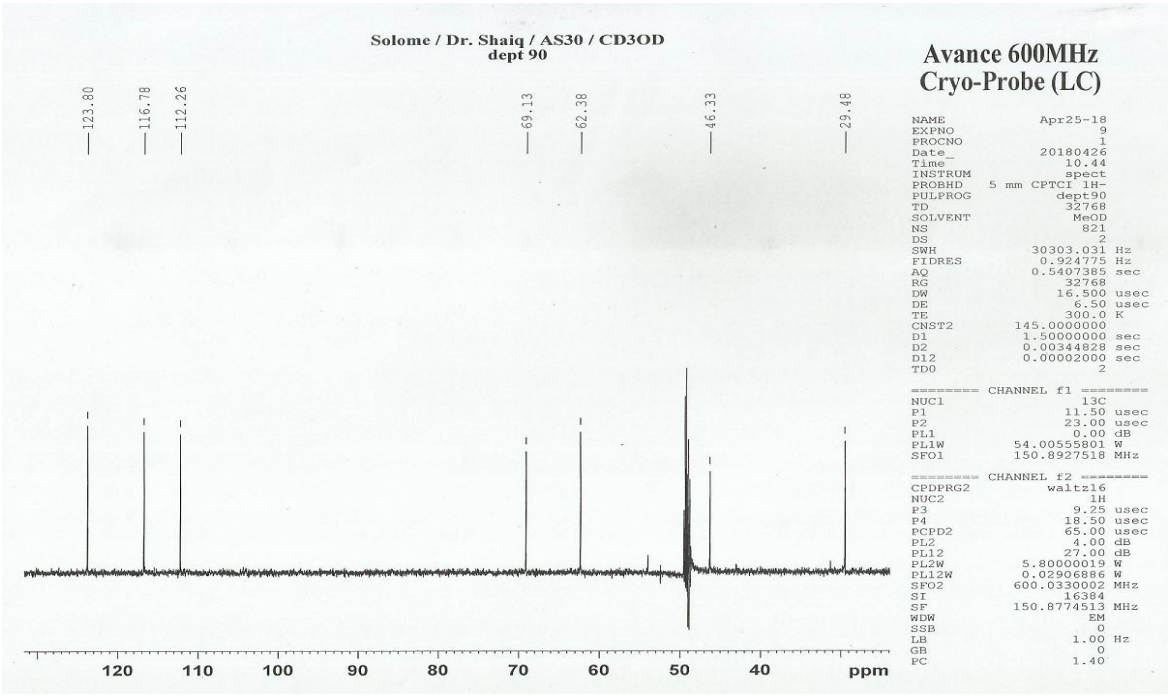

Figure 63: DEPT 90 spectrum of compound 19 (CD_3OD, 150 MHz)

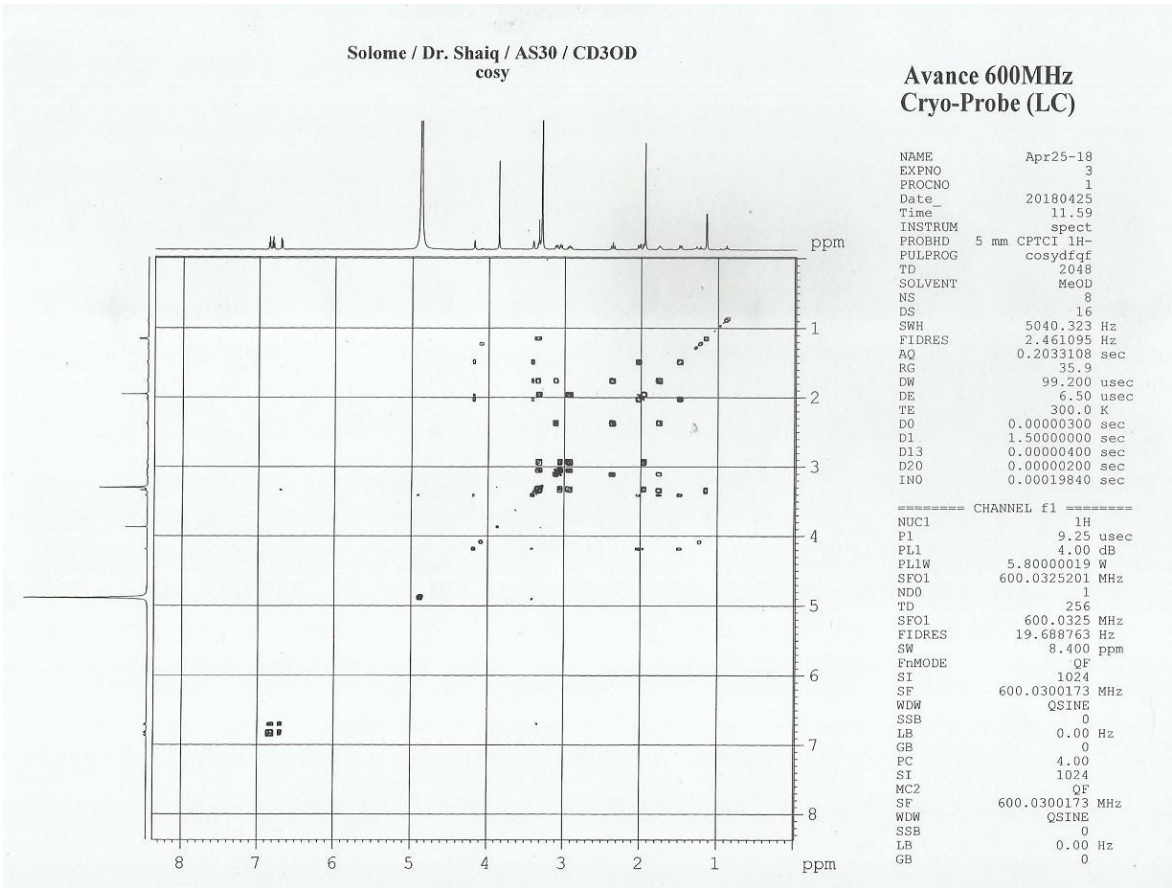

Figure 64: ^{1}H-^{1}H COSY spectrum of compound 19

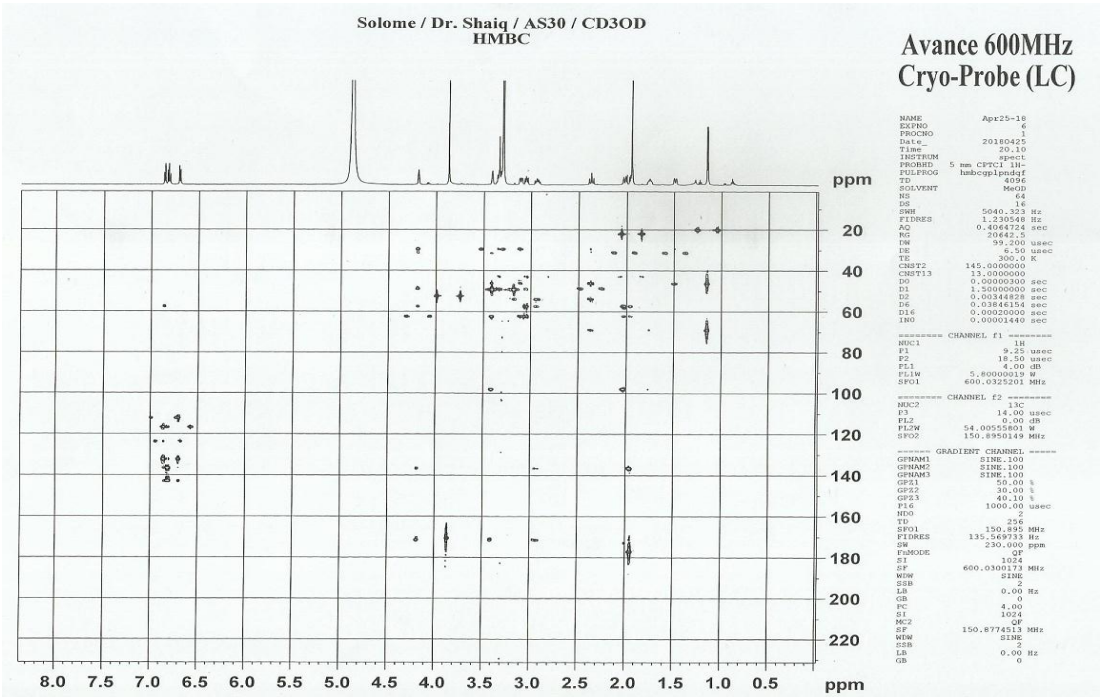

Figure 65: HMBC spectrum of compound 19

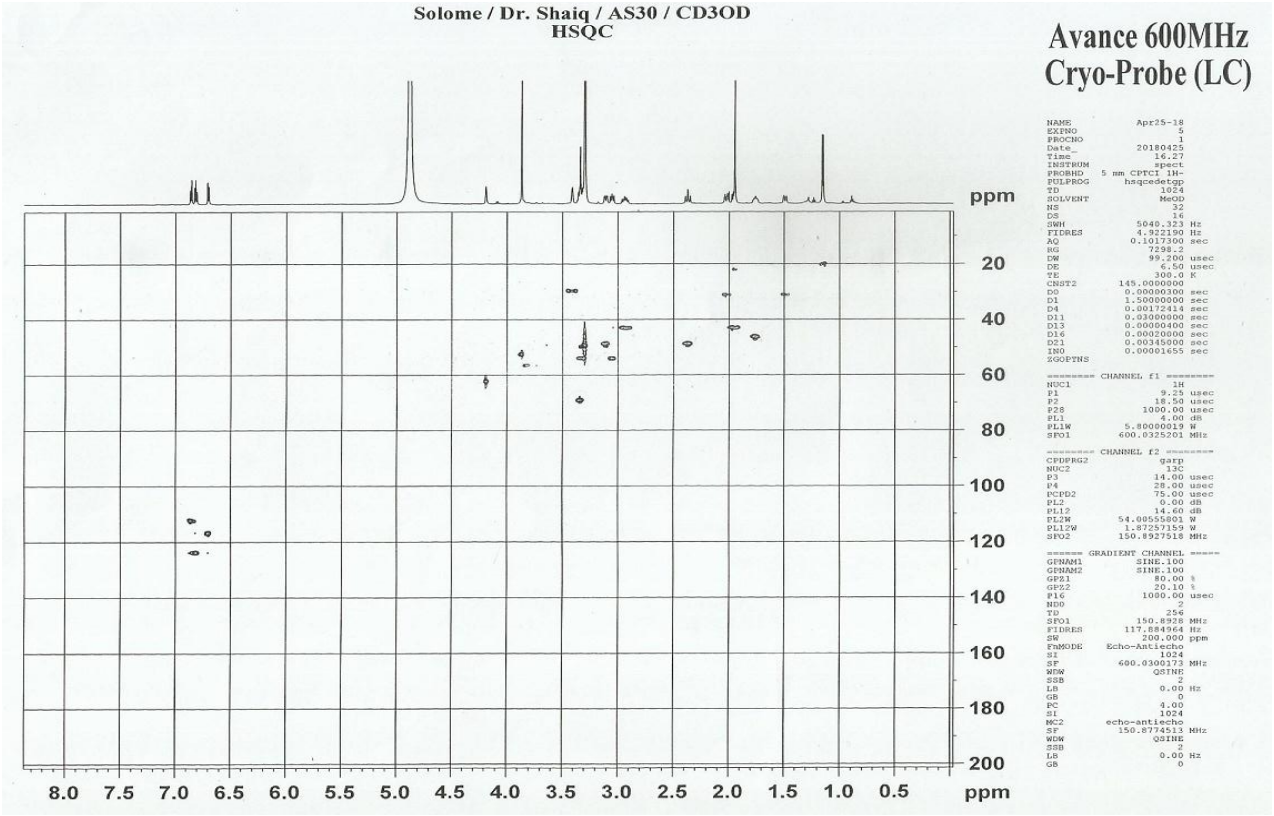

Figure 66: HSQC spectrum of compound 19

II.2.4 Characterisation of phenylpropanoid

II.2.4.1 Identification of compound AS_5

AS_5 was obtained as white powder from hexane/EtOAc 4 % (m.p. 240 °C). Its EI-MS (**Figure 68**) gave a molecular ion peak $[M]^+$ at m/z: 640.2 compartible with the molecular formula $C_{43}H_{76}O_3$ corresponding to six degrees of unsaturations.

Its ^{1}H NMR spectrum (**Figure 69**) exhibited:

- A doublet of two protons at δ 7.62 (*J* = 8.5 Hz) and another doublet of two protons at δ 6.78 (*J* = 8.5 Hz) characteristic of aromatic protons of an AA'BB' spin system.
- A doublet of one proton each at δ 6.82 (*J* = 13 Hz) and δ5.81 (*J* = 13 Hz) attributable to olefinic protons of a double bond conjugated to the aromatic ring
- A singlet of one proton at δ 4.99 attributable to the proton of a hydroxyl group linked to the double bond
- A triplet of two protons at δ 4.09 attributable to an oxymethylene proton
- A triplet of three protons at δ 0.86 attributable to a methyl group linked to a methylene group
- A long peak at δ 1.25 indicative of the methylene protons of the aliphatic chain
- These physical and spectroscopic data were similar to those reported by Wonkam *et al.*, 2020.

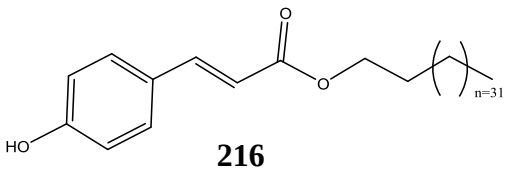

216

Table 25: ^{1}H NMR data of AS_5 and the litterature

AS_5		n -heptadecyl-4-hydroxy- trans-cinnamate (Wonkam et *al.*, 2020)
N_o	**^{1}H (m, *J* in Hz)**	**^{1}H (m, *J* in Hz)**
1	-	-
2/6	7.62 (2H, d, *J* = 8.5 Hz)	7.62 (d, *J* = 8.1 Hz)
3/5	6.78 (2H, d, *J* = 8.5 Hz)	7.16 (d, *J* = 8.1 Hz)
4	-	-
1′	6.82 (2H, d, *J* = 13Hz)	8.01 (d, *J* = 15.9 Hz)
2′	5.81 (2H, d, *J* = 13 Hz)	6.67 (d, *J* = 15.9 Hz)
3′	-	-
1″	4.09 (2H, t, *J* = 6.5 Hz)	4.30 (2H, t, *J* = 6.6 Hz)
2″-16″	1.25 (brs)	1.68 – 1.28 (brs)
17″	0.86 (3H, t, *J* = 13.5 Hz)	0.85 (3H, t, *J* = 6.1 Hz)

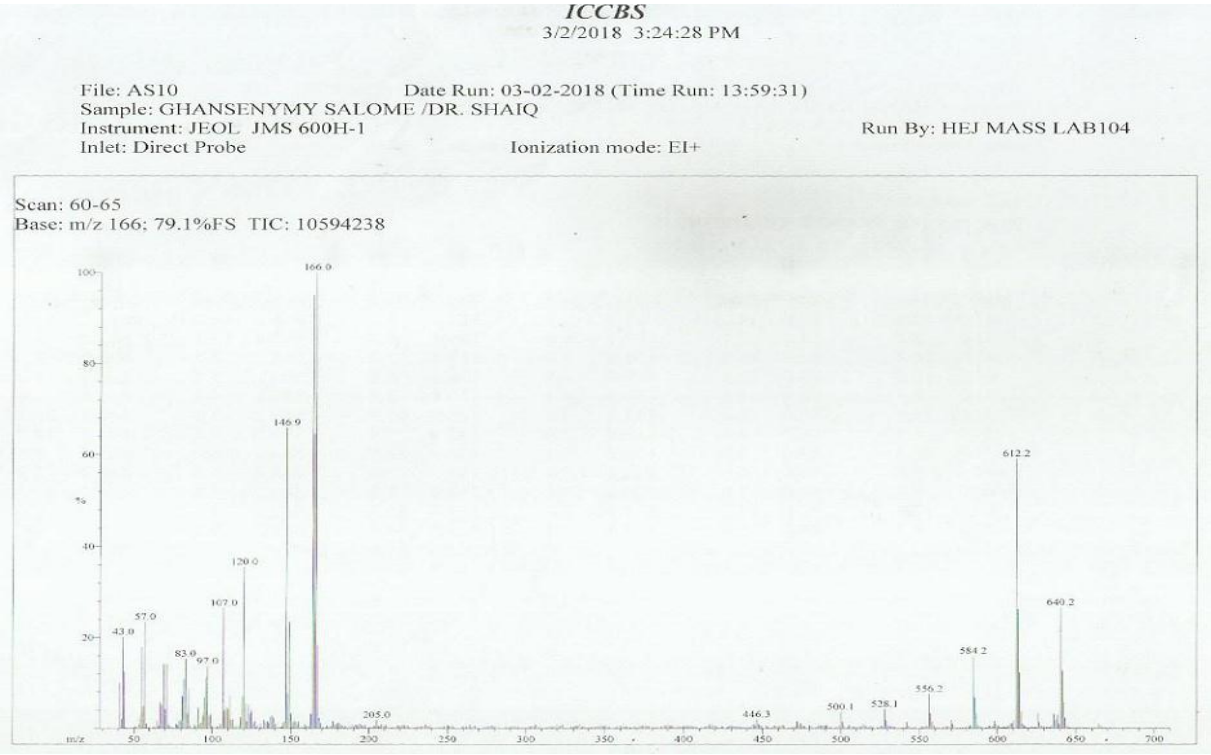

Figure 67: EI-Mass spectrum (HR) of compound 216

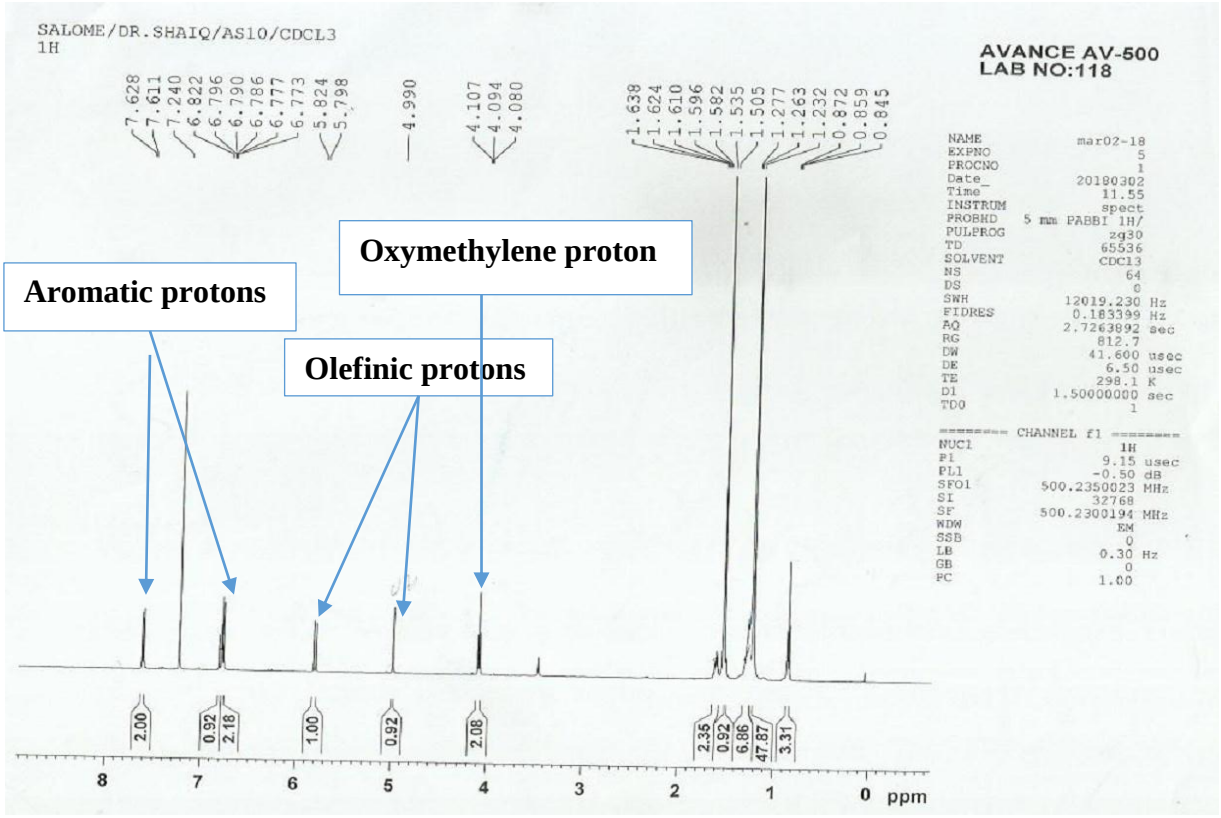

Figure 68: ^{1}H-NMR spectrum of compounds 216 ($CDCl_3$, 500 MHz)

II.3 HEMI- SYNTHESIS

The α-β unsaturated carbonyl function is a privileged medicinal scaffold found in many classes of organic compounds such as flavonoids, chalcones, coumarins and quinones. They are Michael acceptors, containing an electrophile and are generally biologically active. They are involved in the regulation of many signaling pathways in cells and are important tools in chemical biology research **(Zhuang *et al.*, 2017)**. Many techniques and procedures have been developed in the synthesis of α-β unsaturated carbonyl scaffolds and include: Claisen- Schmidt condensation, cross-coupling (Suzuki), Heck reaction, Julia- Kocienski reaction, Wittig reaction, Knoevenagel, Perkin, Reformatski, Peterson and Riley oxidation **(Zhuang *et al.*, 2017)**. The natural products **53, 54, 62** (triterpenes) and **93 & 94** (quinones) were selectively treated with selenium dioxide under reflux conditions in dry dichloromethane. The derivatives were all obtained from silica gel column chromatographic purifcation by gradient elution using hexane/ethyl acetate.

II.3.1 Hemi-synthesis (SeO_2 oxidation) of some triterpenes from *Alstonia scholaris*

To discover derivatives with structure- diversities, we introduced the privileged medicinal α,β-unsaturated function to our triterpene scaffold, which led to a new approach in the conversion of ursane to lupane derivatives and with favorable anti-cancer efficacies against MDA-MB-231 cell line.

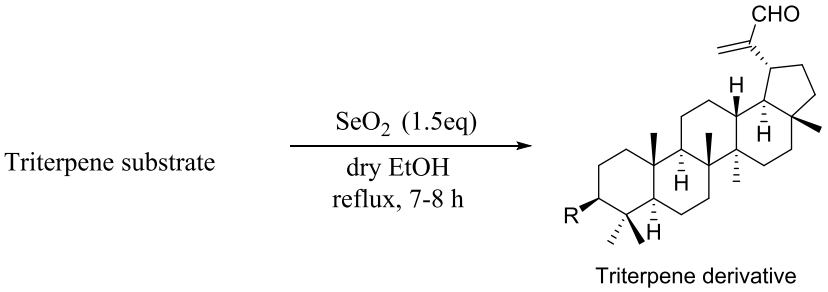

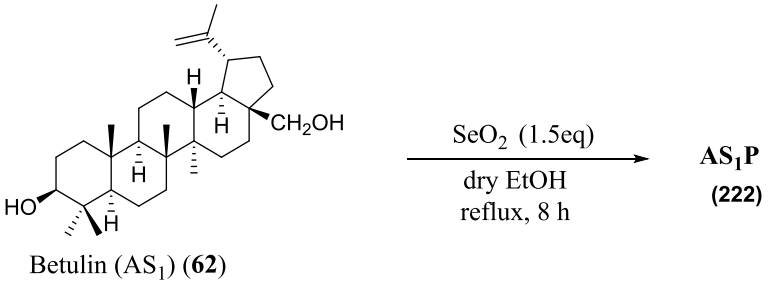

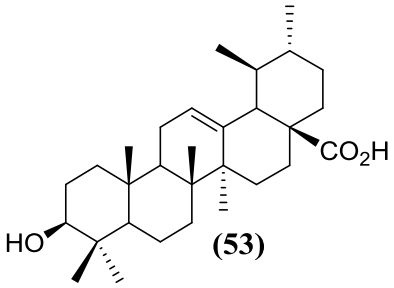

(AS_6): Ursolic acid
m = 25 mg

SeO_2 (1.5eq)
dry EtOH
reflux, 8 h
0 % yield

No reaction

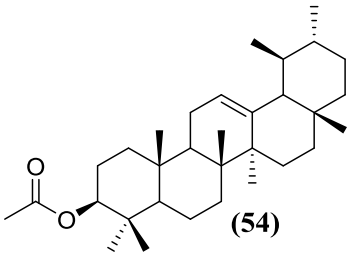

(AS_2): α - amyrin acetate
m = 25 mg

SeO_2 (1.5eq)
dry EtOH
reflux, 8 h

AS_2P (223)

II.3.2 Hemi-synthesis (SeO_2 oxidation) of some quinones from *Psorospermum guineense*

To introduce α,β unsaturated scaffold, the geranyl anthraquinones were equally treated under SeO_2 conditions.

Quinone substrate

SeO_2 (1.5eq)
dry EtOH
reflux, 70°C
7-8 h

Quinone derivatives with aldehyde function on methyl carbon atom alpha to the alkene function

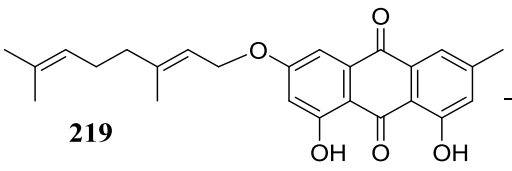

219

3-geranyloxyemodine (PG1)

SeO_2 (1.5eq)
dry EtOH
reflux, 70°C
7-8 h

PG_1P_1 (224)
m = 10 mg
Isolated yield 5.4 %
+
PG_1P_2 (226)
m = 15 mg
Isolated yield 8.2 %

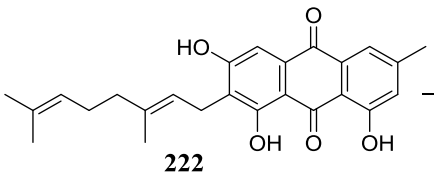

222

2-geranylemodin (PG4)
m=98 mg

SeO_2 (1.5eq)
dry EtOH
reflux, 70°C
7-8 h

PG_4P_1 (225)
m = 30 mg
Isolated yields: 30.6 %
+
PG_4P_2 (227)
m = 5 mg
Isolated yields: 5.1 %

II.3.3 Characterisation of synthesised products

II.3.3.1 Characterisation of synthesised products of triterpenes

The triterpenes betulin **(AS_1)**, ursolic acid **(AS_6)** and α-amyrin acetate **(AS_2)** were selectively treated with selenium dioxide **(Eyong *et al.*, 2018)** under reflux conditions in dry ethanol. There was no reaction with ursolic acid meanwhile, **AS_1** and **AS_2** afford two new lupane derivatives coded as **AS_1P (222)** and **AS_2P (223)** respectively. They were all obtained from silica gel column chromatographic purification by gradient elution using hexane/ethyl acetate.

- **Characterisation of AS_1P (222)**

AS_1P was obtained as a white solid in Hex/AcoEt 27 % (m.p.: 258 °C). It was soluble in CH_2Cl_2/MeOH and was obtained with a yield of 60 %. Interpretation of its LCMS spectrum ([M+H] m/z= 456.368) led us to deduce the molecuar formula $C_{30}H_{48}O_3$ with 7 double bond equivalents. We observe the appearance of a singlet of one proton at about 9.50 ppm characteristic of the aldehyde proton **(Figure 70)** which is absent on the spectrum of the starting material AS_1 (Figure 8) which shows that one of the methyl groups was converted into an aldehyde function. On its carbon -13 NMR spectrum **(Figure 71)**, we also observe the appearance of a peak at 195.0 ppm indicative of the carbonylgroup of an aldeyde. All of this confirms that there was the transformation of a methyl group to an aldehyde function. The NMR data is pesented in Table 26 below along with that for the other synthesised product.

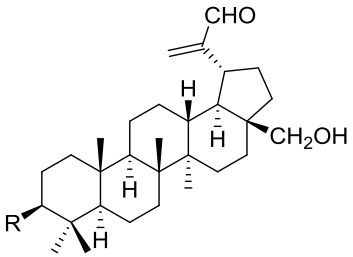

Betulin acryl aldehyde **(222)**

Table 26: ^{1}H and ^{13}C NMR spectral data of the synthesized compounds

N°	δc (DEPT)	δ_H (m, *J* in Hz)	δc (DEPT)	δ_H (m, *J* in Hz)
	AS_1P (222)		**AS_2P (223)**	
1	38.8(CH_2)	0.92(m) ;1.57(br d, *J*= 12.0Hz)	38.8(CH_2)	0.92(m) ;1.57(br d, *J*= 12.0Hz)
2	27.4(CH_2)	1.47(m);1.72(dd, 10 and 12Hz)	27.4(CH_2)	1.47(m);1.72(dd, 10 and 12Hz)
3	77.2(CH)	2.97 (dd, 5 and 10Hz)	80.2(CH)	4.97 (m)
4	38.3(C)	-	38.3(C)	-
5	55.3(CH)	0.72(m)	55.3(CH)	0.72(m)
6	18.3(CH_2)	1.55(m); 1.33(m)	18.3(CH_2)	1.55(m); 1.33(m)
7	34.3(CH_2)	1.44(m); 1.38(m)	34.3(CH_2)	1.44(m); 1.38(m)
8	41.0(C)	-	41.0(C)	-
9	50.1(CH)	1.38(m)	50.1(CH)	1.38(m)
10	37.4(C)	-	37.4(C)	-
11	20.9(CH_2)	1.42(m); 1.22(m)	20.9(CH_2)	1.42(m); 1.22(m)
12	25.6(CH_2)	1.23(m); 1.91(m)	25.6(CH_2)	1.23(m); 1.91(m)
13	37.0(CH)	2.74(m)	37.0(CH)	2.74(m)
14	42.8(C)	-	42.8(C)	-
15	27.1(CH_2)	1.26(m); 1.88(m)	27.1(CH_2)	1.26(m); 1.88(m)
16	29.3(CH_2)	1.55(m); 2.63(m)	29.3(CH_2)	1.55(m); 2.63(m)
17	47.8(C)	-	47.8(C)	-
18	47.8(CH)	1.77(m)	47.8(CH)	1.77(m)
19	48.1(CH)	2.65 (m)	48.3(CH)	2.65 (m)
20	148.3(C)	-	148.3(C)	-
21	29.8(CH_2)	1.53(m); 2.24(m)	29.8(CH_2)	1.53(m); 2.24(m)
22	34.0(CH_2)	1.56(m); 2.15(m)	34.0(CH_2)	1.56(m); 2.15(m)
23	28.0(CH_3)	0.88 (s)	28.0(CH_3)	0.88 (s)
24	15.3(CH_3)	0.66 (s)	15.3(CH_3)	0.66 (s)
25	16.1(CH_3)	0.76 (s)	16.1(CH_3)	0.76 (s)
26	16.1(CH_3)	0.91 (s)	16.1(CH_3)	0.91 (s)
27	14.7(CH_3)	0.98 (s)	14.6(CH_3)	0.98 (s)
28	58.2(CH_3)	3.53 and 3.09 (d, 10 Hz)	18.5(CH_3)	0.70 (s)
29	105.8(CH_2)	6.42 and 6.08 (br s)	105.8(CH_2)	6.40 and 6.05 (br s)
30	196.0(C)	9.51 (s)	196.2(C)	9.51 (s)
1'			170.2(C)	-
2'			21.0(CH_3)	2.02(s)

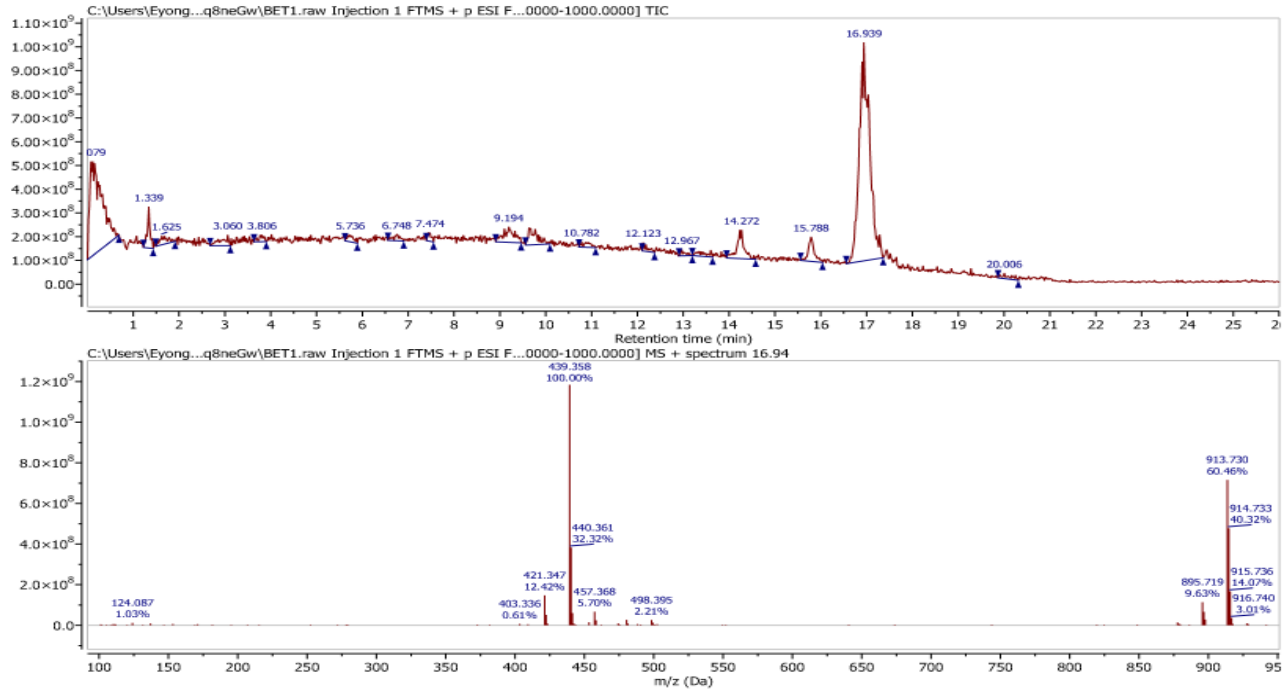

Figure 69: LC-MS Spectrum of compound 222

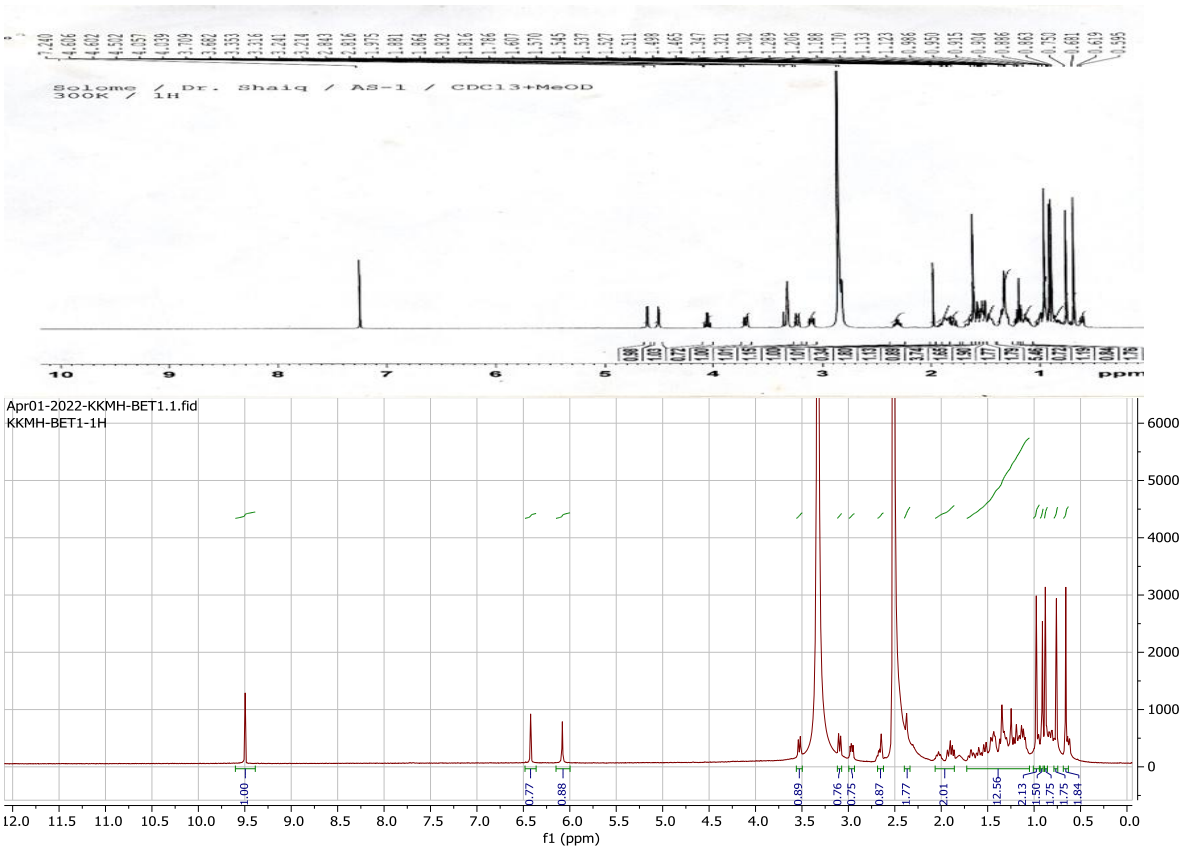

Figure 70: ^{1}H-NMR of compound 222 ($CDCl_3$/MeOD, 400 MHz) superimposed with that of compound 62

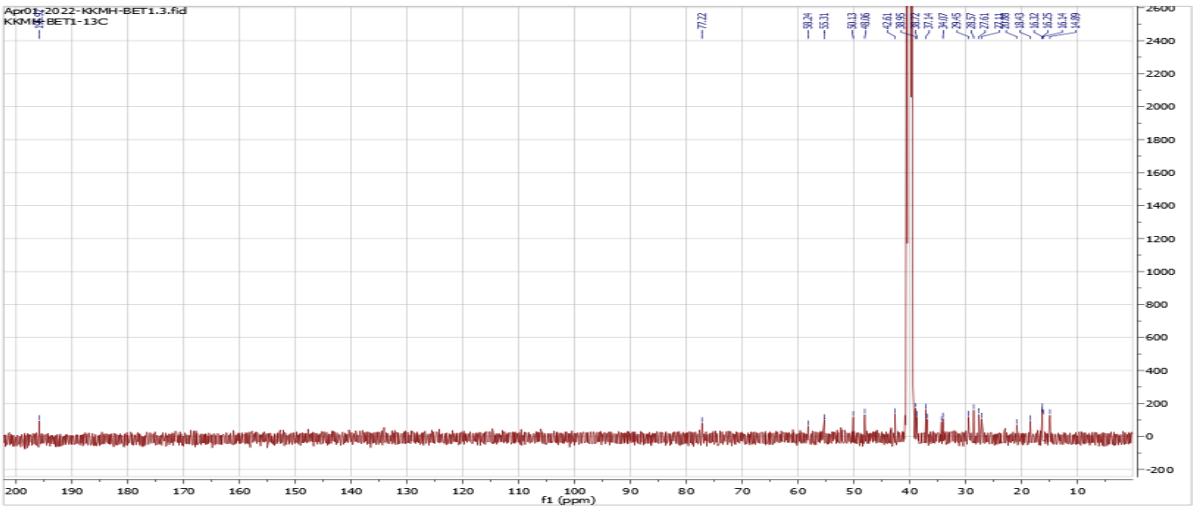

Figure 71: ^{13}C-NMR spectrum of compound 222 ($CDCl_3$/MeOD, 100 MHz)

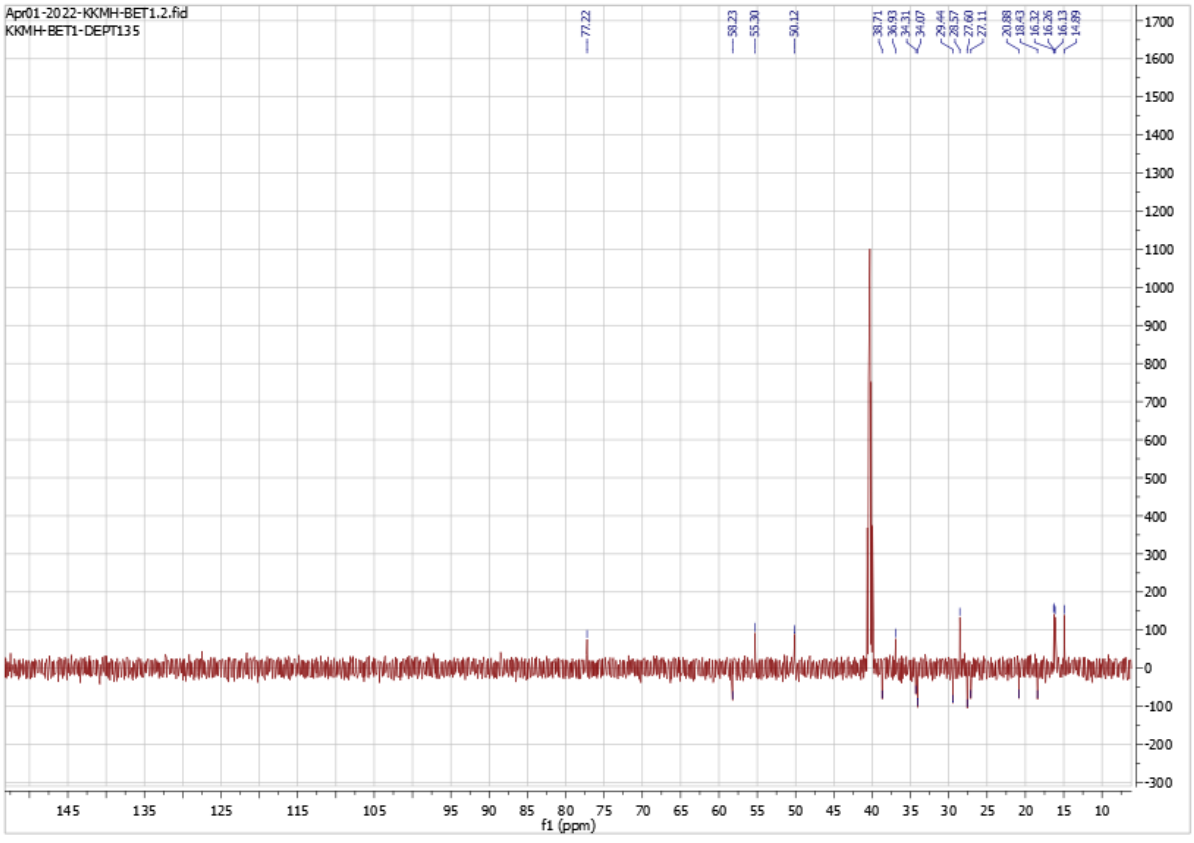

Figure 72: DEPT 135 of compound 222 ($CDCl_3$, 100 MHz)

- **Characterisation of AS_2P (223)**

AS_2P was obtained a white solid from Hex/AcoEt 7.5% (m.p.: 230 °C). It was soluble in CH_2Cl_2/MeOH and was obtained at a yield of 50 %. Analyses of its HRMS ([M-2H]; m/z=480.5138) **(Figure 73)** & NMR spectra led us to deduce the molecular formula $C_{32}H_{50}O_3$ with 8 double bond equivalents.

Physical and spectroscopic data for **AS_2P (223)** were similar to those reported for lupeol **(Machado et *al.*, 2018; Castro et *al.*, 2018).** The ^{1}H NMR spectrum **(500 MHz, $CDCl_3$)** of compound **222 (Figure 74)** showed signals indicative of aldehyde proton at δ_H = 9.51 (1H, s), two down field terminal olefin protons at δ_H = 5.95 (1H, br s) and 6.30 (1H, br s), five methyl groups at δ_H = 0.98 (3H, s), 0.91 (3H, s), 0.88 (3H, s), 0.76 (3H, s) and 0.66 (3H, s), seventeen methylene and methine groups, amongst which two of which are attached to oxygen atoms; a diastereotopic protons at δ_H = 3.53 (1H, d, 10 Hz; H-28a) and δ_H = 3.09 (1H, d, 10 Hz; H-28b) and δ_H = 2.97 (1H, dd, 5, 10.2 Hz; H-3) and the disappearance of methyl-30 at δ_H = 1.59 (3H, s).

The ^{13}C NMR spectrum **(Figure 75, 125 MHz, $CDCl_3$)** showed 30 carbon signals that were assigned by a DEPT experiment as one carbonyl atom at δ_C = 196.2 (CHO), five methyl (δ_C 28.0, 15.3, 16.1, 16.1, 14.7), twelve methylene including one –CH_2(OH) at δ_C = 58.2, six methine including one –CH(OH) (δ_C = 77.2), six quaternary carbons (δ_C = 38.3, 41.0, 37.4, 42.8, 47.7, 148.3) and the disappearance of methyl carbon at δ_C = 18.2 (CH_3-30).

However, the appearance of α,β-unsaturated olefin peaks were not observed on the ^{13}C NMR spectrum. The presence of these peaks at δ_C = 105.8 and δ_C = 148.3 were made evidence thanks to their HSQC **(Figure 78)** and HMBC **(Figure 77)** spectra. The disappearance of these peaks during ^{13}C NMR measurements maybe due to weak absorbance. This can happen if the delay between pulses was too short, particularly for carbon-13 nuclei lacking attached protons.

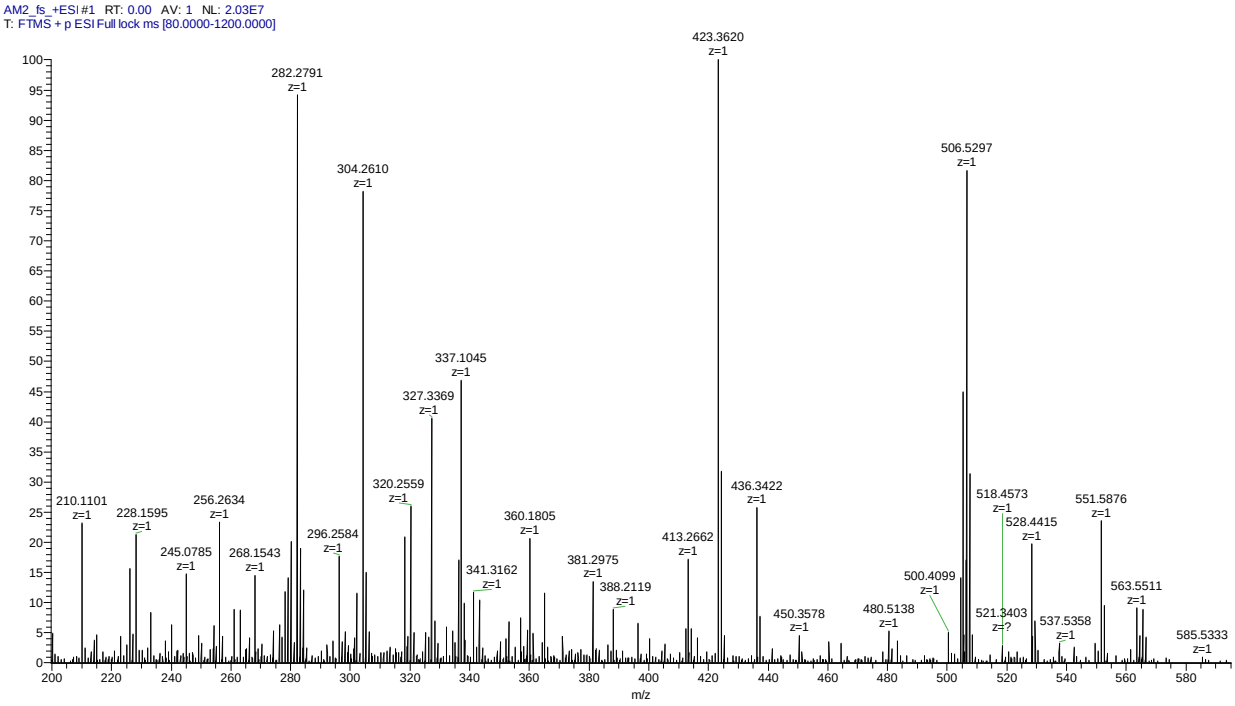

Figure 73: HR-ESI-Mass spectrum of compound 223

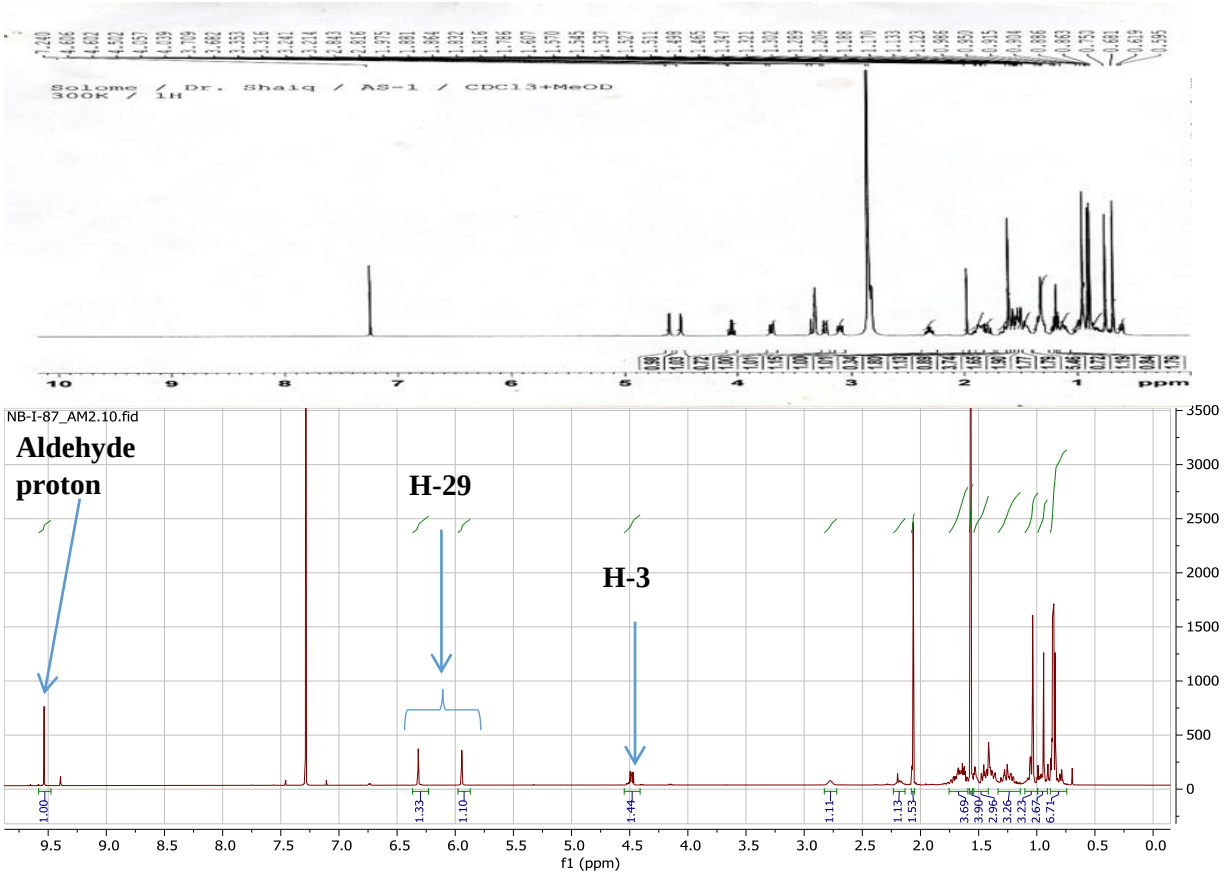

Figure 74: ^{1}H NMR of compound 223 ($CDCl_3$, 400 MHz) superimposed with that of compound 54

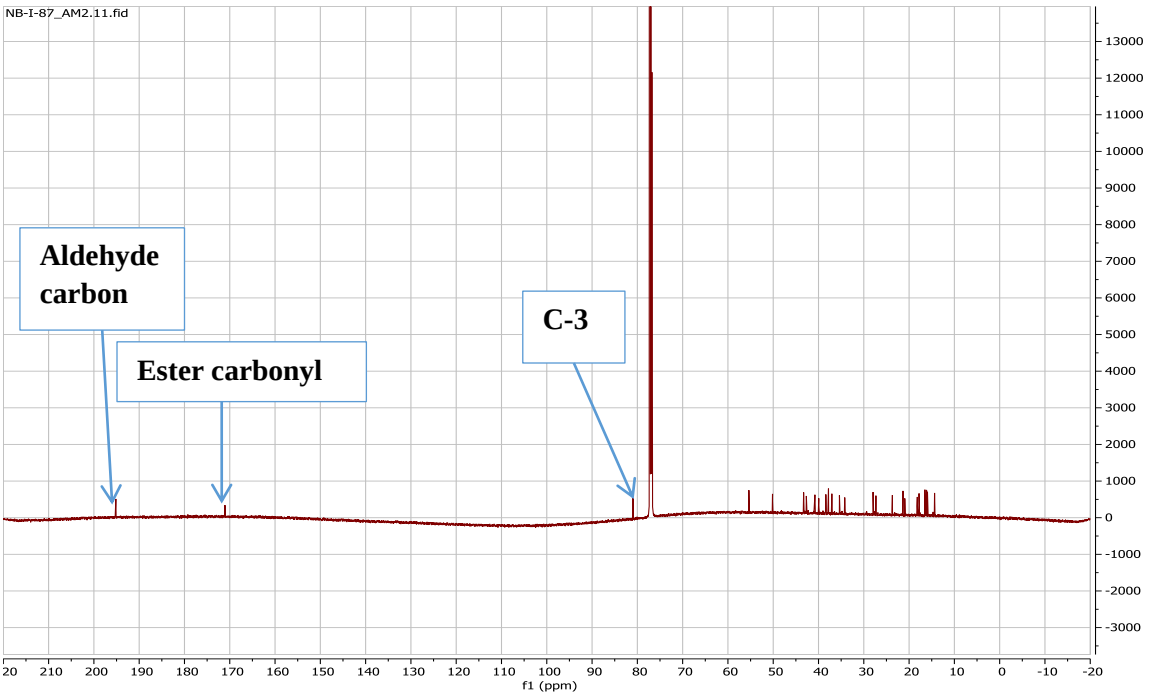

Figure 75: ^{13}C NMR of compound 223 ($CDCl_3$, 100 MHz)

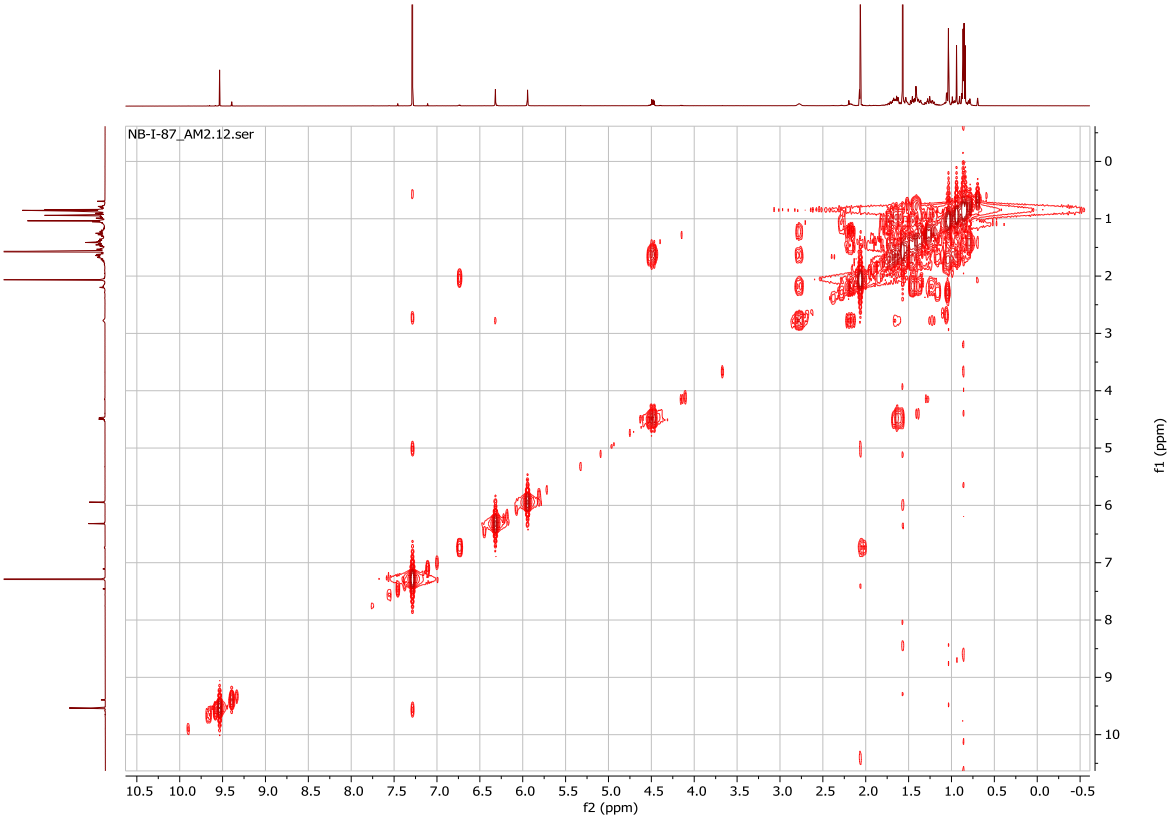

Figure 76: ^{1}H-^{1}H COSY of compound 223

Figure 77: HMBC of compound 223

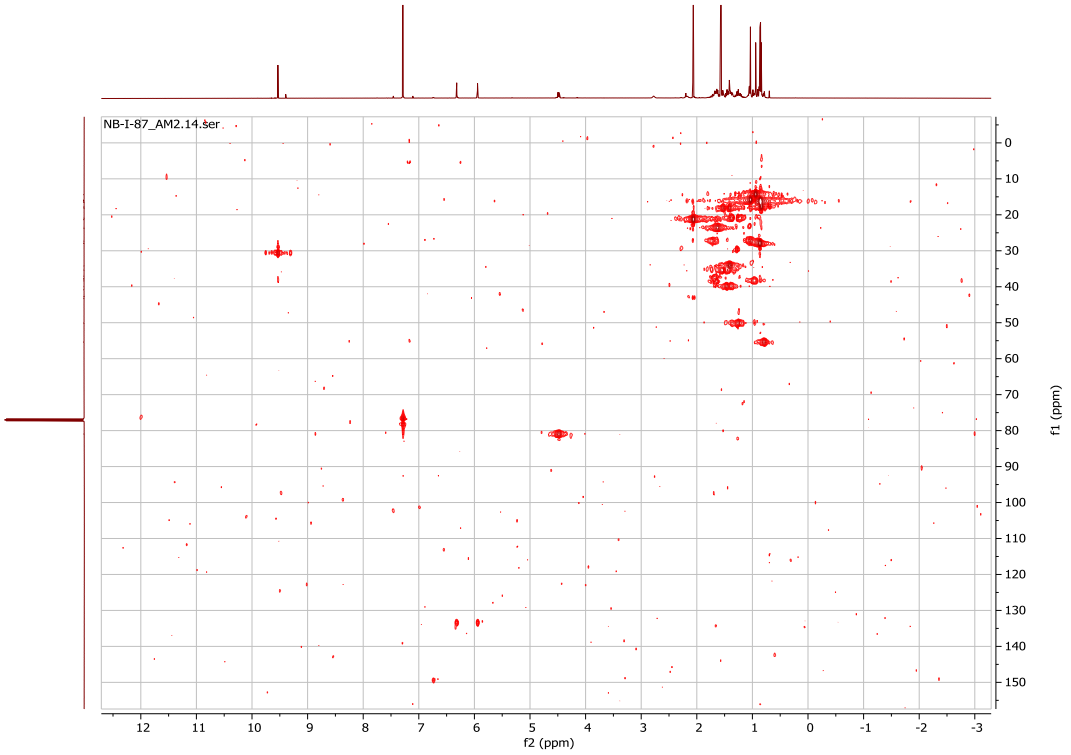

Figure 78: HSQC of compound 223

To gain insights in the unusual conversion of the ursane **AS_2** to lupane **AS_2P (223)**, ursolic acid (**AS_6)** with structural similarities to compound **AS_2** was equally subjected to SeO_2 oxidation conditions but the reaction didn't take place. Since the two ursane derivatives differ at position C-3 and C-28; with **AS_2** having acetyl group at C-3 and methyl group at C-28 while **AS_6** has hydroxyl group at C-3 and acid group at C-28. The difference in functional groups might contribute greatly in the mechanism of the reaction. The proposed mechanism of formation is presented below.Table 26 presents the 1D (^{1}H and ^{13}C) NMR spectral data of this compound.

II.3.3.2 Proposed mechanism for the formation of the synthesized compounds 222 and 223 (conversion of ursane triterpene to lupane triterpene)

i. Proposed mechanism for the rearrangement of 6 member ring of ursane triterpene to a 5 member ring

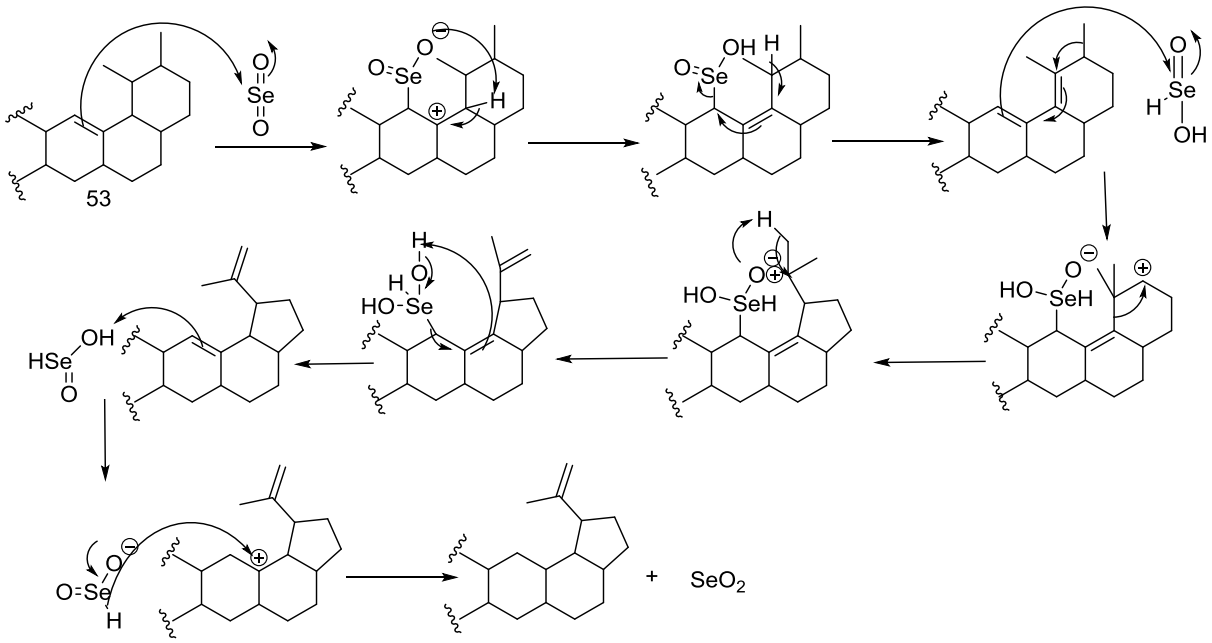

Scheme 22: Proposed mechanism for the rearrangement of 6 member ring of ursane triterpene to a 5 member ring

ii. Proposed mechanism for formation of adehyde by allylic oxidation

The mechanism of allylic oxidation using SeO2 is a series of three steps in which an ene reaction (the reaction between an alkene having a hudrogene in allylic position and the compound containing a multiple bond) is followed by a [2,3] sigmatropic rearrangement leading to the formation of selenium II ester which is susceptible to solvolysis. In this type of mechanism, the ene reaction step can explain the selectivity of the reaction while the rearrangement reaction can explain the preference for the formation of the allylic alcohol with an (E) geometry **(Riley, 1947 ; Patel et *al.*, 2011)**

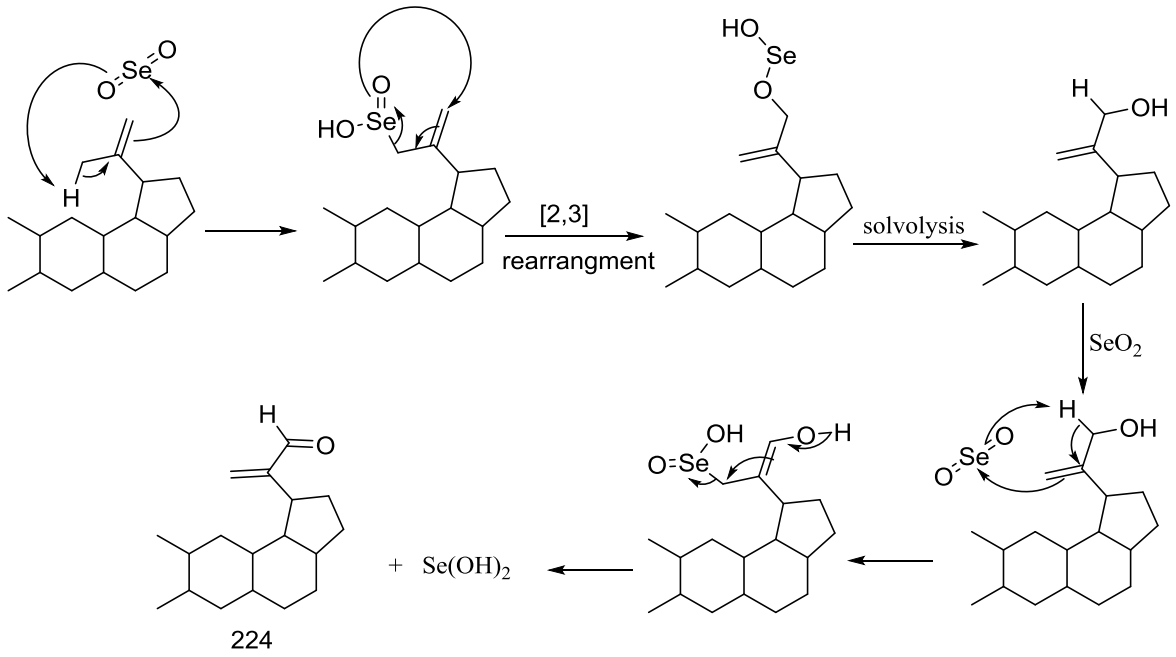

Scheme 23: Proposed mechanism for the formation of α, β-unsaturated aldehydes by allylic oxidation using SeO_2

II.3.3.3 Characterisation of synthesis products of quinones

- Characterisation of PG_1P_1 (224)

PG_1P_1 was obtained as a yellow solid in Hex/AcoEt 39 % and was soluble in CH_2Cl_2. Its yield was 5.4 %. Analyses of its NMR spectra led to the deduction of the molecular formular, $C_{25}H_{24}O_6$ with 14 degrees of unsaturations.

Its ^1H NMR spectrum **(Figure 79)** shows a singlet of one proton at 9.40 ppm indicative of the formation of an aldehyde functional group which is absent from the corresponding spectrum of the starting material PG_1 **(Figure 29)**. The 13C NMR spectrum also shows the presence of an additional signal in the carbonyl region (190 -200 ppm) characteristic of an aldehyde carbonyl which is absent from the corresponding spectrum of the starting material PG_1 (Figure 30). All these led us to establish the structure of PG_1P_1 as (2E,6E)-8-((4,5-dihydroxy-7-methyl-9,10-dioxo-9,10-dihydroanthracen-2-yl)oxy)-2,6-dimethylocta-2,6-dienal (**224**) or 3-geranyloxyemodine aldehyde (**224**).

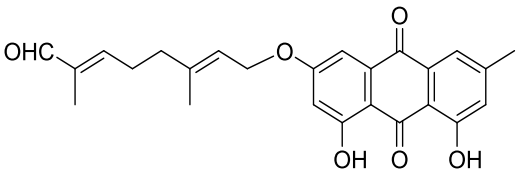

224

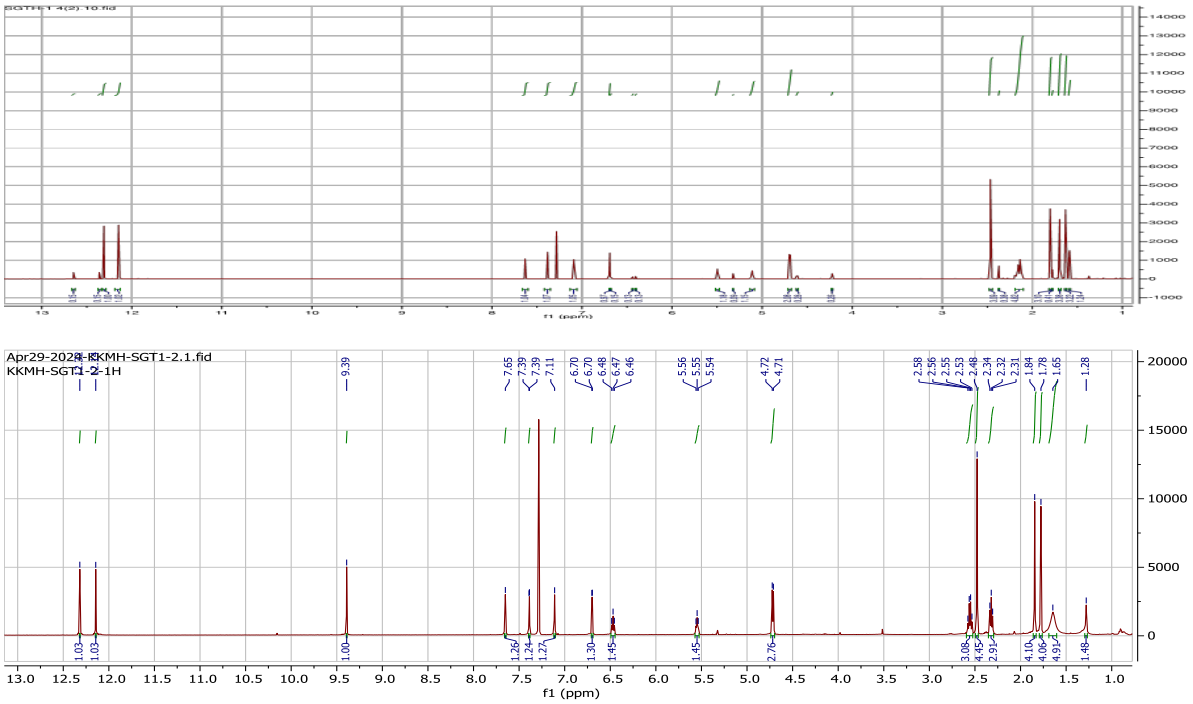

Figure 79: ^{1}H NMR of compound 224 ($CDCl_3$, 400 MHz) superimposed with that of compound 94

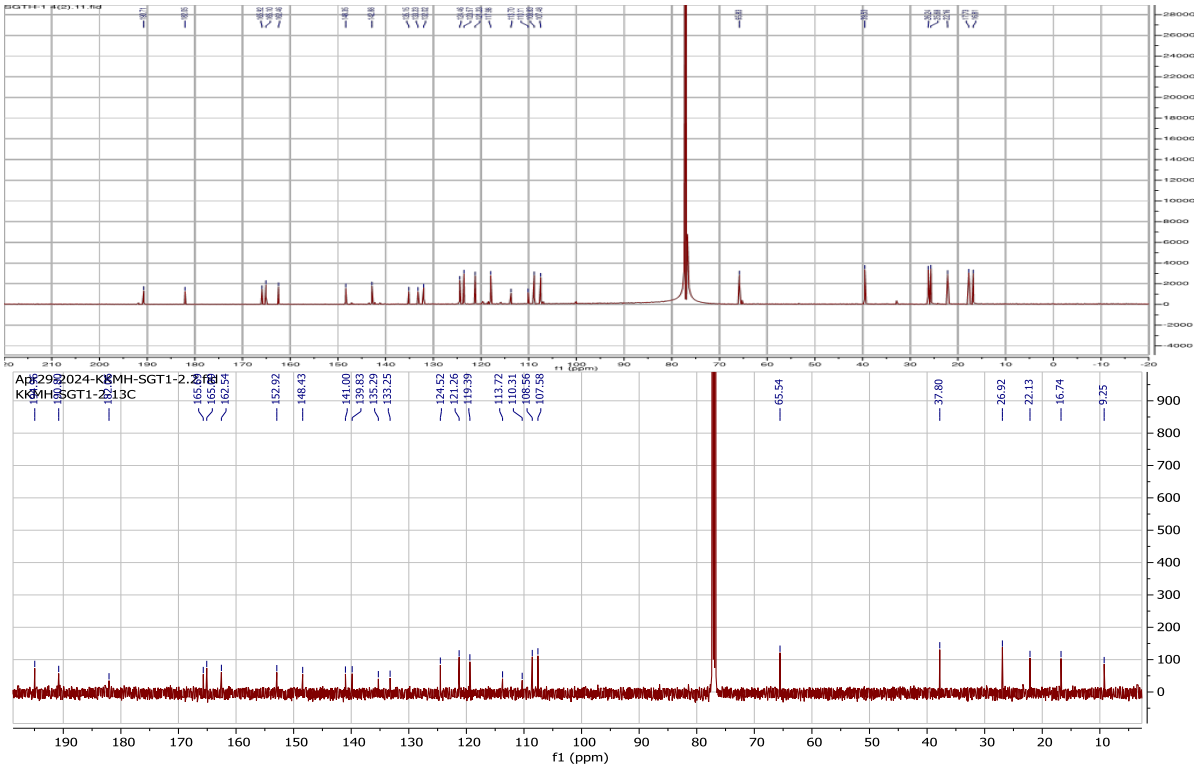

Figure 80: ^{13}C NMR of compound 224 ($CDCl_3$, 100 MHz) superimposed with that of compound 94

- **Characterisation of PG_4P_1 (225)**

PG_4P_1 was obtained as a yellow solid in Hex/AcoEt 45 % and was soluble in CH_2Cl_2. Its yield was 30.6 %. Analyses of its NMR spectra led to the deduction of the molecular formular, $C_{25}H_{24}O_5$ with 14 degrees of unsaturations.

Its ^1H NMR spectrum (Figure 81) shows a singlet of one proton at 9.40 ppm indicative of the formation of an aldehyde functional group which is absent from the corresponding spectrum of the starting material PG_4 **(Figure 37)**. The ^{13}C NMR spectrum also shows the presence of an additional signal at 195 ppm (Figure 82) characteristic of an aldehyde carbonyl which is absent from the corresponding spectrum of the starting material PG_4 **(Figure 30).** All these led us to establish the structure of PG_4P_1 as (2E,6E)-2,6-dimethyl-8-(1,3,8-trihydroxy-6-methyl-9,10-dioxo-9,10-dihydroanthracen-2-yl) - octa-2,6-dienal (**225**) or 2-geranylemodine aldehyde (**225**).

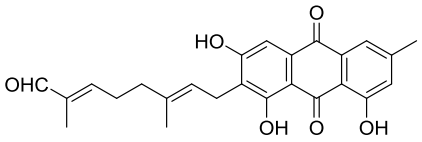

(2*E*,6*E*)-2,6-dimethyl-8-(1,3,8-trihydroxy-6-methyl-9,10-dioxo-9,10-dihydroanthracen-2-yl) octa-2,6-dienal (225)

0

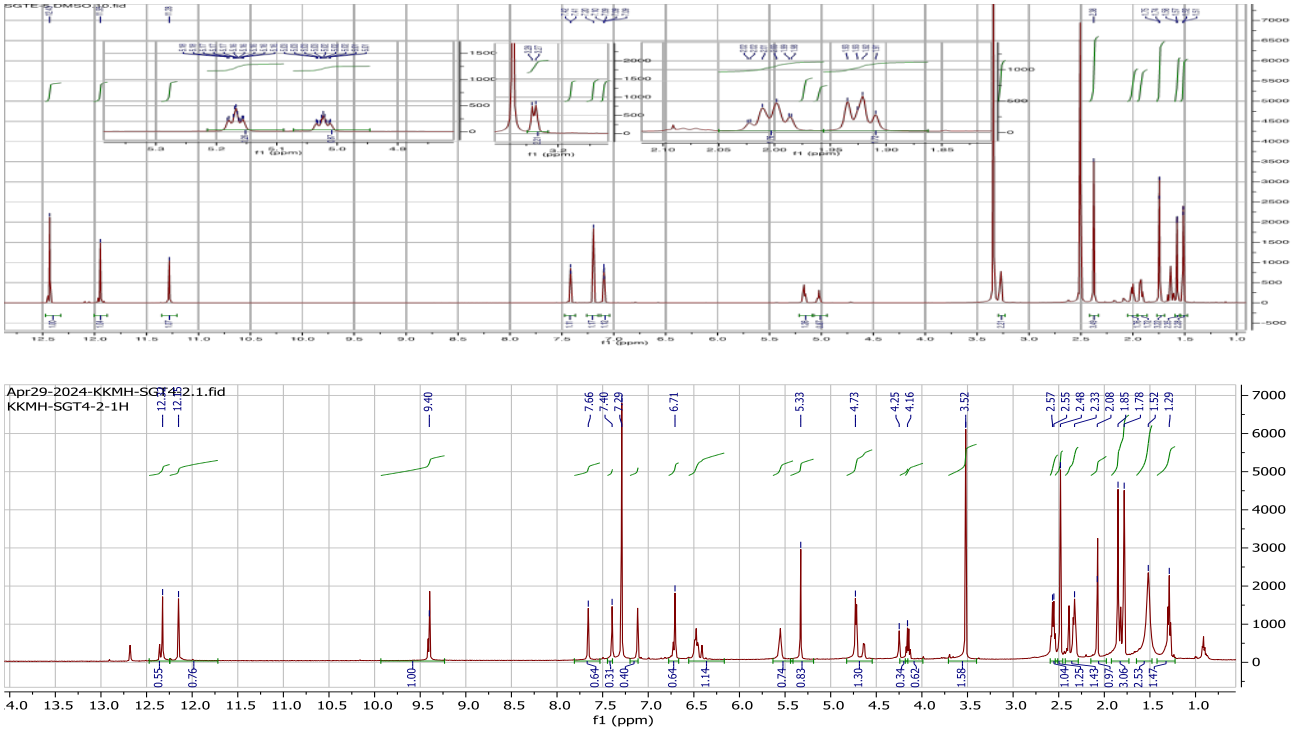

Figure 81: ^1H NMR of compound 225 ($CDCl_3$, 400 MHz) superimposed with that of Spectrum of compound 93

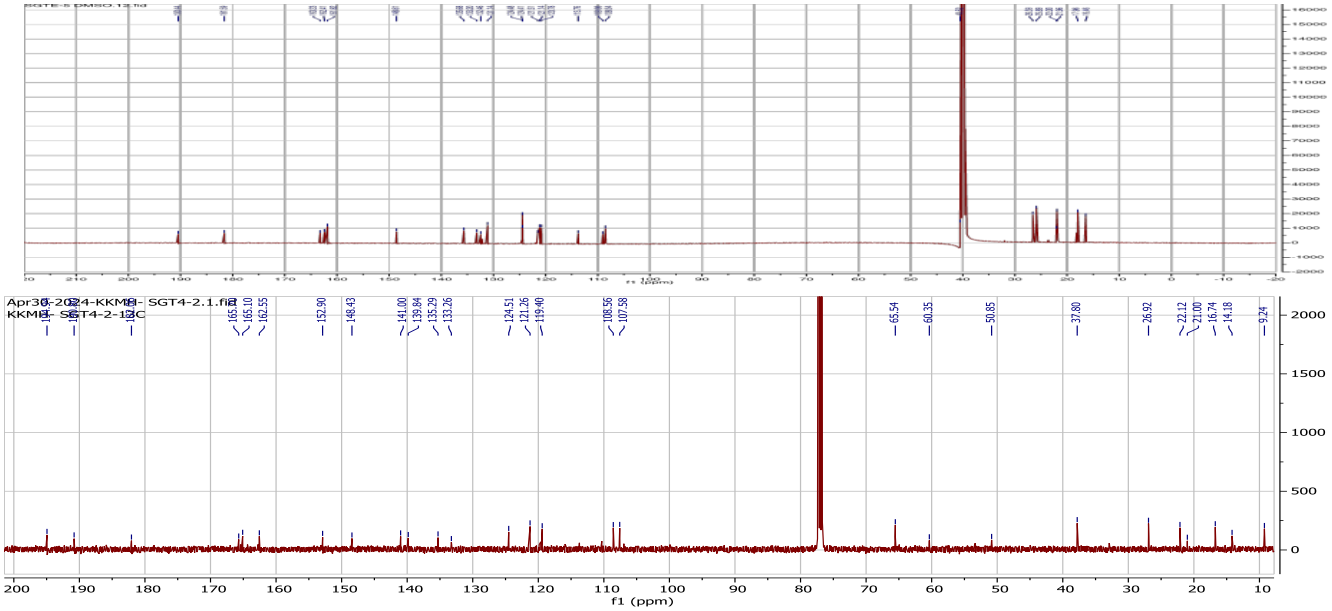

Figure 82: ^{13}C-NMR of compound 225 ($CDCl_3$, 100 MHz) superimposed with that of compound 93

- Characterisation of Compound PG_1P_2

PG_1P_2 was obtained as a yellow solid in Hex/AcoEt 56 % and was soluble in CH_2Cl_2. Its yield was 8.2 %. Analyses of its NMR spectra led to the deduction of the molecular formular, $C_{25}H_{26}O_6$ with 13 degrees of unsaturations.

Its ^{1}H NMR spectrum (Figure 83) shows a singlet of one proton at 4.0 ppm indicative of the formation of an alcohol functional group which is absent from the corresponding spectrum of the starting material PG_1 **(Figure 29)**. The ^{13}C NMR spectrum also shows the presence of an additional signal in the region around 70.0 ppm characteristic of an sp^2 oxygenated carbon atom which is absent from the corresponding spectrum of the starting material PG_1 **(Figure 30)**. All these led us to establish the structure of PG_1P_2 as 1,8-dihydroxy-3-(((2E,6Z)-8-hydroxy-3,7-dimethylocta-2,6-dien-1-yl)oxy)-6-methylanthracene-9,10-dione (**226**) or 3-geranyloxyemodine alcohol (**226**).

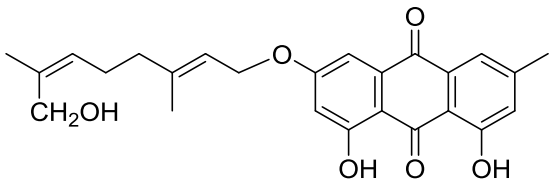

226

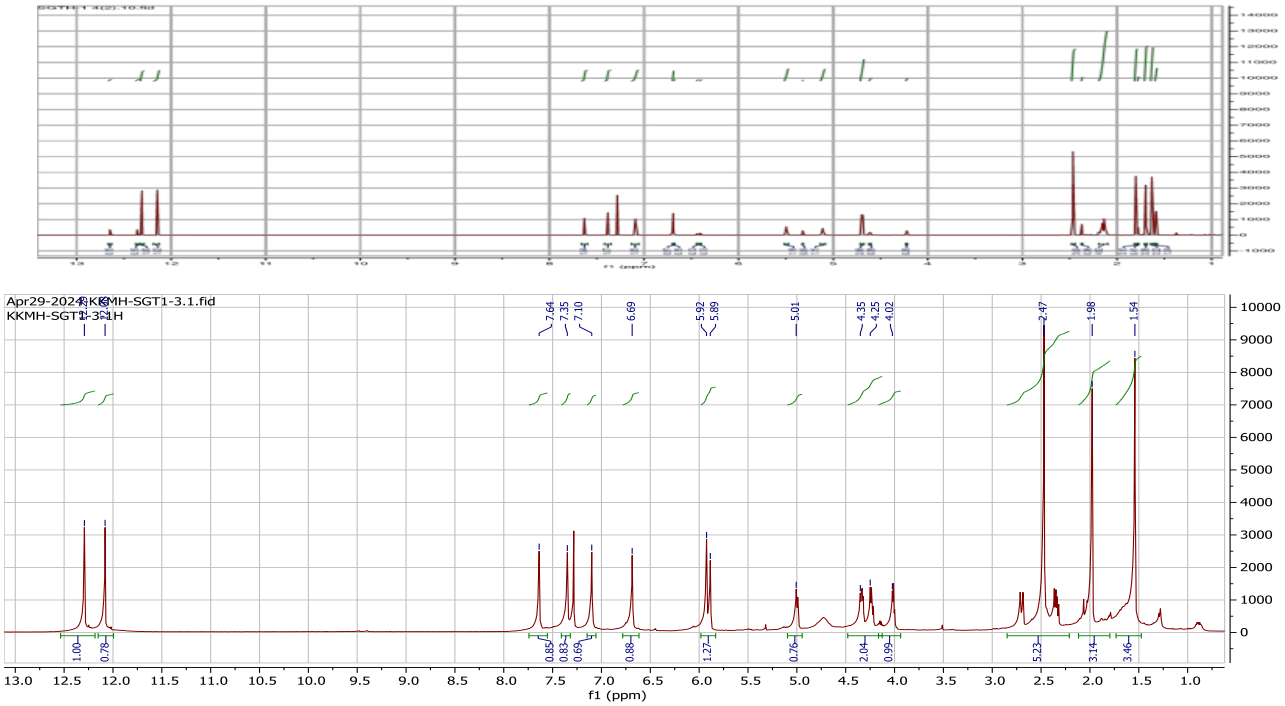

Figure 83: ^{1}H NMR of compound 226 ($CDCl_3$, 400 MHz) superimposed with that of compound 94

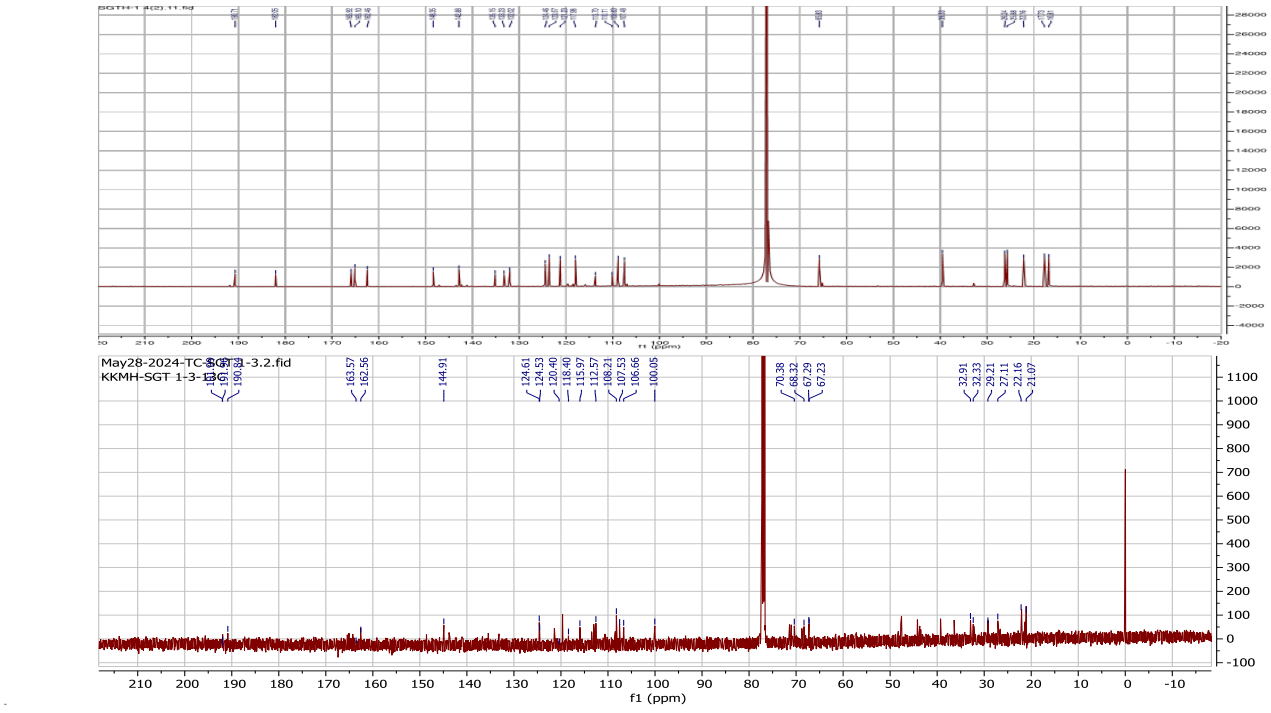

Figure 84: ^{13}C NMR for compound 226 ($CDCl_3$, 100 MHz) superimposed with that of 94

- **Characterisation of PG_4P_2 (227)**

PG_4P_2 was obtained as a yellow solid in Hex/AcoEt 49 % and was soluble in CH_2Cl_2. Its yield was 5.1 %. Analyses of its NMR spectra led to the deduction of the molecular formular, $C_{25}H_{26}O_6$ with 13 degrees of unsaturations.

Its ^1H NMR spectrum (**Figure 85**) shows a singlet of one proton at 4.2 ppm indicative of the presence of an alcohol functional group which is absent from the corresponding spectrum of the starting material PG_4 (**Figure 37**). The ^{13}C NMR spectrum also shows the presence of an additional signal in the region around 70.0 ppm characteristic of an sp^2 oxygenated carbon atom which is absent from the corresponding spectrum of the starting material PG_1 (**Figure 38**). All these led us to establish the structure of $PG4P_2$ as 1,8-dihydroxy-3-(((2E,6Z)-8-hydroxy-3,7-dimethylocta-2,6-dien-1-yl)oxy)-6-methylanthracene-9,10-dione (**227**) or 3-geranyloxyemodine alcohol (**227**).

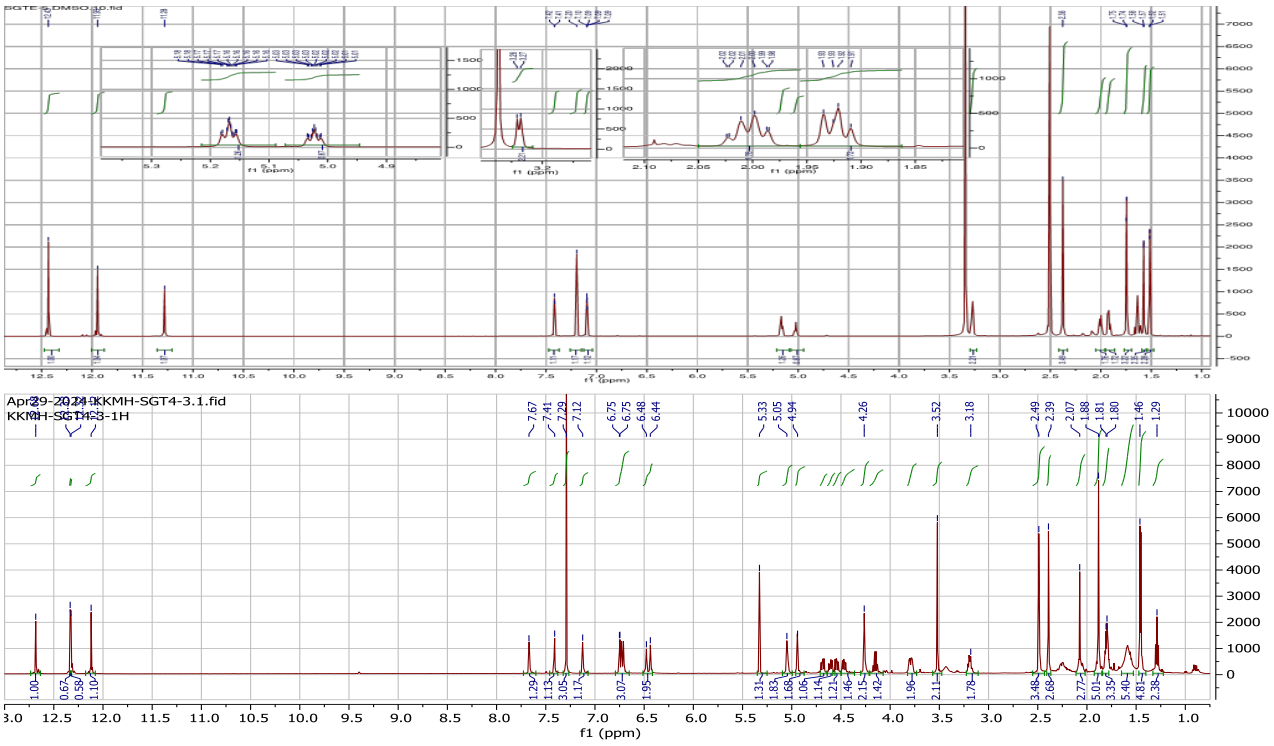

Figure 85: ^1H NMR spectrum of compound 227 ($CDCl_3$, 400 MHz) superimposed with of compound 93

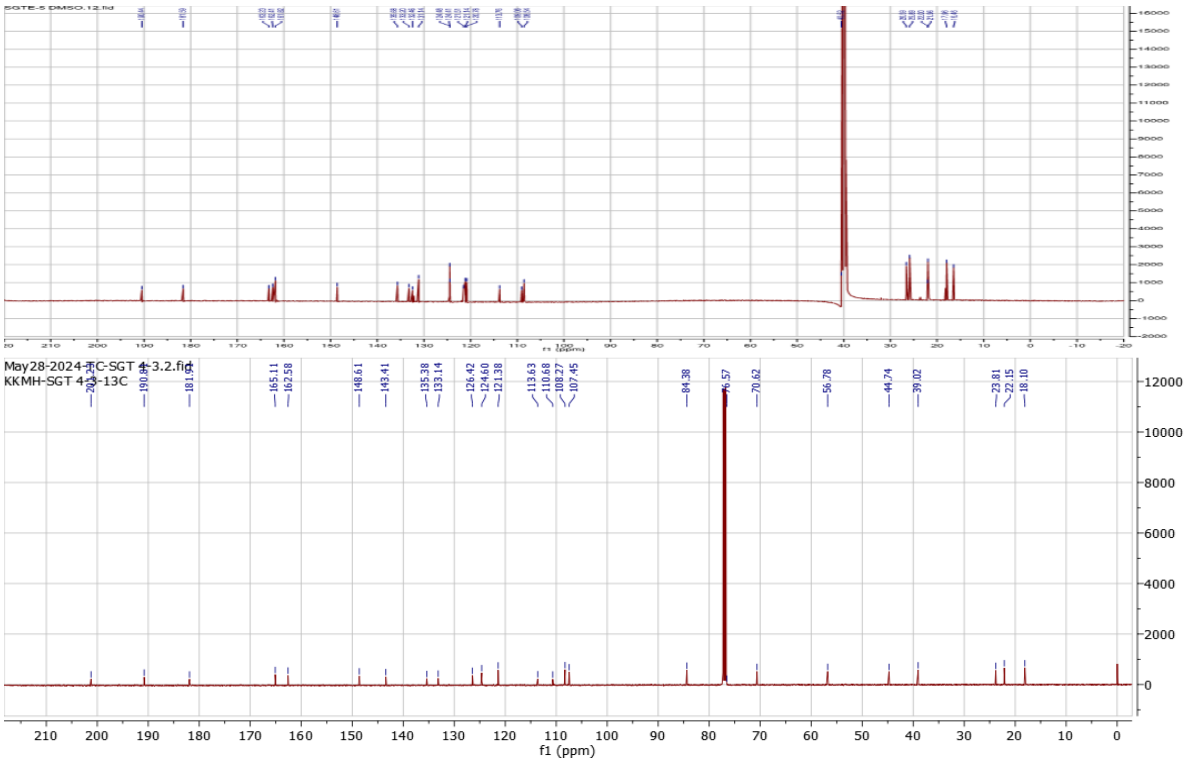

Figure 86: ^{13}C NMR spectrum of compound 227 ($CDCl_3$, 100 MHz) superimposed with that of compound 93

II.4 BIOLOGICAL ACTIVITIES

II.4.1 Triple negative breast cancer activity

The relative viability of the MDA-MB-231 breast cancer cell line exposed to these compounds at multiple concentrations was analyzed to ascertain if any of the isolates exhibited cytotoxic activity. MDA MB 231 cells were plated in a 96-well format. The indicated compounds, dissolved in DMSO, were serially diluted in culture media prior to addition to the culture. After a 3-day incubation time, relative viability was indirectly determined by measuring total ATP in each well using CellTiter-Glo. Following this assay, the IC_{50} value was determined with 95% confidence interval. Several compounds showed moderate cytotoxic activity against MDA-MB-231 breast cancer cells. Compound **55** (ursolic acid) gave the best activity with an IC_{50} of 9.88 µM and 95% CI of 9.03-10.5 µM.

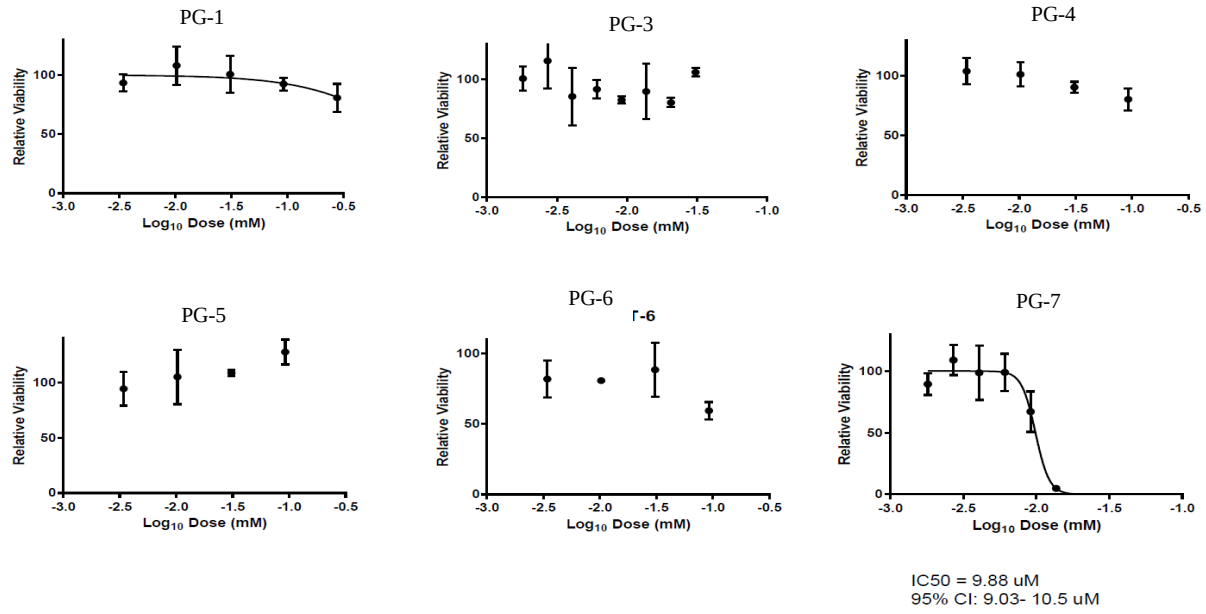

Figure 87: Cytotoxic activity of compounds PG_1 (94) and PG_3-PG_7 (218, 93, 95, 63, and 53)

To ascertain if any of the synthesize compounds also exhibited cytotoxic activity; the relative viability of the MDA-MB-231 breast cancer cell line exposed to triterpenoids at multiple concentrations was assayed **(Dasari *et al.*, 2015)**. The lupeolacetate acryl aldehyde **(223)** was more active than betulin acryl aldehyde **(222)** against the MDA-MB-231 breast cancer cell line, which may be due to greater cell permeability.

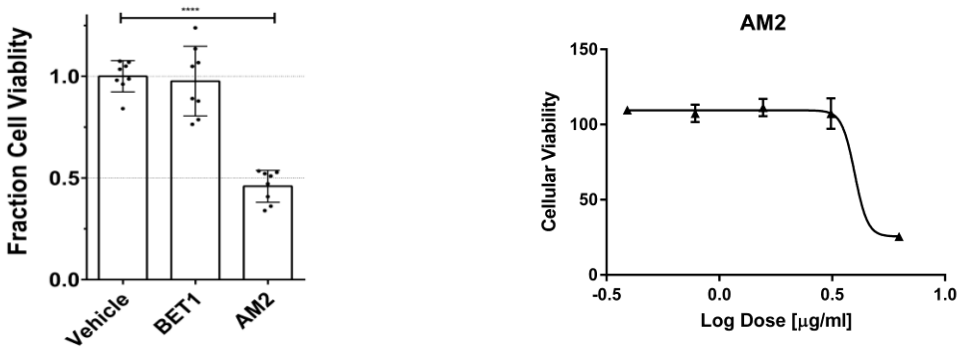

A **b**

Figure 88: Viability (% of DMSO) for compounds 222 (BET_1) and 223 (AM_2)

IC_{50} values for compound 174 on MDA-MB-231 cells: Mean of 4.63µg/ml and Standard Deviation of 0.09 µg/ml.

To determine cell viability, MDA-MB-231 cells were plated in a 96-well format. The indicated compounds, dissolved in DMSO, were serially diluted in culture media prior to addition to the culture.[20] After a 3-day incubation time, relative viability was determined indirectly through the measurement of mitochondrial reductive activity using Cell-Titer Blue

(Figure 89 a). Following this assay, the IC_{50} value was determined with 95% confidence interval **(Figure 89 b**).

II.4.2 Anti-oxidant, lipoxygenase inhibition and urease inhibition activities

To get a deeper insight on the possible mechanism of action, these compounds were tested on some known cancer targets.

The isolated compounds were equally tested for their LOX inhibitory activity, antioxidant activity and urease inhibition activity. The alkaloid scholaricine (**19**) exhibited better lipoxygenase inhibitory activity (IC_{50} = 11.5 ± 0.38 µM) and lipoxygenase inhibitory activity (IC_{50} = 15.2 ± 0.41 µM) compared to the reference drugs; β-hydroxyl acid (BHA) (44.2 ± 0.07 µM) and baicalein (22.6 ± 0.08 µM) respectively. None of the isolated compounds were more active than Thiourea for urease inhibition activity. The rest of the isolated compounds showed moderate activity, as shown in Table 27. All of the isolates exhibited their inhibitory activity in a concentration-dependent manner. Baicalein (IC_{50} = 22.6 ± 0.08 µM). β-hydroxyl acid (BHA) (44.2 ± 0.07 µM) and Thiourea (24.2± 0.09 µM) were used as a positive control.

Table 27: Antioxidant, lipoxygenase inhibition and urease inhibition activities of compounds from the twigs of *Psorospermum guineense* and the leaves of *Alstonia scholaris*

Sr. #	Compound	Antioxidant Activity IC_{50} value (µM)	Lipoxygenase Inhibition Activity IC_{50} value (µM)	Urease Inhibition Activity IC_{50} value (µM)
1.	3-geranyloxyemodin (**94**)	85.6 ± 0.05	98.6 ± 0.36	65.6± 0.17
2.	2-geranylemodin **(93)**	25.7± 0.11	28.7± 0.81	55.1± 0.82
3.	3-geranyloxyemodin anthrone (**220**)	53.4± 0.29	76.6± 0.93	52.1± 0.71
4.	Acetylvismione D **(95)**	35.6± 0.86	38.9± 0.25	44.8± 0.16
5.	3-β-fridelanol **(219)**	20.8± 0.15	19.8± 0.16	38.9± 0.18
6.	Betulinic acid (**63**)	78.8± 0.79	91.1± 0.77	66.5± 0.22
7.	Ursolic acid (**53**)	79.7± 0.57	87.7± 0.10	81.6± 0.30
8.	Betulin **(62)**	45.4 ± 0.41	65.2 ± 0.29	**29.5 ± 0.91**
9.	α-amyrin acetate (**54**)	42.2 ± 0.29	68.8 ± 0.15	32.7 ± 0.28
10.	Mixture of β-sitosterol and stigmasterol (**128** &**129**)	51.2 ± 0.42	62.5 ± 0.69	35.2 ± 0.18
12.	Tetratriacontyl-*trans-p*-coumarate (**216**)	22.4 ±0.82	32.4 ± 0.21	62.4 ± 0.22
13.	β-sitosterol glucoside (**218**)	25.5 ± 0.61	18.5 ± 0.14	45.2 ± 0.35
14.	Picralstonine (**217**)	38.5 ± 0.96	25.4 ± 0.26	49.5 ± 0.47
15.	Scholaricine **(19)**	**11.5 ± 0.38**	**15.2 ± 0.41**	>100
16.	BHA	44.2 ± 0.07	-	
17.	Baicalein[b]	-	22.6 ± 0.08	
18.	Thiourea			24.2± 0.09

[a] Values are the mean ± SEM of three experiments ($p < 0.05$) ; [b] Positive control.

We shall now look at the results of the molecular docking which was carried out.

II.5 MOLECULAR DOCKING

II.5.1 Molecular docking of some compounds from *Alstonia scholaris*

To explore the activities of the present compounds and binding interactions between ligands and lipoxygenase, the structures of some compounds isolated from ***Alstonia scholaris*** (Ursolic acid (**53**), Betulin **(61),** α-amyrin acetate (**54**), β-sitosterol glucoside (**218**), picralstonine (**217**) and scholaricine **(19))**, were docked into the active site of LOX (PDB code: 1HU9). Some significant results of the *in silico* studies are summarized in Table 28. The experimental IC_{50} values of isolates revealed that the better result was obtained for compounds **(19)** and β-sitosterol glucoside (**218**). This is in agreement with the estimated free energies of binding of tested compounds (Table 28). Docking analysis showed that of all the isolates, compounds scholaricine **(19)** and β-sitosterol glucoside (**218**) formed the most stable complexes with the enzyme's active site indicated by their low binding energies (ΔG Binding = + 13.38 and + 0.86 kcal/mol, respectively). These results were in agreement with the experimental IC_{50} values of the isolates summarized in table 30. Docking studies indicated that only the two alkaloid compounds scholaricine **(19)** and β-sitosterol glucoside (**218**) formed hydrogen bonds with the active site residues (through the amine hydrogen atom). In as much as compound β-sitosterol glucoside (**218**) formed a hydrogen bond with histidine 518 (HIS 518) it also forms 3 unfavorable bumps with the active site of 1HU9 **(Fig. 91)**. This can explain why the complex formed with compound β-sitosterol glucoside (**218**) is more stable than that formed with compound (**218**). The estimated free energies of binding for tested molecules could confirm the experimental results. The standard anti lipoxygenase drug-baicalein formed two hydrogen bonds with the enzyme's active site, with a very low binding energy but exhibited moderate *in vitro* inhibitory activity. The analyses also showed that compound **(19)** formed a hydrogen bond with glutamine 514 (GLN 514) in the active site of LOX **(Figure 90)**.

Table 28: Summary of the important docking results of compounds from *Alstonia scholaris*. The H-bond distances have been measured between related atoms

Compound	Estimated $\Delta G_{Binding}$ (kcal/mol)	Hydrogen bonding		
		Interacted ligand functional group	Interacted amino acid	Distance (Å)
Betulin **(62)**	+ 96.16	-	-	-
α-amyrin acetate **(54)**	+ 145.73	-	-	-
Ursolic acid **(53)**	+ 95.54	-	-	-
Picralstonine **(217)**	+ 66.85	NH	HIS 518	2.121
β-sitosterol glucoside **(218)**	+ 13.38	-	-	-
Scholaricine **(19)**	+ 0.86	NH	GLN 514	2.226
Baicalein	-5.74	-	-	-

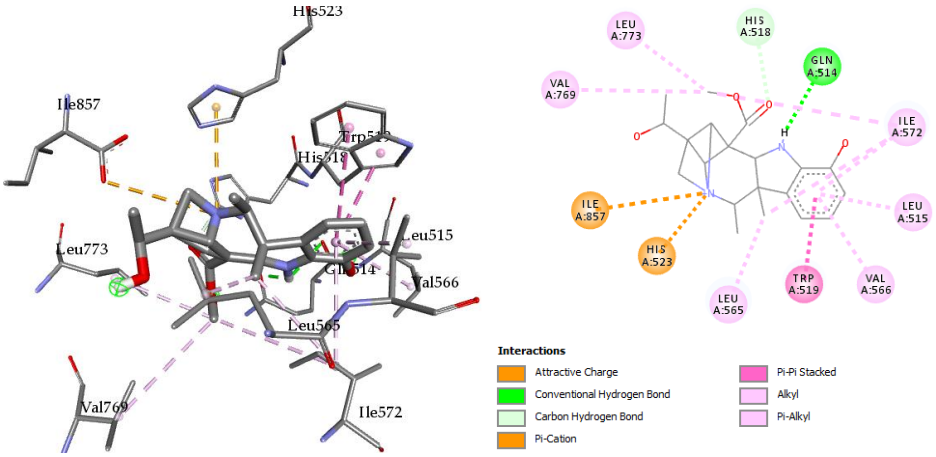

Figure 89: Interactions between scholaricine (19) and the active site of the 1HU9

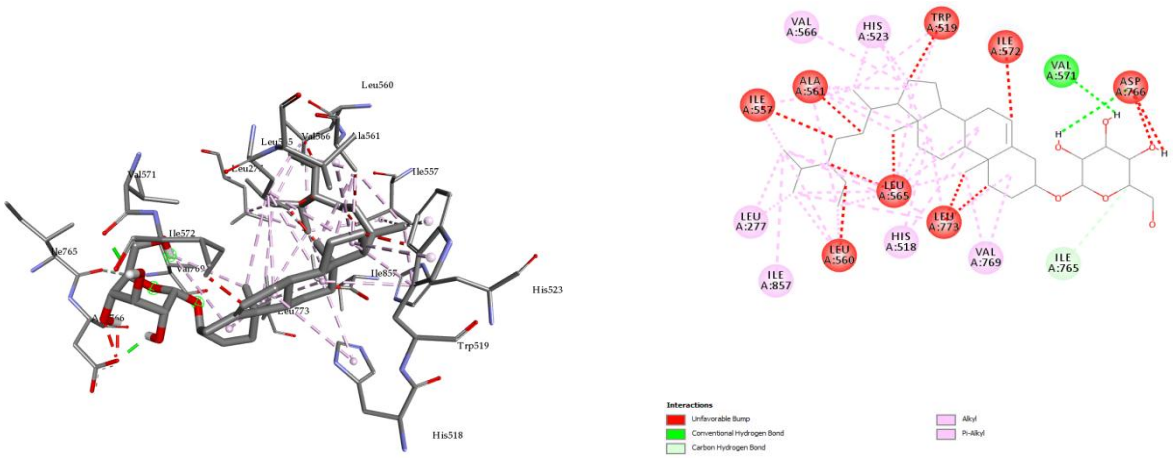

Figure 90: Interactions between β-sitosterol glucoside (218) and the active site of the 1HU9

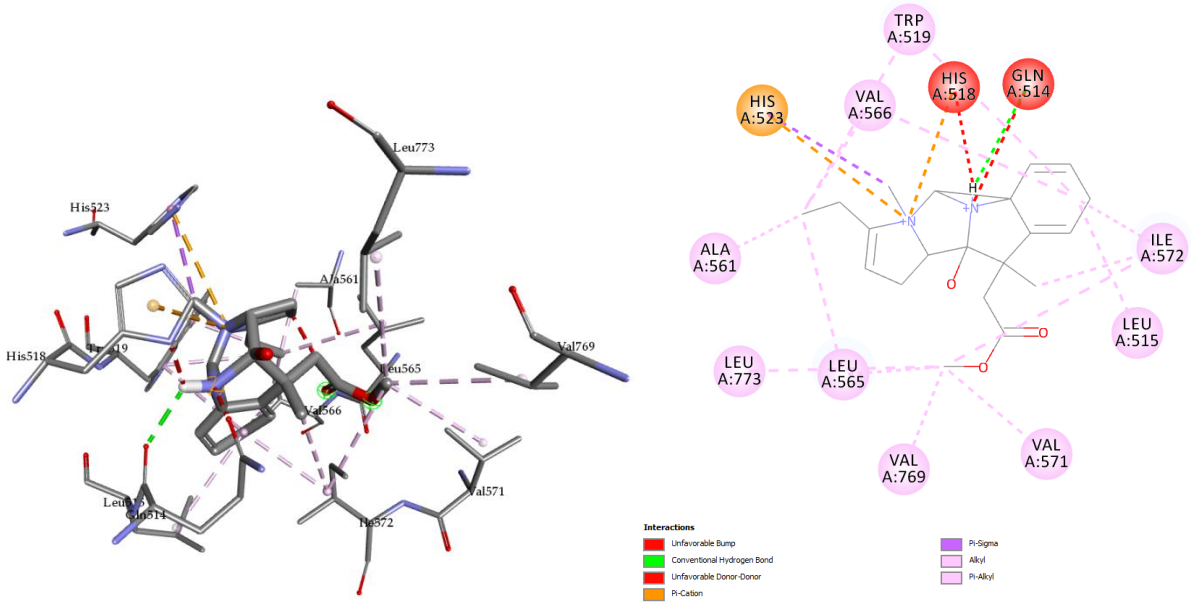

Figure 91: Interactions between picralstonine (217) and the active site of the 1HU9

II.5.2 Molecular docking of some compounds from *Psorospermum guineense*

Some significant results of the *in silico* studies on the compounds from *Psorospermum guineense* are summarized in Table 29. The experimental IC_{50} values of isolates from *Psorospermum guineense* (3-geranyloxyemodin (**94**), 2-geranylemodin **(93)**, 3-geranyloxyemodin anthrone (**220**), Acetylvismione D **(95)**, 3-β-fridelanol **(219),** Betulinic acid (**63**) and Ursolic acid (**53**)) revealed that the better LOX result was obtained for acetylvismione D (Table 29). This is in agreement with the estimated free energies of binding of acetylvismione D and Baicalein (Table 29). Docking analysis showed that, acetylvismione D created conventional H-bonding, carbon-H bond, Pi-Pi T-shape, alkyl and Pi-alkyl interactions with amino acids in the active site of LOX **(Figure 94)** and had lowest binding affinity (ΔG Binding = -8.14 kcal/mol). Also, docking studies indicated that Baicalein had no carbon-H bond but Van der Waals, conventional H-bonding, Pi-donor H-bond, Pi-Lone Pair, Pi-Pi T-shaped, Amide Pi-stacked and Pi-alkyl interactions with amino acids of the active site residues of LOX **(Figure 93)** and had higher binding affinity (ΔG Binding = - 7.81 kcal/mol).

Table 29: Summarizing the important docking results of compounds from *Psorospermum guineense*. The H-bond distances have been measured between related atoms

Compound	Estimated $\Delta G_{Binding}$ (kcal/mol)	Hydrogen bonding		
		Interacted ligand functional group	Interacted amino acid	Distance (Å)
3-geranyloxyemodin **(219)**	- 7.81	C=O	ALA 672	2.76
2-geranylemodin **(222)**	- 8.76	OH C=O	ALA 672 GLN 557	2.03 2.74
3-geranyloxyemodin anthrone **(220)**		C=O	PHE 177	2.68
Acetylvismione D **(95)**	- 8.14	O	PHE 177	2.67
3-β-fridelanol **(219)**	- 9.02	OH	ASN 554	1.81
Betulinic acid **(63)**	- 9.17	OH	ASN 554	2.27
Ursolic acid **(53)**	- 9.79	COOH OH	PHE 177 ASN 554	2.63 1.89
Baicalein	- 7.81	OH	VAL 671 ALA 672	1.95 2.00

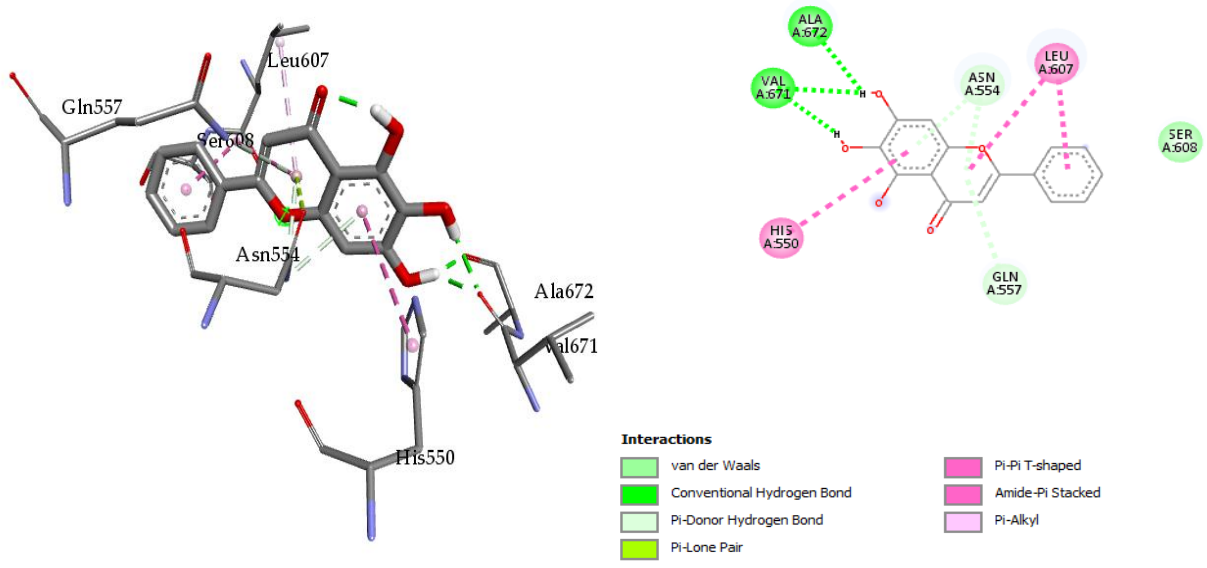

Figure 92: Interactions between Baicalein and the active site of the 3V99

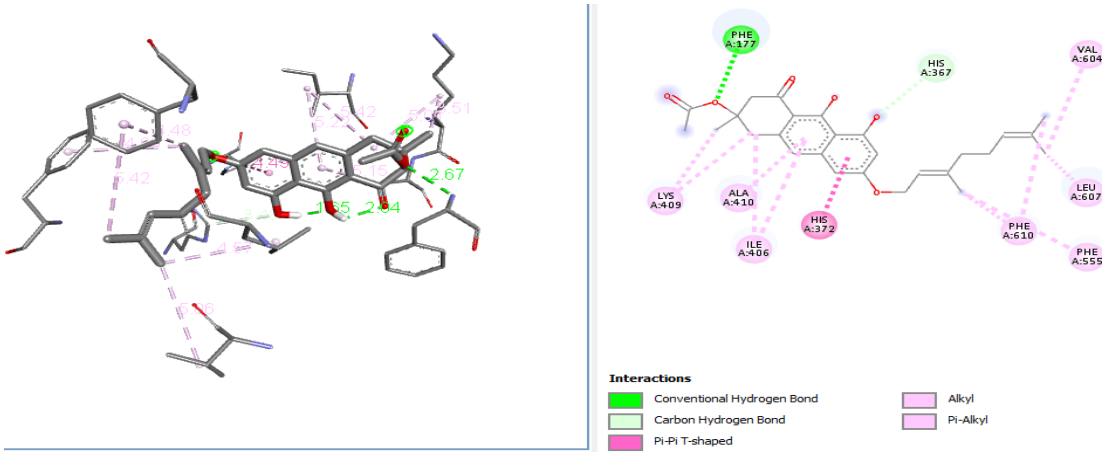

Figure 93: Interactions between Acetylvismione D and the active site of the 3V99

CONCLUSION AND PERSPECTIVES

In our attempts to isolate natural products for drug discovery and development from a rational viewpoint, the cancer disease, its mode of inhibition (antioxidant) or possible targets (lipoxygenase or urease) were evaluated. Bioactive constituents have been isolated from the twigs of *Psorospermum guineense* and the leaves of *Alstonia scholaris*. Eight (8) compounds were isolated from the twigs of *Psorospermum* 3-geranyloxyemodin, 3-β-fridelanol, 3-geranyloxyemodin anthrone, 2- geranylemodin, acetylvismione D, betulinic acid, ursolic acid and emodin and nine (9) compounds were isolated from the leaves of *Alstonia scholaris* betulin, α-amyrin acetate, mixture of β-sitosterol and stigmasterol, tetratriacontyl-trans-*p*-coumarate, ursolic acid, β-sitosterol glucoside, picralstonine and scholaricine. The stereochemistry and conformation of the geranyl sub unit of PG_1 (3-geranyloxyemodin**)** were established from single crystal x-ray analysis.

To introduce privilege medicinal scaffold, five (05) of these compounds (3-geranyloxyemodin, 2- geranylemodin, betulin, α-amyrin acetate and ursolic acid were subjected to SeO_2 oxidation. Betulin afforded Betulin acrylaldehyde while α-amyrin acetate afforded lupeolacetate acryl aldehyde in an intriguing mechanism with the conversion of ursane to lupane scaffold. Betulin and α-amyrin acetate under SeO2 conditions afforded new acrylaldehyde derivatives.

The structures of these compounds were determined by interpretation of theirUV, IR, MS (ESI-MS, EI-MS, LCMS), 1D (^1H, ^{13}C, DEPT) and 2D (HSQC, HMBC, ^1H -^1H COSY) NMR data and in some cases by comparison of their data with those reported in the literature or by comparative TLC with available authentic samples.

Preliminary cytotoxicity assays against the triple negative (MDA-MB-231) breast cancer cell indicated that Ursolic acid **(53)** was the most active amongst the isolated compounds, with an IC_{50} value of 9.88 µM and 95% CI of 9.03-10.5 µM. On the other hand, the transformed compound **175** with the privilege αβ-unsaturated carbonyl scaffold showed an increase in activity against MDA MB 231 breast cancer cell line with an IC_{50} of 4.63 ± 0.09 µg/ml. To determine possible mode of action for these compounds, they were screened on some cancer targets. Acetylvismione D **(95)** exhibited best antioxidant activity (20.8 ± 0.15 µM), scholaricine exhibited best lipoxygenase inhibitory activity (15.2 ± 0.41 µM) which were all better compared to the reference drugs Beta hydroxyl acid (BHA) (44.2 ± 0.07 µM) and baicalein (22.6 ± 0.08 µM) respectively. Betulin gave the best urease inhibition activity (29.5 ± 0.91 µM) whose IC_{50} value was slightly higher than that of the reference compound

used thiourea (24.2± 0.09 µM). To know the type of interactions that were between the enzyme lipoxygenase and the compounds tested for lipoxygenase inhibition activity, molecular docking studies were conducted and we observed conventional H-bonding, carbon-H bond, Pi-Pi stacked, alkyl and Pi-alkyl interactions between enzyme and substrate. Also, the molecular docking analysis predicted the potential of the studied compounds for future drug discovery investigations.

In perspective, we envisage to:

- Study the anti-breast cancer, anti-oxidant and enzyme (lipoxygenase and urease) inhibition activities of the hemi-synthesized quinone derivatives.
- Carry out quantitative structure activity relationship (QSAR) and kinetic studies to understand the inhibitory mechanism of corresponding compounds and relative derivatives.
- Carry out molecular docking studies of the hemi-sythesised derivatives.

CHAPTER III: INSTRUMENTALISATION AND PLANT MATERIAL

III.1 GENERAL EXPERIMENTAL PROCEDURE

1D (1H, 13C and DEPT) and 2D (COSY, HSQC and HMBC) NMR spectra were recorded on a Bruker Ascend 400, 500, 600, (1H 400, 500, 600 MHz and 13C 100, 152, 150 MHz) NMR spectrometer equipped with a 5 mm cryoprobe. 1H NMR chemical shifts are reported as δ values in ppm relative to CD3OD (4.87 and 3.31 ppm), C3D6O (2.05 ppm), CDCl3 (7.26 ppm), coupling constants (J) are reported in Hertz (Hz), and diversity follows convention. Unless indicated otherwise, CD3OD (49.1 ppm), C3D6O (206.7 and 29.9 ppm), CDCl3 (77.2 ppm) served as an internal standard for all 13C spectra. The chemical shifts are quoted relative to TMS. X-ray data were recorded on a Bruker400 Machine. HR-ESI-TOF-MS data were acquired on a Thermo LTQ Orbitrap mass spectrometer. The melting points were measured using a BUCHI SMP-20 instrument (maximum 300 ^{o}C). The Masses of the samples and compounds were measured using an electronic balance of mark SARTORIUS and of type 1265OO1. Column chromatography was carried out with silica gel Kiesegel 60; 70–230 mesh). TLC was carried out on pre-coated silica-gel F254 aluminum sheets (0.25 mm thickness). These plates were eluted with diverse solvents and upon their migration, the chromatograms were examined under UV at 254 and 366 nm and subsequently with iodine vapour and in some cases, the spots were detected by heating the cards after spraying with cerium (IV) sulfate reagent. Cytotoxicity was determined through cells plated in 96-well plates (Nest Scientific) at a density of 2000 cells per well in 100 μL of media per well. The free radical scavenging (antioxidant) activity was measured using 1, 1-diphenyl-2-picryl-hydrazine (DPPH). A spectrophotometer (Spectra Max, Molecular Devices, CA, USA) was used to measure enzyme inhibition. The AutoDockTools was used to prepare the ligand and receptor structures for molecular docking.

III.2 PLANT MATERIAL

Psorospermum guineense twigs were harvested from Limbo, a small locality between Wainamah and Ndop plane in the North West Region of Cameroon, (September, 2016) by a botanist Dr. Tacham Walters, of the University of Bamenda and a voucher specimen deposited at the Cameroon National Herbarium (HNC), (14432/SRFCam). The twigs collected, were cut into small pieces, dried at room temperature and powdered.

The leaves of *Alstonia scholaris* were harvested in May 2017 from the University of Karachi campus. The plant was identified by the Plant Taxonomist of the Department of Botany, University of Karachi, Pakistan, where a voucher specimen (No. G.H-94482) has been deposited in the Karachi Herbarium in Pakistan.

III.3 EXTRACTION

III.3.1 Extraction of twigs of *Psorospermum guineense*

Powdered twigs (1.5 kilograms) of *Psorospermum guineense* were extracted by sonication in MeOH/CH_2Cl_2 (1:1 v/v) at room temperature. The filtrates were concentrated on a rotary evaporator under reduce pressure to yield 300 g of crude extract. A portion of the crude extract (150 g) was subjected to fractionation using hexanes, EtOAc and n-BuOH to afford hexane (30g), EtOAc (25g) and n-BuOH (20g) fractions. The LCMS analyses of the various fractions indicated that the hexane and EtOAc fractions were rich in secondary metabolites.

III.3.2 Extraction of leaves of *Alstonia scholaris*

The air-dried and powdered leaves of *A. scholaris* (25 Kg) were successively extracted with ethanol (3 × 20 L × 120 h) by maceration at room temperature. The extract was concentrated *in vacuo* to obtain 637 g of dark coloured ethanol extract. To it was added 500 mL of water, acidified with 20.5 mL of 1.5 N H_2SO_4 and extracted with CH_2Cl_2. The organic phase was concentrated to afford 260 g of the non-alkaloid fraction. The aqueous phase was basified with 500 mL of 3 N Na_2CO_3 to release the alkaloids which were then extracted with CH_2Cl_2. Concentration of the resulting organic phase afforded 9.33g of the alkaloidal fraction, while the aqueous fraction upon treatment with n-butanol afforded 40 g of the n-butanol fraction.

III.4 COLUMN CHROMATOGRAPHY OF PLANT EXTRACTS

III.4.1 Column chromatography of *Psorospermum guineense* twigs extract

III.4.1.1 Column chromatography of hexane fraction of *Psorospermum guineense* twigs

The hexane fraction of *P. guineense* twigs (30 g) was fixed with about 30g of silica gel. As eluents we had; hexane, hexane-EtOAc, EtOAc, EtOAc-MeOH and MeOH in increasing polarity. The elutions were collected in volumes of 100 mL and the solvent recovered using the rotary evaporator and combined based on TLC profiles as shown in Table 30 below.

Table 30: Chromatogram of the hexane fraction of *Psorospermum guineense* twigs

Eluent	Fraction	TLC	Observation	Series
Hexane 100 %	1-5	Hexane 100 %	Oily spot	
Hex/EtOAc 1 %	6-10	Hex/EtOAc 1%	2 spots	F1
Hex/EtOAc 2 %	11-15	Hex/EtOAc 2 %	2 spots	
Hex/EtOAc 3 %	16-20	Hex/EtOAc 3 %	2 spots	
Hex/EtOAc 4 %	21-25	Hex/EtOAc 4 %	1 spot: PG_1	F2
Hex/EtOAc 5 %	26-30	Hex/EtOAc 5 %	1 spot: PG_2	F3
Hex/EtOAc 6 %	31-35	Hex/EtOAc 6 %	1 spot: PG_3	F4
Hex/EtOAc 7 %	36-40	Hex/EtOAc 7 %	1 spot: PG_4	F5
Hex/EtOAc 8 %	41-45	Hex/EtOAc 8 %	2 spots	F6
Hex/EtOAc 9 %	46-50	Hex/EtOAc 9 %	2 spots	
Hex/EtOAc 10 %	51-55	Hex/EtOAc 10 %	3 spots	F7
Hex/EtOAc 12.5 %	56-60	Hex/EtOAc 12.5 %	3 spots	
Hex/EtOAc 15 %	61-65	Hex/EtOAc 15 %	3 spots	
Hex/EtOAc 17.5 %	66-70	Hex/EtOAc 17.5 %	3 spots	
Hex/EtOAc 22.2 %	71-75	Hex/EtOAc 22.2 %	3 spots	
Hex/EtOAc 25 %	76-80	Hex/EtOAc 25 %	3 spots	
Hex/EtOAc 27.5 %	81-85	Hex/EtOAc 27 %	3 spots	
Hex/EtOAc 30 %	86-90	Hex/EtOAc 30 %	3 spots	
Hex/EtOAc 35 %	91-95	Hex/EtOAc 35 %	2 -3 spots	F8

Hex/EtOAc 40 %	96-100	Hex/EtOAc 40 %	2 -3 spots	
Hex/EtOAc 45 %	101-105	Hex/EtOAc 45 %	2 spots	F9
Hex/EtOAc 50 %	106-110	Hex/EtOAc 50 %	2 spots	
Hex/EtOAc 60 %	111-115	DCM/MeOH 2 %	2 spots	
Hex/EtOAc 70 %	116-120	DCM/MeOH 4 %	2 spots	
Hex/EtOAc 80 %	121-125	DCM/MeOH 6 %	3 spots	F10
Hex/EtOAc 90 %	126-130	DCM/MeOH 8 %	3 spots	
EtOAc 100 %	131-135	DCM/MeOH 10 % plus some drops of acetic acid	3 spots	F11
EtOAc/MeOH 10 %	136-140	DCM/MeOH 10 % plus some drops of acetic acid	3 spots	
EtOAc/MeOH 25 %	141-145	DCM/MeOH 10 % plus some drops of acetic acid	4 spots	F12
MeOH 100 %	146-150	DCM/MeOH 10 % plus some drops of acetic acid	5 spots	F13

- **Treatment of series F2, F3, F4 and F5 to obtain the pure compounds PG_1, PG_2, PG_3 and PG_4**

- Treatment of Series F2

F2 (fractions 21-25) crystallised from hexane and was filtered to afford PG_1 (100 mg).

- Treatment of Series F3

F3 (fractions 26-30) crystallised from hexane and was filtered to afford PG_2 (10 mg).

- Treatment of Series F4

F4 (fractions 31-35) crystallised from hexane and was filtered to afford PG_3 (100 mg).

- Treatment of Series F5

F5 (fractions 36-40) crystallised from hexane and was filtered to afford PG_4 (75 mg).

III.4.1.2 Column chromatography of EtOAc fraction of *Psorospermum guineense* twigs

The EtOAc fraction of ***Psorospermum guineense*** twigs (25 g) was fixed with about 25 g of silica gel. As eluents we had; hexane, hexane-EtOAc, EtOAc, EtOAc-MeOH and MeOH in increasing polarity. The elutions were collected in volumes of 100 mL and the solvent recovered using the rotary evaporator and combined based on TLC profiles as shown in Table 31 below.

Table 31: Chromatogram of the EtOAc fraction of *Psorospermum guineense* twigs

Eluent	Fraction	TLC	Observation	Series
Hexane 100 %	1-5	Hexane 100 %	0 spot	
Hex/EtOAc 1%	6-10	Hex/EtOAc 1%	0 spot	
Hex/EtOAc 2 %	11-15	Hex/EtOAc 2 %	2 spots	F1
Hex/EtOAc 3 %	16-20	Hex/EtOAc 3 %	2 spots	
Hex/EtOAc 4 %	21-25	Hex/EtOAc 4 %	1 spot: PG_1	F2
Hex/EtOAc 5 %	26-30	Hex/EtOAc 5 %	2 spots	F3
Hex/EtOAc 6 %	31-35	Hex/EtOAc 6 %	1 spot: PG_3	F4
Hex/EtOAc 7 %	36-40	Hex/EtOAc 7 %	1 spot: PG_4	F5
Hex/EtOAc 8 %	41-45	Hex/EtOAc 8 %	2 spots	F6
Hex/EtOAc 9 %	46-50	Hex/EtOAc 9 %	2 spots	
Hex/EtOAc 10 %	51-55	Hex/EtOAc 10 %	2 spots	
Hex/EtOAc 12.5 %	56-60	Hex/EtOAc 12.5 %	2 spots	
Hex/EtOAc 15 %	61-65	Hex/EtOAc 15 %	1 spot: PG_5	F7
Hex/EtOAc 17.5 %	66-70	Hex/EtOAc 17.5 %	2 spots	F8
Hex/EtOAc 20 %	71-75	Hex/EtOAc 20 %	2 spots	
Hex/EtOAc 22.5 %	76-80	Hex/EtOAc 22.5 %	2 spots	
Hex/EtOAc 25 %	81-85	Hex/EtOAc 25 %	1 spot: PG_6	F9
Hex/EtOAc 27 %	86-90	Hex/EtOAc 27 %	1 spot: PG_6	
Hex/EtOAc 30 %	91-95	Hex/EtOAc 30 %	2 spots	F10
Hex/EtOAc 35 %	96-100	Hex/EtOAc 35 %	2 spots	
Hex/EtOAc 40 %	101-105	Hex/EtOAc 40 %	1 spot: PG_7	F12
Hex/EtOAc 45 %	106-110	Hex/EtOAc 45 %	1 spot: PG_7	
Hex/EtOAc 50 %	111-115	Hex/EtOAc 50 %	1 spot: PG_7	

Hex/EtOAc 60 %	116-120	DCM/MeOH 2 %	1 spot: PG_7	
Hex/EtOAc 70 %	121-125	DCM/MeOH 4 %	2 spots	F13
Hex/EtOAc 80 %	126-130	DCM/MeOH 6 %	2 spots	
Hex/EtOAc 90 %	131-135	DCM/MeOH 8 %	3 spots	F14
EtOAc 100 %	136-140	DCM/MeOH 10 % plus some drops of acetic acid	3 spots	
EtOAc/MeOH 10 %	141-145	DCM/MeOH 10 % plus some drops of acetic acid	3 spots	
EtOAc/MeOH 25 %	146-150	DCM/MeOH 10 % plus some drops of acetic acid	4 spots	F16
MeOH 100 %	151-155	DCM/MeOH 10 % plus some drops of acetic acid	5 spots	F17

- **Treatment of series F2, F4, F5, F7, F9 and F12 to obtain the pure compounds PG_1, PG_3, PG_4, PG_5, PG_6, and PG_7**

- Treatment of Series F2

F2 (fractions 21-25) crystallised from hexane and was filtered to afford PG_1 (200 mg).

- Treatment of Series F4

F4 (fractions 31-35) crystallised from hexane and was filtered to afford PG_3 (200 mg).

- Treatment of Series F5

F5 (fractions 36-40) crystallised from hexane and was filtered to afford PG_4 (150 mg).

- Treatment of Series F7

F9 (fractions 61-65) crystallised from hexane and was filtered to afford PG_5 (25 mg).

- Treatment of Series F9

F9 (fractions 81-90) crystallised from hexane and was filtered to afford PG_6 (250 mg).

- Treatment of Series F12

F12 (fractions 101-120) crystallised from hexane and was filtered to afford PG_7 (250 mg).

III.4.1.3 Column chromatography of n-Butanol fraction of *Psorospermum guineense* twigs

The n-Butanol fraction of ***Psorospermum guineense*** twigs (20 g) was fixed with about 20 g of silica gel. As eluents we had; hexane, hexane-EtOAc, EtOAc, EtOAc-MeOH and MeOH in increasing polarity. The elutions were collected in volumes of 100 mL and the solvent recovered using the rotary evaporator and combined based on TLC profiles as shown in Table 32 below.

Table 32: Table of elution of 20 g of the n-Butanol fraction of *Psorospermum guineense* twigs

Eluent	Fraction	TLC	Observation	Series
Hexane 100 %	1-5	Hexane 100 %	0 spot	
Hex/EtOAc 1%	6-10	Hex/EtOAc 1%	2 spots	F1
Hex/EtOAc 2 %	11-15	Hex/EtOAc 2 %	3 spots	F2
Hex/EtOAc 3 %	16-20	Hex/EtOAc 3 %	3 spots	
Hex/EtOAc 4 %	21-25	Hex/EtOAc 4 %	3 spots	
Hex/EtOAc 5 %	26-30	Hex/EtOAc 5 %	3 spots	
Hex/EtOAc 6 %	31-35	Hex/EtOAc 6 %	3 spots	
Hex/EtOAc 7 %	36-40	Hex/EtOAc 7 %	3 spots	
Hex/EtOAc 8 %	41-45	Hex/EtOAc 8 %	3 spots	
Hex/EtOAc 9 %	46-50	Hex/EtOAc 9 %	3 spots	
Hex/EtOAc 10 %	51-55	Hex/EtOAc 10 %	2 spots	F3
Hex/EtOAc 12.5 %	56-60	Hex/EtOAc 12.5 %	2 spots	
Hex/EtOAc 15 %	61-65	Hex/EtOAc 15 %	2 spots	
Hex/EtOAc 17.5 %	66-70	Hex/EtOAc 17.5 %	2 spots	
Hex/EtOAc 20 %	71-75	Hex/EtOAc 20 %	1 spot: PG_8 orange precipitate	F4
Hex/EtOAc 22.5 %	76-80	Hex/EtOAc 22.5 %	2 spots	F5
Hex/EtOAc 25 %	81-85	Hex/EtOAc 25 %	3 spots	F6
Hex/EtOAc 27 %	86-90	Hex/EtOAc 27 %	3 spots	
Hex/EtOAc 30 %	91-95	Hex/EtOAc 30 %	2 spots	F7
Hex/EtOAc 35 %	96-100	Hex/EtOAc 35 %	2 spots	

Hex/EtOAc 40 %	101-105	Hex/EtOAc 40 %	2 spots	
Hex/EtOAc 45 %	106-110	Hex/EtOAc 45 %	3 spots	F8
Hex/EtOAc 50 %	111-115	Hex/EtOAc 50 %	2 spots	F9
Hex/EtOAc 60 %	116-120	DCM/MeOH 2 %	2 spots	
Hex/EtOAc 70 %	121-125	DCM/MeOH 4 %	3 spots	F10
Hex/EtOAc 80 %	126-130	DCM/MeOH 6 %	3 spots	
Hex/EtOAc 90 %	131-135	DCM/MeOH 8 %	3 spots	
EtOAc 100 %	136-140	DCM/MeOH 10 % plus some drops of acetic acid	3 spots	
EtOAc/MeOH 10 %	141-145	DCM/MeOH 10 % plus some drops of acetic acid	4 spots	F11
EtOAc/MeOH 25 %	146-150	DCM/MeOH 10 % plus some drops of acetic acid	4 spots	
MeOH 100 %	151-155	DCM/MeOH 10 % plus some drops of acetic acid	5 spots	F12

- **Treatment of series F4 to obtain the pure compound PG_8**

- Treatment of Series F4

F4 (fractions 71-75) crystallised from hexane and was filtered to afford PG_8 (100 mg).

III.4.2 Column chromatography of the leaves of *Alstonia scholaris* extract

The non-alkaloid fraction of the leaves of *Alstonia scholaris* (260 g) was fixed with about 260 g of silica gel. As eluents we had; hexane, hexane-EtOAc, EtOAc, EtOAc-MeOH and MeOH in increasing polarity. The elutions were collected in volumes of 500 mL and the solvent recovered using the rotary evaporator and combined based on TLC profiles as shown in Table 33 below.

Table 33: Chromatogram of the non-alkaloid fraction of leaves of *Alstonia scholaris*

Eluent	Fraction	TLC	Observation	Series
Hex 100 %	1-25	Hex 100 %	1-3 0 spots 4 white oil 5-21 red oil	 F1 F2

			22-25 whitish yellow oil (2 spots)	F3
Hex/EtOAc 10 %	26-65	Hex/EtOAc 10 %	26-30 whitish yellow oil (2 spots) 31-32 brown oil (2 spots) 33-40 brown green oil (2 spots) 41-44 brown oil 45-60 dark oil (4 spots) 61-65 dirty ash (4 spots)	F3 F4 F5 F6 F7 F7
Hex/EtOAc 20 %	66-85	Hex/EtOAc 20 %	66-70 3 spots black oil 71-73 2 spots black oil 74-75 dirty ash 76-85 one main spot and 2-3 minor spots	F8 F9 F10 F11
Hex/EtOAc 30 %	86-105	Hex/EtOAc 30 %	86-89 one main spot and some minor spots 90-97 one main spot with much chlorophyle on the second spot 98-105 one main spot with much chlorophyle on the second spot and some other minor spot	F12 F13 F14
Hex/EtOAc 40 %	106-115	Hex/EtOAc 40 %	106-109 3 spots 110-115 2 spots and oily stuffs	F15 F16
Hex/EtOAc 50 %	116-125	Hex/EtOAc 50 %	116-125 2 main spots	F17
Hex/EtOAc 60 %	126-135	DCM/MeOH 2 %	126-135 3 main spots	F18
Hex/EtOAc 70 %	136-145	DCM/MeOH 4 %	136-141 142-145 3 spots	F19 F20
Hex/EtOAc 80 %	146-155	DCM/MeOH 6 %	146-155 4 spots	F21
Hex/EtOAc 90 %	156-165	DCM/MeOH 8 %	156-159 3 spots	F22

			160-165 4 spots	F23
EtOAc 100 %	166-175	DCM/MeOH 8 %	166-169 3 spots 170-175 3 spots	F24 F25
EtOAc/MeOH 10 %	176-185	DCM/MeOH 10 %	176-180 2-3 spots 176′-180′ 2-3 spots 181-184 4-5 spots 185 2 spots with trails	F26 F27 F28 F29
EtOAc/MeOH 25 %	186-195	DCM/MeOH 10 %	186-189 5 spots 190-195 4 spots with trails	F30 F31
MeOH 100 %	196-205	DCM/MeOH 10 % + some drops of acetic acid	196-198 4 spots with trails 199-205 3 spots	F31 F32

- **Treatment of series F3, F7, F10, F20 and F31 to obtain the pure compound AS_1 to AS_9.**

- **Treatment of Series F3**

F3 was steeped in Hexane/EtoAc 3-4 % for about 9 hours and then filtered and washed using hexane to obtain AS_1 (500 mg).

- **Treatment of Series F7**

F7 (45-65) (8 g) was fixed with silica gel and subjected to column chromatography on silica gel. One hundred and eleven (111) sub fractions of 100 mL each were collected, evaporated on a rotary evaporator and combined on the basis of TLC profiles. Subfractions 12 – 17 (~22 mg) and 22-23 (20 mg) crystallised in hexane respectively to afford, a misture of A_3 and AS_4 (20 mg) and AS_5 (18 mg).

- **Treatment of Series F10**

F3 was steeped in Hexane/EtoAc 3-4 % for about 9 hours and then filtered and washed using hexane to obtain AS_1 (500 mg).

F4 (fractions 71-75) crystallised from hexane and was filtered to afford PG_8 (100 mg).

III.5 CHEMICAL TESTS

III.5.1 Test for triterpenes

Liebermann-Burchard's test: 2 mg of dry extract is dissolved in acetic anhydride, heated to boiling, cooled and then 1 ml of concentrated sulphuric acid is added along the sides of the test tube. Formation of a violet colored ring indicates the presence of triterpenoids.

III.5.2 Test for alkaloids

Dragendorff's test: The sample is mixed with few drops of acetic acid followed by Dragendorff's reagent. Orange red precipitate is formed indicating the presence of alkaloids.

III.5.3 Test for quinones

Borntrager Test: Powdered sample is mixed with ether, which is filtered, and to the filtrate add caustic soda and aqueous ammonia. Red, pink or violet colour produced indicates the presence of anthraquinone.

III.6 HEMI-SYNTHESIS

To a dry DCM or Dioxane solution of the olefin(AS_1, AS_2, AS_6=PG_7, PG_1 and PG_4) in a 100 mL conical flask, SeO_2 was added (1.5 eq) at room temperature. The reaction mixture was refluxed while stirring for 7-8 h and monitored using TLC. After partial evaporation of the solvent to reduce the volume of the mixture, the residue was fixed to silica gel and submitted to column chromatography using Hex/AcOEt in various proportions.

III.7 BIOLOGICAL SCREENING

III.7.1 Cytotoxicity

Cytotoxicity was determined through cells plated in 96 - well plates (Nest Scientific) at a density of 2000 cells per well in 100 μL of media per well. On the following day, the media was aspirated and 100 μL of media in which a serial dilution of DMSO - dissolved compound (or DMSO as a control) was added to wells in triplicate. Three days later, the relative number of metabolically active cells was determined by the addition of the CellTiter - Glo reagent (Promega) and measurement of chemilumines c ence according to the manufacturer's protocol

using a Fluoroskan Ascent FL (Thermo Scientific). To calculate the percent viability, the signal from background wells (media only) was subtracted from each well, and then the remaining chemilumines c ence value was normalized to the signal from w ells with the equivalent amounts of DMSO. Graphing was done using GraphPad Prism 6 (GraphPad Software). IC_{50} values were calculated by fitting a non-linear curve using the "log - inhibitor vs normalized response" function given by the equation Y=100/{1+10[(X - LogIC50)]}.

III.7.2 Lipoxygenase inhibitory activity

Lipoxygenase (LOX) inhibiting activity was measured by modifying the spectrophotometri c method developed by Tappel. Lipoxygenase solution was prepared so that the reaction mixture's enzyme concentra tion was adjusted to a 0.05 absorbance/min rate. The reaction mixture comprised 160 µL of 100 mM sodium phosphate buffer at pH 8, 10 µL of the test solution and 20 µL of LOX solution. The contents were mixed and incubated for 10 min at 25 °C. It was then in itiated by adding 10 µ L substrate solution (linoleic acid, 0.5 mM, 0.12 %w/v tween 20 in a ratio of 1:2) and the change in absorbance at 234 nm was followed for 6 min. The concentration of the test compound that inhibited lipoxygenase activity by 50 % (IC_{50}) was determined by monitoring the effect of increasing concentrations of these compounds in the assays on the degree of inhibition. The IC 50 values were calculated using EZ - Fit, Enzyme kinetics Program (Perrella Scientific In., Amhherset, USA).

III.7.3 Evaluation of urease inhibition activity

Urease (Jack bean) solution (25 µl) was mixed with the 5 µl compound (500 µg) and incubated at 30°C for 15 min. Aliquots were taken and immediately transferred to assay mixtures containing urea (100mM) in buffer (40 µl) and re-incubated for 30 min in 96 well plates. The indophenol method determined urease activity based on measuring ammonia produced. 50 µl each of phenol reagent (1% w/v phenol and 0.005% w/v sodium nitroprusside) and 70 µl of alkali reagent (0.5% w/v NaOH and 0.1% active chloride NaOCl) were added to wells. An increase in absorbance was measured after 50 min at 630 nm on a microtitre plate reader (Spectramax Plus 384 Molecular Device, USA). The f inal volume of the reaction is 200 µl at pH 8.2 (0.01 M K_2HPO_4 . $3H_2O$, 1mM EDTA and 0.01 M $LiCl_2$). All reactions were performed in triplicates. The standard used in this assay was Thiourea, and percentage inhibitions were calculated by the formula:

$$\% \text{ inhibition} = 100 - \left[\frac{\text{optical density of test compound}}{\text{optical density of control (with no compound)}}\right]$$

III.7.4 Determination of DPPH radical scavenging (anti oxidant) activity

1,1-diphenyl-2-picrylhydrazyl radical (DPPH) is a quick method most researchers use to determine antioxidant activities. The free radical scavenging activity was measured by 1, 1 - diphe nyl - 2 - picryl - hydrazi ne (DPPH). DPPH solution (0.3 mM) was prepared in ethanol. The activity was measured in different concentrations of each compound ranging 62.5 µg - 500 µg. 5 µl of different concentrations ranging (62.5 µg - 500 µg) of each sample was mixed with 95 µl of DPPH solution in ethanol. The prepared dilutions were dispersed in 96 well plate and incubated at 37°C for 30 min. The absorbance was measured at 515 nm in microtitre plate reader (Spectramax Plus 384 Molecular Device, USA). The percent radical scavenging activity of root extracts was determined against methanol treated control.

$$\text{DDPH scavenging effect (\%)} = \left[\frac{Ac - As}{Ac}\right] \times 100$$

Where:

Ac = Absorbance of Control (DMSO treated)

As = Absorbance of Sample

III.8 MOLECULAR DOCKING STUDIES

- **Preparation of Ligand**

The 3D structures of the phytoconstituents were saved in .pdb format using Chem3D 15.0. The ligands were imported to the workspace and preparation was done for docking studies.

- **Preparation of Enzyme**

The target for docking studies selected was lipoxygenase. Docking analysis was done by initially selecting the target for the disease and followed by obtaining the 3D structure of lipoxygenase from protein data bank in.pdb format.

The AutoDockTools (ADT) was used to prepare the ligand and receptor structures, add appropriate Gasteiger and Kollman charges, identify and modify ligand rotatable bonds. The potential binding sites of target were calculated using the Lamarckian GA (4.2) algorithm

implemented in Autodock4. The population size, maximum number of evaluation (medium) and maximum number of generations were set at 150, 27 000 and 2 500 000 respectively. The water molecules were removed from the enzyme to decrease interactions between functional group of ligands and water molecules.

III.9 PHYSICAL PROPERTIES OF COMPOUNDS

III.9.1 Physical properties of the isolated triterpenoides

Aspect : White powder
Solubility : CH_2Cl_2
m.p. : 287 ^{0}C
Elution system : Hexane-Ethyl acetate 40-60%
m/z : 442.3 corresponding to $C_{30}H_{50}O_2$

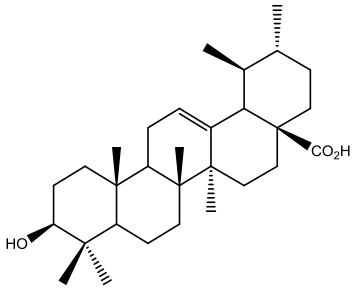

Ursolic acid (53)

Aspect : White powder
Solubility : CH_2Cl_2
m.p. : 284^{0}C
Elution system : Hexane-Ethyl acetate 20 %
m/z : 442.3 corresponding to $C_{30}H_{50}O_2$

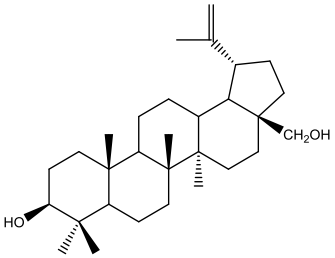

betulin (62)

Aspect : White powder
Solubility : CH_2Cl_2
m.p. : 186 ^{0}C
Elution system : Pure Hexane
m/z : 468.3 corresponding to $C_{32}H_{52}O_2$

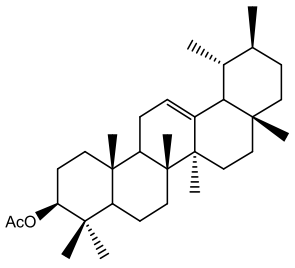

α-amyrin acetate (54)

Aspect	:	White powder
solubility	:	CH_2Cl_2
m.p.	:	288 ^{0}C
Elution system	:	Hexane-Ethyl acetate 25-27 %
m/z	:	456.20 corresponding to $C_{30}H_{47}O_3$

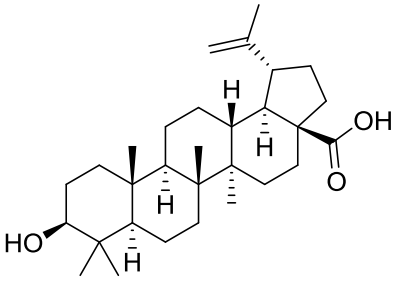

Betulinic acid (63)

Aspect	:	White powder
solubility	:	CH_2Cl_2
m.p.	:	135-137 ^{0}C m.p.
Elution system	:	Hexane-Ethyl acetate 4 %
m/z	:	*m/z*: 414.3 corresponding to $C_{29}H_{50}O$/ $C_{29}H_{48}O$

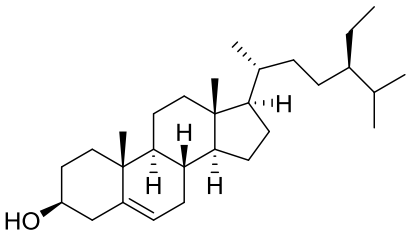

(128)

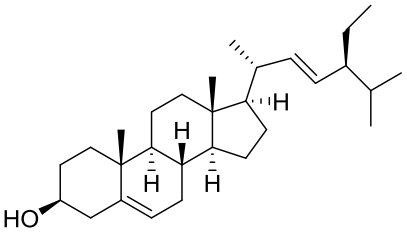

mixture of β-sitosterol and stigmasterol (129)

Spect	:	Brownish-black powder
solubility	:	MeOH
m.p.	:	138 ^{0}C
Elution system	:	CH_2Cl_2/MeOH 5 %
m/z	:	576.8 corresponding to $C_{35}H_{60}O_6$

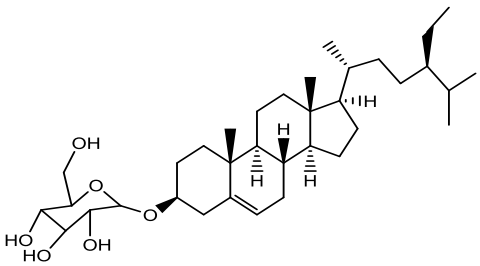

β-sitosterol glucoside (218)

Aspect	:	White powder
solubility	:	CH_2Cl_2
m.p.	:	160 ^{0}C
Elution system	:	Hexane-Ethyl acetate 5 %
m/z	:	428.40 corresponding to
		$C_{30}H_{52}O$

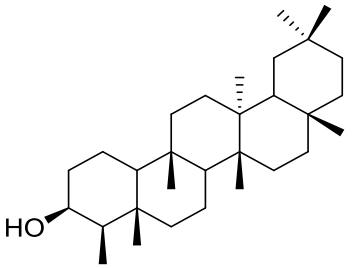

3-β-friedelanol (220)

III.9.2 Physical properties of the isolated quinones

Aspect	:	Orange powder
solubility	:	CH_2Cl_2
m.p.	:	120 ^{0}C
Elution system	:	Hexane-Ethyl acetate 4 %
m/z	:	406.03 corresponding to
		$C_{25}H_{26}O_5$

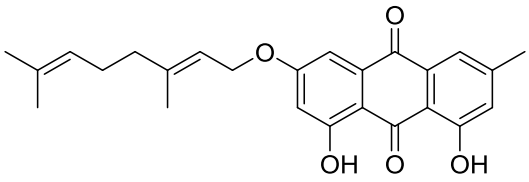

3-geranyloxyemodin (219)

Aspect	:	Yellow powder
solubility	:	CH_2Cl_2
m.p.	:	118 ^{0}C
Elution system	:	Hexane-Ethyl acetate 6 %
m/z		392.07 corresponding to
	:	$C_{25}H_{28}O_4$

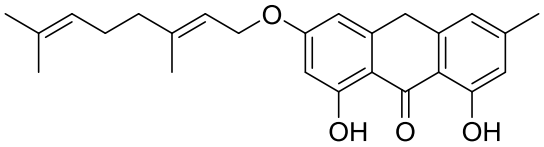

3-geranyloxyemodin anthrone (**220**)

Aspect	:	Yellow powder
solubility	:	CH_2Cl_2
m.p.	:	78-80 ^{0}C
Elution system	:	Hexane-Ethyl acetate 7 %
m/z	:	406.02 corresponding to
		$C_{25}H_{26}O_5$

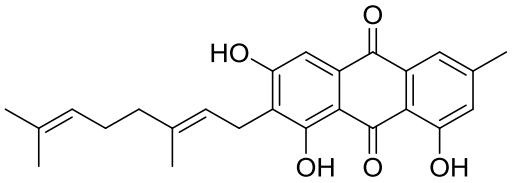

2-geranylemodin (222)

Aspect : Yellow powder
solubility : CH_2Cl_2
m.p. : 216 ^{0}C
Elution system : Hexane-Ethyl acetate 15 %
m/z : 452.07 corresponding to $C_{27}H_{32}O_6$

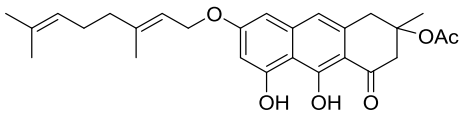

Acetylvismione D (95)

Aspect : Yellow powder
solubility : CH_2Cl_2
m.p. : 240 ^{0}C
Elution system : Hexane-Ethyl acetate 20 %
m/z : 270.045 corresponding to $C_{15}H_{10}O_5$

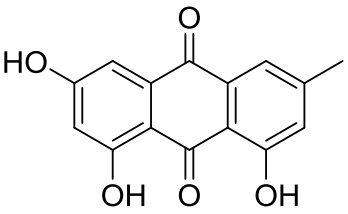

Emodin (111)

III.9.3 Physical properties of the isolated alkaloids

Aspect : Greenish brown powder
solubility : Acetone
m.p. : 180 ^{0}C
Elution system : Ethyl acetate 100%
m/z : 356.2 corresponding to $C_{20}H_{24}N_2O_4$

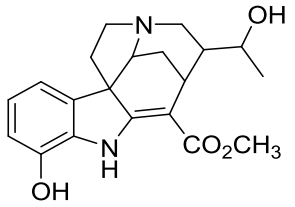

Scholaricine (19)

Aspect : Greenish brown powder
solubility : Acetone
m.p. : 501.1 ^{0}C
Elution system : CH_2Cl_2/MeOH 2 %
m/z : 338.2 corresponding to $C_{20}H_{22}N_2O_3$

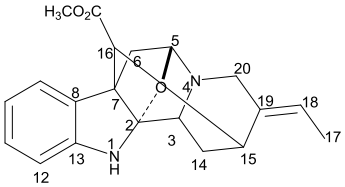

Picralstonine (217)

III.9.4 Physical properties of the isolated phenylpropanoid

Aspect	:	White powder
Solubility	:	CH_2Cl_2
m.p.	:	240 ^{0}C
Elution system	:	Hexane-Ethyl acetate 4 %
m/z	:	640.2 corresponding to $C_{43}H_{76}O_3$

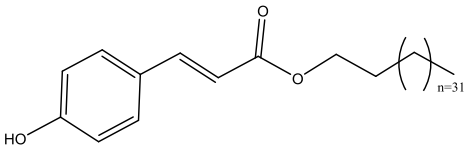

Tetratriacontyl-trans-*p*-coumarate (216)

III.9.5 Physical properties of the new hemisynthesized compounds

Aspect	:	White solid
Solubility	:	MeOH
Elution system	:	Hexane-Ethyl acetate 27 %
Molecular formula	:	$C_{30}H_{48}O_3$
Yield	:	60%

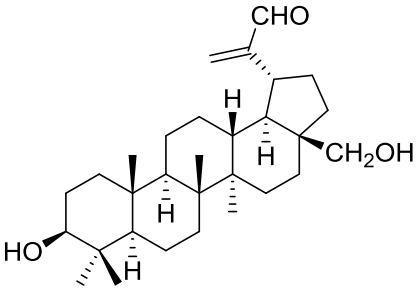

Betulin acrylaldehyde (222)

Aspect	:	White solid
Solubility	:	CH_2Cl_2/MeOH
m.p.	:	230 ^{0}C
Elution system	:	Hexane-Ethyl acetate 50 %
m/z	:	$C_{32}H_{50}O_3$
Yield	:	50 %

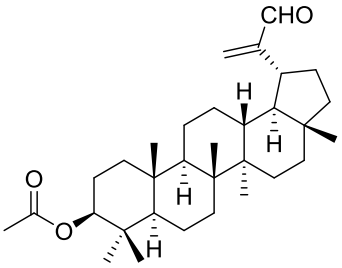

Lupeolacetate acrylaldehyde (223)

Aspect : Yellow solid

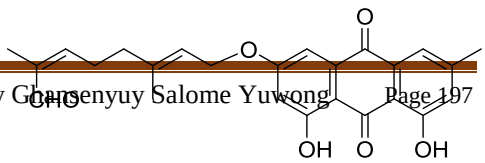

(2*Z*,6*E*)-8-((4,5-dihydroxy-7-methyl-9,10-dioxo-9,10-dihydroanthracen-2-yl)oxy)-2,6-dimethylocta-2,6-dienal (224)

solubility : CH_2Cl_2
Elution system : Hexane-Ethyl acetate 39 %
Molecular formula : $C_{25}H_{24}O_6$
Yield : 5.4 %

Aspect : Yellow solid
solubility : CH_2Cl_2
Elution system : Hexane-Ethyl acetate 56 %
Molecular formula : $C_{25}H_{26}O_6$
Yield : 8.2 %

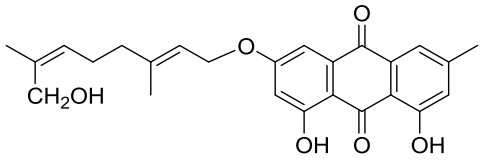

1,8-dihydroxy-3-(((2*E*,6*Z*)-8-hydroxy-3,7-dimethylocta-2,6-dien-1-yl)oxy)-6-methylanthracene-9,10-dione (226)

Aspect : Yellow solid
solubility : CH_2Cl_2
Elution system : Hexane-Ethyl acetate 45 %
Molecular formula : $C_{25}H_{24}O_5$
Yield : 30.6 %

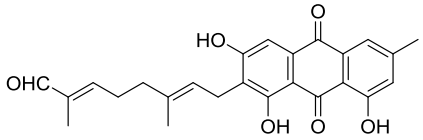

(2*E*,6*E*)-2,6-dimethyl-8-(1,3,8-trihydroxy-6-methyl-9,10-dioxo-9,10-dihydroanthracen-2-yl) octa-2,6-dienal (225)

Aspect : Yellow solid
solubility : CH_2Cl_2
Elution system : Hexane-Ethyl acetate 49 %
Molecular formula : $C_{25}H_{26}O_6$
Yield : 5.1 %

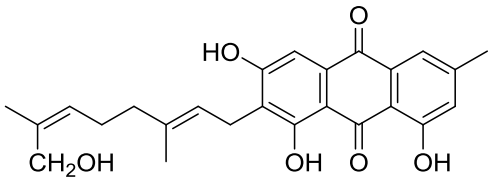

1,3,8-trihydroxy-2-((2*E*,6*Z*)-8-hydroxy-3,7-dimethylocta-2,6-dien-1-yl)-6-methylanthracene-9,10-dione (227)

REFERENCES

Abegaz B.M., 2002. Novel phenylanthraquinones, isofuranonaphthoquinones, homoisoflavonoids and biflavonoids from African plants in the genus Bulbine, Scilla, Ledebouria and Rhus. Phytochemistry Review, 1:299-310.

Abhijit D., 2011. *Alstonia scholaris* R.Br. (Apocynaceae): Phytochemistry and pharmacology: A concise review. Journal of Applied Pharmaceutical Science, 1:51–57.

Adejokea H.T., Louis H., Amusana O.O., Apebende G., 2019. A Review on classes, extraction, purification and pharmaceutical importance of plant alkaloid. Journal of Medicinal and Chemical Sciences, 2:130–139.

Adenot M., 2000. Initiation à la Chimie médicinale, les voies de la découverte du médicament. Ellipses edition marketing, 32 rue Bargue 75740 Paris cedex, 15:81–85.

Agarwal S., Mehrotra R., 2016. An overview of Molecular Docking. JSM Chemistry, 4:1–4.

Anupam M., Subash C. V., Rampratap M., Jayanthy A., Anupam S., Madhira B. S., Rajeev K. S., 2016. Phytochemistry and chromatographic analysis of *Alstonia scholaris* R.Br. Used as a Traditional Medicine: A Review. World Journal of Pharmaceutical Research, 5:1503–1519.

Ata A., Salar U., Saleem F, Lateef M., Khan S.A, Khan K.M., Taha M., Haider S.M., Ul-Haq Z., 2023. Identification of potential urease inhibitors and antioxidants based on saccharin derived analogs: Synthesis, *in vitro*, and *in silico* studies. Journal of Molecular Structure, 1274:1–13.

Atta-Ur-Rahman M., Asif M., Ghazala J.F., Alvi K.A., 1985. Scholaricine, an alkaloid from *Alstonia scholaris*. Phytochemistry, 24:2771–2773.

Banerji A., Siddhanta A.K., 1981. Scholarine: an indode alkaloids of *Alstonia scholaris*. Phytochemistry, 20:540–542.

Bao C., Lu Y., Chen J., Chen D., Lou W., Ding B., Xu L., 2019. Fan W. Exploring specific prognostic biomarkers in triple-negative breast cancer. Cell Death & Disease, 10:1–14.

Bilia A.R., Yusuf A.W., Braca A., Keita A., Morelli I., 2000. New Prenylated Anthraquinones and xanthones from *Vismia guineensis*. Journal of Natural Products, 63:16–21.

Bonfill M., Mangas S., Cusidó R. M., Osuna L., Piñol M.T., Palazón J., 2006. Identification of triterpenoid compounds of *Centella asiatica* by thin-layer chromatography and mass spectrometry. Biomedical Chromatography, 20:151–153.

Boonchuay W., Court W.E., 1976. Minor alkaloids from *Alstonia scholaris* roots. Phytochemistry, 15:821–26.

Boonsri S., Karalai C., Ponglimanont C., Kanjana-opas A., Chantrapromma K., 2006. Antibacterial and cytotoxic xanthones from the roots of *Cratoxylum formosum*. Phytochemistry, 67:723–727.

Botta B., Delle Monache F., Delle Monache G., Marini Bettolo G.B., Oguakwa J.U., 1983. 3-Geranyloxy-6-Methyl-1,8-Dihydroxyanthraquinone and Vismiones C, D and E From *Psorospermum Febrifugum*. Phytochemistry, 22:539–542.

Bräutigam K., Mitzlaff K., Uebel L., Köster F., Polack S., Pervan M., Steinert G., Rody A., Liedtke C., 2016. Subtypes of triple-negative breast cancer cell lines react differently to eribulin mesylate. Anticancer Research, 36:2759–2766.

Bruneton J., 1999. *Pharmacognosie, phytochimie et plantes médicinales. 3ème edition, technique et documentation*, Paris, 82.

Cai X.H., Du Z.Z., Luo X.D., 2007. Unique monoterpenoid indole alkaloids from *Alstonia scholaris*. Organic Letters, 9:1817–1820.

Castro M.J., Richmond V., Faraoni M.B., Murray A.P., 2018. Oxidation at C-16 enhances butyrylcholinesterase inhibition in lupane triterpenoids. Bioorganic Chemistry, 79:301–309.

Chan-Zapata I., Borges-Argáez R., Ayora-Talavera G., 2023. Quinones as promising compounds against respiratory viruses: A Review. Molecules, 2:1–30.

Chao-Min W., Kuei-Lin Y., Shang-Jie T., Yun-Lian J., Chang-Hung C., 2017. Anti-proliferative activity of triterpenoids and sterols isolated from *alstonia scholaris* against non-small-cell lung carcinoma cells. Molecules, 22:2119.

Chatterjee A., Mukherjee B., Ray A.B., Das B., 1965. The alkaloids of the leaves of *Alstonia scholaris* R.Br.. Tetrahedron Letters, 6:3633–3637.

Chavez K.J., Garimella S.V., Lipkowitz S., 2011. Triple negative breast cancer cell lines: One tool in the search for better treatment of triple negative breast cancer. Breast Disease, 32: 35–48.

Dasari S., Wudayagiri R., Valluru L., 2015. Cervical cancer: Biomarkers for diagnosis and treatment. Clinica Chimica Acta, 445:7–11.

Dewi R.T., Minarti, Darmawan A., Mulyani H., 2008. Emodin, an anthraquinone from ethyl acetate extract of *Aspergillus terreus koji*. Proceeding of The International Seminar on Chemistry, 731–734.

Dey A., 2011. *Alstonia scholaris* R.Br. (Apocynaceae): Phytochemistry and pharmacology: A concise review. Journal of Applied Pharmaceutical Science, 1:51–57.

Dhruti M., Bhavika P., Meonis P., 2016. Studies on phytochemical constituents and antioxidant activity of *Alstonia scholaris*. International Journal of Life Sciences, 4:529–538.

Djerassi C., Budzikiewicz W., Dudley H., 1964. Structure elucidation of natural products by mass spectrometry volume II: steroids, terpenoids, sugars, and miscellaneous classes. Standford Univeristy, California, 575–598.

Dutta S.C., Battacharya S.K., Ray A.B., 1976. Flower alkaloids of *Alstonia scholaris* R. Br.. Planta Medica, 30:86–89.

Epifano F., Fiorito S., Genovese S., 2013. Phytochemistry and pharmacognosy of the genus *Psorospermum*. Phytochemistry Reviews, 1:1–12.

Eyong K.O., Chinthapally K., Senthilkumar S., Lamshöft M., Folefoc G.N., Baskaran S., 2016. Conversion of lapachol to lomatiol: synthesis of novel naphthoquinone derivatives. New Journal of Chemistry, 39:9611–9616.

Faisal S., Badshah L., Kubra B., Emwas A.H., Jaremko M., 2023. Alkaloids as potential antivirals. A comprehensive review. Natural Products and Bioprospecting, 13:1–38.

Faizi S., Ali M., Saleem R., Irfanullah, Bibi S., 2001. Complete ^{1}H and ^{13}C NMR assignments of stigma-5-en-3-O-β-glucoside and its acetyl derivative. Magnetic Resonance Chemistry, 39:399–405.

Feng T., Cai X.H., Zhao P.J., Du Z.Z., Li W.Q., Luo X.D., 2009. Monoterpenoid indole alkaloids from the bark of *Alstonia scholaris*, Planta Medica, 75:1537–1541.

Feng T., Caia X.H., Du Z.Z., Luo X.D., 2008. Iridoids from the bark of *Alstonia scholaris*. Helvetica Chimica Acta, 91:2247–2251.

Fernandez J.R.E., Eckhardt B.L., Lee J., Lim B., Pearson T., Seitz R.S., Hout D.R., Schweitzer B.L., Nielsen T.J., Ryne Lawrence O.R., Wang Y., Rao A., Ueno N.T., 2020. Identification of triple-negative breast cancer cell lines classified under the same molecular subtype using different molecular characterization techniques: Implications for translational research. Plos One, 15:1–8.

Gorman R., Kaloga M., Li X.C., Ferreira D., Bergenthal D., Kolodziej H., 2003. Furanonaphthoquinones, atraric acid and a benzofuran from the stem barks of *Newbouldia laevis*. Phytochemistry, 64:5837.

Gurupriya S., Cathrine L., 2021. Molecular docking studies of isolated compounds andrographolide and betulin from methanolic leaves extract of andrographis echioides as α-amylase and α-glucosidase activators. International Journal of Applied Pharmaceutics, 13:1–10.

Han J., Lim W., You D., Jeong Y., Kim S., Lee J.E., Shin T.H., Lee G., Park S., 2019. Chemoresistance in the human triple-negative breast cancer cell line mda-mb-231 induced by doxorubicin gradient is associated with epigenetic alterations in histone deacetylase. Journal of Oncology, 209:1–13.

Holliday D.L., Speirs V., 2015. Choosing the right cell line for breast cancer research. Breast Cancer Research, 13:1–7.

https://www.cdc.gov/cancer/breast/basic_info/risk_factors.htm consulted on 29th August 2023.

https://www.cdc.gov/cancer/breast/basic_info/risk_factors.htm consulted on 29th August 2023.

https://www.botany.hawaii.edu consulted on 29th August 2023.

https://www.inaturalist.org consulted on 6th June 2024.

https://www.plants.jstor.org consulted on 18th June 2024.

https://www.researchgate.net/figure/Geographical-distribution-of-*A-scholaris*-Color-figure-online_fig1_339273223 consulted on 9th May 2024.

Islam R., Iftekhar A, Al A. S., Mohammad R. H., Abdullah A., Mansoor A., Munawar R. and Mohammad A. R., 2014. Chemical investigation of *Mesua nagassarium* (Burm. f.) *Kosterm*. Journal of Basic & Applied Sciences, 10:124-128.

Kam T.S., Nyeoh K.T., Sim K.M., Yoganathyan K., 1997. Alkaloids from *Alstonia scholaris*. Phytochemistry, 45:1303–1305.

Kemboi D., Langat M.K., Siwe‑Noundou X., Krause R.W.N., Isaacs L.M., Tembu V.J., 2022. In vitro antibacterial and cytotoxic efects of *Euphorbia grandicornis* blanc chemical constituents. BMC Complimentary Medicine and Therapies, 22:1–10.

Khana K.M., Alia,M., Wadood A., Zaheer-ul-Haqc, Khana,M., Lodhia M.A., Perveend S., Choudharya M.I., Voelter W., 2011. Molecular modeling-based antioxidant arylidene barbiturates as urease inhibitors. Journal of Molecular Graphic Modelling, 30:153–156.

Kuete V., Nguemeving J.R., Beng V.P., Azebaze A.G.B., Etoa F.X., Meyer M., Bodo B., Nkengfack A.E., 2007. Antimicrobial activity of the methanolic extracts and compounds from *Vismia laurentii* De Wild (Guttiferae). Journal of Ethnopharmacology, 109:372–379.

Lanning N.J., Castle J.P., Singh S.J., Leon A.N., Tovar E.A. Sanghera A., MacKeigan J.P., Filipp F.V., Graveel C.R., 2017. Metabolic profiling of triple-negative breast cancer cells reveals metabolic vulnerabilities. Cancer & Metabolism, 5:1–14.

Lenta B.N., Devkota K.P., Ngouela S., Boyom F.F., Naz Q., Choudhary M.I., Tsamo E., Rosenthal P.J., Sewald N., 2008. Anti-plasmodial and Cholinesterase Inhibiting Activities of some Constituents of *Psorospermum glaberrimum*. Chemical and Pharmaceutical Bulletin, 56:222–226.

Liu E., Becker N., Sudha P., Dong C., Liu Y., Keats J., Morgan G., Walker B.A., 2023. Alternative splicing in multiple myeloma is associated with the non-homologous end joining pathway. Blood Cancer Journal, 13:1–11.

Lobo V., Patil A., Phatak A., Chandra N., 2010. Free radicals, antioxidants and functional foods: Impact on human health. Pharmacology Reviews, 4:118–126.

Machado V.R., Sandjo L.P., Pinheiro G.L., Moraes M.H., Steindel M., Pizzolatti M.G., Biavatti M.W., 2018. Synthesis of lupeol derivatives and their antileishmanial and antitrypanosomal activities. Natural Products Resonance, 32: 275–281.

Mahato S.B., Kundu A.P., 1994. ^{13}C NMR spectra of pentacyclic triterpenoids: a compilation and some salient features. Phytochemistry, 37:1517–1575.

Manjeshwar S.B., 2011. Review of the Phytochemical, pharmacological and toxicological properties of *Alstonia Scholaris* Linn. R. Br (Saptaparna). Chinese Journal of Integrated Medicine, 1:1–14.

Mashima R., Okuyama T., 2015. The role of lipoxygenases in pathophysiology; new insights and future perspectives. Redox Biology, 6:297–310.

Mbachu K.A., E-Farwa U., Khan M.A., Hameed S., Lateef M., Atta L., Ul-Haq Z., Khan K.M., Ekundayo O., 2023. Urease inhibitory activity on 1,2,3-triazoles-linked indomethacin derivatives; *in vitro* and *in silico* studies. Journal of Molecular Structure, 1278:1–14.

Merchanta N., Bhaskarb L.V.K.S., Momina S., Sujathac P., Reddyd A.B.M., Nagaraju G.P., 2018. 5-Lipoxygenase: Its involvement in gastrointestinal malignancies. Critical Reviews in Oncology/Hematology, 127:50–55.

Mertens-Talcott S.U., Chintharlapalli S., Li X., Safe S., 2007. The oncogenic microrna-27a targets genes that regulate specificity protein transcription factors and the g2-m checkpoint in mda-mb-231 breast cancer cells. Cancer Research, 67:11001–11011.

Monache G.D., Botta B., Oguakwa J.U., Monache F.D., 1987. New vismiones from *Psorospermum tenuifolium*. Bullein of the Chemical Society of Ethiopia, 1:42–46.

Nagaraju P., Ravichandra S., Pradeep K.T., 2017. Computer-aided docking: an invaluable tool in drug discovery and molecular biology, International Journal of Pharmaceutical. Chemical and Biological Sciences, 7:453–458.

Neve R.M., Chin K., Fridlyand J., Yeh J., Baehner F.L., Fevr T., Clark L., Bayani N., Coppe J.P., Tong F., Speed T., Spellman P.T., DeVries S., Lapuk A., Wang N.J., Kuo W.L., Stilwell J.L., Pinke D., Albertson D.G., Waldman F.M., McCormick F., Dickson R.B., Johnson M.D., Lippman M., Ethier S., Gazdar A., Gray J.W., 2016. A collection of breast cancer cell lines for the study of functionally distinct cancer subtypes. Cancer Cell, 10:515–552.

Nguemeving J.R., Azebaze A.G.B., Kuete V., Nono N.E.C., Beng V.P., Meyer M., Blond A., Bodo B., Nkengfack A.E., 2006. Laurentixanthones A and B, antimicrobial xanthones from *Vismia laurentii*. Phytochemistry, 67:1341–1346.

Noungoue D.T., Antheaume C., Chaabi M., Ndjakou B.L., Ngouela S., Lobstein A., Tsamo E., 2008. Anthraquinones from the fruits of *Vismia laurentii*. Phytochemistry, 69:1024–1028.

Ogunkoya L., 1981. Application of mass spectrometry in structural problems in triterpenes. Phytochemistry, 19:121–126.

Okoye N.N., Ajaghaku D.L., Okeke H.N., Ilodigwe E.E., Nworu C.S., Okoye F.B.C., 2014. β-Amyrin and α-amyrin acetate isolated from the stem bark of *Alstonia boonei* display profound anti-inflammatory activity. Pharmaceutical Biology, 52:1478–1486.

Omara T., Kiprop A.K., Ramkat R.C., Cherutoi J., Kagoya S., Nyangena D.M., Tebo T.A., Nteziyaremye P., Karanja L.N., Jepchirchir A., Maiyo A., Kiptui B.J., Mbabazi I., Nakiguli C.K., Nakabuye B.V., Koske M.P., 2020. Medicinal plants used in traditional management of cancer in uganda: a review of ethnobotanical surveys, phytochemistry, and anticancer studies. Evidence-Based Complimentary Alternative Medicine, 1:1-26.

Pankti K., Payal G., Manodeep C., Jagadish K. A., 2012. Phytopharmacological Review of *Alstonia Scholaris*: A panoramic herbal medecine. International Journal of Research in Ayurveda and Pharmacy, 3:367–371.

Patel R.M., Puranik V.G., Argade N.P., 2011. Regio-and stereoselective selenium dioxide allylic oxidation of (E)-dialkyl alkylidenesuccinates to (Z)-allylic alcohols: Synthesis of natural and unnatural butenolides. Organic and Biomolecular Chemistry, 9:6312.

Patrick A.G., Macabeo, Krohn K., Gehle D., Read R.W., Brophy J.J., Cordell G.A., Franzblau S.G., Aguinaldo A.M., 2005. Indole alkaloids from the leaves of Philippine *Alstonia scholaris*. Phytochemistry, 66: 1158–62.

Politi M., Sanogo R., Ndjoko K., Guilet D., Wolfender J.-L., Hostettmann K., Morelli I., 2004. HPLC-UV/PAD and HPLC-MS^n Analyses of leaf and root extracts of *Vismia guineensis* and isolation and identification of two new bianthrones. Phytochemical Analysis, 15:355–364.

Prasanta D., Amit K., Anoop K., Meenakshi G., Byung M.L., Tejendra B., Suvakanta D., Hyung S.K., 2020. Analysis of alkaloids (indole alkaloids, isoquinoline alkaloids, tropane alkaloids). Recent Advances in Natural Products Analysis, 15, 505–567.

Rahman Atta-Ur., Asif M., Firdous S, Fatima J., Alvi K.A., 1986. ^{1}H and ^{13}C NMR Studies on picralstonine. Journal of the American Chemical Society, 8:421–423.

Rahman Atta-Ur-., Asif M., Ghazala M., Fatima K.J., Alvi A., 1985. Scholaricine an alkaloid from *Alstonia scholaris*. Phytochemistry, 24:2771–2773.

Rastogi R.C., Kapil R.S., Popli S.P., 1990. Picralinal: a key alkaloid of picralima group from *Alstonia scholaris* R. Br.. Experimentia, 26:1056.

Riley H.L., 1947. Oxidation activity of selenium dioxide. Nature 159:571-572.

https://chem.libretexts.org/@go/page/182339, consulted on 30th May 2023.

Salim A.A., Garson M.J., Craik D.J., 2004. New indole alkaloids from the bark of *Alstonia scholaris*. Journal of Natural Products, 67:1591–1594.

Seebacher W., Simic N., Weis R., Saf R., Kunert O., 2023. Complete assignments of ^{1}H and ^{13}C NMR resonances of oleanolic acid, 18α-oleanolic acid, ursolic acid and their 11-oxo derivatives. Magnetic Resonance Chemistry, 41:636–638.

Siegel R.L., Miller K.D., Wagle N.S., Ahmedin J.D.V.M., 2023. Cancer statistics. Cancer Journal for Clinicians, 73:17–48.

Singh J., Singh J. A., 1986. Bianthraquinone and a triterpenoid from the seeds of *Cassia hirsute*. Phytochemistry, 25:1985–1987.

Steele V.E., Holmes C.A., Hawk E.T., Kopelovich L., Lubet R.A., Crowell J.A., Sigman C.C., Kelloff G.J., 1999. Lipoxygenase Inhibitors as Potential Cancer Chemopreventives. Cancer Epidemiology, Biomarkers & Prevention, 8:467–483.

Sultana N., Saeed S.Z., Saleem M., Kamal M., 2013. Two new triterpenes from *Alstonia scholaris* flowers. Natural Product Research, 27:1277–1286.

Surya S. P., Jayanthi G. Smitha K.R., 2012. In vitro evaluation pf the anticancer effect of methanolic extract of *Alstonia scholaris* leaves on mammary carcinoma. Journal of Apllied Pharmaceutical Science, 2: 142-149.

Suryawanshi P., Vidyasagar G.M., 2016. Phytochemical screening for secondary metabolites of *Opuntia dillenii* Haw. Journal of Medicinal Plants Studies, 4:39–43.

Tala F.M., Krohn K., Hussain H., Kouam F.S., Wabo K.H., Tane P., Schulz B., Hu Q., 2007. Laurentixanthone C: A New Antifungal and Algicidal Xanthone from Stem Bark of *Vismia laurentii*. Zeitschrift für Naturforschung, 62:565–568.

Tingting H., Yun S., Liping Z., Wen G., 2009. Flavonoids in leaves of *Alstonia scholaris*. China Journal of Chineese Materia Medica., 34:1111–1113.

Toma F., Bouhet J.C., Van Chuong P.P., Fromageot P., Haar W., Ruterjans H., Maurer W., 1975. Carbon-13 NMR Spectroscopy of the Biological Pigments Luteoskyrin and Rugulosin and some Polyhydroxyanthraquinone Analogues. Organic Magnetic Resonance, 7:496–503.

Vanita K., Deepali J. M., 2018. A Pharmacognostic and Pharmacological Review on *Alstonia Scholaris*. Asian Journal of Pharmaceutics Clinical Research, 11:22-26.

Wells J.M., Cole R.J., Kirksey J.W., 1975. Emodin, a Toxic Metabolite of *Aspergillus wentii* Isolated from Weevil-Damaged Chestnuts. Applied Microbiology, 30:26–28.

Wilcox M., Sanogo R., Diakite C., Giani S., 2012. Smestad Paulsen B. Improved traditional medicines in Mali. Journal of Alternative and Complimentary Medicine, 18:212–220.

Wisastra R. Dekker F.J., 2014. Inflammation, Cancer and Oxidative Lipoxygenase Activity are Intimately Linked. Cancers, 6:1500–1521.

Wongseripipatana S., Chaisri L., Sritularak B., Likhitwitayawuid K., 2004. Indole alkaloids from the fruits of *Alstonia scholaris*. Thailand Journal of Pharmaceutical Science, 28:173-180.

Wonkam A.K.N., Ngansop C.A.N., Wouamba S.C.N., Jouda J.B., Happi G.M., Boyom F.F., Sewald N., Lenta B.N., 2020. Rothmanniamide and other constituents from the leaves of *Rothmannia hispida* (K.Schum.) fagerl. (Rubiaceae) and their chemophenetic significance. Biochemical Systems Ecology, 93:104137.

Wurdack K.J., Davis C.C., 2009. "Malpighiales phylogenetics: Gaining ground on one of the most recalcitrant clades in the angiosperm tree of life". American Journal of Botany, 96:1551–1570.

Xiaofeng D., Cheng H., Zhonghu B., Jia L., 2017. Breast cancer cell line classification and its relevance with breast tumor subtyping. Journal of Cancer, 8:3131–3141.

Yang M., Wang X., Guan S., Xia J., Sun J., Guo H., Guo D., 2014. Analysis of Triterpenoids in *Ganoderma lucidum* Using liquid chromatography coupled with electrospray ionization mass spectrometry. Journal of the American Society for Mass Spectrometry, 18:927–939.

Yemback P., Eyong K.O., Efange N.M., Kamdem M.H.K., Ndinteh D.T., Odumosu P.O., Folefoc G.N., Ayong L., 2023. Lupane derivatives: design, isolation, synthesis and evaluation of antiplasmodial activity against *Plasmodium falciparum* 3D7 strain. Phytochemistry Letters, 57:26–35.

Zhou H., He H.P., Luo X.D., Wang Y.H., Yang X.W., Di Y.T., Hao X.J., 2005. Three new indole alkaloids from the leaves of *Alstonia scholaris*. Helvetica Chimica Acta, 88:2508–2512.

Zhuang C., Zhang W., Sheng C., Zhang W., Xing C., Miao Z., 2017. Chalcone: a privileged structure in medicinal chemistry. Chemistry Reviews, 117: 7762–7810.

Zingue S., Atuenguena E. O., Zingue L.L., Tueche A. B., Nkoum D. N. A. B., Ndom P., 2021. Epidemiological and clinical profile, and survival of patients followed for breast cancer between 2010 and 2015 at the Yaounde General Hospital, Cameroon. Pan African Medicinal Journal, 39: 1-8.

ANNEXES

LIST OF PUBLICATIONS

1. K.O. Eyong, **S.Y. Ghansenyuy**, P. Yemback, L. Mehreen, G.N. Folefoc, **2023**. Constituents from *Psorospermum guineense* twigs**,** MDA-MB-231, Lipoxygenase, Anti-oxidant and Molecular Docking Studies. **Pakistan Journal of Chemistry 13 (1-2), 11-17**.

2. Salome Y. Ghansenyuy, Kenneth O. Eyong, Pierre Yemback, Vincent de Paul N. Nziko, Muhammad S. Ali, Gabriel N. Folefoc, **2023**. Lipoxygenase Inhibition and Molecular Docking studies of secondary metabolites from the leaves of *Alstonia scholaris*. ***European Journal of Medicinal Chemistry Reports*** **9(101108), 1-5**.

3. **Salome Yuwong Ghansenyuy**, Kenneth Oben Eyong, Pierre Yemback, Vincent de Paul Nzuwah Nziko, Muhammad Shaiq Ali, Gabriel Ngosong Folefoc, Samantha Davis, Jenna Tobin, Haleigh Parker and Joseph Taube, **2023**. Phytochemical Studies of ***Alstonia scholaris***, Chemical Transformation and Biological Evaluation against a Breast Cancer Cell Line. ***The Natural Products Journal X*** **(XX), 1-8**. (**Accepted**)

LIST OF COMMUNICATIONS

Salome Y. Ghansenyuy, Kenneth O. Eyong, Gabriel N. Folefoc. Phytochemical studies of *Psorospermum guineense* Hochr (HYPERICACEAE) and *Alstonia scholaris* (l) r. br. (APOCYNACEAE), Synthesis, Biological Activities and Molecular Docking Studies. Goethe-Institut Kamerun, *Sciences Slam*, **November 9, 2016 (*Oral presentation*).**

Salome Y. Ghansenyuy, Kenneth O. Eyong, Pierre Yemback, Gabriel N. Folefoc. Phytochemical studies of *Psorospermum guineense* Hochr (HYPERICACEAE) and *Alstonia scholaris* (l) r. br. (APOCYNACEAE), Synthesis, Biological Activities and Molecular Docking Studies. University of Yaounde 1, *Doctoriales Chimie*, **June 14-15, 2017 (*Oral presentation*).**

Salome Y. Ghansenyuy, Kenneth O. Eyong, Pierre Yemback, Lateef Mehreen, Gabriel N. Folefoc. Anti breast cancer activity and molecular docking studies of constituents of *Psorospermum guineense* hochr, a Cameroonian medicinal plant of the Hypercaceae family,**.** Chicago - USA, *American Society of Tropical Medicine and Hygiene 2023 Annual meeting*, **October 18-22, 2023 (*Poster presentation*).**

Ghansenyuy Salome Yuwong, Eyong Kenneth Oben, Yemback Piere, Mehreen Lateef, Vincent de Paul N. Nziko, Muhammad Shaiq Ali, Folefoc Gabriel Ngosong. Lipoxygenase Inhibition and Molecular Docking Studies of Secondary Metabolites from the Leaves of ***Alstonia scholaris.*** Online, *American Society of Pharmacognosy Younger Members' Symposium 2025*, May 8, 2025 **(*Oral presentation*).**

PUBLICATIONS

ATTESTATIONS OF SCHOLARSHIPS RECEIVED AND ATTESTATIONS OF PARTICIPATION IN NATIONAL & INTERNATIONAL CONFERENCES/WORKSHOPS ATTENDED AND ATTESTATIONS OF PROFESSIONAL AFFILIATIONS, DURING THE DOCTORATE/PhD THESIS RESEARCH PERIOD

Pak. J. Chem. 13(1-2): 11-17, 2023 Research article
ISSN (Print): 2220-2625
ISSN (Online): 2222-307X DOI: 10.15228/2023.v13.i01-2.p02

Constituents from *Psorospermum guineense* twigs, MDA-MB-231, lipoxygenase, antioxidant and Molecular Docking Studies

K.O. Eyong[1]*, S.Y. Ghansenyuy[1], P. Yemback[1], L. Mehreen[2], G.N. Folefoc [1]
[1]Department of Organic Chemistry, Faculty of Science, University of Yaounde I, P.O. Box 812, Yaounde, Cameroon.
[2]Multidisciplinary research Lab, Bahria University Medical and Dental College, Bahria University, Karachi, Pakistan
Email address: eyongkk@yahoo.com

Abstract
Cancer is one of the leading causes of mortality worldwide, characterized by the irregular proliferation of malignant cells and increasing resistance to known drugs. The importance of developing new chemotherapeutic agents is necessary. The present study focuses on *Psorospermum guineense*, used in traditional medicine to treat cancer, and associated carcinogenic processes such as tumour cell proliferation, differentiation, and apoptosis. A study of the chemical constituents of the twigs of *Psorospermum guineense* has resulted in the isolation and characterization of eight known compounds, namely: 3-geranyloxyemodine **1**, 3-β-fridelanol **2**, 3-geranyloxyemodine anthrone **3**, 2-geranylemodine **4**, Acetylvismione D **5**, Betulinic acid **6**, Ursolic acid **7** and Emodine **8** through LC-MS and selected 1D and 2D–NMR experiments. Single crystal x-ray diffraction analysis was used to confirm the relative configuration and conformation of compound **1**. Preliminary cytotoxicity assays against the MDA-MB-231 breast cancer cell indicated that Ursolic acid **7** was the most active, with an IC_{50} value of 9.88 μM and 95% CI of 9.03-10.5 μM. Acetylvismione D **5** exhibited better lipoxygenase inhibitory activity (19.8±0.16) and antioxidant activity (20.8±0.15) compared to the reference drugs baicalein (22.6 ± 0.08 μM) and Beta hydroxyl acid (BHA) (44.2 ± 0.07) respectively. Molecular docking studies were conducted to support lipoxygenase inhibitory activities of the test compounds.

Keywords: *Psorospermum guineense*, Breast Cancer, Antraquinones, single crystal x-ray, Lipoxygenase, Molecular Docking

1. INTRODUCTION

Cancer is one of the leading causes of mortality worldwide [1]. The irregular proliferation of malignant cells characterizes it in various stages with different biochemical, molecular and cellular events [2]. Cancer is caused by both internal factors (such as mutations, hormones and immune conditions) and external factors like chemicals, radiation and infectious microorganisms [3,4]. This is attributed to changes in lifestyle, such as smoking, unhealthy eating, lack of physical exercise and excessive consumption of alcohol [5].

In 2021, 18.1 million new cancer cases and 9.6 million deaths were reported globally [6]. The International Agency for Research on Cancer (IARC) reported that cancer's incidence, mortality and prevalence worldwide were attributed to 36 different types of cancer [6]. Lung cancer registered 11.6% of cancer incidences with 18.4% mortality. It was followed by breast cancer (11.6%), prostate cancer (7.1%), and colorectal cancer (6.1%) in mortality. Colorectal cancer (9.2%), stomach cancer (8.2%), and liver cancer (8.2%) were listed among the top four deadliest tumours. Lung, prostate, liver and stomach cancers represented the most deadly among males, while among females, breast, lung and colorectal cancers dominated [7]. In Africa, cancer recorded over 1 million cases yearly, and the most common include cervix, breast, liver and prostate cancers [5]. Cancer management is not a priority in developing countries, despite the increasing burden, largely due to limited resources and other pressing public health concerns such as HIV/AIDS, malaria and tuberculosis [1].

Cancer treatment is costly, and the resistance of tumour cells to the available antineoplastic drugs has exacerbated this [8]. Due to their lack of specificity, conventional cancer therapies, such as radiotherapies, present severe side effects and, in most developing countries, are inaccessible to cancer patients [9]. Thus, traditional medicine is gaining more attention in the chemoprotective management of cancer in Africa [1,10-11]. Over 3,000 plant species have been reported to have anticancer properties [12]. An example is *Taxus brevifolia*, from which taxol was isolated, a well-known cancer drug in the United States of America [13].

Psorospermum guineense Hochr. (sin. *P. glaucum* Hochr.) is a plant typically growing in French Guinea, Mali, Senegal, Tanzania, and Nigeria, where it is also known by the common name‘‘kari-diakouma" and the local population uses it to treat skin diseases (eczema, psoriasis, scabies, cold sores, and leprosy), syphilis, cancer and neuralgia [14]. Extracts of the leaves and root bark of *P. guineense* have shown anti-leishmanial and anticancer activity [14]. Previous phytochemical investigations of *Psorospermum* species reported the presence of bioactive xanthones, anthraquinones, vismiones and psorolactones [15].

In our attempts to isolate natural products for drug discovery and development from a rational approach as a part of a laboratory project on re-investigating Cameroon medicinal plants, we initiated a study to isolate constituents of *P. guineense*, with biological activity and search for potential targets or mode of action studies. In this paper, we have reported on the phytochemical studies of the twigs of *P. guineense*, single crystal x-ray diffraction analysis and their bioactivity against MDA MB-231 breast cancer cell lines. The mechanism of action was determined by

evaluating their antioxidant activity, lipoxygenase and urease enzyme inhibition activities. Moreover, molecular docking studies to support the better lipoxygenase inhibitory activities of the test compounds were also conducted.

2. MATERIALS AND METHODS

General Experimental Procedures. 1D (^{1}H, ^{13}C and DEPT) and 2D (COSY, HSQC, HSQC-TOCSY, HMBC, TOCSY, NOESY, and ROESY) NMR spectra were recorded on a Bruker Ascend 600 (^{1}H 600 MHz and ^{13}C 150 MHz) NMR spectrometer equipped with a 5 mm cryoprobe. ^{1}H NMR chemical shifts are reported as δ values in ppm relative to $CDCl_3$ (7.26 ppm,), coupling constants (J) are reported in Hertz (Hz), and diversity follows convention. Unless indicated otherwise, $CDCl_3$ served as an internal standard (77.2 ppm) for all ^{13}C spectra. The chemical shifts are quoted relative to TMS. X-ray data were recorded on a Bruker400 Machine. HRESIMS data were acquired on a Thermo LTQ Orbitrap mass spectrometer.

2.1. Sample Collection. *Psorospermum guineense* twigs were harvested from Limbo, a small locality between Wainamah and Ndop plane in the North West region of Cameroon (September, 2016) by a botanist Dr. Tacham Walters, of the University of Bamenda and a voucher specimen deposited at the Cameroon National Herbarium (HNC), (14432/SRFCam). The twigs collected were cut into small pieces, dried at room temperature and powdered.

2.2. Extraction and Isolation. At room temperature, powdered twigs (1.5 kilograms) were extracted by sonication in MeOH:CH2Cl2 (1:1 v/v). The filtrates were concentrated on a rotary evaporator under reduced pressure to yield 300 g of crude extract. A portion of the crude extract (150 g) was subjected to fractionation using hexanes, EtOAc and n-BuOH to afford hexane (30g), EtOAc (25g) and n-BuOH (20g) fractions. The LCMS analyses of the various fractions indicated that the hexane, EtOAc and n-BuOH fractions were rich in secondary metabolites. These fractions were each subjected to silica gel 60 (0.063 – 0.200 mm) column chromatography using hexanes, hexanes-EtOAc gradient systems and EtOAc. Fractions (150) of 150 mL each were collected and concentrated under a vacuum. The hexane fraction afforded four compounds namely; 3-geranyloxyemodine **1** (100 mg), 3-β-fridelanol **2** (10 mg), 3-geranyloxyemodine anthrone **3** (100 mg) and 2-geranylemodine **4** (75 mg). While the EtOAc fraction afforded; 3-geranyloxyemodine **1** (200 mg), 3-geranyloxyemodine anthrone **3** (200 mg), 2-geranylemodine **4** (150 mg) Acetylvismione D **5** (25 mg), Betulinic acid **6** (250mg), Ursolic acid **7** (250 mg). The n-butanol fraction afforded Emodine **8**(100mg)

3-geranyloxyemodine: Orange powder; 120^{0}C; Hexane-Ethyl acetate 4%; LR-MS *m/z*: 406.03 (calcd for $C_{25}H_{26}O_5$, 406.02). The 1D NMR spectra show complete agreement with those reported in the literature [15] (See supplementary information)

3-β-fridelanol: White powder; 60^{0}C; eluting using Hexane-Ethyl acetate 5%; LR-MS *m/z*: 428.40 (calcd for $C_{30}H_{52}O$, 428.38). The 1D NMR spectra show complete agreement with those reported in the literature [15] (See supplementary information)

3-geranyloxyemodine anthrone: Yellow powder; 118^{0}C; eluting using Hexane-Ethyl acetate 6%; LR-MS *m/z*: 392.07 (calcd for $C_{25}H_{28}O_4$, 392.05). The 1D NMR spectra show complete agreement with those reported in the literature [15] (See supplementary information)

2-geranylemodine: Yellow powder; 78-80^{0}C; eluting using Hexane-Ethyl acetate 7%; LR-MS *m/z*: 406.02 (calcd for $C_{25}H_{26}O_5$, 406.01). The 1D NMR spectra show complete agreement with those reported in the literature [15] (See supplementary information)

Acetylvismione D: Yellow powder; 216^{0}C; eluting using Hexane-Ethyl acetate 15%; LR-MS *m/z*: 452.07 (calcd for $C_{27}H_{32}O_6$, 452.05). The 1D NMR spectra show complete agreement with those reported in the literature [15] (See supplementary information)

Betulinic acid: White powder; 288^{0}C; eluting using Hexane-Ethyl acetate 25-27%; LR-MS *m/z*: 456.20 (calcd for $C_{30}H_{47}O_3$, 256.20). The 1D NMR spectra show complete agreement with those reported in the literature [15] (See supplementary information)

Ursolic acid: White powder, 270^{0}C; eluting using Hexane-Ethyl acetate 40-60%; LR-MS *m/z*: 456.35 (calcd for $C_{30}H_{48}O_3$, 456.33). The 1D NMR spectra show complete agreement with those reported in the literature [15] (See supplementary information)

Emodine: Yellow powder; 240^{0}C; eluting using Hexane-Ethyl acetate 20%; HR TOF-MS ESI *m/z*: 270.045 corresponding to $C_{15}H_{10}O_5$. The 1D NMR spectra show complete agreement with those reported in the literature [15] (See supplementary information)

2.3. Biological screening.

2.3.1 Cytotoxicity

Cytotoxicity was determined through cells plated in 96-well plates (Nest Scientific) at a density of 2000 cells per well in 100 μL of media per well. On the following day, the media was aspirated, and 100 μL of media in which a serial dilution of DMSO-dissolved compound (or DMSO as a control) was added to wells in triplicate. Three days later, the relative number of metabolically active cells was determined by the addition of the CellTiter-Glo reagent (Promega) and measurement of chemiluminescence according to the manufacturer's protocol using a Fluoroskan Ascent FL

(Thermo Scientific). To calculate the percent viability, the signal from background wells (media only) was subtracted from each well, and then the remaining chemiluminescence value was normalized to the signal from wells with the equivalent amounts of DMSO. Graphing was done using GraphPad Prism 6 (GraphPad Software). IC_{50} values were calculated by fitting a non-linear curve using the "log-inhibitor vs normalized response" function given by the equation Y=100/{1+10[(X-LogIC50)]}.

2.3.2 Lipoxygenase inhibitory activity

Lipoxygenase (LOX) inhibiting activity was measured by modifying the spectrophotometric method developed by Tappel [16]. Lipoxygenase solution was prepared so that the reaction mixture's enzyme concentration was adjusted to a 0.05 absorbance/min rate. The reaction mixture comprised 160 µL of 100mM sodium phosphate buffer at pH 8, 10 µL of the test solution and 20 µL of LOX solution. The contents were mixed and incubated for 10 min at 25 °C. It was then initiated by adding 10 µL substrate solution (linoleic acid, 0.5mM, 0.12 %w/v tween 20 in a ratio of 1:2) and the change in absorbance at 234 nm was followed for 6 min. The concentration of the test compound that inhibited lipoxygenase activity by 50 % (IC_{50}) was determined by monitoring the effect of increasing concentrations of these compounds in the assays on the degree of inhibition. The IC_{50} values were calculated using EZ-Fit, Enzyme kinetics Program (Perrella Scientific In., Amhherset, USA).

2.3.3 Evaluation of urease inhibition activity

Urease (Jack bean) solution (25 µl) was mixed with the 5 µl compound (500 µg) and incubated at 30°C for 15 min. Aliquots were taken and immediately transferred to assay mixtures containing urea (100mM) in buffer (40 µl) and re-incubated for 30 min in 96 well plates. The indophenol method determined urease activity based on measuring ammonia produced [17]. 50 µl each of phenol reagent (1% w/v phenol and 0.005% w/v sodium nitroprusside) and 70 µl of alkali reagent (0.5% w/v NaOH and 0.1% active chloride NaOCl) were added to wells. An increase in absorbance was measured after 50 min at 630 nm on a microtitre plate reader (Spectramax Plus 384 Molecular Device, USA). The final volume of the reaction is 200 µl at pH 8.2 (0.01 M K_2HPO_4. $3H_2O$, 1mM EDTA and 0.01 M $LiCl_2$). All reactions were performed in triplicates. The standard used in this assay was Thiourea, and percentage inhibitions were calculated by the formula:

$$\% \text{ inhibition} = 100 - \left[\frac{\text{Optical Density of test cpd}}{\text{Optical Density of control(with no cpd)}} \right]$$

2.3.4 Determination of DPPH radical scavenging activity

1, 1-diphenyl-2-picrylhydrazyl radical (DPPH) is a quick method most researchers use to determine antioxidant activities.

The free radical scavenging activity was measured by 1, 1-diphenyl-2-picryl-hydrazine (DPPH) [18]. DPPH solution (0.3mM) was prepared in ethanol. The activity was measured in different concentrations of each compound ranging 62.5 µg- 500 µg. 5 µl of different concentrations ranging (62.5 µg - 500 µg) of each sample was mixed with 95 µl of DPPH solution in ethanol. The prepared dilutions were dispersed in 96 well plate and incubated at 37°C for 30 min. The absorbance was measured at 515 nm in microtitre plate reader (Spectramax Plus 384 Molecular Device, USA). The percent radical scavenging activity of root extracts was determined against methanol treated control.

$$\text{DPPH Scavenging effect (\%)} = \frac{Ac - As}{Ac} \times 100$$

Where:

Ac = Absorbance of Control (DMSO treated)

As = Absorbance of Sample

Molecular docking studies

Molecular docking studies were performed using AutoDock 4.2 software [19, 20] to study the molecular interaction and binding mode of the purified compounds. For this purpose, the crystal structure of human lipoxygenase (PDB code: 3V99) was obtained from the protein data bank (http://www.rcsb.org). All water molecules of 3V99 were removed. The polar hydrogen atoms, Kollman and Gasteiger charges, were added to the protein structure's amino acid residues using AutoDock Tools (ADT, version 1.5.6) [21]. The 3D molecular structures of the compounds were optimized using ChemDraw 3D. Then, the required AutoDock format (pdbqt) of the receptor and ligands were obtained using AutoDock Tools 1.5.6. A total of 200 docking calculations of the purified compounds were carried out using the Lamarckian genetic algorithm method (LGA). The population size, the maximum number of evaluations (medium), and the maximum generation were set at 150; 2,500,000 and 27,000, respectively. The grid box was

centered on the enzyme's active site with x, y, and z coordinates of 17.778 -80.36, -30.62 Å. The number of points in the x, y and z dimensions was 40 × 50 × 50. The spacing between grid points was set at 0.375 Å. The molecular visualizations were executed in Python3.4.

2.4. X-ray Crystallographic Analysis. Red crystals of compound **1** were obtained from AcOEt-hexanes. Data for complex **1** were collected at 150 K on a Bruker D8 Quest with IμS microfocus source using Mo Kα radiation (λ = 0.71073 Å). The structure was solved by direct methods and refined by full-matrix least-squares refinement on F2 after multiscan absorption correction of the data using SADABS [22,23]. Data was processed using the Bruker AXS SHELXTL software, version 6.14 [24]. Crystallographic data of **1**: C25 H26 O5 (M = 406.46); Triclinic crystal (0.358 x 0.101 x 0.040 mm^3); space group P-1; unit cell dimensions a = 4.5662(6) Å, b = 12.7014(19) Å, c = 18.1090(2) Å, α= 100.464(7)°, β = 93.846(5)°, γ=95.467(4)°, V = 1024.3(2) $Å^3$; Z = 2; ρ_{calcd} = 1.318Mg/m^3; μ = 0.091 mm^{-1}; 15 280 reflections measured (2.557° ≤ θ ≤ 28.354°), 4925 unique (Rint = 0.0590), which were used for all calculations; the final refinement produced R1 = 0.0852, wR2 = 0.1932 (all data); and R indices (all data) R1 = 0.1604, wR2 = 0.2299. The crystallographic data of **1** were deposited at the Cambridge Crystallographic Data Centre under deposition number CCDC 2022971. Copies 18 of the crystallographic data can be obtained for freefrom the Cambridge Crystallographic Data Centre, 12 Union Road,Cambridge CB2 1EZ, UK e-mail: deposit@ccdc.cam.ac.uk or fax:(+44) 1223-336-033] or by www.ccdc.cam.ac.uk/conts/retrieving.html

3. RESULTS AND DISCUSSION

The air-dried twigs of *Psorospermum guineense* used in traditional medicine to treat cancer (1.5 Kg) were extracted using a mixture of CH_2Cl_2-MeOH (1:1) in a sonicator bath to afford 300 g of extract. 150 g of the extract was partitioned using hexanes, EtOAc and n-BuOH to afford hexane (30 g), EtOAc (25 g) and n-BuOH (20 g) fractions. Analysis of the high-resolution LC-MS of the various fractions revealed the presence of different compounds. The major compounds were isolated from these fractions, characterized based on the interpretation of their 1D and 2D NMR values, and compared with those described in the literature. The hexane extract was subjected to repeated column chromatography to yield 3-geranyloxyemodine **1**, 3-β-fridelanol **2**, 3-geranyloxyemodine anthrone **3** and 2-geranylemodine **4**, the EtOAc fraction afforded; 3-geranyloxyemodine **1**; 3-geranyloxyemodine anthrone **3**, 2-geranylemodine **4**, Acetylvismione D **5**, Betulinic acid **6**, and Ursolic acid **7** while the n-butanol fraction afforded 3-geranyloxyemodine **1**, 3-β-fridelanol **2**, 3-geranyloxyemodine anthrone **3** and 2-geranylemodine **4**, Acetylvismione D **5** and Emodine **8**. See Figure 1[15]. The stereochemistry of the double bonds and conformation of the geranyl moiety of compound **1** was attributed based on single crystal x-ray analyses (Figure 2).

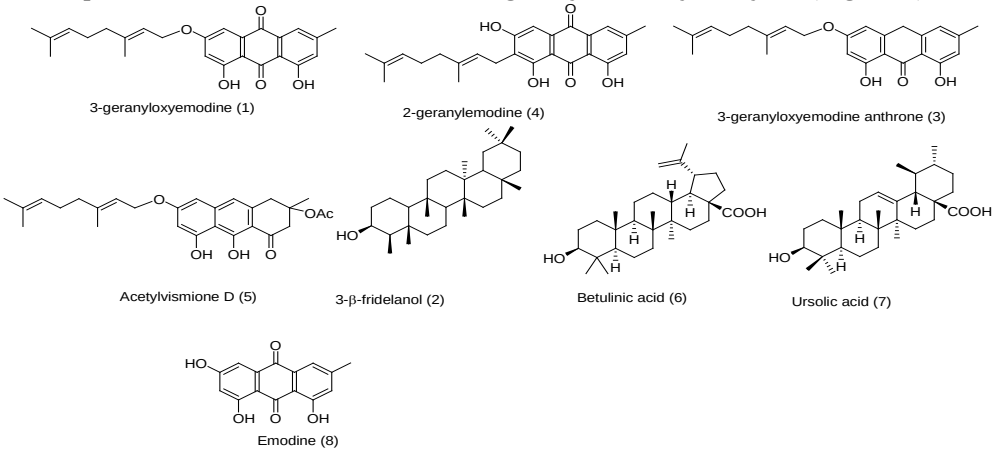

Figure 1: Isolates from the Hexane, EtOAc and nBuOH extracts of the twigs of *Psorospermum guineense* [15].

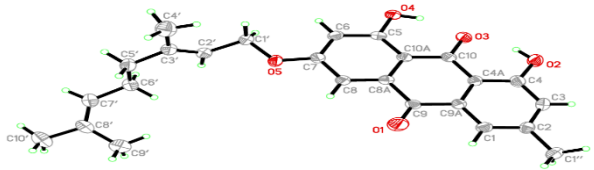

Figure 2: Single crystal X-ray structure of 3-geranyloxy Emodine **1**

The relative viability of the MDA-MB-231 breast cancer cell line exposed to these compounds at multiple concentrations was analyzed to ascertain if any of the isolates exhibited cytotoxic activity. MDA MB 231 cells were plated in a 96-well format. The indicated compounds, dissolved in DMSO, were serially diluted in culture media prior

to addition to the culture. After a 3-day incubation time, relative viability was indirectly determined by measuring total ATP in each well using CellTiter-Glo (Promega, Figure 3). Following this assay, the IC_{50} value was determined with 95% confidence interval. Several compounds showed moderate cytotoxic activity against MDA-MB-231 breast cancer cells. Compound **7** (ursolic acid) gave the best activity with an IC_{50} of 9.88 µM and 95% CI of 9.03- 10.5 µM.

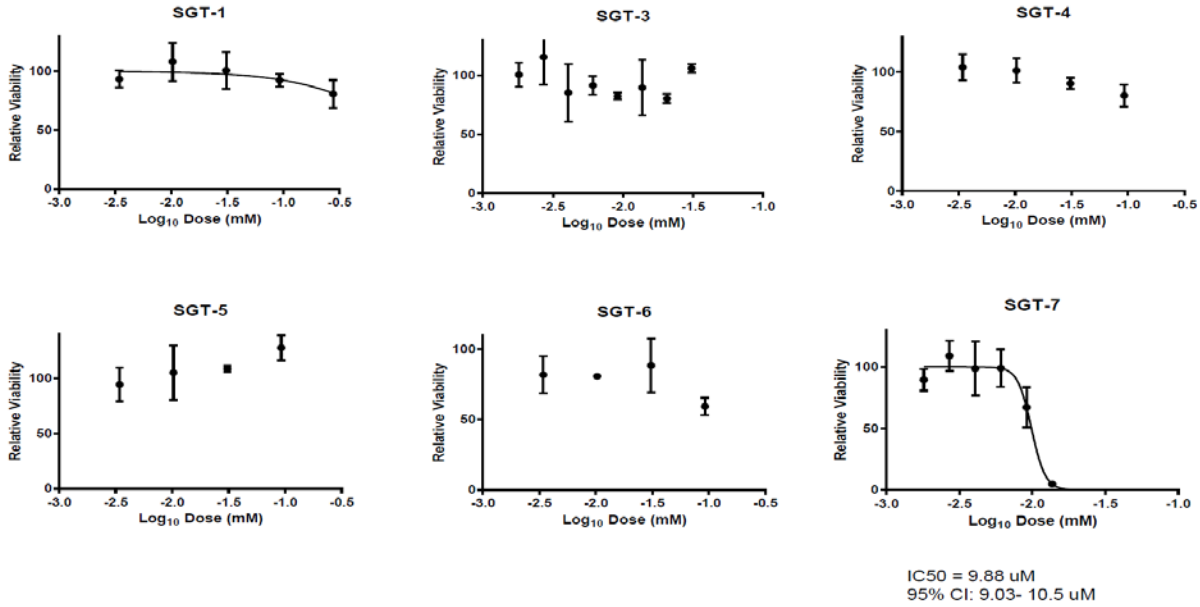

Figure 3: Cytotoxic activity of compounds **1** and **3-7**

To get a deeper insight on the possible mechanism of action, these compounds were tested on some known cancer targets [16].

The isolated compounds were equally tested for their LOX inhibitory activity, antioxidant activity and urease inhibition activity. The quinone, Acetylvismione D **5** exhibited better lipoxygenase inhibitory activity (19.8±0.16 µM) and antioxidant activity (20.8±0.15 µM) compared to the reference drugs baicalein (22.6 ± 0.08 µM) and Beta hydroxyl acid (BHA) (44.2 ± 0.07 µM) respectively. None of these compounds were more active than Thiourea for urease inhibition activity. The rest of the isolated compounds showed moderate activity, as shown in Table 1. All of the isolates exhibited their inhibitory activity in a concentration-dependent manner. Baicalein (IC_{50} = 22.6 ± 0.08 µM). Beta hydroxyl acid (BHA) (44.2 ± 0.07 µM) and Thiourea (24.2± 0.09 µM) were used as a positive control.

Table 1 Antioxidant activity, lipoxygenase inhibitory activity and urease inhibition activity of compounds from the twigs of *Psorospermum guineense*[a]

Sr. #	Compound	Antioxidant Activity IC_{50} value (µM)	Lipoxygenase Inhibition Activity IC_{50} value (µM)	Urease Inhibition Activity IC_{50} value (µM)
1.	**SGT 1 (1)**	85.6 ± 0.05	98.6 ± 0.36	65.6± 0.17
2.	**SGT 2 (2)**	25.7± 0.11	28.7± 0.81	55.1± 0.82
3.	**SGT 3 (3)**	53.4± 0.29	76.6± 0.93	52.1± 0.71
4.	**SGT 4 (4)**	35.6± 0.86	38.9± 0.25	44.8± 0.16
5.	**SGT 5 (5)**	20.8± 0.15	19.8± 0.16	38.9± 0.18
6.	**SGT 6 (6)**	78.8± 0.79	91.1± 0.77	66.5± 0.22
7.	**SGT 7 (7)**	79.7± 0.57	87.7± 0.10	81.6± 0.30
8.	**BHA**	44.2 ± 0.07	-	
9.	**Baicalein**[b]	-	22.6 ± 0.08	
10.	**Thiourea**			24.2± 0.09

[a] Values are the mean ± SEM of three experiments ($p < 0.05$).
[b] Positive control

Some significant results of the *in silico* studies are summarized in Table 2. The experimental IC_{50} values of isolates revealed that the better LOX result was obtained for compound **5** (Table 1). This is in agreement with the estimated free energies of binding of compound **5** and Baicalein (Table 2). Docking analysis showed that, the compound **5** created conventional H-bonding, carbon-H bond, Pi-Pi T-shape, alkyl and Pi-alkyl interactions with amino acids in the active site of LOX (Fig. 5) and had lowest binding affinity (ΔG Binding = -8.14 kcal/mol). Also, docking studies indicated that Baicalein had no carbon-H bond but Van der Waals, conventional H-bonding, Pi-donor H-bond, Pi-Lone Pair, Pi-Pi T-shaped, Amide Pi-stacked and Pi-alkyl interactions with amino acids of the active site residues of LOX (Fig. 4) and had higher binding affinity (ΔG Binding = - 7.81 kcal/mol),

Table 2 Summarizing the important docking results. The H-bond distances have been measured between related atoms

Compound	**Estimated $\Delta G_{Binding}$ (kcal/mol)**	**Hydrogen bonding**		
		Interacted ligand functional group	**Interacted amino acid**	**Distance (Å)**
3-geranyloxyemodine	- 7.81	C=O	ALA 672	2.76
2-geranylemodine	- 8.76	OH C=O	ALA 672 GLN 557	2.03 2.74
3-geranyloxyemodine anthrone		C=O	PHE 177	2.68
Acetylvismione D	- 8.14	O	PHE 177	2.67
3-β-fridelanol	- 9.02	OH	ASN 554	1.81
Betulinic acid	- 9.17	OH	ASN 554	2.27
Ursolic acid	- 9.79	COOH OH	PHE 177 ASN 554	2.63 1.89
Baicalein	- 7.81	OH	VAL 671 ALA 672	1.95 2.00

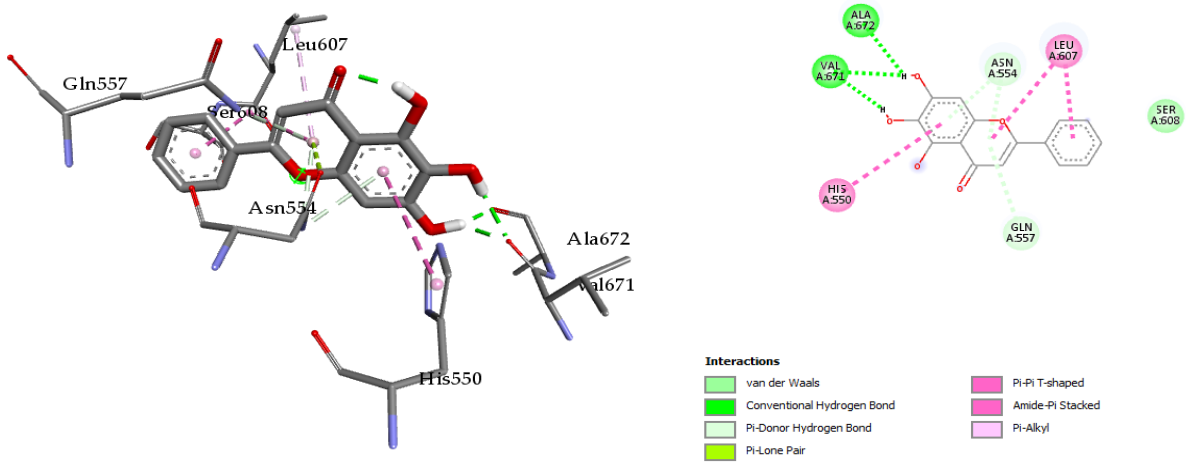

Figure 4 Interactions between Baicalein and the active site of the 3V99

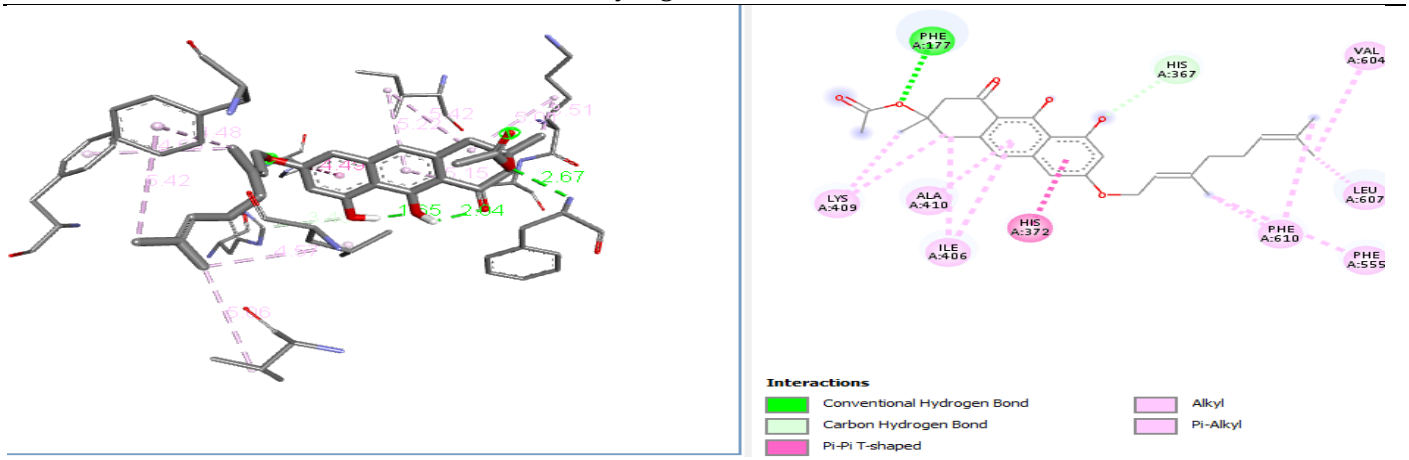

Figure 5 Interactions between Acetylvismione D and the active site of the 3V99

4. DISCUSSION

Antioxidants can track down and neutralize free radicals preventing chain reactions which can cause cancer. More body cells are kept healthy and less susceptible to cancer. Lipoxygenases or ureases could cause oxidative stress or inflammation.

LOX-mediated products elicit diverse biological activities needed for neoplastic cell growth, influencing growth factor and transcription factor activation, oncogene induction, tumour cell adhesion stimulation, and apoptotic cell death regulation [25]. Agents that block LO-catalyzed activity may effectively prevent cancer by interfering with signalling events needed for tumour growth. Enzyme activity inhibitors may be better candidates for chemopreventive intervention, because these enzymes' inhibition directly reduces fatty acid metabolite production, with concomitant damping of the associated inflammatory, proliferative, and metastatic activities that contribute to carcinogenesis. So, the discovery of new lipoxygenase inhibitors with more inhibitory activity is needed. In fact, in a few studies, LOX inhibitors have prevented carcinogen-induced lung adenomas and rat mammary gland cancers [25]. Bacteria can produce urease, which is a major virulence factor that may also play a role in carcinoma development.

To explore the activities of the present compounds and binding interactions between ligands and lipoxygenase, the structures of isolated compounds (**1-8**) were docked into the active site of LOX (PDB code: 3V99). The structure and conformation of compound **1** was unambiguously confirmed from single crystal analysis. The analysis revealed that the geranyl group was not a linear chain. This conformation was a very important factor which was considered for the docking.

5. CONCLUSION

In our attempts to isolate natural products for drug discovery and development from a rational viewpoint, the cancer disease, its mode of inhibition (antioxidant) or possible targets (lipoxygenase or urease) was evaluated. Bioactive constituents have been isolated from the twigs of *Psorospermum guineense*, the stereochemistry and conformation of the geranyl sub unit of compound **1** were established from single crystal x-ray analysis, and the isolates evaluated for their biological activities. Ursolic acid **7** was the most active compound tested for triple-negative breast cancer. All the quinolic derivatives (1-4) tested showed better antioxidant activity than BHA, which was used as a reference drug. The lipoxygenase (15-LOX) inhibitory activity of the isolated compounds was investigated for the first time with Acetylvismione D showing the best activity with IC_{50} value in the micromolar range. *In silico* study of isolated compounds showed possible binding modes on the enzyme target lipoxygenase (15-LOX) (Observed were conventional H-bonding, carbon-H bond, Pi-Pi stacked, alkyl and Pi-alkyl interactions between enzyme-substrate.) and confirmed the experimental results. Also, the molecular docking analysis confirmed the potential of the studied compounds for future drug discovery investigations. Further QSAR and kinetic studies are needed to understand the inhibitory mechanism of corresponding compounds and relative derivatives.

Acknowledgements We are grateful to TWAS-ICCBS Scholarship program to Ghansenyuy Salome Yuwong at the International Center for Chemical and Biological Sciences, University of Karachi- Karachi, Pakistan

References

1. R. Siegel, K. Miller, N. Wagle, and A. Jemal, Cancer J. Clin. 73(1):17-48, **(2023)**
2. T. Omara, A. K.Kiprop, R. C.Ramkat, J. Cherutoi, S. Kagoya, D. M.Nyangena, T. A.Tebo, P. Nteziyaryemye, L. N.Karanja, A. Jephchirchir, A. Maiyo, B. J.Kiptui, I. Mbabazi, C. K.Nakiguli, B. V. Nakabuye, Koske, M. Chepkemoi, Evid-Based.Compl.Alternat.Med. 20, 1-26. **(2020)**
3. P. Guglielmelli, C. Maccari, B. Sordi, M. Balliu, A. Atanasio, C. Mannarelli, G. Capecchi, I. Sestini, G. Coltro, G. G.Loscocco, G. Rotunno, E. Angori, F. C.Borri, A. Tefferi, A. M.Vannucchi, Blood.Cancer.J. 13, 21. **(2023).**

4. E. Liu, N. Becker, P. Sudha, C. Dong, Y. Liu, J. Keats, G. Morgan, B. Walker, Blood.Cancer.J. 13, 16. **(2023).**
5. A. J.Muller, S. Thomas, and G. C.Prendergast, Cancer J. 29(1):34-37, **(2023)**
6. https://www.wcrf.org/cancer-trends/worldwide-cancer-data/
7. https://www.who.int/news-room/fact-sheets/detail/cancer.
8. https://www.theeastafrican.co.ke/scienceandhealth/Prevalence-of-cancer-is-on-the-rise-in-EA-despite-progress/3073694-4994142-12rle39/index.html.
9. C. Nguyen, A. Mehaidli, K. Baskaran, S. Grewal, A. Pupulin, I. Ruvinov, S. Pandey, Evid-Based.Compl.Altern.Med. 19, 1-12. **(2019)**
10. D. O.Ochwang'i, C. N.Kimwele, J. A.Oduma, P. K.Gathumbi, J. M. Mbaria, S. G.Kiama, Ethnopharmacol. 151, 1040-1055. **(2014)**
11. D. Z.Matata, O. D.Ngassapa, F. Machumi, M. J.Moshi, Evid-Based.Compl.Altern.Med. 201, 1-16. **(2018)**
12. R. Kaur, K. Kapoor, H. Kaur, J.Nat.Prod.Plant.Resour. 1, 119-124. **(2011)**
13. I. Tasius, British.J.Pharm.Res. 6, 214-227. **(2015)**
14. F. Epifano, S. Fiorito, S. Genovese, Phytochem.Rev. 12, 673–684. (2013)
15. B. N.Lenta, K. P.Devkota, S. Ngouela, F. F.Boyom, Q. Naz, M. I. Choudhary, E. Tsamo, P. J.Rosenthal, N. Sewald, Chem.Pharm.Bull. 56, 222-226. **(2008)**
16. A. L.Tappel, Vita.Horm. 20, 493-510. **(1962)**
17. M. W.Weatherburn, Anal.Chem. 39, 971- 974. **(1967)**
18. N. Cotelle, J. L.Bernier, J. P.Catteau, J. Pommery, J. C.Wallet, E. M. Gaydou, Free.Rad.Biol.Med. 20, 35-43. **(1996)**
19. G. M.Morris, D. S.Goodsell, R. S.Halliday, R. Huey, W. E.Hart, R. K.Belew, A. J.Olson, J.Comput.Chem. 19, 1639–1662. **(1998)**
20. C. S. Sundaram, L. Krishnasamy, T. Ramesh, M. Mohanapriya, U.S. M.Rao and M. Iqbal, Pak. J. Chem. 12(1):08-12, **(2022)**
21. M. F.Sanner, J.Mol.Graph.Model, 17, 57–61. **(1999)**
22. BRUKER APEX2 (version 1.0-28) and SAINT-PLUS (version 6.25) Bruker AXS Inc.: Madison, WI, USA, **(2003)**
23. G. M.Sheldrick, SHELXS97 and SHELXL97, University of Gottingen: Germany, **(1997)**
24. G. M.Sheldrick, SHELXTL Version 6.14; Bruker AXS, Inc.: Madison, WI, USA, **(2000)**
25. E. S.Vernon, A. H.Cathy, T. H.Ernest, K. Levy, A. L.Ronald, A. C.James, C. S.Caroline, J. K.Gary, Cancer.Epidem.Bio.Prev. 8, 467– 483. **(1999)**

Received: 12th December 2022 **Accepted: 5th February 2023**

European Journal of Medicinal Chemistry Reports 9 (2023) 100108

HOSTED BY

Contents lists available at ScienceDirect

European Journal of Medicinal Chemistry Reports

journal homepage: www.editorialmanager.com/ejmcr/default.aspx

Lipoxygenase inhibition and molecular docking studies of secondary metabolites from the leaves of *Alstonia scholaris*

Salome Y. Ghansenyuy [a], Kenneth O. Eyong [a,*], Pierre Yemback [a], Lateef Mehreen [b], Vincent de Paul N. Nziko [c], Muhammad S. Ali [d], Gabriel N. Folefoc [a]

[a] Department of Organic Chemistry, Faculty of Science, University of Yaounde I, P.O. Box 812, Yaounde, Cameroon
[b] Department of Biochemistry, Bahria University Medical and Dental College, Bahria University, Karachi, Pakistan
[c] Department of Chemistry, Hampton University, Hampton, VA, 23668, USA
[d] H.E.J. Research Institute of Chemistry, International Center for Chemical and Biological Sciences, University of Karachi, Karachi, 75270, Pakistan

ARTICLE INFO

Keywords:
Alstonia scholaris
Lipoxygenase
Cancer
Docking study
β-Sitosterol glucoside
Scholaricine

ABSTRACT

The phytochemical study was carried out on the ethanolic extract of the leaves of *Alstonia scholaris*. This plant has been used traditionally for medicinal purposes in the treatment of several diseases such as cancer, jaundice, malaria, gastrointestinal troubles, dysentery, snake-bite and diarrhea. Chromatographic purification of this extract led to the isolation and characterization of nine compounds. Their structures were elucidated as betulin (**1**), α-amyrin acetate (**2**), mixture of β-sitosterol (**3**) and stigmasterol (**4**), tetratriacontyl-trans-*p*-coumarate (**5**), ursolic acid (**6**), picralstonine (**7**), β-sitosterol glucoside (**8**) and scholaricine (**9**). Scholaricine and *β*-sitosterol-glucoside exhibited potent lipoxygenase inhibitory activity with IC_{50} of 15.2 ± 0.41 and 18.5 ± 0.14 respectively compared to Baicalein (22.6 ± 0.08) used as positive control. Molecular docking studies were conducted to support lipoxygenase inhibitory activities of the test compounds.

1. Introduction

The genus *Alstonia* (Apocynaceae) comprises about 60 species [1]. Previous chemical studies of *A. scholaris* revealed the presence of alkaloids [2], triterpenes [3] and phenolics compounds [1]. Biological activities such as anti-inflammatory, analgesic, antidiabetic, antioxidant, antimalarial, anticancer and cytotoxic have been reported for various species from the genus *Alstonia* [4–6]. Lipoxygenase (LOX) mediated products elicit diverse biological activities needed for neoplastic cell growth, influencing growth factor and transcription factor activation, oncogene induction, stimulation of tumor cell adhesion, and regulation of apoptotic cell death [7]. Agents that block LOX-catalyzed activity effectively prevent cancer by interfering with signaling events needed for tumor growth. Enzyme activity inhibitors may be better candidates for chemopreventive intervention because these enzymes' inhibition directly reduces fatty acid metabolite production, with concomitant damping of the associated inflammatory, proliferative, and metastatic activities that contribute to carcinogenesis. So, the discovery of new lipoxygenase inhibitors with more inhibitory activity is needed. In fact, in a few studies, LOX inhibitors have prevented carcinogen-induced lung adenomas and rat mammary gland cancers [7].

In our attempts to isolate natural products for drug discovery and development from a rational approach as a part of a laboratory project on re-investigating medicinal plants, we initiated a study to isolate constituents of *A. scholaris*, with biological activity and search for potential targets or mode of action studies. In this paper, we have reported on the phytochemical studies of the leaves of *A. scholaris*, and their lipoxygenase enzyme inhibition activities. Moreover, molecular docking studies to support the better lipoxygenase inhibitory activities of the test compounds were also conducted.

2. Materials and methods

2.1. General experimental procedures

NMR spectroscopic data were recorded on Bruker AMX 600 MHz spectrometers (^{1}H: 600 MHz, ^{13}C: 150 MHz). HR-TOF-ESI-MS were calculated on an Applied Biosystems QSTAR XL LC-MS-MS spectrometer. EI-MS were measured on a JEOL MS Route spectrometer (Direct Probe). IR and UV spectra were recorded on JASCO A-302 and Hitachi U-3200 spectrophotometers, respectively. Column chromatography was conducted on silica gel (Kiesegel 60; 70–230 mesh). TLC was carried out on pre-coated silica-gel F254 aluminum sheets (0.25 mm thickness). The

* Corresponding author.
E-mail addresses: eyongkk@yahoo.com, eyongkk@gmail.com (K.O. Eyong).

https://doi.org/10.1016/j.ejmcr.2023.100108
Received 27 April 2023; Received in revised form 9 July 2023; Accepted 18 July 2023
Available online 18 July 2023

List of abbreviations

LOX	Lipoxygenase
NMR	Nuclear Magnetic Resonance
HR-MS	High Resolution Mass Spectrometry
TOF	(Time of flight analyser

spots were detected by heating the cards after spraying with cerium (IV) sulfate reagent. A spectrophotometer (Spectra Max, Molecular Devices, CA, USA) was used to measure enzyme inhibition.

2.2. Chemicals

Chloroform-*d*, methanol-d_4 and pyridine-d_5 used for NMR were purchased from Armar Chemicals. Silica gel (mesh 230–400), DTNB and baicalin were obtained from Merck (Germany).

2.3. Plant material

The leaves of *A. scholaris* were harvested in May 2017 from the University of Karachi campus. The plant was identified by the Plant Taxonomist of the Department of Botany, University of Karachi, Pakistan, where a voucher specimen (No. G.H-94482) has been deposited in the Herbarium.

2.4. Extraction and isolation

The air-dried and powdered leaves of *A. scholaris* (25 Kg) were successively extracted with ethanol (3 × 20 L × 120 h) by maceration at room temperature. The extract was concentrated *in vacuo* to obtain 637 g of dark colored ethanolic extract. To it was added 500 mL of water, acidified with 20.5 mL of 1.5 N H_2SO_4 and extracted with CH_2Cl_2. The organic phase was concentrated to afford the non-alkaloid fraction (260 g). The aqueous phase was basified with 500 mL of 3 N Na_2CO_3 to release the alkaloids which were then extracted with CH_2Cl_2. Concentration of the resulting organic phase afforded 9.33 g of the alkaloid fraction, while the aqueous fraction upon treatment with n-butanol afforded 40 g of the n-butanol fraction. The non-alkaloid fraction was subjected to column chromatography eluting with mixtures of n-hexane-EtOAc to afford 20 fractions F_1–F_{20}.3.55 g of F_1 fraction was infused in 3–4% n-hexane/EtOAc for about 9 h and to produce 0.5 g of a white substance. The resulting white substance was filtered and washed with hexane and called betulin (**1, 500 mg**). 5 g of F_2 fraction was purified by soaking it in hexane to give α-amyrin acetate (**2, 300 mg**). Column chromatography of 8 g of fraction F_3 using hexane-EtOAc as eluent afforded a 20 mg of β-sitosterol (**3**) and stigmasterol (**4**) mixture and tetratriacontyl-trans-*p*-coumarate (**5, 18 mg**). Another column chromatography of 8.9 g of fraction F_9 using hexane-EtOAc as eluent afforded ursolic acid (**6, 20 mg**). Column chromatography of 20 g of fraction F_{17} using hexane-EtOAc as eluent afforded picralstonine (**7, 10 mg**) and β-sitosterol glucoside (**8, 3 mg**). Finally, column chromatography of the 6.9 g of alkaloid fraction using DCM-MeOH as eluent afforded scholaricine (**9, 8 mg**).

Compound 1 or betulin: White powder, 284 °C; eluting using Hexane-Ethyl acetate 20%; EI *m/z*: 442.3 corresponding to $C_{30}H_{50}O_2$. ^{1}H NMR ($CDCl_3$/MeOH-d_4, 500 MHz): δ = 4.61–4.60 (each 1H, d, *J* = 1.5Hz, H-29), 3.71 and 3.32 (each 1H, m, H-28), 3.21 (1H, m, H-3), 2.84 (1H, m, H-19), 1.77 (3H, s, H-30), 0.88, 0.86 and 0.85 (each 3H, s, 3xCH_3), 0.73 (3H, s, CH_3), 0.65 (3H, s, CH_3);

^{13}C NMR ($CDCl_3$, 125 MHz): δ = 198.4 (C, C-30), 180.9 (C, C-28), 148.3 (C, C-20), 105.8 (CH_2, C-29), δ = 79.01 (C, C-3). The 1D and 2D NMR spectra show complete agreement with those reported in the literature [1–3]. (See supplementary information).

Compound 2 or α-amyrin acetate: White powder, 186 °C; eluting using Hexane 100%; EI *m/z*: 468.3 corresponding to C $_{32}H_{52}O_2$. ^{1}H NMR ($CDCl_3$/MeOH-d_4, 500 MHz): δ = 5.01 (1H, m, H-12), 4.44 (1H, d, *J* = 9Hz, H-3), 2.00 (3H, s, $COOCH_3$-3), 1.02, 0.96 and 0.93 (each 3H, s H-27, 26, 25), 0.88 (3H, br s, H-30), 0.83, 0.82, 0.75 (each 3H, s, H-24, 23, 28), 0.74 (3H, d, 4Hz, H-29);

The 1D and 2D NMR spectra show complete agreement with those reported in the literature [1–3]. (See supplementary information).

Compounds 3 or β-sitosterol: White powder, 135–137 °C; eluting using Hexane/Ethyl acetate 4%; EI *m/z*: 414.3 corresponding to $C_{29}H_{50}O$. ^{1}H NMR ($CDCl_3$, 500 MHz): δ = 5.37 (t, 1 H, J = 6,4 Hz), 3.54 (1H, m, H-3), 1.4 (3H s, H-29), 0.91 (3H, d, *J* = 6.5 Hz, H-19), 0.83 (3H, d, J = 6,6 Hz, H-26), 0.82 (3H, d, *J* = 6.4 Hz, H-27), 0.70 (3H, s, H-28).

^{13}C NMR ($CDCl_3$, 125 MHz): 142.1, 122.1, 71.8, 56.8, 56.1, 50.2, 45.9, 42.3, 39.8, 37.3, 36.5, 36.1, 33.9, 31.9, 31.7, 29.2, 28.2, 26.2, 24.3, 23.1, 21.1, 19.8, 19.2, 19.1, 18.8.

The 1D NMR spectra show complete agreement with those reported in the literature [1–3]. (See supplementary information).

Compounds 4 or stigmasterol: White powder, 135–137 °C; eluting using Hexane/Ethyl acetate 4%; EI *m/z*: 412.3 corresponding to $C_{29}H_{48}O$. ^{1}H NMR ($CDCl_3$, 500 MHz): δ = 5.37 (t, 1 H, J = 6,4 Hz), 5.04 and 5.17 (each 1H m, H-20, 21) 3.54 (1H, m, H-3), 1.4 (3H s, H-29), 0.91 (3H, d, *J* = 6.5 Hz, H-19), 0.83 (3H, d, J = 6,6 Hz, H-26), 0.82 (3H, d, *J* = 6.4 Hz, H-27), 0.70 (3H, s, H-28).

The 1D NMR spectra show complete agreement with those reported in the literature [1–3]. (See supplementary information).

Compound 5 or tetratriacontyl-trans-*p*-coumarate: white powder; 240 °C; eluting using Hexane-Ethyl acetate 4%; HR TOF-MS ESI *m/z*: 640.2 corresponding to $C_{43}H_{76}O_3$. ^{1}H NMR ($CDCl_3$, 500 MHz): δ = 7.62 (2H, d, J = 8,5 Hz, H-2, 6), 7.24–6.77 (3H, m, H-3, 5, 7), 5.81 (1H, d, J = 8,5 Hz, H-8), 4.99 (1H, s, 4-OH), 4.09 (2H, t, *J* = 6.5 Hz, H-1'), 0.86 (3H, t, *J* = 13.5 Hz, H-32).

The 1D NMR spectra show complete agreement with those reported in the literature [1–3]. (See supplementary information).

Compound 6 or ursolic acid: White powder; 285–290 °C; eluting using DCM/M 1%; EI-MS *m/z*: 456.2 corresponding to $C_{30}H_{40}O_3$. ^{1}H NMR (Pyr-d_5, 500 MHz): δ = 5.50 (1H, br s, H-12), 3.44 (1H, d, *J* = 8.0, 12.0 Hz, H-3), 2.65 (1H, d, *J* = 14.0 Hz, H-18), 1.23 (3H, d, *J* = 9.0 Hz, H-30), 1.03 (3H, d, *J* = 8.0 Hz, H-29), 1.02, 0.96 and 0.93 (each 3H, s H-27, 26, 25), 0.88 (3H, br s, H-30), 0.83, 0.82, 0.75 (each 3H, s, H-24, 23, 28), 0.86 (3H, s, H-25).

^{13}C NMR (MeOH-d_4, 125 MHz):178.7, 138.6, 125.0, 77.3, 55.3, 52.8, 47.5, 47.3, 42.1, 39.0, 38.9, 38.8, 38.7, 36.9, 36.8, 33.2, 28.7, 27.5, 23.7, 23.3, 21.5, 18.5, 17.5, 17.4, 16.5, 15.7.

The 1D NMR spectra show complete agreement with those reported in the literature [1–3]. (See supplementary information).

Compound 7 or picralstonine: Greenish brown powder, 519.5 °C; eluting using DCM/MeOH 2%; EI *m/z*: 338.2 corresponding to $C_{20}H_{22}N_2O_3$. ^{1}H NMR (C_3D_6O, 500 MHz): δ = 7.05–6.65 (4H, m, H-9, 10, 11, 12), 6.74 (1H, s, NH), 5.23 (1H, m, H-18), 4.69 (1H, d, *J* = 2 Hz, H-5), 3.50 (3H, s, $COOCH_3$), 1.46 (3H, d, *J* = 7.0 Hz, H-19).

^{13}C NMR (CD_3OD, 125 MHz): δ = 173.9 (CO ester), 149.7 (C-13), 136.6 (C-16), 136.4 (C-), 129.0 (C-11), 125.4 (C-9), 122.1 (C-10), 120.9 (C-18), 111.0 (C-12), 88.1 (C-5), 53.2 (C-20), 53.0 (C-3), 52.0 (C-17, CH_2), 49.8 (C-7), 46.7 C-1', CH_3), 41.0 (C-6, CH_2), 32.2 (C-15), 26.6 (C-14, CH_2), 13.2 (C-19, CH_3).

The 1D NMR spectra show complete agreement with those reported in the literature [1–3]. (See supplementary information).

Compound 8 or β-sitosterol glucoside: Brownish-black powder; >212 °C; eluting using DCM/M 5%; EI-MS *m/z*: 576.8 corresponding to $C_{35}H_{60}O_6$. ^{1}H NMR (CD_3OD, 500 MHz): δ = 5.37 (t, 1H, J = 6,4 Hz), 4.89 (1H, m, H-1′), 3.65 (1H, m, H-3), 3.00–4.00 (6H, m, H-2′, H-3′, H-4′, H-5′, H-6'), 0.87–0.97 (12H, m, H-21, H-26, H-27, H-29), 0.71 (3H, s, H-18).

The 1D NMR spectra show complete agreement with those reported in the literature [1–3]. (See supplementary information).

Compound 9 or scholaricine: White powder, 519.5 °C; eluting using Ethyl acetate 100%; EI *m/z*: 356.2 corresponding to $C_{20}H_{24}N_2O_4$. ^{1}H

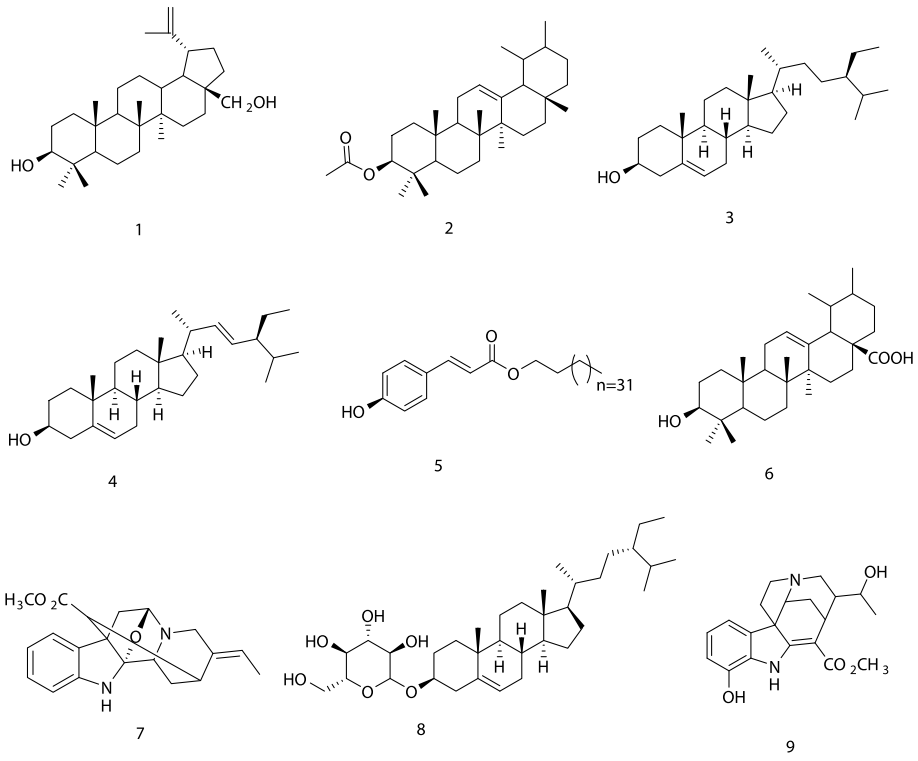

Fig. 1. Structures of isolated compounds.

NMR (C_3D_6O, 500 MHz): δ = 6.90–6.69 (3H, m, H-9, 10, 11), 3.87 (3H, s, OCH_3), 3.40 (1H, d, J = 6.5 Hz, H-18), 1.15 (3H, d, J = 6.5 Hz, H-19).

^{13}C NMR (CD_3OD, 125 MHz): δ = 172.3 (C-2), 170.8 (CO ester), 142.9 (C-12), 138.0, (C-8), 132.4 (C-13), 123.7 (C-10), 116.6 (C-9), 112.2 (C-11), 97.9 (C-5), 69.3 (C-6), 62.3 (C-18), 58.2 (C-7), 54.2 (C-16, CH_2), 52.4 (C-14), 46.7(C-13), 43.7 (C-17), 32.6 (C-5), 29.8 (C-4), 20.2 (C-19, CH_3).

The 1D NMR spectra show complete agreement with those reported in the literature [1–3]. (See supplementary information).

2.5. Lipoxygenase inhibitory activity

Lipoxygenase (LOX) inhibiting activity was measured by modifying the spectrophotometric method developed by Tappel [8]. Lipoxygenase solution was prepared so that the reaction mixture's enzyme concentration was adjusted to a rate of 0.05 absorbance/min. The reaction mixture comprised 160 μL of 100 mM sodium phosphate buffer at pH 8, 10 μL of the test solution and 20 μL of LOX solution. The contents were mixed and incubated for 10 min at 25 °C. It was then initiated by adding 10 μL substrate solution (linoleic acid, 0.5 mM, 0.12 %w/v tween 20 in ratio of 1:2) and the change in absorbance at 234 nm was followed for 6 min. The concentration of the test compound that inhibited lipoxygenase activity by 50% (IC_{50}) was determined by monitoring the effect of increasing concentrations of these compounds in the assays on the degree of inhibition. The IC_{50} values were calculated using EZ-Fit, Enzyme kinetics Program (Perrella Scientific In., Amhherset, USA).

Table 1
Lipoxygenase inhibitory activity of compounds from the ethanolic leaf extract of *A. scholaris*[a].

Compound	IC_{50} (μM)
Betulin (**1**)	65.2 ± 0.29
α-Amyrin acetate (**2**)	68.8 ± 0.15
Mixture of B-Sitosterol (**3**) and Stigmasterol (**4**)	62.5 ± 0.69
Tetratriacontyl-trans-*p*-coumarate (**5**)	57.2 ± 0.28
Ursolic acid (**6**)	32.4 ± 0.21
Picralstonine (**7**)	25.4 ± 0.26
β-Sitosterol glucoside (**8**)	18.5 ± 0.14
Scholaricine (**9**)	15.2 ± 0.41
Baicalein[b]	22.6 ± 0.08

[a] Values are the mean ± SEM of three experiments ($p < 0.05$).
[b] Positive control.

2.6. Molecular docking studies

Molecular docking studies were performed using AutoDock 4.2 software [9] to study the purified compound's molecular interaction and binding mode. For this purpose, the crystal structure of human lipoxygenase (PDB code: 1HU9) was obtained from the protein data bank (http://www.rcsb.org). All water molecules of 1HU9 were removed. The polar hydrogen atoms, Kollman and Gasteiger charges, were added to the protein structure's amino acid residues using AutoDock Tools (ADT, version 1.5.6) [10]. The 3D molecular structures of the compounds were optimized using ChemDraw 3D. Then, the required AutoDock format (pdbqt) of the receptor and ligands were obtained using AutoDock Tools 1.5.6. A total of 200 runs of docking calculations of the purified compounds were carried out using Lamarckian genetic algorithm method (LGA). The population size, maximum number of evaluation (medium), and maximum generation were set at 150, 2,500,000 and 27,000 respectively. The grid box was centered on the enzyme's active site with x, y, and z coordinates of 20.267 6.719, 18.507 Å. The number of points in the x, y and z dimensions was 40 × 40 × 40. The spacing between grid points was set at 0.375 Å. The molecular visualizations were executed in Python3.4.

3. Results and discussion

3.1. Structure elucidation of isolated compounds

The ethanolic extract of the leaves of *A. scholaris* was subjected to silica gel column chromatography and yielded betulin (**1**), α-amyrin acetate (**2**), mixture of β-sitosterol (**3**) & stigmasterol (**4**), tetratriacontyl-

Table 2
Summarizing the important docking results. The H-bond distances have been measured between related atoms.

Compound	Estimated $\Delta G_{Binding}$ (kcal/mol)	Hydrogen bonding		
		Interacted ligand functional group	Interacted amino acid	Distance (Å)
Betulin (1)	+96.16	–	–	–
α-amyrin acetate (2)	+145.73	–	–	–
Ursolic acid (6)	+95.54	–	–	–
Picralstonine (7)	+66.85	NH	HIS 518	2.121
β-sitosterol glucoside (8)	+13.38	–	–	–
Scholaricine (9)	+0.86	NH	GLN 514	2.226
Baicalein	−5.74	–	–	–

trans-*p*-coumarate (**5**), ursolic acid (**6**), picralstonine (**7**), β-sitosterol glucoside (**8**) and scholaricine (**9**) (Fig. 1). Their structures were determined based on 1D and 2D NMR spectra as well as by a comparison of their spectral data with those reported in the literature [2,11,12]. The Compound **5** is reported for the first time from this species.

3.2. Lipoxygenase inhibitory activity

The isolated compounds were tested for their LOX inhibitory activity. The alkaloid, scholaricine (**9**) showed potent enzyme inhibition activity with an IC_{50} value of 15.2 ± 0.41 μM, followed by β-sitosterol glucoside (**8**) (IC_{50} = 18.5 ± 0.14 μM). Significant activities were also exhibited by picralstonine (**7**) and ursolic acid (**6**) with IC_{50} values of 25.4 ± 0.26 μM and 32.4 ± 0.21 μM respectively. The rest of the isolated compounds showed moderate activity as shown in Table 1. All of the isolates exhibited their inhibitory activity in a concentration-dependent manner. Baicalein was used as a positive control (IC_{50} = 22.6 ± 0.08 μM).

3.3. Molecular modeling

To explore the activities of the present compounds and binding interactions between ligands and lipoxygenase, the structures of isolated compounds (**1**–**9**) were docked into the active site of LOX (PDB code: 1HU9) [8–10,13–16]. Some significant results of the *in silico* studies are summarized in Table 2. The experimental IC_{50} values of isolates revealed that the better result was obtained for compounds **8** and **9**. This is in agreement with the estimated free energies of binding of tested compounds (Table 2). Docking analysis showed that of all the isolates, compounds **8** and **9** formed the most stable complexes with the enzyme's active site indicated by their low binding energies (ΔG Binding = + 13.38 and + 0.86 kcal/mol, respectively). These results were in agreement with the experimental IC_{50} values of the isolates summarized in Table 1. Docking studies indicated that only the two alkaloid compounds **7** and **9** formed hydrogen bonds with the active site residues (through the amine hydrogen atom). Inasmuch as compound **7** formed a hydrogen bond with histidine 518 (HIS 518) it also forms 3 unfavorable bumps with the active site of 1HU9 (Fig. 4). This can explain why the complex formed with compound **8** (Fig. 3) is more stable than that formed with compound **7**. The estimated free energies of binding for tested molecules could confirm the experimental results. The standard anti lipoxygenase drug-baicalein, formed two hydrogen bonds with the enzyme's active site, with a very low binding energy but exhibited moderate *in vitro* inhibitory activity.

The analyses also showed that compound **9** formed a hydrogen bond with glutanamine 514 (GLN 514) in the active site of LOX (Fig. 2) while compound **7** did not form hydrogen bonds.

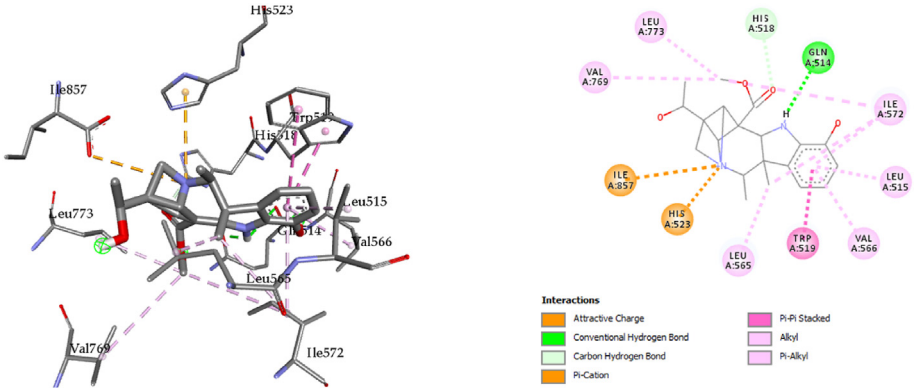

Fig. 2. Interactions between scholaricine (**9**) and the active site of the 1HU9.

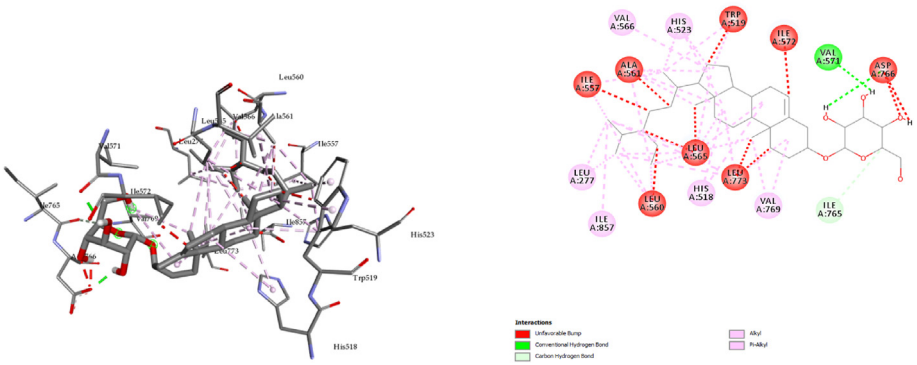

Fig. 3. Interactions between β-sitosterol glucoside (**8**) and the active site of the 1HU9.

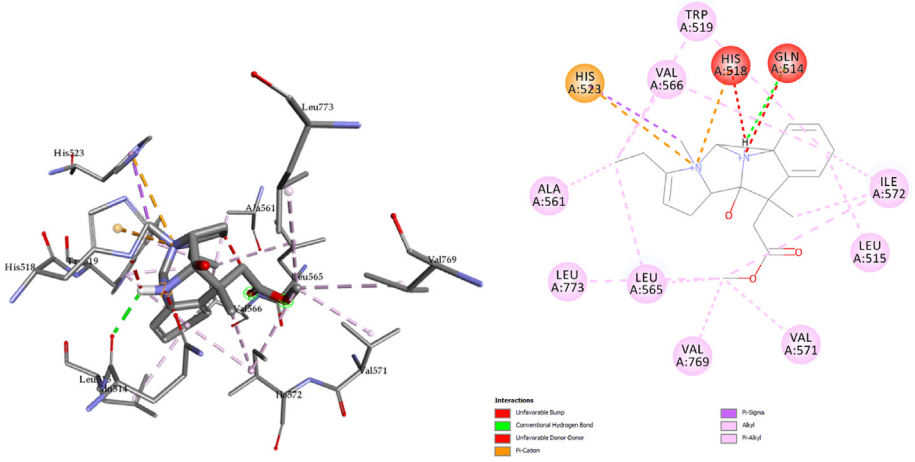

Fig. 4. Interactions between picralstonine (**7**) and the active site of the 1HU9.

4. Conclusion

Bioactive constituents have been isolated from the leaves of *A. scholaris*. The lipoxygenase (15-LOX) inhibitory activity of the isolated compounds was investigated for the first time with scholaricine showing the best activity with IC_{50} value in micro molar range. *In silico* study of isolated compounds showed possible binding modes and confirmed the experimental results. Also the molecular docking analysis confirmed the potential of studied compounds for future drug discovery investigations. Further QSAR and kinetic studies are needed to understand the inhibitory mechanism of corresponding compounds and relative derivatives.

Declaration of competing interest

Authors declare no conflict of interest.

Data availability

No data was used for the research described in the article.

Acknowledgements

This research was supported by the Third World Academy of Sciences (TWAS) and the International Center of Chemical and Biological Sciences (ICCBS), University of Karachi, Pakistan. We also thank Dr. Nzuwah V.D.P. Nziko of the Department of Chemistry, Hampton University, USA for running the NMR spectra of compound **5**. MSA is also thankful for the financial support to conduct this research through a Project of Higher Education Commission, Islamabad, Pakistan (# NRPU 5758).

Appendix A. Supplementary data

Supplementary data to this article can be found online at https://doi.org/10.1016/j.ejmcr.2023.100108.

References

[1] S. K Mahendra, M. K Deepak, P. V Nityanand, *Alstonia scholaris* (L.) R. Br. and *Alstonia macrophylla* Wall. ex G. Don: a comparative review on traditional uses, phytochemistry and pharmacology, J. Ethnopharmacol. 153 (2014) 1–18.
[2] A. Atta-Ur-Rahman, M. Asif, M. Ghazala, K. J Fatima, A alvi, scholaricine an alkaloid from Alstonia *scholaris*, Phytochemistry 24 (1986) 2771–2773.
[3] K. Toh-Seok, N. Kok-Tih, S. Kooi-Mow, K. Yoganathan, Alkaloids from *Alstonia scholaris*, Phytochemistry 45 (1997) 1303–1305.
[4] V. Kanase, D. J Mane, A pharmacognostic and pharmacological review *Alstonia scholaris*, Asian J. Pharmaceut. Clin. Res. 11 (12) (2018) 22–26.
[5] T. Shin-Jowl, L. Yun-yee, C. Yeun-Mun, A. Zanariah, E. Tadahiro, H. Masahiko, K. Kanki, K. Toh-Seok, Strychnan and secoangustilobine A type alkaloids from *Alstonia spatula*. Revision of the C-20 configuration of scholaricine, J. Nat. Prod. 73 (2010) 1891–1897.
[6] S. P Surya, G. Jayanthi, K. R Smitha, *In Vitro* Evaluation of the anticancer effect of metabolic Extract of *Alstonia scholaris* leaves on mammary carcinoma, J. Appl. Pharmaceut. Sci. 2 (2012) 142–149.
[7] E.S. Vernon, A. H Cathy, T. H Ernest, K. Levy, A. L Ronald, A. C James, C. S Caroline, J. K Gary, Lipoxygenase inhibitors as potential cancer chemopreventives, Cancer Epidemiol. Biomark. Prev. 8 (1999) 467–483.
[8] A.L. Tappel, Methods of Enzymology, vol. 5, Academic Press, New York, 1962, p. 539.
[9] G. M Morris, D.S. Goodsell, R. S Halliday, R. Huey, W. E Hart, R. K Belew, A. J Olson, Automated docking using a Lamarckian genetic algorithm and an empirical binding free energy function, J. Comput. Chem. 19 (1998) 1639–1662.
[10] M. F Sanner, Python, A programming language for software integration and development, J. Mol. Graph. Model. 17 (1999) 57–61.
[11] M. Anupam, C. V Subash, M. Rampratap, A. Jayanthy, S. Anupam, B. S Madhira, K. S Rajeev, Phytochemistry and chromatographic analysis of *Alstonia scholaris* L. R.Br. used as a traditional medicine, World J. Pharmaceut. Res. 5 (2015) 1503–1519.
[12] W. Chao-Min, Y. Kuei-Lin, T. Shang-Jie, J. Yun-Lian, C. Chang-Hung, Anti-proliferative activity of triterpenoids and sterols isolated from *Alstonia scholaris* against non-small-cell lung carcinoma cells, Molecules 22 (2017) 1–13.
[13] S. Nighat, S. S Zafar, S. Muhammad, K. Mustafa, Two new triterpenes from *Alstonia scholaris* flowers, Nat. Prod. Res. 27 (2014) 1277–1286.
[14] W. Rosalina, J.D. Frank, Inflammation, cancer and oxidative lipoxygenase activity are intimately linked, Cancers 6 (2014) 1500–1521.
[15] L. Cheng-tan, Z. Wei-ping, S. San-hua, L. Yun-bi, Z. Li-hui, Q. Ling-ling, H. Xue-qin, H. Xiao-jia, W. Er-qing, Baicalin attenuates oxygen-glucose deprivation-induced injury by inhibiting oxidative stress-mediated 5-lipoxygenase activation in PC12 cells, Acta Pharmacol. Sin. 31 (2010) 137–144.
[16] S. Raeisi, Molecular docking studies of squalene synthase inhibitors as potential anti-cardiovascular disease drugs: insights into drug-protein interaction discovery, Pharmaceut. Sci. 19 (2013) 39–44.

The Natural Products Journal, 2024, *14*, e050124225279

RESEARCH ARTICLE

Phytochemical Studies of *Alstonia scholaris*, Chemical Transformation and Biological Evaluation against a Breast Cancer Cell Line

Salome Ghansenyuy[1], Eyong Kenneth Oben[1,*], Pierre Yemback[1], Nziko Vincent de Paul Nzuwah[2], Ali Muhammad Shaiq[3], Folefoc Gabriel Ngosong[1], Davis Samantha[4], Tobin Jenna[4], Haleigh Parker[4] and Taube Joseph[4]

[1]*Department of Organic Chemistry, Faculty of Science, University of Yaounde I, Yaounde, Cameroon;* [2]*Department of Chemistry, Hayden Dr. Virginia State University, Petersburg VA, 23803, USA;* [3]*H.E.J. Research Institute of Chemistry, International Center for Chemical and Biological Sciences, University of Karachi, Karachi 75270, Pakistan;* [4]*Department of Biology, Institute for Biomedical Sciences, Baylor University, Waco, TX, 76798, USA*

ARTICLE HISTORY

Received: May 03, 2023
Revised: August 25, 2023
Accepted: September 11, 2023

DOI:
10.2174/0122103155260546231113052349

Abstract: ***Background*:** Some *Alstonia* species are used in traditional medicine to treat diseases such as cancer, dysentery, diarrhea, jaundice, malaria, gastrointestinal troubles, and snake-bites.

***Objective*:** In this study, we aim to evaluate the ethanol leaf extract of *Alstonia scholaris* for anti-cancer constituents and structural modification to introduce a privilege medicinal α,β-unsaturated scaffold.

***Methods*:** The relative viability of the MDA-MB-231 breast cancer cell line exposed to isolated compounds at different concentrations was assayed. Chemical analysis was carried out by high resolution mass spectrometry and one and two-dimensional NMR techniques.

***Results*:** Structures of purified compounds were determined as betulin **1**, α-amyrin acetate **2**, mixture of β-sitosterol **3** and stigmasterol **4**, tetratriacontyl-trans-*p*-coumarate **5**, ursolic acid **6**, β-sitosterol glucoside **7**, picralstonine **8** and scholaricine **9**. To introduce privilege medicinal scaffold, compounds **1** and **2** under SeO_2 oxidation condition afford new acrylaldehye derivatines. Compound **1** afforded Betulin acrylaldehyde **10** while compound **2** afforded lupeolacetate acryl aldehyde **11** in an intriguing mechanism with the conversion of ursane to lupane scafford. Compound **11** equally showed interesting activity against MDA MB 231 breast cancer cell line with an IC_{50} of 4.63 ± 0.09 µg/ml.

***Conclusion*:** From these findings, the medicinal α,β-unsaturated scaffold could have pharmacological effects in treating MDA-MB-231 breast cancer.

Keywords: *Alstonia scholaris,* α-amyrin acetate, SeO_2 oxidation, lupeolacetate acrylaldehyde, MDA-MB-231 cell line, breast cancer cell line.

1. INTRODUCTION

Alstonia is a genus of the Apocynaceae family and comprises about 60 species [1]. Some of these species are used traditionally in the treatment of several diseases, such as cancer, dysentery, diarrhea, jaundice, gastrointestinal troubles, malaria, and snakebite [1-4]. Biological activities such as antiphlogistic, antidiabetic, antimalarial, anticancer, antioxidant, and cytotoxic activities have been reported for the genus [1, 5]. A broad band of isolated compounds such as alkaloids, triterpenes, and phenolics have been reported from different Alstonia species [6-12].

A. scholaris is an important species of this genus used in traditional medicine to treat various diseases [1]. This plant has been previously investigated and has resulted in the isolation of triterpenes, alkaloids, and sterols [13-15]. A recent study of this plant has reviewed a pharmacological perspective toward drug discovery [16].

We have initiated a study to isolate the major constituents of *A. scholaris*, and the introduction of the privileged α,β-unsaturated medicinal scaffold. We report herein on the phytochemistry of the leaves of *A. scholaris*, chemical transformation, and activities against a breast cancer cell line.

2. MATERIAL AND METHODS

2.1. Materials

^1H, 2D ^1H-^1H COSY, ^{13}C, 2D HSQC, and HMBC NMR spectra data were recorded on Bruker AMX 600 MHz spec-

*Address correspondence to this author at the Department of Organic Chemistry, Faculty of Science, University of Yaounde I, Yaounde, Cameroon; Tel: ++237-677-95-1126; E-mail: eyongkk@yahoo.com

2210-3163/24 $65.00+.00

trometers. HR-TOF-ESI-MS and EI-MS were measured on a Bruker machine. IR and UV spectra were recorded on NICOLET 510PFT-IR and UV-2101PC spectrophotometers, respectively. The melting points were determined using a 'BUCHI' B-540 instrument.

2.2. Methods

2.2.1. Chemicals

Chemicals and reagents for synthesis and solvents for NMR analysis were obtained from Merck (Germany).

2.2.2. Plant Material

The plant material was harvested from the University of Karachi campus in May 2017 and identified by Dr. Muneeba Khan, Plant Taxonomist, Department of Botany, University of Karachi, Karachi, with a voucher No. G.H-94482.

2.2.3. Extraction and Isolation

The air-dried and powdered leaves of *A. scholaris* (25 Kg) were extracted with ethanol at room temperature. The suspensions were filtered and the filtrate was concentrated using a rota vapor to obtain 637 g of extract. The crude extract was subjected to acid-base extraction using 1.5 N H_2SO_4 and 3 N Na_2CO_3 to afford 260 g of the non-alkaloid fraction and 9.33 g of the alkaloidal fraction, while the resulting aqueous fraction afforded 40 g of the n-butanol fraction. Successive column chromatographic separation of the non-alkaloid fraction afforded AS_1 and identified as betulin (compound **1**), 0.3 g of AS_2 and identified as α-amyrin acetate (compound **2**), 20 mg of AS_3 as a mixture of compound **3** (β-sitosterol) and **4** (stigmasterol), and 18 mg of AS_4 and identified as tetratriacontyl-trans-*p*-coumarate (compound **5**). Further column chromatographic separation afforded 20 mg of AS_5 and identified as ursolic acid (compound **6**), 10 mg of AS_6 identified as β-sitosterol glucoside (compound **7**), and 3 mg of AS_7 identified as picralstonine (compound **8**). Finally, column chromatography of 6.9 g of alkaloid fraction using CH_2Cl_2-MeOH as eluent afforded 8 mg of AS_8 and identified as scholaricine (compound **9**).

2.2.3.1. Compound 1 or Betulin

White powder, 284°C; Hexane-Ethyl acetate 20% as eluent; EI *m/z*: 442.3 corresponding to $C_{30}H_{50}O_2$ [17]. (Supplementary material).

2.2.3.2. Compound 2 or α-amyrin Acetate

White powder, 186°C; Hexane 100 % as eluent; EI *m/z*: 468.3 corresponding to $C_{32}H_{52}O_2$ [18]. (See supporting information).

2.2.3.3. Compounds 3 and 4 or Mixture of β-sitosterol and Stigmasterol

White powder, 135-137°C; Hexane/Ethyl acetate 4 % as eluent; EI *m/z*: 414.3 corresponding to $C_{29}H_{50}O$/ $C_{29}H_{48}O$ [19]. (Supplementary material).

2.2.3.4. Compound 5 or Tetratriacontyl-trans-p-coumarate

White powder; 240°C; Hexane-Ethyl acetate 4% as eluent; HR TOF-MS ESI *m/z*: 640.2 corresponding to $C_{43}H_{76}O_3$ [20]. (Supplementary material).

2.2.3.5. Compound 6 or Ursolic Acid

White powder; 285-290°C; DCM/MeOH 1% as eluent; EI-MS *m/z*: 456.2 corresponding to $C_{30}H_{40}O_3$ [21]. (Supplementary material).

2.2.3.6. Compound 7 or β-sitosterol Glucoside

Brownish-black powder; > 212°C; DCM/MeOH 5% as eluent; EI-MS *m/z*: 576.8 corresponding to $C_{35}H_{60}O_6$ [22]. (Supplementary material).

2.2.3.7. Compound 8 or Picralstonine

Greenish brown powder, 519.5°C; DCM/MeOH 2% as eluent; EI *m/z*: 338.2 corresponding to $C_{20}H_{22}N_2O_3$ [3]. (Supplementary material).

2.2.3.8. Compound 9 or Scholaricine

White powder, 519.5°C; Ethyl acetate 100% as eluent; EI *m/z*: 356.2 corresponding to $C_{20}H_{24}N_2O_4$ [23]. (Supplementary material).

2.3. Synthesis

To the compounds in dry DCM or Ethanolic solution, 1.5 eq. of SeO_2 was added at room temperature. The reaction mixture was refluxed while stirring for 1-3 h and monitored on a TLC plate. The compounds were obtained after column chromatography separation of the reaction medium using Hex/AcOEt in various proportions [24].

3. RESULTS AND DISCUSSION

3.1. Phytochemistry

In this study, we report the isolation and identification of three triterpenoids, two alkaloids, one sterol glucoside, a mixture of two sterols, and one cinnamate propanoate from the ethanol extract of the leaves of *A. scholaris* on the basis of 1D and 2D NMR data and identified as betulin **1**, α-amyrin acetate **2**, a mixture of β-sitosterol **3** and stigmasterol **4** tetratriacontyl-trans-*p*-coumarate **5**, ursolic acid **6**, β-sitosterol glucoside **7**, picralstonine **8** and scholaricine **9** (Fig. **1**).

3.2. Chemical Transformation

We introduced the privilege medicinal α,β-unsaturated function to our triterpene scaffold in an approach to discover derivatives with structure-diversities. We obtained a new approach in the conversion of ursane to lupane derivatives with favorable anti-cancer efficacies against the MDA-MB-231 cell line.

New lupane derivatives **10**-**11** were obtained on treatment with triterpenes **1** and **2** with selenium dioxide [24] under reflux conditions in dry DCM or ethanol (Table **1**).

The oxidation of the terminal methylene group in compound **1** proceeded with enough selectivity under SeO_2 oxidizing conditions to afford the required product **10** in 60% yield while the formation of compound **11** involves a possible rearrangement in an intriguing mechanism from ursane to lupane scaffold under SeO_2 oxidation conditions (Scheme **1**).

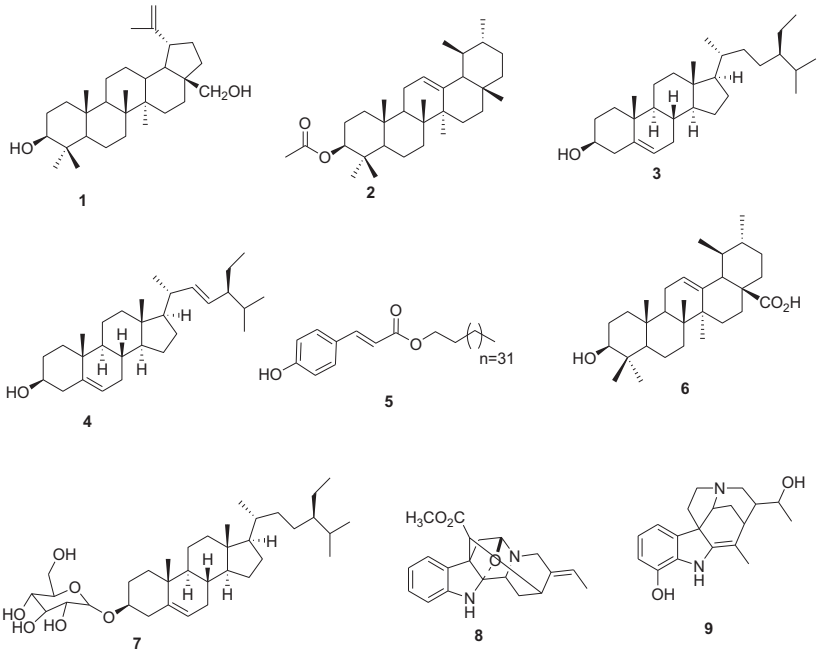

Fig. (1). Structure of isolated compounds from *A. scholaris.*

Table 1. Allylic oxidation of triterpene derivatives.

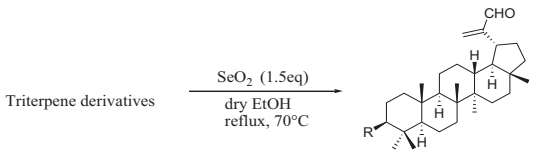

Substrate	Product(s)	Isolated Yield	Time
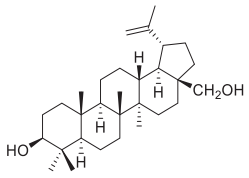 **1**	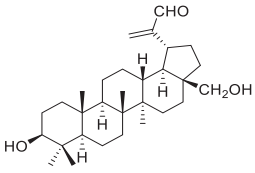 **10**	60%	7
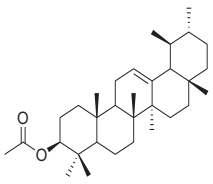 **2**	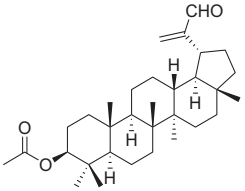 **11**	50%	8

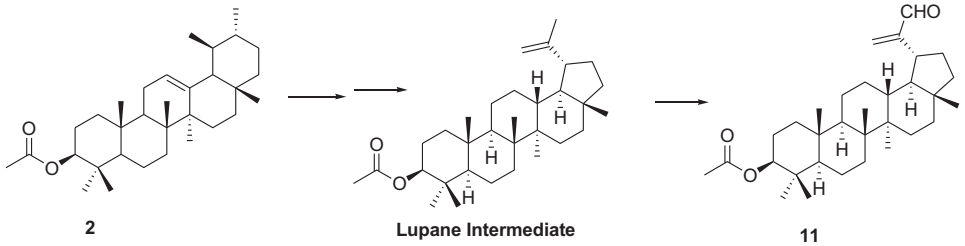

Scheme 1. unusual rearrangement of ursane **2** to lupane intermediate under SeO_2 oxidation conditions to afford compound **11**.

Table 2. ^{1}H and ^{13}C NMR spectral data of the synthesized compounds.

S. No.	δc (DEPT)	δ_H (m, *J* in Hz)	δc (DEPT)	δ_H (m, *J* in Hz)
10		**11**		**-**
1	38.4(CH_2)	0.91(m) ;1.55(br d, *J*= 12.0Hz)	38.8(CH_2)	0.92 (m); 1.57 (br d, *J* = 12.0 Hz)
2	27.4(CH_2)	1.47(m);1.70(m)	27.4(CH_2)	1.47 (m); 1.72 (dd, *J* = 10 and 12 Hz)
3	77.2(CH)	2.97 (dd, *J*= 5 and 10Hz)	80.2(CH)	4.97 (m)
4	38.3(C)	-	37.3(C)	-
5	55.1(CH)	0.70(m)	55.3(CH)	0.72 (m)
6	18.3(CH_2)	1.55(m); 1.30(m)	18.0(CH_2)	1.56 (m); 1.33 (m)
7	34.1(CH_2)	1.44(m); 1.38(m)	34.3(CH_2)	1.45 (m); 1.37 (m)
8	41.0(C)	-	41.0(C)	-
9	50.1(CH)	1.38(m)	51.1(CH)	1.38 (m)
10	37.4(C)	-	37.4(C)	-
11	20.9(CH_2)	1.43(m); 1.22(m)	30.0(CH_2)	1.42 (m); 1.20 (m)
12	24.6(CH_2)	1.27(m); 1.91(m)	25.6(CH_2)	1.23 (m); 1.90 (m)
13	37.0(CH)	2.74(m)	37.0(CH)	2.74 (m)
14	42.6(C)	-	42.8(C)	-
15	27.1(CH_2)	1.23(m); 1.87(m)	27.0(CH_2)	1.26 (m); 1.88 (m)
16	29.3(CH_2)	1.55(m); 2.63(m)	30.3(CH_2)	1.52 (m); 2.61 (m)
17	47.8(C)	-	47.8(C)	-
18	47.8(CH)	1.78(m)	47.8(CH)	1.77 (m)
19	48.0(CH)	2.65(m)	48.2(CH)	2.62 (m)
20	148.3(C)	-	148.3(C)	-
21	29.8(CH_2)	1.52(m); 2.22(m)	29.6(CH_2)	1.53 (m); 2.24 (m)
22	34.1(CH_2)	1.56(m); 2.13(m)	34.0(CH_2)	1.56 (m); 2.15 (m)
23	28.0(CH_3)	0.86 (s)	27.0(CH_3)	0.88 (s)
24	15.3(CH_3)	0.66 (s)	15.0(CH_3)	0.67 (s)
25	16.1(CH_3)	0.77 (s)	16.1(CH_3)	0.76 (s)
26	16.1(CH_3)	0.91 (s)	16.1(CH_3)	0.91 (s)
27	14.7(CH_3)	0.98 (s)	14.6(CH_3)	1.02 (s)
28	58.2(CH_2)	3.53 and 3.09 (d, *J*= 10 Hz)	18.5(CH_3)	0.70 (s)
29	105.6(CH_2)	6.42 and 6.08 (br s)	105.8(CH_2)	6.40 and 6.05 (br s)
30	196.0(C)	9.51 (s)	196.2(C)	9.51 (s)
1’	-	-	170.2(C)	-
2’	-	-	21.0(CH_3)	2.02 (s)

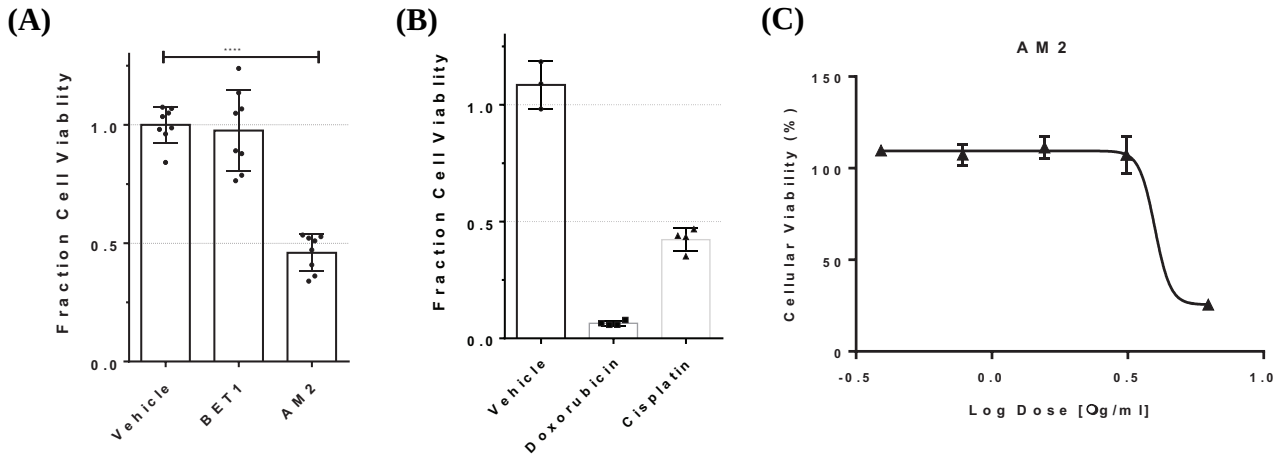

Fig. (2). Cytotoxicity of compounds **10** (BET1) and **11** (AM2) towards MDA-MB-231 cells. (**A**) MDA-MB-231 cells were treated with indicated compounds at 4 μg/ml concentration. (**B**) MDA-MB-231 cells were treated with doxorubicin at 5 μM and cisplatin at 50 μM. (**C**) Representative IC_{50} determination for AM2. Note the log scale on the x-axis. All data were gathered in biological triplicate.

To further understand the formation of compound **11**, ursolic acid **6** and other ursane derivatives available in our laboratory with structural similarities to compound **2** were equally subjected to SeO_2 oxidation conditions but the reaction didn't take place. Thus the methyl at C-18 and the acetyl at C-3 functions of compound **2** might play a role in this unusual conversion. However, the detailed mechanism is still under study. Physical and spectroscopic data for **10** and **11** were similar to those reported for lupeol [25, 26]. The ^1H NMR spectrum (500 MHz, $CDCl_3$) of compound **10** showed signals indicative of aldehyde proton at δ_H = 9.51 (1H, s), two downfield terminal olefin protons at δ_H = 5.95 (1H, br s) and 6.30 (1H, br s), five methyl groups at δ_H = 0.98 (3H, s), 0.91 (3H, s), 0.88 (3H, s), 0.76 (3H, s) and 0.66 (3H, s), seventeen methylene and methine groups, amongst which two of which are attached to oxygen atoms; a diastereotopic protons at δ_H = 3.53 (1H, d, 10 Hz; H-28a) and δ_H = 3.09 (1H, d, 10 Hz; H-28b) and δ_H = 2.97 (1H, dd, 5, 10.2 Hz; H-3) and the disappearance of methyl-30 at δ_H = 1.59 (3H, s).

The ^{13}C NMR spectrum (125 MHz, $CDCl_3$) showed 30 carbons signals that were assigned by a DEPT experiment as one carbonyl atom at δ_C = 196.0 (CHO), five methyl (δ_C 28.0, 15.3, 16.1, 16.1, 14.7), twelve methylene including one –CH_2(OH) at δ_C = 58.2, six methine including one –CH(OH) (δ_C = 77.2), six quaternary carbons (δ_C = 38.3, 41.0, 37.4, 42.8, 47.7, 148.3) and the disappearance of methyl carbon at δ_C = 18.2 (CH_3-30) (Table **2**).

However, the appearance of α,β-unsaturated olefin peaks was not observed on the ^{13}C NMR spectrum. The presence of these peaks at δ_C = 105.8 and δ_C = 148.3 was made as evidence thanks to their HSQC and HMBC spectra. The disappearance of these peaks during ^{13}C NMR measurements maybe due to the inability of these bonds to come into resonance due to weak absorbance. This can happen if the delay between pulses is set too short, particularly for carbon-13 nuclei lacking attached protons.

The structures of the synthesized compounds **10**, and **11** were analyzed from the interpretation of their 1D and 2D NMR spectral data (Table **2**).

3.2.1. Betuline Acrylaldehyde 10

White solid (CH_2Cl_2/MeOH); (Hex/AcOEt 27%); mp 258°C; yield: 60%; ^1H NMR ($CDCl_3$, 500 MHz): δ = 9.51 (1H, s, H-30), δ = 6.42 and 6.08 (each 1H, br s, H-29), 0.98 and 0.91 (each 3H, 2XCH_3), 0.88-0.76 (6H, s, 2XCH_3), 0.66 (3H, s, CH_3); ^{13}C NMR ($CDCl_3$, 125 MHz): δ = 196.0 (C, C-30), 58.2 (C, C-28), 148.3 (C, C-20), 105.6 (CH_2, C-29), δ = 77.2 (C, C-3).

3.2.2. Lupeolacetate Acrylaldehyde 11

White solid (CH_2Cl_2/MeOH); (Hex/AcOEt 7.5%) mp 230°C; yield: 50%; ^1H NMR ($CDCl_3$, 500 MHz): δ = 9.51 (1H, s, H-30), δ = 6.40 and 6.05 (each 1H, br s, H-29), 2.02 (3H, s, methyl acetate), 1.01-0.66 (18H, s, 6x CH_3); ^{13}C NMR ($CDCl_3$, 125 MHz): δ = 196.2 (C, C-30), 170.2 (C, C-acetate), 148.3 (C, C-20), 105.8 (CH_2, C-29), δ = 80.2 (C, C-3).

3.3. Cytotoxic Activity

To ascertain if any of the synthesized compounds exhibited cytotoxic activity, the relative viability of the MDA-MB-231 breast cancer cell line exposed to triterpenoids at multiple concentrations was assayed [27]. The lupeol acetate acryl aldehyde **11** was more active than the lupeol acryl aldehyde **10** against the MDA-MB-231 breast cancer cell line, which may be due to greater cell permeability.

To determine cell viability, MDA-MB-231 cells were plated in a 96-well format. The indicated compounds, dissolved in DMSO, were serially diluted in culture media prior to addition to the culture [28]. After a 3-day incubation time, relative viability was determined indirectly through the measurement of mitochondrial reductive activity using Cell-Titer Blue (Promega, Fig. **2a**). Following this assay, the IC_{50} value was determined with a 95% confidence interval (Fig. **2c**).

CONCLUSION

Phytochemical studies on the ethanol leaves extract of *A. scholaris* afforded nine known compounds **1-9**. We intro-

duced the privileged medicinal α,β-unsaturated function to our triterpene scaffold, which led to the discovery of new lupane derivatives that possess favorable anti-cancer efficacies against MDA-MB-231 cell line with an IC_{50} of 4.63 ± 0.09 μg/ml. An intriguing mechanism with the conversion of ursane to lupane scaffold is reported for the first time under SeO_2 oxidation conditions. This mechanism is under investigation.

ETHICS APPROVAL AND CONSENT TO PARTICIPATE

Not applicable.

HUMAN AND ANIMAL RIGHTS

Not applicable.

CONSENT FOR PUBLICATION

Not applicable.

AVAILABILITY OF DATA AND MATERIALS

Not applicable.

FUNDING

Authors are thankful for the financial support to conduct this research through a Project of the Higher Education Commission, Islamabad, Pakistan (# NRPU 5758).

CONFLICT OF INTEREST

The authors declare no conflict of interest, financial or otherwise.

ACKNOWLEDGEMENTS

This research was supported by the Third World Academy of Sciences (TWAS) and the International Center of Chemical and Biological Sciences (ICCBS), University of Karachi, Pakistan. We also thank Dr. Nzuwah V.D.P. Nziko of the Department of Chemistry, Virginia State University, USA for running the NMR spectra of compound **5**.

SUPPLEMENTARY MATERIAL

Supplementary material is available on the publisher's website along with the published article.

REFERENCES

[1] Khyade, M.S.; Kasote, D.M.; Vaikos, N.P. Alstonia scholaris (L.) R. Br. and Alstonia macrophylla Wall. ex G. Don: A comparative review on traditional uses, phytochemistry and pharmacology. *J. Ethnopharmacol.,* **2014**, *153*(1), 1-18. http://dx.doi.org/10.1016/j.jep.2014.01.025 PMID: 24486598

[2] Tan, S.J.; Low, Y.Y.; Choo, Y.M.; Abdullah, Z.; Etoh, T.; Hayashi, M.; Komiyama, K.; Kam, T.S. Strychnan and secoangustilobine A type alkaloids from Alstonia spatulata. Revision of the C-20 configuration of scholaricine. *J. Nat. Prod.,* **2010**, *73*(11), 1891-1897. http://dx.doi.org/10.1021/np100552b PMID: 21043460

[3] Atta-Ur-Rahman, A.; Asif, M.; Ghazala, M.; Fatima, J.; Alvi, K.A. ^{1}H and ^{13}C NMR studies on picralstonine. *J. Chem. Soc.,* **1986**, *8*, 421-423.

[4] Toh-Seok, K.; Kok-Tih, N.; Kooi-Mow, S.; Yoganathan, K. Alkaloids from alstonia scholaris. *Phytochemistry,* **1997**, *45*(6), 1303-1305. [https://doi.org/10.1016/S0031-9422(97)00106-4]. http://dx.doi.org/10.1016/S0031-9422(97)00106-4

[5] Surya, S.P.; Jayanthi, G.; Smitha, K.R. *In Vitro* evaluation of the anticancer effect of methanolic extract of alstonia scholaris leaves on mammary carcinoma. *J. Appl. Pharm. Sci.,* **2012**, *2*, 142-149. http://dx.doi.org/10.7324/JAPS.2012.2526

[6] Wiart, C. Antiparasitic asian medicinal plants in the clade lamiids. In: *Med. Plants Asia and Pacific Paras. Infec*; Academic press, **2021**; pp. 363-463. http://dx.doi.org/10.1016/B978-0-12-816811-0.00010-X

[7] Chadha, N.; Silakari, O. Indoles as therapeutics of interest in medicinal chemistry: Bird's eye view. *Eur. J. Med. Chem.,* **2017**, *134*, 159-184. http://dx.doi.org/10.1016/j.ejmech.2017.04.003 PMID: 28412530

[8] Mitra, S.; Prova, S.R.; Sultana, S.A.; Das, R.; Nainu, F.; Emran, T.B.; Tareq, A.M.; Uddin, M.S.; Alqahtani, A.M.; Dhama, K.; Simal-Gandara, J. Therapeutic potential of indole alkaloids in respiratory diseases: A comprehensive review. *Phytomedicine,* **2021**, *90*, 153649. http://dx.doi.org/10.1016/j.phymed.2021.153649 PMID: 34325978

[9] Mason, J.D.; Weinreb, S.M. The alstoscholarisine alkaloids: Isolation, structure determination, biogenesis, biological evaluation, and synthesis. *Alkaloids Chem. Biol.,* **2019**, *81*, 115-150. http://dx.doi.org/10.1016/bs.alkal.2018.09.001 PMID: 30685049

[10] Singh, H.; Bhushan, S.; Arora, R.; Singh Buttar, H.; Arora, S.; Singh, B. Alternative treatment strategies for neuropathic pain: Role of Indian medicinal plants and compounds of plant origin-A review. *Biomed. Pharmacother.,* **2017**, *92*, 634-650. http://dx.doi.org/10.1016/j.biopha.2017.05.079 PMID: 28578258

[11] Lee, S.; Sperry, J. Isolation and biological activity of azocine and azocane alkaloids. *Bioorg. Med. Chem.,* **2022**, *54*, 116560. http://dx.doi.org/10.1016/j.bmc.2021.116560 PMID: 34923389

[12] Anand, U.; Nandy, S.; Mundhra, A.; Das, N.; Pandey, D.K.; Dey, A. A review on antimicrobial botanicals, phytochemicals and natural resistance modifying agents from Apocynaceae family: Possible therapeutic approaches against multidrug resistance in pathogenic microorganisms. *Drug Resist. Updat.,* **2020**, *51*, 100695. http://dx.doi.org/10.1016/j.drup.2020.100695 PMID: 32442892

[13] Sultana, N.; Saify, Z.S.; Saleem, M.; Kamal, M. Two new triterpenes from *Alstonia scholaris* flowers. *Nat. Prod. Res.,* **2013**, *27*(14), 1277-1286. http://dx.doi.org/10.1080/14786419.2012.730046 PMID: 23075080

[14] Anupam, M.; Subash, C.V.; Rampratap, M.; Jayanthy, A.; Anupam, S.; Madhira, B.S.; Rajeev, K.S. Phytochemistry and chromatographic analysis of Alstonia scholaris (L.) R.Br. used as a traditional medicine: a review. *World J. Pharm. Res.,* **2015**, *5*(1), 1503-1519.

[15] Wang, C.M.; Tsai, S-J.; Jhan, Y-L.; Yeh, K-L.; Chou, C.H. Antiproliferative activity of triterpenoids and sterols isolated from alstonia scholaris against non-small-cell lung carcinoma cells. *Molecules,* **2017**, *22*(12), 2119. http://dx.doi.org/10.3390/molecules22122119 PMID: 29194373

[16] Pandey, K.; Shevkar, C.; Bairwa, K.; Kate, A.S. Pharmaceutical perspective on bioactives from Alstonia scholaris: Ethnomedicinal knowledge, phytochemistry, clinical status, patent space, and future directions. *Phytochem. Rev.,* **2020**, *19*(1), 191-233. http://dx.doi.org/10.1007/s11101-020-09662-z

[17] Gurupriya, S.; Cathrine, L. molecular docking studies of isolated compounds andrographolide and betulin from methanolic leaves extract of Andrographis echioides as alphaamylase and alpha-glucosidase activators. *Int. J. Appl.Pharmac.,* **2021**, *13*(3), 121-129. [https://dx.doi.org/10.22159/ijap.2021v13i3.39641]. http://dx.doi.org/10.22159/ijap.2021v13i3.39641

[18] Okoye, N.N.; Ajaghaku, D.L.; Okeke, H.N.; Ilodigwe, E.E.; Nworu, C.S.; Okoye, F.B.C. beta-Amyrin and alpha-amyrin acetate isolated from the stem bark of *Alstonia boonei* display profound anti-inflammatory activity. *Pharm. Biol.,* **2014**, *52*(11), 1478-1486. http://dx.doi.org/10.3109/13880209.2014.898078 PMID: 25026352

[19] Luhata, L.P.; Munkombwe, N.M. Isolation and characterisation of stigmasterol and β-sitosterol from odontonema strictum (acanthaceae). *J. Innov. Pharm. Biol. Sci.,* **2015**, *2*(1), 88-96.

[20] Mahmood, U.; Kaul, V.K.; Acharya, R.; Jirovetz, L. p -Coumaric acid esters from Tanacetum longifolium. *Phytochemistry,* **2003**, *64*(4), 851-853. http://dx.doi.org/10.1016/j.phytochem.2003.08.023 PMID: 14559280

[21] Seebacher, W.; Simic, N.; Weis, R.; Saf, R.; Kunert, O. Spectral assignments and reference data. complete assignments of ^{1}H and ^{13}C NMR resonances of oleanolic acid, 18a-oleanolic acid, ursolic acid and their 11-oxo derivatives. *Magn. Reson. Chem.,* **2003**, *41*, 636-638. http://dx.doi.org/10.1002/mrc.1214

[22] Faizi, S.; Ali, M.; Saleem, R.; Irfanullah Bibi, S. Spectral assignments and reference data. complete ^{1}H and ^{13}C NMR assignments of stigma-5-en-3-O-β-glucoside and its acetyl derivative. *Magn. Reson. Chem.,* **2001**, *39*, 399-405. http://dx.doi.org/10.1002/mrc.855

[23] Atta-Ur-Rahman, A.; Asif, M.; Ghazala, M.; Fatima, J.; Alvi, K.A. Scholaricine, an alkaloid from alstonia scholaris. *Phytochemistry,* **1985**, *24*(11), 2771-2773. [https://doi.org/10.1016/S0031-9422(00)80725-6]. http://dx.doi.org/10.1016/S0031-9422(00)80725-6

[24] Eyong, K.O.; Chinthapally, K.; Senthilkumar, S.; Lamshöft, M.; Folefoc, G.N.; Baskaran, S. Conversion of lapachol to lomatiol: Synthesis of novel naphthoquinone derivatives. *New J. Chem.,* **2015**, *39*(12), 9611-9616. http://dx.doi.org/10.1039/C5NJ01484K

[25] Machado, V.R.; Sandjo, L.P.; Pinheiro, G.L.; Moraes, M.H.; Steindel, M.; Pizzolatti, M.G.; Biavatti, M.W. Synthesis of lupeol derivatives and their antileishmanial and antitrypanosomal activities. *Nat. Prod. Res.*, **2018**, *32*(3), 275-281. http://dx.doi.org/10.1080/14786419.2017.1353982 PMID: 28715940

[26] Castro, M.J.; Richmond, V.; Faraoni, M.B.; Murray, A.P. Oxidation at C-16 enhances butyrylcholinesterase inhibition in lupane triterpenoids. *Bioorg. Chem.,* **2018**, *79*, 301-309. http://dx.doi.org/10.1016/j.bioorg.2018.05.012 PMID: 29793143

[27] Dasari, S.; Wudayagiri, R.; Valluru, L. Cervical cancer: Biomarkers for diagnosis and treatment. *Clin. Chim. Acta,* **2015**, *445*, 7-11. http://dx.doi.org/10.1016/j.cca.2015.03.005 PMID: 25773118

[28] Lacroix, M.; Leclercq, G. Relevance of breast cancer cell lines as models for breast tumours: An update. *Breast Cancer Res. Treat.,* **2004**, *83*(3), 249-289. http://dx.doi.org/10.1023/B:BREA.0000014042.54925.cc PMID: 14758095